Title Page

Report Title: Feasibilities of a Coal-Biomass to Liquids Plant in Southern West Virginia

Type of Report: Final Scientific/Technical Report

Reporting Period Start Date: October 18th, 2012

Reporting Period End Date: October 17th, 2016

Principal Author:

Jingxin Wang
West Virginia University
PO Box 6125
322 Percival Hall
Morgantown, WV 26506
Email: jxwang@wvu.edu
Phone: 304-293-7601

Co-Authors:

Debangsu Bhattacharyya, David DeVallance, Greg Henthorn and Shawn Grushecky

Date Report Issued: November 10, 2016

DOE Award Number: DE-FE0009997

DUNS Number: 191510239

Name and Address of Submitting Organization:

West Virginia University Research Corporation
PO Box 6216
886 Chestnut Ridge Rd
Morgantown, WV 26505

Disclaimer

Abstract

This project has generated comprehensive and realistic results of feasibilities for a coal-biomass to liquids (CBTL) plant in southern West Virginia; and evaluated the sensitivity of the analyses to various anticipated scenarios and parametric uncertainties. Specifically the project has addressed economic feasibility, technical feasibility, market feasibility, and financial feasibility.

In the economic feasibility study, a multi-objective siting model was developed and was then used to identify and rank the suitable facility sites. Spatial models were also developed to assess the biomass and coal feedstock availabilities and economics. Environmental impact analysis was conducted mainly to assess life cycle analysis and greenhouse gas emission. Uncertainty and sensitivity analysis were also investigated in this study. Sensitivity analyses on required selling price (RSP) and greenhouse gas (GHG) emissions of CBTL fuels were conducted according to feedstock availability and price, biomass to coal mix ratio, conversion rate, internal rate of return (IRR), capital cost, operational and maintenance cost. The study of siting and capacity showed that feedstock mixed ratio limited the CBTL production. The price of coal had a more dominant effect on RSP than that of biomass. Different mix ratios in the feedstock and conversion rates led to RSP ranging from $104.3 - $157.9/bbl. LCA results indicated that GHG emissions ranged from 80.62 kg CO_2 eq to 101.46 kg CO_2 eq/1,000 MJ of liquid fuel at various biomass to coal mix ratios and conversion rates if carbon capture and storage (CCS) was applied. Most of water and fossil energy were consumed in conversion process. Compared to petroleum-derived-liquid fuels, the reduction in GHG emissions could be between -2.7% and 16.2% with CBTL substitution.

As for the technical study, three approaches of coal and biomass to liquids, direct, indirect and hybrid, were considered in the analysis. The process models including conceptual design, process modeling and process validation were developed and validated for different cases. Equipment design and capital costs were investigated on capital coast estimation and economical model validation. Material and energy balances and techno-economic analysis on base case were conducted for evaluation of projects. Also, sensitives studies of direct and indirect approaches were both used to evaluate the CBTL plant economic performance. In this study, techno-economic analysis were conducted in Aspen Process Economic Analyzer (APEA) environment for indirect, direct, and hybrid CBTL plants with CCS based on high fidelity process models developed in Aspen Plus and Excel. The process thermal efficiency ranges from 45% to 67%. The break-even oil price ranges from $86.1 to $100.6 per barrel for small scale (10000 bbl/day) CBTL plants and from $65.3 to $80.5 per barrel for large scale (50000 bbl/day) CBTL plants. Increasing biomass/coal ratio from 8/92 to 20/80 would increase the break-even oil price of indirect CBTL plant by $3/bbl and decrease the break-even oil price of direct CBTL plant by about $1/bbl. The order of carbon capture penalty is direct > indirect > hybrid. The order of capital investment is hybrid (with or without shale gas utilization) > direct (without shale gas utilization) > indirect > direct (with shale gas utilization). The order of thermal efficiency is direct > hybrid > indirect. The order of break-even oil price is hybrid (without shale gas utilization) > direct (without shale gas utilization) > hybrid (with shale gas utilization) > indirect > direct (with shale gas utilization).

In the marketing study, a plan for proposed CBTL facility was plotted after expanding the integrated model, analyzing demographics, needs, competition, and buyer information. Also, SWOT and PESTE analyses were conducted. Subsequently, risks related to the marketing of CBTL fuels were evaluated on breakeven certainty and risk reduction strategies.

While in the financial study, the cash flow and income statement were developed. The direct, indirect and hybrid CBTL cases were accordingly analyzed. Sensitivity analysis were evaluated using direct, indirect and hybrid models on factors including prices of coal, biomass, shale gas, and electricity, life span and subsidy. In addition, investor interest were studied by adapting the financial modes to allow for certain financial subsidies and incentives, including subsidizing the capital expenditures of the project as well as mechanisms to increase revenue on a per-unit basis. Various factors were considered, including: investment conditions, commodity pricing environment, regulatory framework, project development models and financing options.

The obvious impacts of this project is on reducing the levels of greenhouse gasses that are currently emitted during petroleum fuel refining, and reducing domestic dependence on foreign oil. Furthermore, development of a CBTL fuel facility in the proposed study region can promote job creation and economic benefits that will enhance rural economic development.

Table of Contents

Executive Summary

The goal of this proposed project is to generate comprehensive and realistic results of feasibilities for a coal-biomass to liquids (CBTL) plant in southern West Virginia; and evaluate the sensitivity of the analyses to various anticipated scenarios and parametric uncertainties. Specifically the project addresses economic feasibility, technical feasibility, market feasibility, and financial feasibility. The important accomplishments under proposed tasks are as following:

Task 1 Project Management

- ✓ The meetings' agenda and related documents have been posted on the team's GoogleDoc site at https://sites.google.com/site/cbtlfeasibility/.

Task 2 Economic Feasibility

Task 2.1 Multi-objective Siting Model

- ✓ Developed and refined the multi-objective siting model
- ✓ Identified the suitable facility site and ranked the suitability

Task 2.2 Feedstock Assessments

- ✓ Development of Spatial Models for feedstock extraction.
- ✓ Biomass feedstocks: data collection and geographical coverage.
- ✓ Transportation networks, including storage and processing facilities
- ✓ Extraction of factors that impact the productivity of harvest operations.
- ✓ Determine break-even cost to each node for direct approach.

Task 2.3 Economic Impact Assessments

- ✓ Calibration and parameter configuration for direct approaches
- ✓ Model development and calibration and parameter configuration for direct approach

Task 2.4 Environmental Impact Analysis

- ✓ Emissions and fuel use data for harvesting equipment was collected.
- ✓ Developed GHG flow.
- ✓ LCA model for direct and indirect approaches was finished.
- ✓ Conducted the uncertainty analysis for indirect approach.
- ✓ Conducted Sensitivity analysis based on different feedstock mix ratio

Task 3 Technical Feasibilities

Task 3.1 Development and Validation of the Process Models for Different Cases

- ✓ Conceptual design
- ✓ Process modeling
- ✓ Process model validation

Task 3.2 Equipment Design and Capital Costs

- ✓ Capital cost estimation
- ✓ Economic model validation

Task 3.3 Evaluation of Projects

- ✓ Material and energy balance (base case)
- ✓ Techno-economic analysis (base case)

Task 3.4 Sensitivity Studies

- ✓ Effect of key design parameters on the indirect CBTL plant performance
- ✓ Effect of key design and investment parameters on the indirect CBTL plant economic performance
- ✓ Effect of key design parameters on the direct CBTL plant performance
- ✓ Effect of key design and investment parameters on the direct CBTL plant economic performance
- ✓ Effect of plant configuration and summary of case studies

Task 4 Market Feasibility

Task 4.1 Develop a marketing plan for the proposed CBTL facility

- ✓ Expanded Integrated Model of Marketing Plan
- ✓ Market/Industry Summary, Demographics, Needs, Competition, and Buyer Analysis
- ✓ SWOT and PESTE Analysis
- ✓ Competitive Market Strategies

Task 4.2 Evaluate risks related to the marketing of CBTL fuels

- ✓ Determination of Break Even Certainty
- ✓ Evaluation of Risk Reduction Strategies

Task 5 Financial Feasibility

Task 5.1 Cash flow and Income Statement Development

- ✓ The project team has reviewed and completed the financial statements for the indirect, direct, and hybrid CBTL cases, and now has final versions of all documents.
- ✓ The project cost projections include information related to the following: (1) Project Internal Rate of Return (IRR); (2) Net Present Value (NPV); (3) Direct project costs (4) Engineering costs; (5) Other; (6) General and administrative costs; (7)Project development fees; (8) Project contingency estimates.
- ✓ The project income statements include information related to the following: (1) Operating costs; (2) Fixed charges; (3) Plant overhead; (4) General and administrative.

Task 5.2 Sensitivity Analysis

- ✓ The project team has evaluated the key variables driving the sensitivity of the direct, indirect, and hybrid CBTL financial models, including: Coal prices, Biomass prices, Shale gas prices, Electricity prices, and projected project life span.

Task 5.3 Investor Interest and Financing Analysis

- ✓ We have prepared a prospectus that describes the potential impact of certain financial subsidies and incentives, including subsidizing the capital expenditures of the project as well as mechanisms to increase revenue on a per-unit basis.
- ✓ Various factors were considered, including: Investment conditions, Commodity pricing environment, Regulatory framework, Project development models and financing options.

Report Details

Task 1 Project Management

The team has had regular monthly meetings. We discussed the project progress, potential problems, and subtask updates. The meetings' agenda and related documents have been posted on the team's GoogleDoc site at https://sites.google.com/site/cbtlfeasibility/.

Task 2 Economic Feasibility

Planned activities:

- ✓ Identify potential suitable sites for the construction of a CBTL fuels facility.
- ✓ Quantify the amounts of trained or trainable labor.
- ✓ Determine the availability of adequate infrastructure (i.e. rail, road and navigable waterways).
- ✓ Quantify the economic and technically available supply of coal, forest and mill residue, short rotation woody crops (SRWC) from the cultivation of marginal farmland and abandoned mine lands, and biomass as surface mining residue.
- ✓ Perform an economic impact assessment for the local area and region.
- ✓ Quantify the projected impacts on the environment, resource levels and public health.

Accomplishments:

The major accomplishments were listed in the Executive Summary previously. The integrated report regarding to details of the accomplishments in this task for the entire funding period is displayed orderly as in the following four subtasks.

Research Products:

Brar, J., K. Singh, J. Zondlo, and J. Wang. 2013. Co-gasification of coal and hardwood pellets: a case study. American Journal of Biomass and Bioenergy. 2013(1): 11-26. Doi:10.7726/ajbb.2013.1005.

Cheng, Q., B. Via, J. Wang, and J. Zondlo. 2014. Primary study of woody biomass and coal for energy production investigated by TGA-FTIR analysis. BioResources. 9(2): 2899-2906.

Liu, W. and J. Wang. 2015. Life cycle assessment and techno-economic analysis of energy crops utilization for biofuels in the northeastern United States. 2015 FORMEC Forest Engineering: Making a positive contribution. Linz, Austria. October 4-8, 2015.

Liu, W., X. Xie, and J. Wang. Economic and environmental analyses of coal biomass to liquids: a case study in West Virginia. 2015 Gasification systems and coal & coal-biomass to liquids workshop. US Department of Energy National Energy Technology Laboratory. August 10-11, 2015. Morgantown, WV. (Invited)

Liu, W., J. Wang, D. Bhattacharyya, Y. Jiang, and D. DeVallance. (2016). Economic and Environmental analyses of Coal and Biomass to Liquid Fuels. *Submitted to Energy Journal.*

Liu, W. 2015. Economic and environmental analyses of biomass utilization for bioenergy products in the northeastern United States. Ph.D. Dissertation. Division of Forestry and Natural Resources, West Virginia University, Morgantown, West Virginia. 193 pp.

Hartley, D. 2014. Modeling and optimization of woody biomass harvest and logistics in the northeastern United States. Ph.D. Dissertation. Division of Forestry and Natural Resources, West Virginia University, Morgantown, West Virginia. 219 pp.

Task 2.1 Identify potential suitable sites for the construction of a CBTL fuels facility.

Planned Activities:

- ✓ Develop and refine of the multi-objective siting model
- ✓ Identify the suitable facility site and rank the suitability

Accomplishments:

- ✓ Identified criteria for initial siting of candidate facilities
- ✓ Developed a criteria weighting scheme for selecting candidate sites
- ✓ Model was tested and modified for base case.
- ✓ Determined the most suitable facility site for indirect approach

Southern West Virginia area was targeted for this study. The area studied was displayed in Figure 2-1a. In addition, the biomass availability and coal production distribution were shown in Figure 2-1b and Figure 2-1c. Formulated criteria weights based on the factors that have been identified by the research team since these factors are very important to the siting and development of CBTL facilities. The criteria weights were used to define the Minkovsky metric for each cell in a 30 meter raster grid of the state of West Virginia. The highest 5% of the scores were then identified a potentially suitable sites for and will be used for further evaluation.

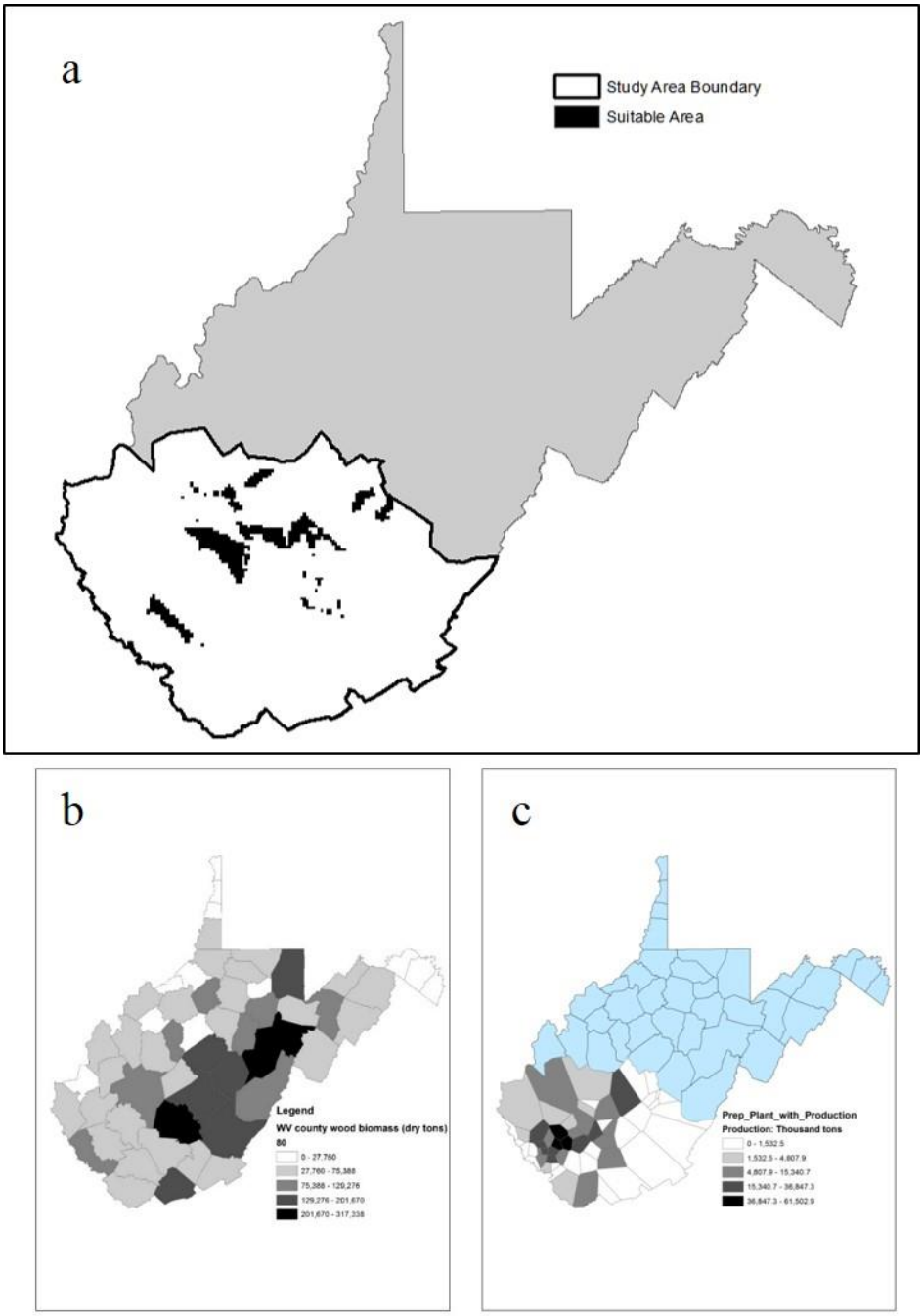

Figure 2-1. Locations and feedstock availabilities: (a) southern West Virginia study boundary; (b) biomass availabilities in West Virginia; (c) coal production in southern West Virginia.

The Figure 2-1 has shown the results of the preliminary analysis showing the locations of preliminary suitable locations across the state. The Table 2-1 below identifies the weights that are given to each criteria. It shows that distance from rail, biomass availabilities and distance to water and distance from electric substations are the four major accountable factors that decides a suitable cite.

Table 2-1. Formulated criteria weights according to each factor.

	Weight
Distance from rail	0.225744
Biomass availability	0.169825
Distance to water	0.169825
Distance from electric substation	0.105682
Distance from demand	0.059818
Flood risk	0.059818
Adjacent land uses	0.059818
Population	0.037078
Landownership	0.037078
Distance from population center	0.025104
Direction to nearest population center	0.025104
Unemployment	0.025104

The following steps were accomplished for suitability evaluation:

(1) Evaluated individual sites to determine which factors were responsible for their suitability scores.
(2) Engaged detailed analysis on most promising locations.
(3) Identified potential feedstock supply points and quantities.
(4) Developed transportation network.

Suitability index of each cell in the study was computed and the top 5% were selected as areas that were suitable for siting a CBTL facility. The suitable sites were ranked based on the index. The locations of suitable areas and sites in the study region are shown in Figure 2-2. According to the distribution of coal and biomass, as well as the suitable candidates, the economic model was solved and the solution provided detailed transportation pattern of feedstocks.

Candidate sites and suitability score were listed in Table 2-2. The locations and ranking of candidate sites for a CBTL facility were shown in Figure 2-2. The candidate #3 was selected to construct CBTL facility with a production of 10,000 bpd liquid fuels in the base case (Fig. 2-2).

Table 2-2. Suitability indices for selected candidate sites.

Site	Nearest City	Suitability Score	Site number
North Gate	Charleston	0.7790	3
Longacre Bottom	Smithers	0.7780	9
Ronald Lane	Charleston	0.7768	6
Handley	Handley	0.7748	2
McDonald	Taplin	0.7744	8
Wash Branch	Danville	0.7743	7
Glade Creek	Summersville	0.7728	1
Mink Shoals	Charleston	0.7722	4
Washington Heights	Charleston	0.7708	5

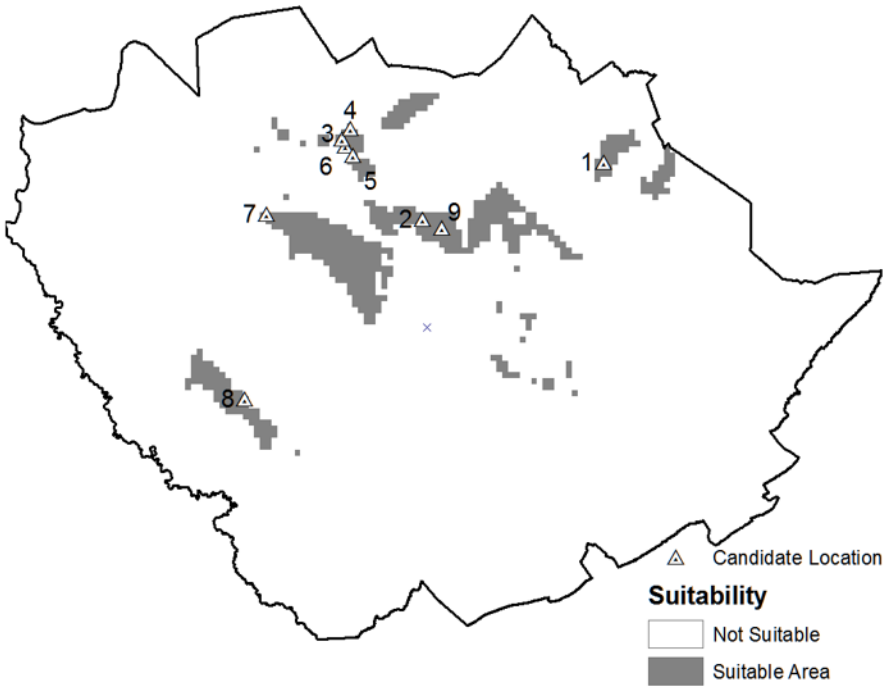

Figure 2-2. Locations and ranking of candidate sites for a CBTL facility.

Explanation of Variance

- ✓ This work has been started before it was planned to provide information to both the Market Feasibility and Financial Feasibility Tasks.

Task 2.2 Quantify the economic and technically available supply of coal, forest and mill residue, SRWC from the cultivation of marginal farmland and abandoned mine lands, and biomass as surface mining residue.

Planned Activities

- ✓ Development of Spatial Models for feedstock extraction.
- ✓ Biomass feedstocks: data collection and geographical coverage.
- ✓ Transportation networks, including storage and processing facilities
- ✓ Extraction of factors that impact the productivity of harvest operations.
- ✓ Determine break-even cost to each node for direct approach.

Accomplishments

- ✓ Assessed the availability of biomass based on the billon ton study and the possible variation of price.
- ✓ Identified harvesting systems for woody biomass and defined machine capacities and capabilities.

- ✓ Identified geospatial factors that affect harvesting efficiency.
- ✓ Road networks for the supply area have been mapped.
- ✓ Transportation networks for distribution of final products have been completed for surrounding states.
- ✓ Test runs on a single county area, validating results to determine if results are within established ranges in the literature.
- ✓ Developed search algorithm to identify candidate landing areas within the forest areas.
- ✓ Generated the list of candidate landing areas to be used in the travel distance analysis.
- ✓ Developed on module to automate the separation of forest land from National Land Cover Data.
- ✓ Developed module that automates the extraction of topographical data for forested Areas.
- ✓ Developed a method to generate feedstock extraction paths based on topography and machine capability.
- ✓ Assessed the biomass availability in the study region based on the billion ton study by KDF (Figure 2-3a).
- ✓ Assessed the coal availability in the study region based on the Annual Coal Report by EPA (Figure 2-3b).
- ✓ Assessed the biomass availability in the study region based on the billion ton study.
- ✓ Assessed the coal availability in the study region based on the Annual Coal Report

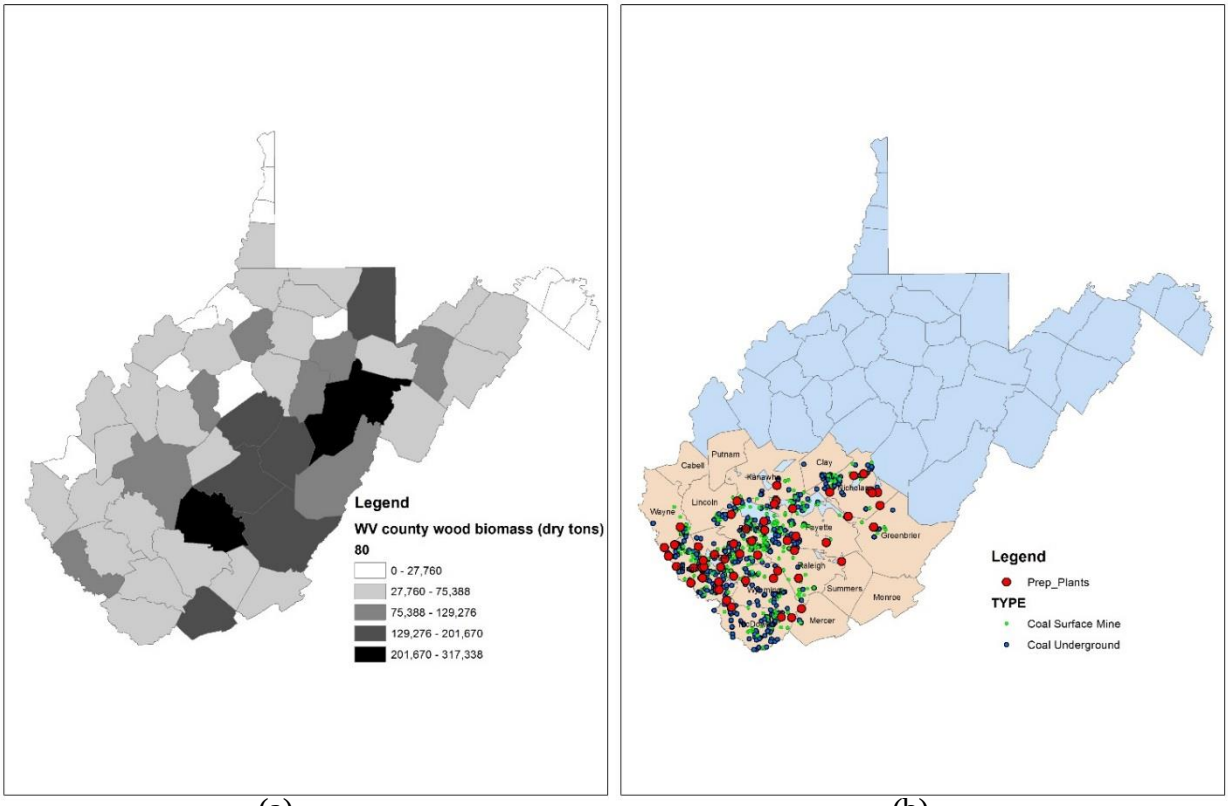

(a) (b)

Figure 2-3. Distribution of available: (a) biomass and (b) coal.

The determination of the break-even cost per Mg for each node, begins with a determination of cycle time. Cycle time is essentially a function of distance and speed with the addition of non-travel working time and delays. The formula for estimating the cycle time in seconds is given by equation 2-1.

$$\text{Cycle time} = (\text{Dist} \div \text{Unloaded Speed}) + (\text{Dist} \div \text{Loaded Speed}) + \text{NonTravel} \quad (2\text{-}1)$$

Where:
Cycle time: the time to complete one productive cycle in seconds.
Dist: the travel distance from the landing to the current node in meters.
Unloaded speed: machine speed when unloaded in m/s.
Loaded Speed: machine speed when loaded in m/s.
NonTravel: time taken for non-travel work and delay.

After cycle time in seconds is determined the cost per cycle is determined through equation 2-2.

$$\text{Cost per cycle} = (\text{Cycle time} \div 3600) \times \text{HMR} \quad (2\text{-}2)$$

Where:
Cost per cycle: the cost in dollars for a productive cycle.
Cycle time: the time to complete a cycle in seconds.
HMR: the hourly cost of the machine in dollars per hour.

Finally, cost per Mg is determined by equation 2-3.

$$\text{Cost per Mg} = \text{Cost per cycle} \div \text{Payload} \quad (2\text{-}3)$$

Where:
Cost per Mg: the cost in dollars per Mg of biomass.
Cost per cycle: the cost per cycle in dollars.
Payload: the payload to the landing in Mg.

Explanation of Variance

- ✓ Nothing to Report

Task 2.3 Perform an economic impact assessment for the local area and region.

Planned activities:

- ✓ Calibration and parameter configuration for direct approaches.
- ✓ Model development and calibration and parameter configuration for direct approach.

Accomplishments

- ✓ A preliminary industry sectoring scheme was developed.

- ✓ Conducted analysis and extraction of data acquired from U.S. Census Bureau, U.S. Department of Commerce, Bureau of Economic Analysis, and the IMPLAN group.
- ✓ Processed data from the U.S. Department of Energy (USDOE), ARC, the U.S. Department of Agriculture (USDA), the Environmental Protection Agency (EPA), and state agencies.
- ✓ Conducted analysis for indirect approach based on the distribution of biomass and coal resulted in a potential facility location in Kanawha County.

County-level databases that provide detailed data on industry sectors, final demand activities, and value added components that are developed annually using U.S. Census Bureau, U.S. Department of Commerce, Bureau of Economic Analysis, and other government-based information has been acquired from the IMPLAN group. Renewable energy, biomass inventory, conventional power generation, coal mining and transportation, energy and environmental policy information and data was obtained from the U.S. Department of Energy (USDOE), ARC, the U.S. Department of Agriculture (USDA), the Environmental Protection Agency (EPA), and state agencies, and was used to supplement the base IO data.

The parameters for direct approach were updated based on the two scenarios where hydrogen was from gasification or shale gas. When the mix ratio was 8/92, the conversion rate were 2.61 and 3.95 bbl-1/ton of feedstock if hydrogen was from gasification and shale gas respectively. The thermal efficiencies were 59% and 64% for each scenario.

Table 2.3. Social Accounting Matrix Frame work.

	1-Industry	2-Commodity	3-Factors	4-Institutions	5-Foreign Trade	6-Domestic Trade
1-Industry		1X2			1X5	1X6
2-Commodity	2X1			2X4		
3-Factors	3X1					
4-Institutions		4X2	4X3	4X4	4X5	4X6
5-Foreign trades	5X1		5X3	5X4	5X5	
6-Domestic Trade	6X1		6X3	6X4		

Table 2-4. Sectoring scheme for the project.

Code	Sector Name	NAICS Code
IND01	Agriculture, Forestry, Fishing and Hunting	11
IND02	Oil and Gas Extraction	2110
IND03	Coal Mining	212100
IND04	All other mining and Support Activities	212X
IND05	Support Activities for Oil and Gas Operations	213112
IND06	Electric Power Generation and Distribution	221100
IND07	Natural Gas Distribution	221200
IND08	Water, Sewage and Other Systems	221300
IND09	Construction	2301, 2302, 2303
IND10	Primary and Fabricated metals	331 & 332
IND11	Machinery	333
IND12	Motor vehicles and Other transportation equipment	3361 & 3364
IND13	Other Durable Manufacturing	321,327, 334,335,337,339
IND14	Other NonDurable Manufacturing	311, 313-323
IND15	Petroleum and coal products	324
IND16	Chemical, Plastics and rubber products	325 & 326
IND17	Wholesale trade	42
IND18	Retail trade	4A
IND19	Gross Output of Air, rail and water transportation	481-483
IND20	Truck transportation	484
IND21	Pipeline transportation	486
IND22	Transit and sightseeing transportation and transportation support services	485, 487 and 488
IND23	Warehousing and storage	493
IND24	Information	51
IND25	Finance, insurance, real estate, rental, and leasing	52 & 53
IND26	Gross Output of Professional, scientific, and technical services	54
IND27	Management of companies and enterprises	55
IND28	Admin and Support and Waste Management and Remediation Services	56
IND29	Educational services, health care and social assistance	6
IND30	Arts, entertainment, recreation, accommodation, and food services	7
IND31	Other Services (except Public Administration)	8
IND32	Government and Non-NAICS	92

Explanation of Variance

- ✓ Progress is halted in the model development until construction budget data is provided by the technical feasibility group.

Task 2.4 Quantify the projected impacts on the environment, resource levels and public health.

Planned activities:

- ✓ Collect emissions and energy use data for harvesting systems.
- ✓ Emissions and energy use data for preprocessing.
- ✓ Identify and define base supply chain design.
- ✓ Perform uncertainty analysis on different biomass to coal mix ratios.
- ✓ Uncertainty analysis of the LCA model with simulation results of ASPEN.
- ✓ Sensitivity analysis based on different feedstock mix ratio.
- ✓ Development of LCA boundary.
- ✓ The LCA model with ASPEN simulation results.
- ✓ Adjust the LCA model for direct and hybrid approach.
- ✓ LCA model for direct approach.

Accomplishments

- ✓ Emissions and fuel use data for harvesting equipment was collected.
- ✓ Emissions and fuel use data for infield processing and handling equipment was collected.
- ✓ Study boundary of this cradle-to-grave LCA was created.
- ✓ Developed GHG flow and LCA.
- ✓ The LCA model with ASPEN simulation results was created.
- ✓ Uncertainty analysis of the LCA model with simulation results of ASPEN was finished.
- ✓ LCA model for direct and indirect approaches was finished.
- ✓ Conducted the uncertainty analysis for indirect approach.
- ✓ Conducted Sensitivity analysis based on different feedstock mix ratio.

LCA and GHG flow

The study collected all the LCA data (includes GHG emissions, emission to water, water consumption and energy consumption) for every process. The study boundary of this cradle-to-grave LCA is shown in Figure 2-4. It includes feedstock collection, transportation, processing, liquid fuels distribution and combustion. Based on the existing study, a LCA model was developed in SimaPro 7.3. The GHG flow was developed for the base case as displayed in Figure 2-5.

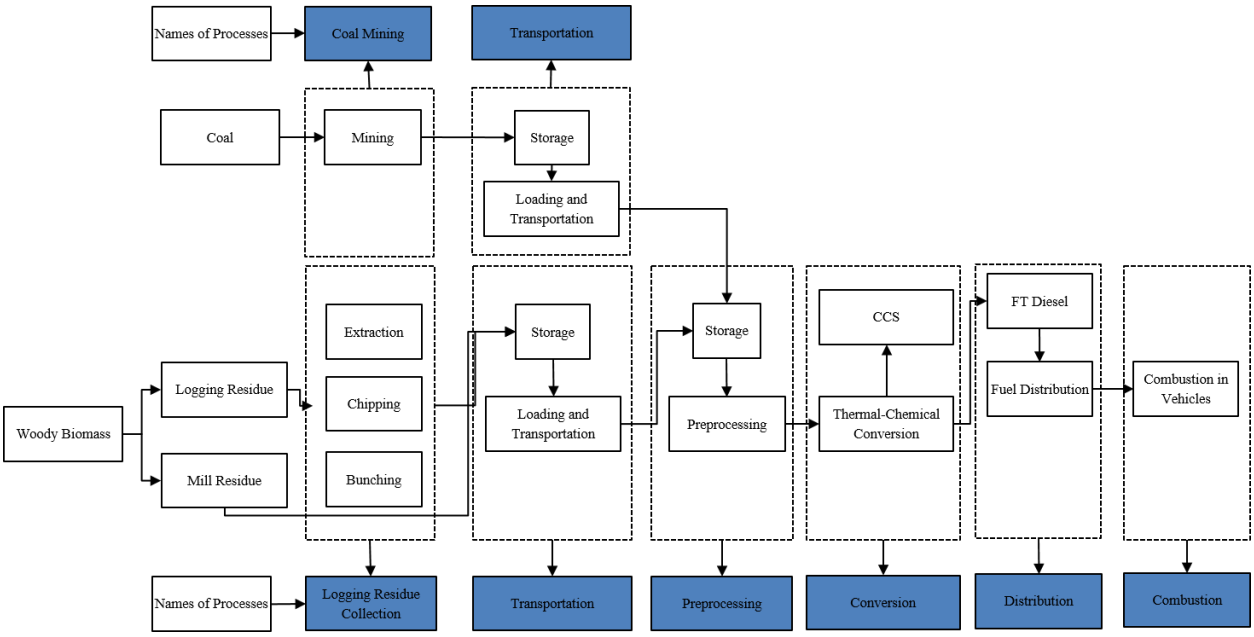

Figure 2-4. The outline of LCA boundary.

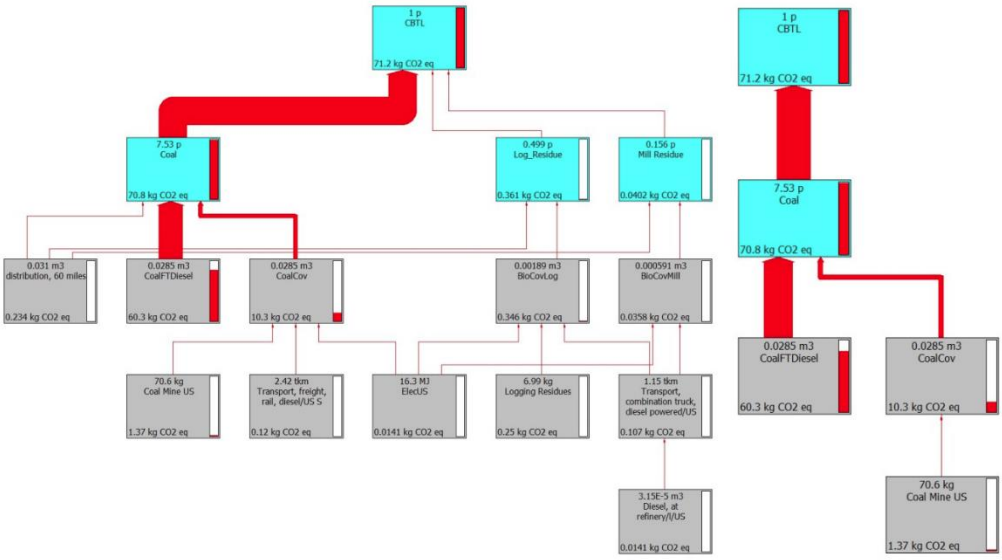

Figure 2-5. Flow of GHG (CO2 eq kg) in every process when the mix ratio is 8/92.

Uncertainty analysis

Uncertainty analysis focused on the conversion rate. The liquid fuels conversion rate from biomass and coal are 0.84-1.26 $barrel \cdot ton^{-1}$ (WTT report 2011) and 1.74-1.89 $barrel \cdot ton^{-1}$ (The American

energy security study, 2006). Triangular distribution was assumed. A total of 1,000 random trials were conducted for every case and a skew normal distribution was fitted for the results.

The uncertainty analysis in Figure 2-6 shows the skew normal distribution simulated from the results of MC simulation for each biomass and coal mix ratio. The life cycle GHG emissions of the liquid fuels have the probability be larger than the GHG emissions from petroleum-derived-diesel. The probability is 0.5%, 1.6% and 7.4% when the biomass and coal mix ratio is 15/85, 8/92 and 0/100. The probability for the other mix ratio is lower than 0.05%. Uncertainty analysis describes a clear picture than how much GHG emissions can be different from petroleum derived diesel. The uncertainty of the GHG emissions in this study is considering the conversion rate. The improvement of the conversion rate and the recovery strategy of captured carbon dioxide could benefit the environment further.

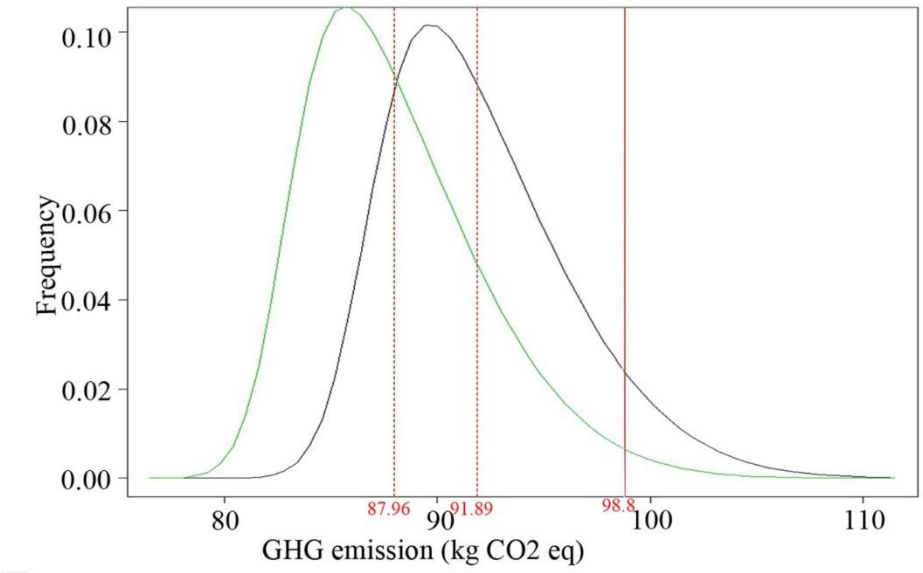

Figure 2-6. Uncertainty analysis of different biomass and coal mix ratio (8/92: black curve; 0/100: green curve); the red vertical broken lines represent the average emission of the mix ratios.

The LCA analysis for indirect approach.

A cradle-to-grave assessment includes feedstock collection, transportation, and storage, liquid fuel production, distribution, final usage and waste disposal. This study focuses on the GHG emissions (GHG), blue water consumption (BWC) and fossil energy consumption (FEC). The functional unit (f.u.) of the system is 1,000 MJ of liquid fuels. The BWC and FEC is pretty low, and most of the BWC is accounted by "Thermochemical conversion" and "Transportation, storage and preprocessing" accounts more than half of the total FEC. The GHG emissions is high because the involvement of coal, "combustion" of liquid fuels has high percentage of GHG. Uncertainty analysis of GHG emissions, blue water and fossil energy consumptions were conduct which were shown in Figure 2-7.

Table 2-5. Environmental impacts of Coal-biomass-to-liquids.

Impact Factor	Percentage of every process						Total
	Feedstock Collection	Transportation, Storage and Preprocessing	Thermochemical conversion	Distribution	Combustion	Waste Disposal	
GHG	14.68	2.38	11.79	0.35	70.71	0.10	89.52
BWC	1.68	8.40	78.55	4.75	0	6.62	49.62
FEC	13.37	57.63	2.30	6.23	0	20.47	12.92

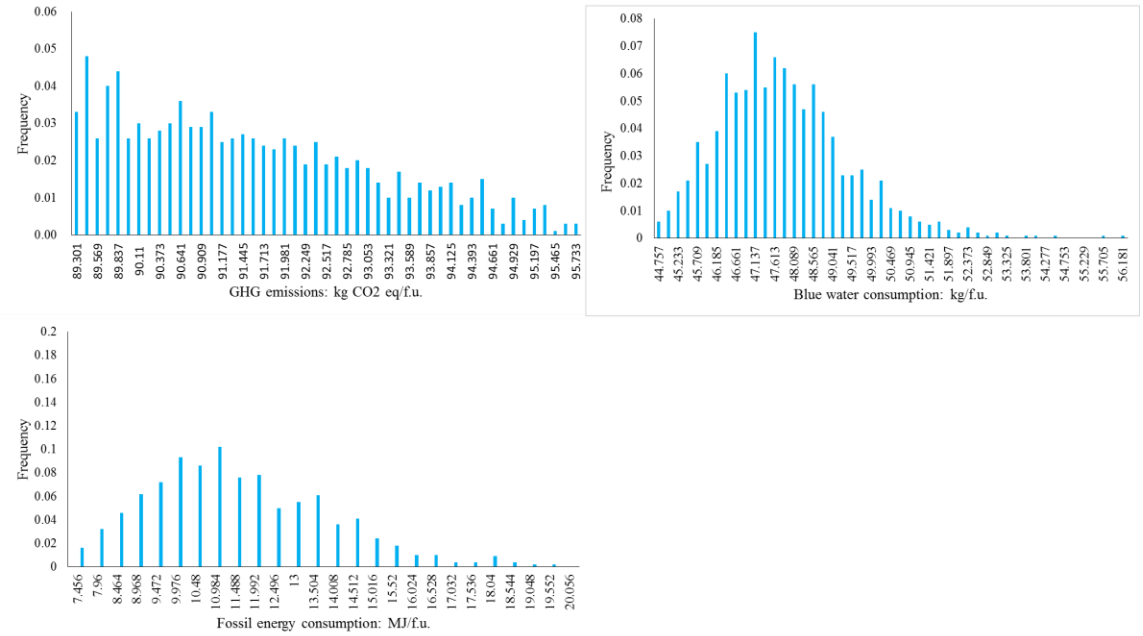

Figure 2-7. Uncertainty analysis of (a) GHG emissions, (b) blue water consumption and (c) fossil energy consumption.

There were seven major processes in the LCA model. For the base case, the GHG emissions, water and fossil energy consumption of each process and the percentage of their total amount of emission were shown in Table 2-6. Most emissions originated from the combustion in vehicles and thermal conversion, which contribute 59.72% and 12.95%, respectively to the overall GHG emissions. The portion of FT fuels derived from biomass was considered as carbon neutral. The emissions from 1,000 MJ of products ranged from 80.62 kg CO2 eq to 101.46 kg CO2 eq for various mix ratio and conversion rates. The CBTL facility consumed over 80% of the water and fossil energy that were consumed in the system.

Table 2-6. Process based environmental impacts for the base case.

Impact	Coal Mining	Transport-Coal	Residue Collection	Transport-Residue	Conversion	Distribution	Combustion	Total
GHG	13.5	0.15	0.17	0.06	12.95	0.64	59.72	87.19
	15.48%	0.17%	0.19%	0.07%	14.85%	0.73%	68.49%	100%
BWC	0.632	0.838	0.0721	0.9979	361.65	1.75	0.75	366.69
	0.17%	0.23%	0.02%	0.27%	98.63%	0.48%	0.2%	100%
FEC	1.05	1.31	0.101	1.639	34	0.584	0.016	38.7
	2.71%	3.39%	0.26%	4.24%	87.86%	1.51%	0.04%	100%

Fig. 2-8 shows the GHG emissions of each mix ratio as a function of conversion rate. GHG emissions are lower when more biomass is mixed with coal. Given the same mix ratio, more GHG emissions occur when the conversion rate is low. The mix ratio and conversion rate also affect the transportation distance of the feedstock, but the emissions due to transportation only account for a low percentage in the entire life cycle.

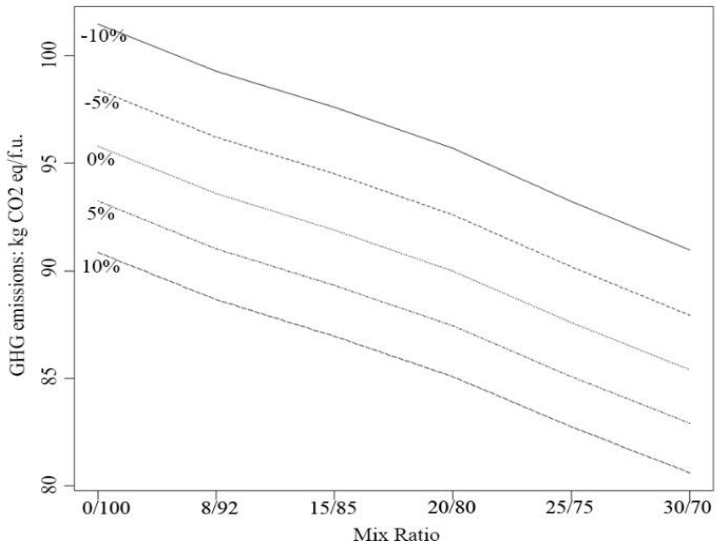

Figure 2-8. Sensitivity analyses by conversion rate and biomass to coal mix ratio for GHG emission kg CO_2 eq/f.u.

Direct approach

The input/output energies and materials were typed in the LCA model for direct approach. The GHG emissions, water and fossil energy consumptions were all much lower than indirect approach. When hydrogen was provided from gasification, the GHG emissions, water consumption, fossil energy consumption were 76.97 kg CO2 eq, 36.49 kg and 35.98 MJ per 1,000 MJ liquid fuels produced, respectively. When hydrogen was provided from shale gas, they were 73.53 kg CO2 eq, 27.84 kg and 26.97 MJ per 1,000 MJ liquid fuels produced. The low impacts of direct approach is because the high energy conversion efficiency. The energy conversion efficiency is 59.99% when hydrogen was from gasification, and is 64.29% when hydrogen was from shale gas. Both are much higher than indirect approach which has an energy conversion efficiency 46.73%.

Table 2-7. LCA results of direct CBTL with H_2 from gasification.

Impact	Coal Mining	Transport Coal	Residue Collection	Transport Residue	Conversion	Distribution	Combustion	Total
GHG (kg CO2 eq)	0.72	0.01	0.12	0.04	12.46	0.31	63.30	76.97
	0.94%	0.01%	0.16%	0.06%	16.19%	0.41%	82.24%	100.00%
BWC (kg)	0.04	0.05	0.05	0.71	33.35	2.21	0.09	36.49
	0.10%	0.13%	0.14%	1.96%	91.37%	6.06%	0.25%	100.00%
FEC (MJ)	0.06	0.08	0.07	1.17	34.00	0.58	0.02	35.98
	0.17%	0.21%	0.20%	3.26%	94.50%	1.62%	0.04%	100.00%

Table 2-8. LCA results of direct CBTL with H_2 from shale gas.

Impact	Coal Mining	Transport Coal	Residue Collection	Transport Residue	Conversion	Distribution	Combustion	Total
GHG (kg CO2 eq)	0.47	0.00	0.08	0.03	9.34	0.31	63.30	73.53
	0.63%	0.01%	0.10%	0.04%	12.71%	0.43%	86.09%	100.00%
BWC (kg)	0.02	0.03	0.03	0.45	25.01	2.21	0.09	27.84
	0.08%	0.11%	0.12%	1.61%	89.82%	7.94%	0.32%	100.00%
FEC (MJ)	0.04	0.05	0.05	0.74	25.50	0.58	0.02	26.97
	0.14%	0.18%	0.17%	2.73%	94.55%	2.17%	0.06%	100.00%

The Coal Biomass to Liquid (CBTL) project can improve GHG reduction when compared to burning raw coal. Taking base case (mix ratio 92/8) as an example, Green House Gas (GHG) emission could reduce from 87.2 to 11.6 kg CO_2 eq. The other mix ratios also displayed a

substantial amount of GHG emission reduction. This indicates that CBTL creates a very critical way to control the GHG emission caused by coal consumption. Under the increasing federal regulations against GHG emission, CBTL acts as an outlet for environmental concerns.

TEA and LCA Indirect Results

The input/output energies and materials were typed in the LCA model of different feedstock mix ratio. The GHG emissions reduced from 95.8 kg CO_2 eq to 85.4 kg CO_2 eq, and water and fossil energy consumptions increased, when the proportion of biomass increased.

Table 2-9. Green house emission reduction of different coal/biomass ratio**.**

Mix Ratio	100/0	92/8	85/15	80/20	75/25	70/30	65/35
GHG	91.5	87.2	83.3	80.5	77.5	74.5	71.2
GHG reduction	7.3	11.6	15.5	18.3	21.3	24.3	27.6

Table 2-10. LCA results of different coal/biomass ratio.

Mix Ratio	100/0	92/8	85/15	80/20	75/25	70/30
GHG	95.8	93.6	91.9	90	87.6	85.4
BWC	0.0489	0.0493	0.0498	0.0501	0.0505	0.0509
FEC	8.99	12.4	15.7	18.2	21.1	24.1

Sensitivity analysis of Capital Cost as well as Operation and Maintenance was conducted both for range 10% with interval change 5% in this case. The analysis was also subject to biomass to coal mix ratio variations. The results show that when Capital Cost was under 10% fluctuation, the percentage change of RSP was between 10% and 12%. In the case of Operation and Maintenance, it was observed that the percentage change of RSP was between 1.9% and 2.3%. Mix ratio variations were taken for consideration in all results.

Table 2-11. Percentage change of RSP

Biomass to Coal Mix ratio	Capital Cost (%)					Operation & Maintenance (%)				
	-10%	-5%	0%	5%	10%	-10%	-5%	0%	5%	10%
0/100	10.01	10.05	10.16	10.19	10.29	2.12	2.14	2.2	2.21	2.26
8/92	10.75	10.96	10.96	11.14	11.14	2.09	2.15	2.15	2.21	2.21
15/85	10.84	10.84	10.84	10.84	10.84	2.12	2.12	2.12	2.12	2.12
20/80	11.3	11.3	11.3	11.3	11.3	2.04	2.04	2.04	2.04	2.04
25/75	11.78	11.75	11.75	11.75	11.75	2.02	2.01	2.01	2.01	2.01
30/70	11.97	11.97	11.97	11.97	11.97	1.93	1.93	1.93	1.93	1.93

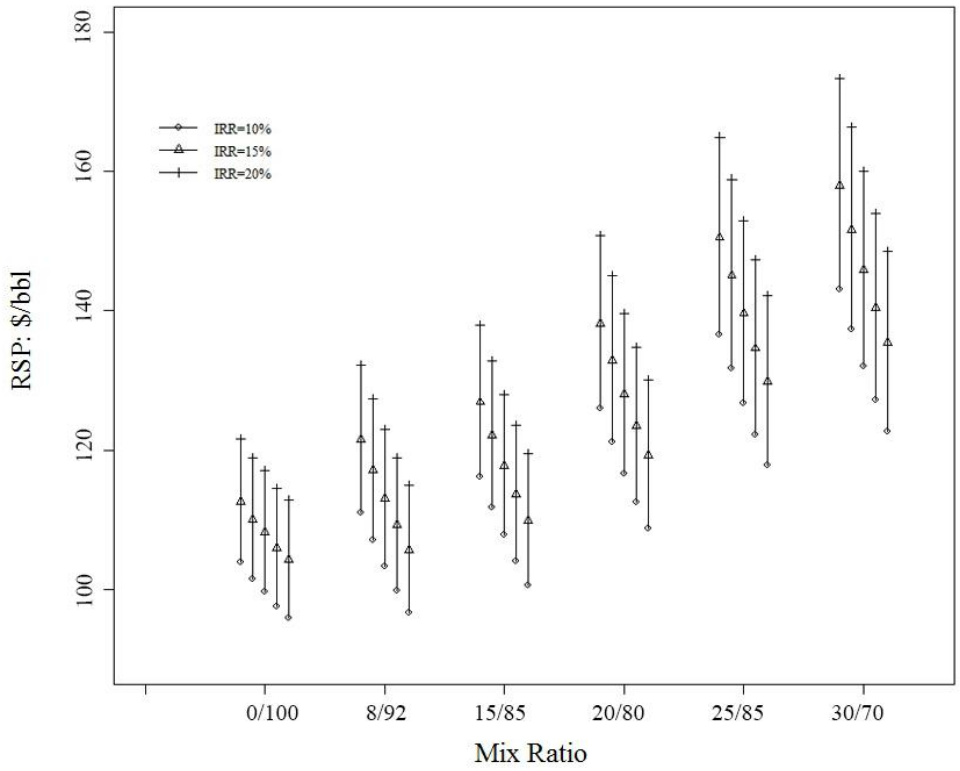

Figure 2-9. Change of RSP based on different IRR at different mix ratio and conversion rate.

Change of RSP based on different IRR were analyzed under different mix ratio and conversion rate (Figure 2-9). The IRR variations are 10%, 15% and 20%. When mix ratio is 0/100, namely no biomass used at the maximum conversion rate, the RSP was $104.3/bbl. For the base case (mix ratio 8/92), the prices keep the same. As more biomass was mixed with coal, the RSP was increasing. The highest RSP is $157.9/bbl which was observed at mix ratio 30/70 with the minimum conversion rate. RSP was more sensitive to the conversion rate of coal at low mix ratio. The RSP reduction was significantly subject to IRR reduction at high biomass ratio.

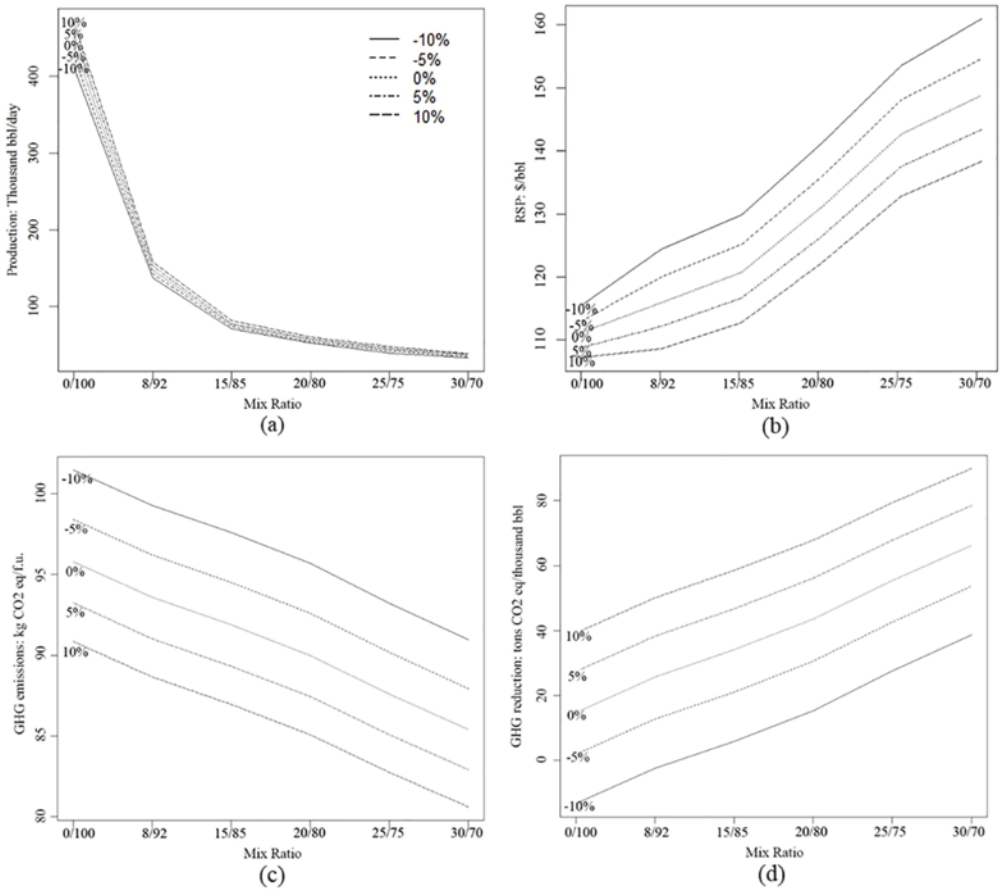

Figure 2-10. Sensitivity analyses by (a) conversion rate and biomass to coal mix ratio for CBTL fuel production in thousand bbl/day; (b) required selling price of CBTL fuels $/bbl; (c) GHG emission kg CO2 eq/f.u.; and (d) GHG reduction compared to petroleum derived diesel in thousand tons CO2 eq/thousand bbl.

CBTL fuel production was subject to sensitivity analysis with fluctuation of 10% (Figure 2-10). The production was decreasing when biomass ratio increased. Sensitivity analysis showed that the production trend was generally consistent with slightly changes observed. The RSP increased when biomass ration increased. The sensitivity analysis displayed that the increasing trends within 10% fluctuation were consistent. GHG emission became lower when biomass ratio increased. Provide fixed mix ratio, GHG emissions increased when conversion rate dropped. The demand of feedstock was also subject to mix ratio and conversion rate. As a result, transportation distance of feedstock was also under the influences of the two parameters. However, emissions caused by transportation was only a small portion in the whole life cycle of liquid fuels. Reduction of GHG was compared under the mix ratio and conversion rate variations. Higher mix ratio generally led to lower GHG emission. When compared to petroleum derived liquid fuels, CBTL could obtain GHG emission reduction between -2.7% to 16.2%. Analysis of 30 years total reduction in GHG emission showed that range from -162 to 555 million tons CO2 eq were obtained under conversion rate and mix ratio variations.

Explanation of Variance

- ✓ Nothing to report

References:

Wu, H., Mora-Pale, M., Miao, J., Doherty, T.V., Linhardt, R.J. and Dordick, J.S., 2011. Facile pretreatment of lignocellulosic biomass at high loadings in room temperature ionic liquids. Biotechnology and bioengineering, 108(12), pp.2865-2875.

Perlack, R.D., Eaton, L.M., Turhollow Jr, A.F., Langholtz, M.H., Brandt, C.C., Downing, M.E., Graham, R.L., Wright, L.L., Kavkewitz, J.M., Shamey, A.M. and Nelson, R.G., 2011. US billion-ton update: biomass supply for a bioenergy and bioproducts industry.

Wang, J., Grushecky, S. and McNeel, J., 2006. Biomass resources, uses, and opportunities in West Virginia. Biomaterials Center, West Virginia University, Morgantown.

Becker, D.R., Abbas, D., Halvorsen, K.E., Jakes, P.J., McCaffrey, S. and Moseley, C., 2009. Conventional wisdoms of woody biomass utilization.

Gan, L. and Yu, J., 2008. Bioenergy transition in rural China: Policy options and co-benefits. Energy Policy, 36(2), pp.531-540.

Hartley, D. S. Modeling and Optimization of Woody Biomass Harvest and Logistics in the Northeastern United States. WEST VIRGINIA UNIVERSITY, Morgantown, WV, 2014.

HMR Hardwood market report; Memphis, TN, 2011.

Hook, M.; Aleklett, K., A review on coal-to-liquid fuels and its coal consumption. International Journal of Energy Research 2010, 34, (10), 848-864.

Jiang, Y.; Bhattacharyya, D., Plant-wide modeling of an indirect coal-biomass to liquids (CBTL) plant with CO2 capture and storage (CCS). International Journal of Greenhouse Gas Control 2014, 31, 1-15.

Keesom, W.; Unnasch, S.; Moretta, J.; Consultancy, J., Life cycle assessment comparison of North American and imported crudes. Alberta Energy Research Institute: 2009.

Kerstetter, J. D.; Lyons, J. K., Logging and agricultural residue supply curves for the Pacific Northwest. Washington State University Energy Program: 2001.

Kumar, D.; Murthy, G. S., Life cycle assessment of energy and GHG emissions during ethanol production from grass straws using various pretreatment processes. International Journal of Life Cycle Assessment 2012, 17, (4), 388-401.

Jiang, Y. and Bhattacharyya D. Modeling and analysis of an indirect coal-biomass to liquids (CBTL) plant integrated with a combined cycle plant and CO2 capture and storage (CCS), Accepted by *Energy & Fuels*, 2015.

Liu, W. Economic and environmental analyses of biomass utilization for bioenergy products in the northeastern United States. West Virginia University: 2015.

Marano, J. J.; Ciferno, J. P., Life-cycle greenhouse-gas emissions inventory for Fischer-Tropsch fuels. Report Prepared for the US Department of Energy, Energy and Environmental Solution, LLC, Gaithersburg, MD, USA 2001.

Murray, A. T., Spatial restrictions in harvest scheduling. Forest Science 1999, 45, (1), 45-52.

Paul, A. D., A Fresh Look at Coal-Derived Liquid Fuels. Power 2009, 153, (1), 46-51.

Saud, P.; Wang, J. X.; Lin, W. S.; Sharma, B. D.; Hartley, D. S., A Life Cycle Analysis of Forest Carbon Balance and Carbon Emissions of Timber Harvesting in West Virginia. Wood and Fiber Science 2013, 45, (3), 250-267.

Sharma, B. D., Modeling of forest harvest scheduling and terrestrial carbon sequestration. West Virginia University: 2010.

Skone, T. J. Case Study: Interagency workgroup on life cycle GHG emissions of alternative aviation fuels; National Energy Technology Laboratory: Pittsburgh, PA, 2011.

Standardization, I. O. f., Environmental Management: Life Cycle Assessment: Principles and Framework. ISO: 2006; Vol. 14040.

Sultana, A.; Kumar, A.; Harfield, D., Development of agri-pellet production cost and optimum size. Bioresource Technology 2010, 101, (14), 5609-5621.

Su, H.; Fletcher, J. J. Carbon capture and storage in China: options for the Shenhua direct coal liquefaction plant. International Association for Energy Economics. Available online: http://citeseerx.ist.psu.edu/viewdoc/download?doi=10.1.1.600.1172&rep=rep1&type=pdf.

Tarka, T. J.; Wimer, J. G.; Balash, P. C.; Skone, T. J.; Kern, K. C.; Vargas, M. C.; Morreale, B. D.; White III, C. W.; Gray, D. In Affordable, low-carbon diesel fuel from domestic coal and biomass, Proc. 25th Annual Pittsburgh Coal Conf., Pittsburgh, PA, 2009.

Tennant, J. B. Overview of coal and coal-biomass to liquids (C&CBTL) program; National Energy Technology Laboratory: Morgantown, WV, 2014.

USGS Download land cover data. http://gapanalysis.usgs.gov/gaplandcover/data/download/ (June 4),

Van Bibber, L.; Thomas, C.; Chaney, R. Alaska coal gasification feasibility studies-Healy coal-to-liquids plant; National Energy Technology Laboratory (United States): 2007.

Wang, M., The GREET spreadsheet model: greenhouse gases and regulated emissions and energy use in transportation, Version 1.8 c. Center for Transportation Research, Energy Systems Division, Argonne National Laboratory 2009.

Wu, J.; Wang, J.; Strager, M. P., A Two-Stage GIS-Based Suitability Model for Siting Biomass-to-Biofuel Plants and its Application in West Virginia, USA. International Journal of Forest Engineering 2011, 22, (2), 28-38.

Wu, J. Z.; Wang, J. X.; Cheng, Q. Z.; DeVallance, D., Assessment of coal and biomass to liquid fuels in central Appalachia, USA. International Journal of Energy Research 2012, 36, (7), 856-870.

Task 3 Technical Feasibility

Summary:

Task 3.1 Development and Validation of the Process Models for Different Cases
- ✓ Conceptual design
- ✓ Process modeling
- ✓ Process model validation

Task 3.2 Equipment Design and Capital Costs
- ✓ Capital cost estimation
- ✓ Economic model validation

Task 3.3 Evaluation of Projects
- ✓ Material and energy balance (base case)
- ✓ Techno-economic analysis (base case)

Task 3.4 Sensitivity Studies
- ✓ Effect of key design parameters on the indirect CBTL plant performance
- ✓ Effect of key design and investment parameters on the indirect CBTL plant economic performance
- ✓ Effect of key design parameters on the direct CBTL plant performance
- ✓ Effect of key design and investment parameters on the direct CBTL plant economic performance
- ✓ Effect of plant configuration and summary of case studies

Research Products:

Publications

1) Jiang Y, Bhattacharyya D, Modeling of Direct Coal-Biomass to Liquids (CBTL) Plants with Shale Gas Utilization and CO_2 Capture and Storage (CCS), *Applied Energy*, 183, 1616-1663, 2016.
2) Jiang Y, Bhattacharyya D, Techno-Economic Analysis of a Novel Indirect Coal-Biomass to Liquids Plant Integrated with a Combined Cycle Plant and CO_2 Capture and Storage, *Industrial & Engineering Chemistry Research*, 55, 1677-1689, 2016.
3) Jiang Y, Bhattacharyya D, Modeling and Analysis of an Indirect Coal-Biomass to Liquids (CBTL) Plant Integrated with a Combined Cycle Plant and CO_2 Capture and Storage (CCS), *Energy & Fuels*, 29, 5434-5451, 2015.
4) Jiang Y, Bhattacharyya D, Plant-Wide Modeling of an Indirect Coal-Biomass to Liquids (CBTL) Plant with CO_2 Capture and Storage (CCS), *International Journal of Greenhouse Gas Control*, 31, 1-15, 2014.
5) Jiang Y, Bhattacharyya D, Techno-Economic Analysis of Direct Coal-Biomass to Liquids (CBTL) Plants with Shale Gas Utilization and CO_2 Capture and Storage (CCS), *submitted to Applied Energy*, 2016.

Presentations

1) Jiang Y, Bhattacharyya D, Modeling and Economic Analysis of Direct Coal-Biomass to Liquids (CBTL) Plant with Shale Gas Utilization and CO_2 Capture and Storage (CCS), Paper 564e, AICHE Annual Meeting, San Francisco, CA, USA, November 13-18, 2016.
2) Jiang Y, Bhattacharyya D, Techno-Economic Analysis of Indirect, Direct and Hybrid Coal-Biomass to Liquids (CBTL) Plant with CO_2 Capture and Storage (CCS), Paper 66c, AICHE Annual Meeting, San Francisco, CA, USA, November 13-18, 2016.
3) Jiang Y, Bhattacharyya D, Techno-Economic Study of an Indirect Coal-Biomass to Liquids (CBTL) Plant with CO_2 Capture and Storage (CCS), Paper 625d, AICHE Annual Meeting, Salt Lake City, UT, USA, November 8-13, 2015.
4) Jiang Y, Bhattacharyya D, Sustainable Engineering Economic and Profitability Analysis, Paper 668b, AICHE Annual Meeting, Salt Lake City, UT, USA, November 8-13, 2015.
5) Jiang Y, Bhattacharyya D, Techno-Economic Analysis of a Direct Coal-Biomass to Liquids (CBTL) Plant with CO_2 Capture and Storage (CCS), Paper 639f, Salt Lake City, UT, USA, November 8-13, 2015.
6) Jiang Y, Bhattacharyya D, Modeling of an Indirect Coal-Biomass to Liquids (CBTL) Plant with CO_2 Capture and Storage (CCS), Paper 249b, AIChE Annual Meeting, Atlanta, GA, November 16-21, 2014.
7) Jiang Y, Bhattacharyya D, Techno-Economic Analysis of a Novel Indirect Coal-Biomass to Liquids (CBTL) Plant Integrated with a Combined Cycle Plant and CO_2 Capture and Storage (CCS), Paper 366a, AIChE Annual Meeting, Atlanta, GA, November 16-21, 2014.
8) Jiang Y, Bhattacharyya D, Plant-Wide Modeling of an Indirect Coal-Biomass to Liquids (CBTL) Plant with CO_2 Capture and Utilization Integrated with a Combined Cycle Plant, Paper 410a, AIChE Annual Meeting, San Francisco, CA, November 3-8, 2013.

Task 3.1 Development and Validation of the Process Models for Different Cases

Planned Activities:

- ✓ **Conceptual design:** Block flow diagrams were generated for indirect, direct and hybrid CBTL plant with CCS.
- ✓ **Process modeling:** Plant-wide models were developed in Aspen Plus for different CBTL plants.
- ✓ **Process model validation:** The results generated from the process model are validated by comparing with the data available in the open literature.

Accomplishments:

- ✓ **Conceptual design**

Block flow diagrams (BFDs) of indirect, direct and hybrid CBTL plants are shown in Figures 3-1. The indirect CBTL plant with CCS (FT_CCS), as shown in Figure 3-1, can be divided into five units-syngas production, CO_2 capture and storage, syncrude production, product upgrading, and combined cycle units. In the syngas production unit, the syngas is first produced by co-gasification of coal and biomass and then shifted in the water gas shift (WGS) reactor to obtain the desired H_2/CO ratio for the Fischer-Tropsch (FT) unit. COS is converted to H_2S in the COS hydrolysis reactor. After selectively removing H_2S and a significant portion of CO_2 in the dual-stage Selexol process, the clean syngas is sent to the syncrude production unit. In the syncrude production unit, clean syngas is converted into syncrude and light hydrocarbons in a Fe-catalyzed slurry bed LTFT reactor. CO_2 produced in the FT reactor is removed in the post-FT CO_2 removal unit. A portion of the light gases from the FT reactors is sent to the hydrogen recovery unit using pressure swing adsorption (PSA) process to supply H_2 for the hydroprocessing units. The remaining portion is recycled back to the FT reactor through an autothermal reformer, where light hydrocarbons are converted into syngas. Heat recovered from the high temperature syngas is utilized in the combined cycle unit for steam and electricity production. Removed H_2S is sent to a Claus unit to be converted to elementary sulfur. Removed CO_2 are vented if not considering CCS or sent to a CO_2 compression unit if considering CCS.

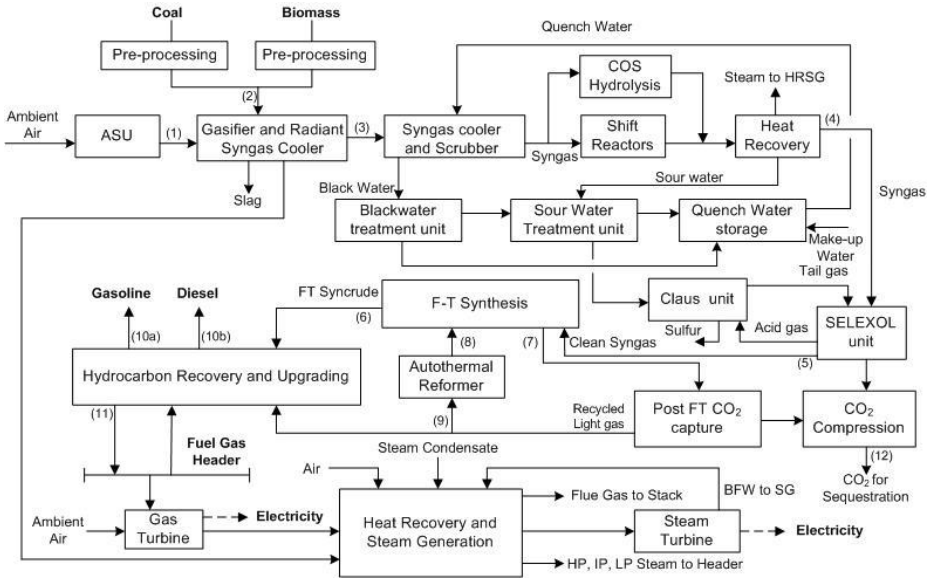

Figure 3-1. BFD of the indirect CBTL plant with CCS (FT_CCS).

Direct liquefaction technology is the core technology of the direct CBTL processes as shown in Figure 3-2 and 3-3. Coal and biomass with a low biomass/coal ratio are mixed with recycled oil in the slurry tank, and then pressurized and preheated before being fed to the catalytic two-stage liquefaction (CTSL) reactors with make-up and recycled H_2 to be liquefied and converted to syncrude. The product from the second liquefaction reactor is sent to a hot HP separator. The vapor product from the hot HP separator is then sent to the inline hydrotreater for stabilization. The hydrotreated liquids from the inline hydrotreater and the liquid product from the hot separator are sent to the hydrocarbon recovery and solid/liquid separation unit to be separated into H_2-rich gases, light gases (C_1- C_4), light naphtha (C_5, C_6), heavy naphtha (C_7-177^{o}C), distillate/gas oil (177-376^{o}C), solvent oil (376-524^{o}C) and liquefaction residues (more than 524^{o}C). H_2-rich gases and solvent oil are recycled back to the CTSL unit. Part of the light gases is used in the process furnaces, while the remaining is sent to the power island for electricity generation. Naphtha and gas oil are sent to the product upgrading unit for generating on-spec gasoline and diesel as main products. The liquefaction residue is sent to the POX unit for H_2 production.

Because considerable amount of H_2 is consumed in the CTSL unit, hydrogen production is also critical for the direct CBTL plants. Considering different H_2 sources and CO_2 control targets, four different configurations are considered in our study. In the SMR_CCS and SMR_VT processes as shown in Figure 3-2, part of the required H_2 is generated from liquefaction residue partial oxidation, while the remaining is generated by shale gas steam reforming. Alternatively, the required H_2 is supplied from coal/biomass/liquefaction residue co-gasification. In the CG_CCS and CG_VT processes as shown in Figure 3-3, pre-processed coal and biomass are fed to the liquefaction unit and the POX unit along with the liquefaction residues, while other blocks remain the same as the SMR_CCS and SMR_VT processes. In all configurations, the syngas from the POX/CG unit and/or the SMR unit is sent to the acid gas removal (AGR) unit for CO_2 and H_2S removal, and then to PSA unit for H_2 purification. Three different CO_2 capture technologies are considered for the AGR unit- Selexol, monoethanolamine (MEA), piperazine- activated methyl diethanolamine (MDEA/PZ). H_2S produced in the POX/CG unit via gasification is removed in the

H_2S absorber of the dual-stage Selexol unit, while H_2S produced in the liquefaction and hydrotreating units is removed by chemical absorption using MDEA as solvent. The removed H_2S is then sent to the Claus unit to be recovered as elemental sulfur. In the SMR_VT and CG_VT processes, CO_2 captured from the syngas is directly vented to the atmosphere. In the SMR_CCS and CG_CCS processes considering high extent of CCS, part of the flue gas produced from the gas turbine or process furnaces also needs to be sent to the AGR unit for post-combustion CO_2 removal, and all CO_2 streams from the AGR unit are sent to the CO_2 compression section for sequestration.

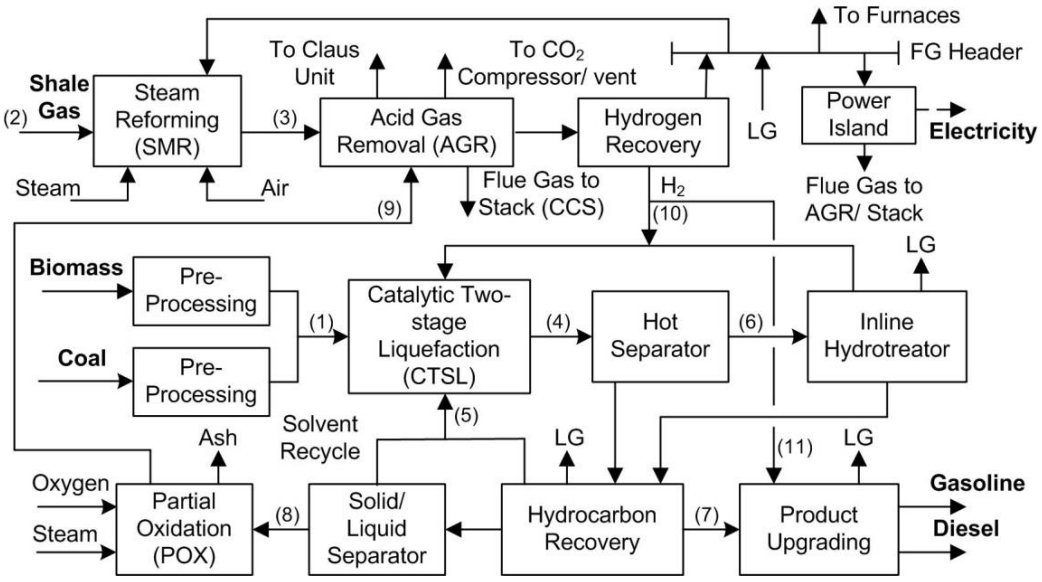

Figure 3-2. BFD of the direct CBTL plant with H_2 from shale gas (SMR_CCS/SMR_VT).

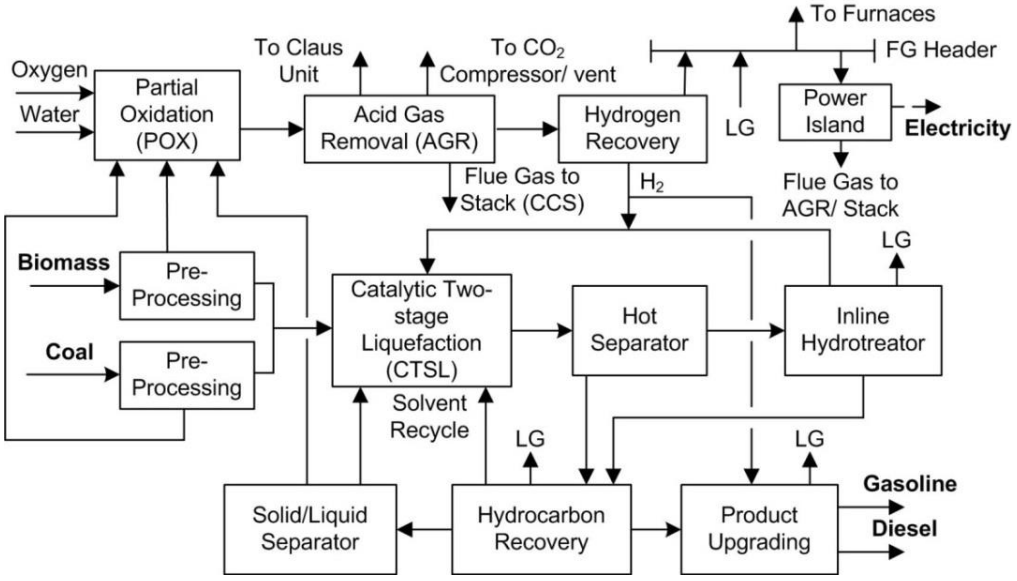

Figure 3-3. BFD of the direct CBTL plant with H_2 from coal and biomass (CG_CCS/CG_VT).

Direct and indirect CBTL plants share a large number of common unit operations, such as coal and biomass pre-processing, gasification unit for producing syngas, AGR, and Claus unit for sulfur recovery. The raw syncrude from direct liquefaction plants using CTSL contains predominantly aromatics and naphthenes with high level heteroatoms. The raw syncrude from indirect liquefaction plants using slurry FT reactors contains predominantly olefins and paraffinic with negligible heteroatoms. Thus, in the hybrid CBTL plants, the raw syncrudes from direct and indirect liquefaction plants have the potential to produce on-spec fuels simply by proper blending by significantly reducing severity and amount of upgrading. The BFD of the hybrid CBTL plant with CCS is shown in Figure 3-4 and 3-5. In the process without shale gas utilization, pre-processed coal and biomass are fed to either the gasification unit to produce syngas or the CTSL unit to produce syncrude directly. After the H_2/CO ratio is adjusted by WGS reactors, syngas is either sent to the hydrogen recovery unit or to the FT synthesis reactors. The split ratio of coal and biomass is determined by the specified direct and indirect syncrude blending ratio. It is noticed that, hydrogen can be produced from shale gas steam reforming instead of co-gasification with less cost and higher efficiency in the hybrid processes, as shown in Figure 3-5. If shale gas utilization is considered, all syngas produced from the gasification unit is sent to the FT synthesis unit, while all syngas produced from the shale gas steam reforming unit is sent to the hydrogen recovery unit.

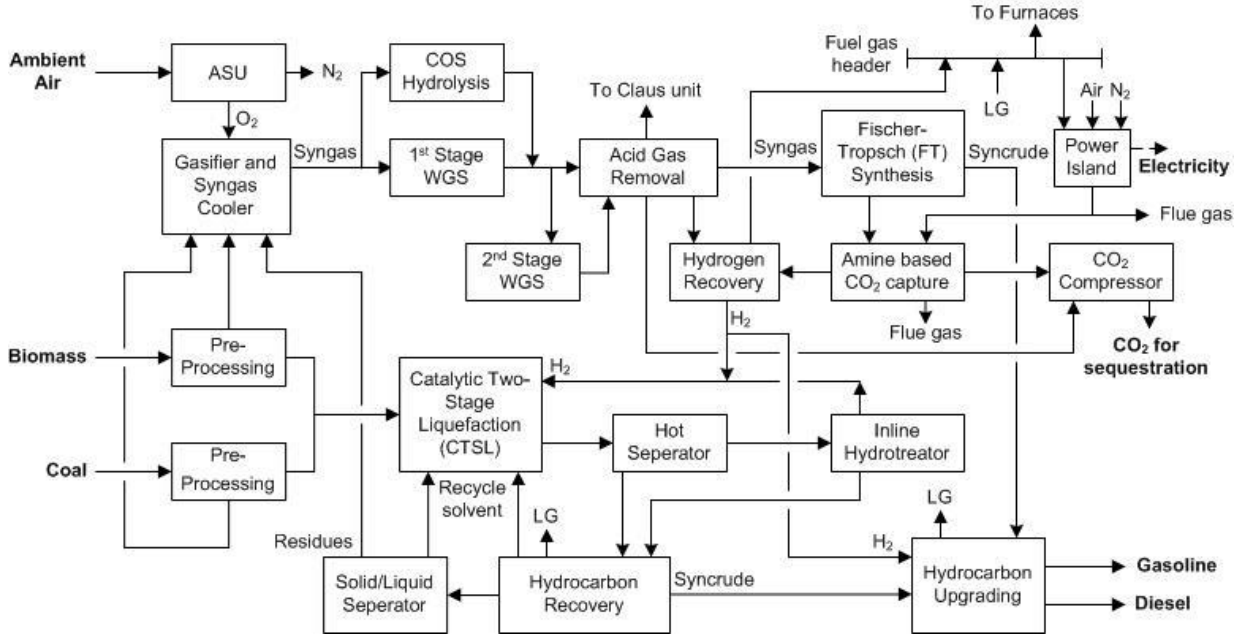

Figure 3-4. BFD of the hybrid CBTL plant with CCS (HCG_CCS).

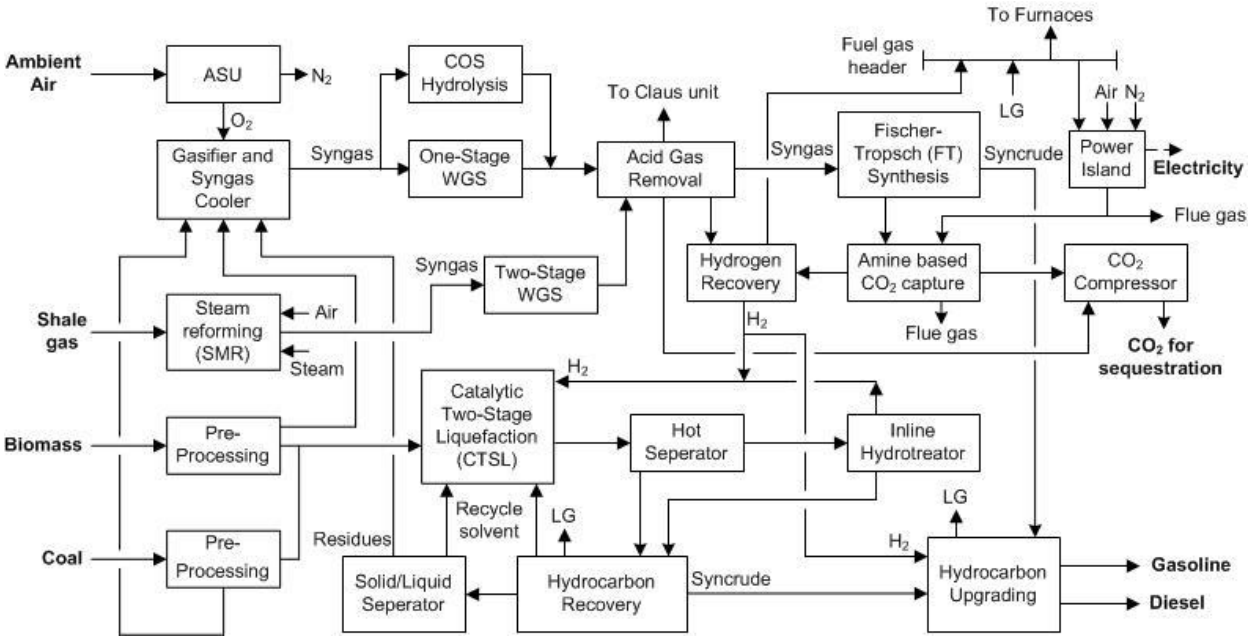

Figure 3-5. BFD of the modified hybrid CBTL plant with CCS (HSMR_CCS).

Process modeling

In this section, the steady-state modeling approach of the CBTL plants is discussed. Most of the unit operations are modeled as standard equipment in Aspen Plus, while yield models are developed in Excel for liquefaction reactors and upgrading units based on the experimental or operational data available in the open literature. Aspen User2 blocks are used to connect Excel with Aspen Plus. In the process model, coal and biomass are specified as unconventional component, while syncrude are specified as either pseudo-components or petroleum assays defined by boiling point ranges. The compositions of Illinois No.6 coal, wood chip, bagasse, torrefied wood and Marcellus shale gas are given in Table 3-1 and Table 3-2 (Jiang and Bhattacharyya, 2015; 2016; Ibrahim et al., 2013).

Table 3-1 Proximate and ultimate analysis of coal and biomass feedstock.

	Proximate analysis (dry basis)				Ultimate analysis (dry basis)					
	M	FC	VM	A	A	C	H	N	S	O
Coal	3.08	50.65	37.85	11.50	11.50	71.00	4.80	1.40	3.20	8.00
Wood chip	9.58	16.55	82.51	0.94	0.94	48.51	6.17	0.12	0.04	44.22
Bagasse	10.60	14.80	82.10	3.10	3.10	47.90	6.20	0.60	0.01	42.19
Torrefied wood	3.80	70.85	27.55	1.60	1.60	58.40	5.70	0.08	0.02	35.80

Table 3-2 Composition of Marcellus shale gas (well 3).

Component	C_1	C_2	C_3	CO_2	N_2
vol%	83.8	12.0	3.0	0.9	0.2

Gasification unit

The gasification unit, as shown in Figure 3-6, is a common section in the indirect, direct and hybrid CBTL plant. In the indirect process (FT_CCS), coal and biomass is co-fed into the gasifier. In the direct process (SMR_CCS), only the hot liquefaction residue from the ROSE-SR unit is gasified in the gasifier. In the direct process without shale gas utilization (CG_CCS) and the hybrid process (HSMR_CCS/HCG_CCS), mixture of coal biomass and residue is fed into the gasifier. In the gasification unit, solid fuel is fed into gasifier along with oxygen from ASU and slurry water. The raw syngas from the gasifier is cooled by heat recovery and then sent to the one-stage or two-stage WGS reactors to adjust H_2/CO ratio.

The co-gasifier is simulated by combining a reactor model for coal or residue gasification based on minimization of the Gibbs free energy with a yield model for biomass gasification, with the assumption that the interaction between coal and biomass is negligible due to the low biomass to coal ratio and the yield of the co-gasifier is a linear combination of these two model. This assumption is consistent with experiment done by Andre (Andre et al., 2005), which shows an approximate linear correlation between syngas composition and biomass to coal ratio. The reactor model for coal gasification has been developed by considering restricted equilibrium and has been reported by our group previously (Bhattacharyya, et al., 2011) since the WGS reaction catalyzed by the ash as well as the uncatalyzed WGS reaction continue till the reaction is quenched. (Kasule et al., 2012)

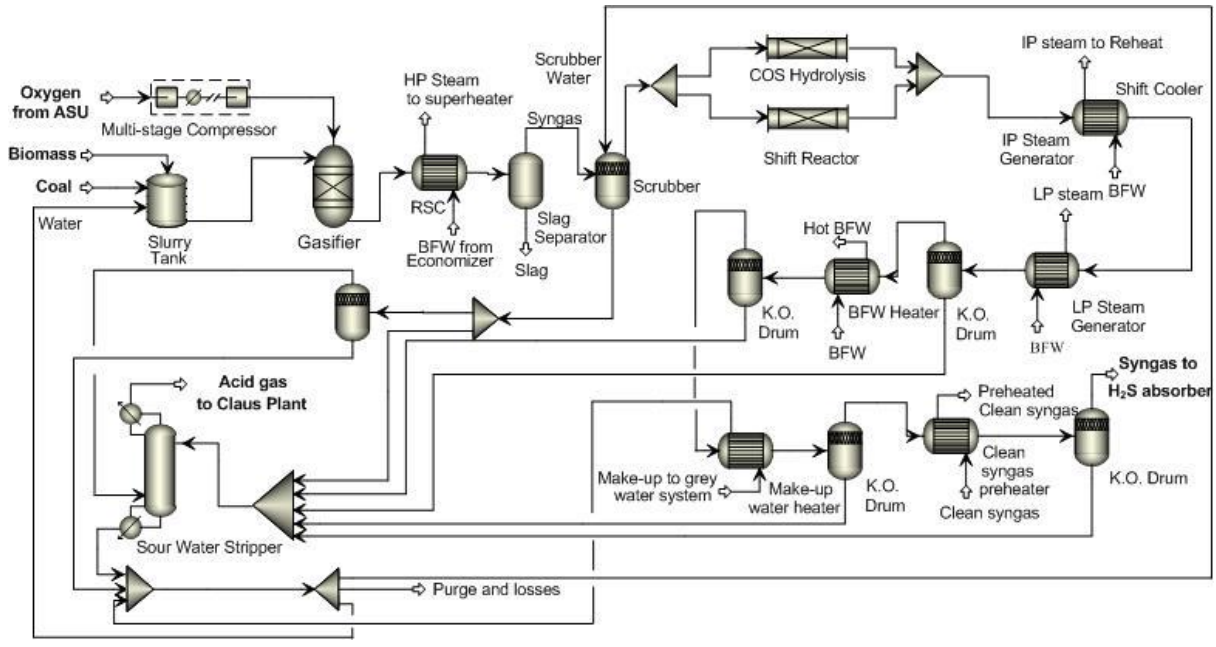

Figure 3-6. Configuration of the syngas production section and water treatment units.

The yield of each species for biomass gasification is generated by the following correlation, $y = A + BT + CT^2$, that has been developed for the fluidized bed IGT gasifier. (Bain, 1992) In the work of Bain, the values of the parameters *A*, *B*, and *C* have been determined from the regression analysis of the experimental data available for a biomass gasifier operating between 754-982 ^{o}C at

2300 kPa. In this work, for satisfying the elemental balance the MGAS model of Syamlal and Bisset (Kasule et al., 2012; Syamlal and Bisset, 1992) is used to obtain the final yield of major gas components from the proximate and ultimate assays, tar and char compositions, and preliminary prediction of product distribution from temperature correlation shown above. Table 3-3 compares the results from our model for biomass gasification with the experimental data (Bain, 1992) obtained at 830 °C. As seen in Table 3-3, the model is satisfactory.

Table 3-3 Model validation for biomass gasification.

Gas (mol%)	Experimental	Our Model	error%
CO	8.73	9.26	-6.14
CO_2	21.31	20.35	4.50
CH_4	8.41	7.69	8.56
H_2	17.07	15.91	6.77
H_2O	43.20	45.72	-5.82
NH_3	0.48	0.48	0

The syngas from the gasifier goes to the radiant syngas cooler (RSC) to generate high pressure (HP) steam, which can be sent to the heat recovery steam generation (HRSG) section for superheating for power generation. As shown in Figure 3-6, syngas is then sent to the scrubber where quench water is used to decrease the temperature of the syngas to the desired value. (Bhattacharyya et al., 2011) After scrubbing, a portion of the syngas enters an adiabatic sour WGS reactor, while the remaining portion enters a COS hydrolysis unit in the indirect and hybrid CBTL processes. The reversible WGS reaction is shown in Reaction 1 with the kinetics given by Eq. (2) for a cobalt molybdenum-based catalyst, which is a sour shift catalyst. (Bhattacharyya et al., 2011; Overstreet, 1974; Berispek, 1975) The equilibrium constant is given by Eq. (3) (Bhattacharyya et al, 2011). The WGS reactor is modeled as an adiabatic plug flow reactor (PFR) in ASPEN Plus.

$$CO + H_2O \leftrightarrow CO_2 + H_2 \quad (1)$$

$$-r_f = 2.6 \times 10^4 \exp\left(-\frac{E_f}{RT}\right)[CO]\frac{kmol}{m^3 s} \quad (2)$$

$$K_{eq} = \exp(-4.33 + \frac{8240}{T}) \quad for\ 1060 \le T \le 1360 \quad (3)$$

Where $E_f = 53127$ kJ/kmol, CO in kmol/m^3 , and T in °R.

The Langmuir-Hinshelwood Hougen-Watson (LHHW) kinetics, Eq (5), is used to simulate the COS hydrolysis reaction shown in Reaction 4. The kinetics captures the inhibiting effect of water and the adsorption or the surface reaction of COS being the rate-determining step, which gives good agreement between the experimental and simulation results. (Williams et al., 1999) The kinetic parameters are obtained from the open literature. (Svoronos and Bruno, 2002; Williams et al., 1999) A design spec is used in Aspen Plus to manipulate the split fraction of the syngas sent to the WGS reactor to obtain the desired H_2/CO ratio.

$$COS + H_2O \rightarrow CO_2 + H_2S \quad (4)$$

$$r = \frac{kP_{COS}}{1+KP_{H_2O}} \quad (5)$$

Where $k = 6.4322\exp\left[\frac{11,144}{R}\left(\frac{1}{T} - \frac{1}{373.73}\right)\right]$, $K = 1.3 \times 10^{-7}\exp\left(\frac{10010}{T}\right)$, T in K, P in kPa, r in kmol/kg-hr.

The syngas from the WGS and the COS hydrolysis reactors is combined and then sent to the heat recovery section where a series of heat exchangers is used to cool down the syngas by generating intermediate pressure (IP) steam, low temperature (LP) steam and heating boiler feed water (BFW). The hot side outlet temperatures of the IP steam generator, the LP steam generator and the BFW heater are set to 191 ^{o}C, 138 ^{o}C, and 121 ^{o}C, respectively. The condensate from the heat recovery section contains very high amount of NH_3 and is sent to a sour water stripper (SWS). The NH_3-rich gas from the SWS is sent to the Claus furnace while the clean water from the bottom of the SWS is recycled to the gasification section. The SWS column is simulated in ASPEN Plus by using 'RadFrac' block. For the thermodynamic model, 'ELECNRTL' is used for liquid phase and 'SRK' is used for the vapor phase.

In the direct liquefaction processes without shale gas utilization, the hot liquefaction residue from the ROSE-SR unit is gasified and converted to H_2-rich syngas in two stage WGS reactors as shown in Figure 3-7. The residue contains mainly 510 ^{o}C plus solid, ash and unconverted coal/biomass. The entrained-flow gasifier fed only with the liquefaction residue is operated at 56 bar and 1315 ^{o}C with a steam to residue ratio of 0.4 and a carbon conversion of 99% similar to the data available in the experimental data in the open literature. (Texaco, 1984; Robin, 1977; Robin, 1976; Penner, 1980; Debyshire, 1984; Gao, 2014) The amount of oxygen fed into the gasifier is manipulated to satisfy the energy balance. The simulation result of the residue gasification shows that the H_2 yield of the POX unit is about 10.2 wt% of the liquefaction residue. (Comolli et al., 1995; Texaco, 1984)

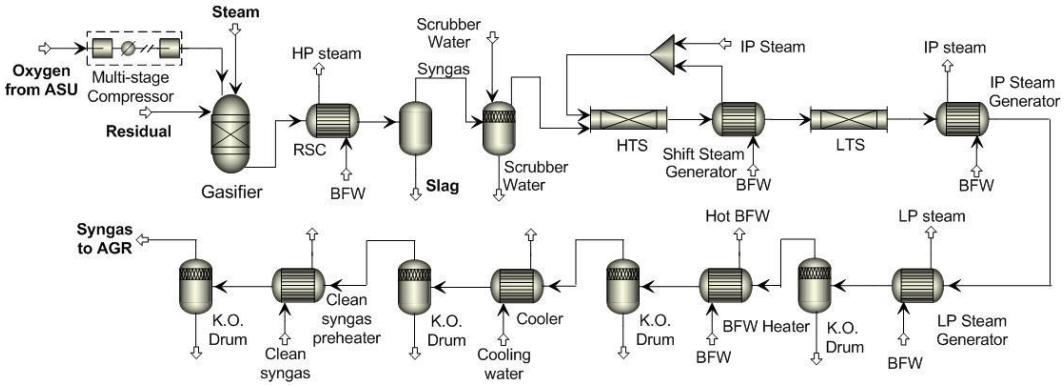

Figure 3-7. Plant configuration of the POX unit.

Selexol unit

In this work, the dual-stage Selexol unit, as shown in Figure 3-8, is used for selectively removing H_2S in the first stage followed by removal of bulk CO_2 in the second stage from the high pressure sour syngas from the gasification unit by using dimethylether of polyethylene glycol (DEPG) as the solvent. (Bhattacharyya et al., 2011) This configuration is similar to the work of Bhattacharyya et al. The tail gas from the Claus unit is recycled to the first stage of the H_2S absorber. The off-gas from the top of the H_2S absorber is sent to the CO_2 absorber. A portion of the loaded solvent from the CO_2 absorber is sent to the H_2S absorber. The remaining portion of the loaded solvent is heated and sent to a series of flash vessels to recover H_2 and flash off CO_2. The CO_2 is flashed off in a series of three separators operating at decreasing pressure levels. The semi-lean solvent from the last separator is cooled by exchanging heat with the loaded solvent and then chilled to 2^{o}C using NH_3 as the refrigerant before returning it to the CO_2 absorber. The flow rate of the refrigerant in the vapor-compression cycle is determined by a design specification considering a minimum temperature approach of 5.5 ^{o}C. Equilibrium stage models are developed for all the columns by using the RadFrac block in Aspen Plus. The PC-SAFT EOS is used for calculating the thermodynamic properties. (Bhattacharyya et al., 2011) Detailed information on the modeling approach of the AGR unit for the IGCC power plant can be found in Bhattacharyya et al. (Bhattacharyya et al., 2011) Due to the considerable difference in the operating pressure of the gasifier between the IGCC power plant and CBTL plant, the operating pressure of the AGR unit in this work is different than the previous work. (Bhattacharyya et al., 2011) The operating pressures of the main equipment are summarized in Section 3.4 Table 3-7. The solvent circulation rate in the AGR unit as part of the CBTL plant is expected to be higher, because of the lower CO_2 partial pressure in the CBTL plant than that in the IGCC plant. The solvent circulation rate is manipulated by a 'design spec' in Aspen Plus to desired extent of CO_2 capture.

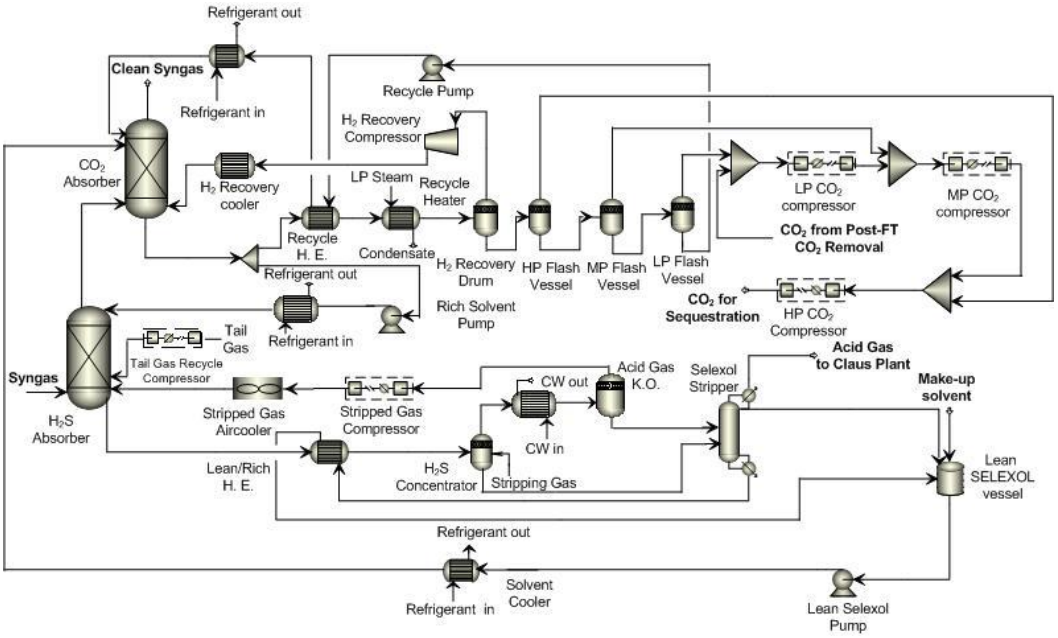

Figure 3-8. Configuration of the Selexol unit and the CO_2 compression section.

It is noted that, the single stage Selexol unit, as shown in Figure 3-9, can be used to treat high pressure syngas without H_2S, i.e. syngas from SMR unit or FT vapor product. In the indirect CBTL plant, the single-stage Selexol technology is considered here as a potential technology to remove CO_2 from the FT product due to its low utility consumption of the downstream CO_2 compression. The drawback of the Selexol technology is hydrocarbon loss. Hydrocarbon loss and utility saving for Selexol are compared with the previous two chemical solvents. The modeling approach is similar to that mentioned in Section 2.4. The rich solvent from the bottom of the absorber is sent to a H_2 recovery vessel to recover 70% of H_2 and then to a series of flash vessels to remove CO_2 from the solvent. Lean solvent out of the flash vessel again is chilled and sent back to the absorber. The temperature of the chilled lean solvent is 2 ^oC, and the operating pressure of the absorber is 1965 kPa. The percentage of CO_2 captured is set to be 93% in this case. It can be noted that the extent of CO_2 capture is lower than the chemical solvents due to the relatively low operating pressure of the post-FT CO_2 capture unit that limits the extent capture for the physical solvent.

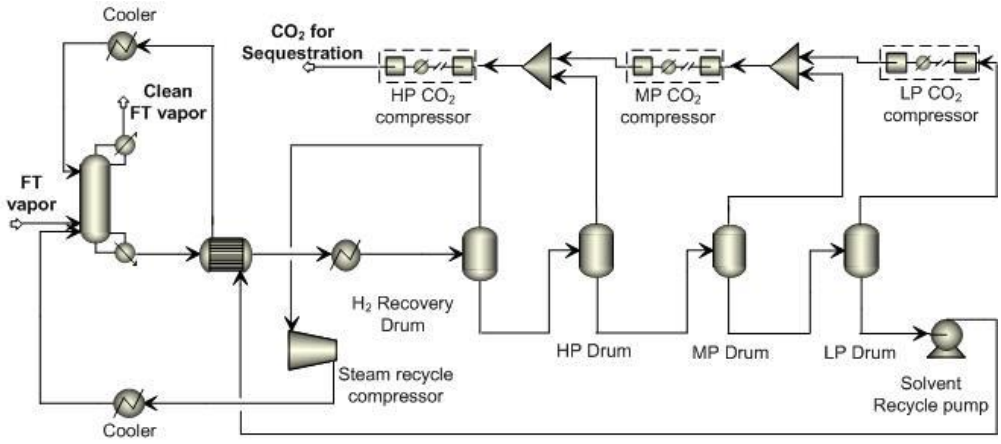

Figure 3-9. Configuration of the single-stage Selexol unit.

Claus unit

The Claus unit is a gas desulfurizing process recovering elemental sulfur from the acid gas stream generated from the gasifier and the SWS column in all CBTL plants. It includes one thermal stage and two catalytic stages. More details about this unit can be found in the work of Bhattacharyya et al. and the plant configuration is shown in Figure 3-10. (Bhattacharyya et al., 2011)

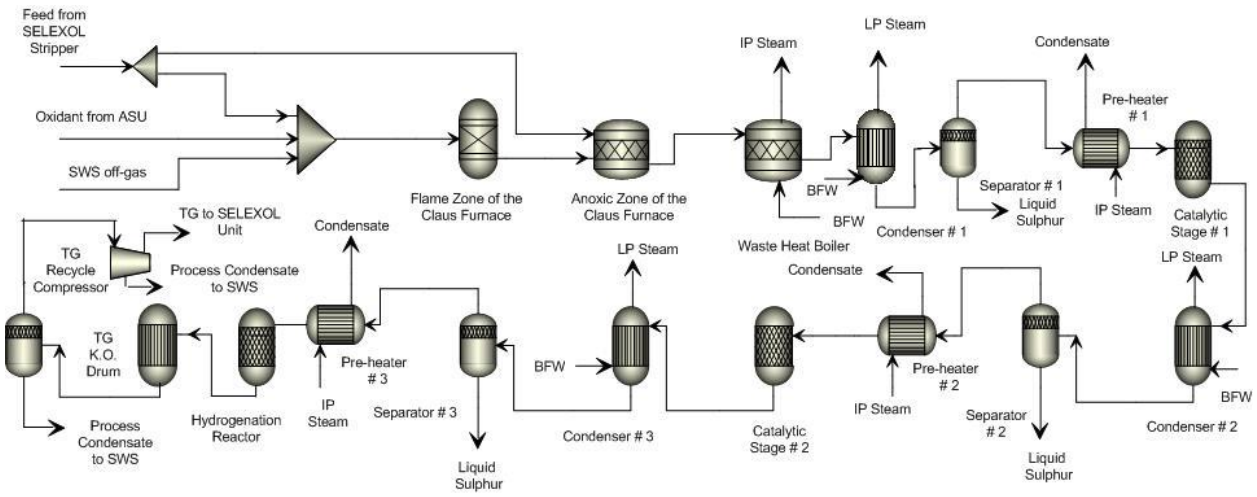

Figure 3-10. Configuration of the Claus Unit.

Fischer-Tropsch synthesis

In FT synthesis unit is the core section of the indirect CBTL plant to convert syngas into syncrude. The model of the FT Synthesis section has been developed in Excel and connected to Aspen Plus via a User2 block, where total mass and atom conservations are satisfied by using a VBA solver code. As mentioned before, a Fe-catalyzed slurry phase low temperature FT (LTFT) technology is considered in this study because of its high efficiency and flexibility. It has been reported that the capital cost of a slurry reactor is only 25% of a multi-tubular system. The slurry reactor has also lesser temperature gradient resulting in higher conversion. The on-line removal and addition of catalyst also allows longer reactor runs for slurry reactor. (Dry, 2002; Espinoza, et al., 1999) In the Fe-catalyzed slurry phase FT reactors, following main reactions take place.

$$\mathrm{CO} + 2\mathrm{H}_2 \rightarrow -(\mathrm{CH}_2) - + \mathrm{H}_2\mathrm{O} \qquad (6a)$$

$$H_2O + CO \rightarrow CO_2 + H_2 \qquad (6b)$$

A yield model is developed for obtaining the product distributions of a LTFT reactor based on the information available in the open literature. (Bechtel, 1992a; Kuo, 1985; Kuo, 1983; Fox and Tam, 1995; Bechtel, 1990) Anderson-Schulz-Flory (ASF) theory is often used to estimate the FT product distribution. As increasing wax yield is the key objective of LTFT process, the wax selectivity (S_{wax}, wt%) is often used as the indicator to calculate the ASF parameters. (Dry, 2002; Bechtel, 1992a) The correlations for wax yield vs. operating conditions were reported in the open literature. (Bechtel, 1992a; Kuo, 1985; Bechtel, 1998) It is modified in this study to generate more accurate estimations of the FT product distribution from operating temperature (*T*), pressure (*P*) and superficial velocity (*S.V.*) in the low operating temperature range shown in Eq. (7) and Eq. (8). The coefficients determined via linear regression of 12 sets of experimental data obtained from the Mobil's pilot plant data (Kuo, 1985) are as follows: *a=-0.1306, b=121.0773, c=271.6, d=-112.21*, where all the terms are in SI unit. The selectivity of CO_2 is calculated by WGS ratio (K_{WGS}) defined in Eq. (9), with a value of 2.69 for LTFT reactors when a low CO_2 -selective Fe-based catalyst is used. (Fox and Tam, 1995; Bai et al., 2002)

$$S_{wax} = aT + \frac{bP}{S.V.} \quad (7)$$

$$\text{Syngas Conversion } (\%) = c\left(\frac{k \cdot P}{S.V.}\right) + d \qquad \text{where } k = \exp\left(-\frac{100}{RT}\right) \quad (8)$$

$$K_{WGS} = \frac{(H_2)(CO_2)}{(H_2O)(CO)} \quad (9)$$

$$S_{wax} = 33.6 + \frac{13.1}{H_2/CO} \quad (10)$$

Because the H_2/CO ratio in the syngas has a strong effect on the product distribution from the FT process, another correlation is developed to estimate the wax selectivity at different inlet H_2/CO ratios at a constant temperature, shown in Eq. (10). It has been reported that the slurry reactors tend to produce more wax than the fixed bed reactors with Fe-based catalysts at similar operating conditions, the product selectivity of the fixed bed reactors is more sensitive to H_2/CO ratio in comparison to the slurry bed reactors, and the wax selectivity could be correlated to the inlet H_2/CO ratio. (Jager and Espinoza, 1995; Dry, 1981; Espinoza and Steynberg, 1999; Steynberg and Dry, 2004) For regressing the parameters *a* and *b* in Eq. (10), experimental data for wax selectivity in slurry bed reactors due to changes in the H_2/CO ratio are needed. However, there are very few experimental data in the open literature for wax selectivity in the Fe-catalyst based LTFT reactors for low H_2/CO ratio. (Kuo, 1985; Kuo, 1983) Therefore, it was decided to regress the parameters with the data for low H_2/CO ratio, extrapolate the correlation for high H_2/CO ratio, and compare with the data available for the fixed bed reactors at high H_2/CO ratio to see if the trends are similar. Figure 3-11 shows that the trend of wax selectivity estimated by the correlation for the slurry bed reactors is similar to that for the fixed bed reactors. It should be noted that the wax selectivity for the fixed bed reactor has been reported by Dry. (Dry, 2002; Steynberg and Dry, 2004)

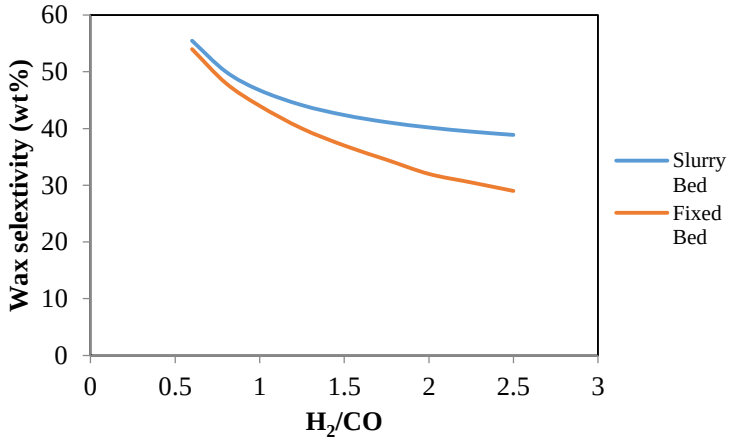

Figure 3-11. Effect of syngas composition on wax selectivity.

By using the calculated wax yield, the chain growth probabilities (α) in the ASF theory can be calculated by the polynomial $\alpha - S_{wax}$ correlations shown in Eq. (11a) – (11c). (Bechtel, 1992a) Then Eq. (11 d) – (11f) are used for predicting the carbon number distribution in the hydrocarbon products. In these equations, W_n denotes the weight fraction of hydrocarbon with n carbon atoms

and *M* is the methane factor, which is applied for methane selectivity estimation and defined as the actual methane yield divided by what would be predicted from the observed value of α_2. (Fox and Tam, 1995) This model has been proven to match the LTFT experimental data. (Bechtel, 1992a) Triple values of α are used to explain the high methane yield and change in the chain growth probability at certain point due to the vapor-liquid equilibrium in the reactor, which cannot be accounted for by the conversional single α value method. The two break point is set to be n_1=1, and n_2=21. It should be noted that n_2 is also set to be the starting carbon number for wax.

$$S_{wax} = 1401-4427(\alpha_2) + 3375(\alpha_2)^2 \quad (11a)$$

$$S_{wax} = -36687 + 125834(\alpha_3) + 1439067(\alpha_3)^2 \ + 54888(\alpha_3)^3 \quad (11b)$$

$$M = \frac{(1-\alpha_1)^2}{(1-\alpha_2)^2} = 6.413 - 0.0580(S_{wax}) + 0.00165(S_{wax})^2 + 7.986 \times 10^{-6}(S_{wax})^3 \quad (11c)$$

$$W_1 = (1-\alpha_1)^2 x \quad (11d)$$

$$W_n = n(1-\alpha_2)^2 \alpha_2^{n-1} y \qquad n = 2,3,4,\dots,20 \quad (11e)$$

$$W_n = n(1-\alpha_3)^2 \alpha_3^{n-1} z \qquad n = 21,22,\dots \quad (11f)$$

where x, y, z are given by:

$$x/y = \alpha_2/(M\alpha_1)$$

$$z/y = [(1-\alpha_2)^2\alpha_2^{20}]/[(1-\alpha_3)^2\alpha_3^{20}]$$

$$y = 1/(\sum_{n=2}^{20} W_n + \sum_{n=21}^{\infty} W_n\, z/y + W_1\, x/y)$$

For the same carbon number, components in the FT liquid are not only normal paraffin, but also olefin, and oxygenates. (Kuo, 1985) The olefin components have to be hydrotreated before sending them to the upgrading blocks. Since the olefin content in the FT crude can be high, the olefins fraction γ is an important variable that should be satisfactorily estimated. The olefins fraction will decrease with an increase in the carbon number, and the value finally settles down to 0.7 when the carbon number is larger than 6. (Fox and Tam, 1995) Table 3-4 lists the typical value of γ obtained experimentally. (Kuo, 1985)

Table 3-4. Olefins fraction versus carbon number in FT hydrocarbons (Kuo, 1985).

C_n	2	3	4	5	6	7+
olefins%	0.72	0.82	0.72	0.72	0.72	0.7

The wax obtained from the FT reactor can be treated as a single lumped C_{20+} wax pseudo component. From the modified ASF theory, the average carbon number of the C_{20+} wax can be calculated using the following equation (Fox and Tam, 1995):

$$C_{avg} = n + \alpha_3/(1-\alpha_3) \tag{12}$$

Besides alkenes, oxygenates produced at the FT reaction also need to be hydrogenated for stability of final products. Hence, it is also important to predict the oxygenate yield correctly. The total oxygenate yield in our model is obtained by using a polynomial correlation, given by Eq. (13), published in the open literature (Bechtel, 1992a; Fox and Tam, 1995). The species distributions for oxygenates are the average value of the reported pilot data. (Kuo, 1983; Kuo, 1985) It can be noted that the species distributions for oxygenates are not strong function of operating condition. (Bechtel, 1992a; Kuo, 1983; Kuo, 1985)

$$S_{OxyV} = 0.39 \tag{13a}$$

$$S_{OxyW} = 1.128(S_{wax}) + 0.05558(S_{wax})^2 \tag{13b}$$

$$S_{OxyHC} = 1.351(S_{wax}) + 0.1331(S_{wax})^2 + 0.1105(S_{wax})^3 \tag{13c}$$

Where $S_{OxyV}, S_{OxyW}, S_{OxyHC}$ denote oxygenate weight percent in vapor, water, and oil phase.

16 sets of experimental data from Run 256-7 conducted by Mobil in 1985 (Kuo, 1985) are used for validating the model at several different operating conditions. Figure 3-12 shows a comparison, between the results of the modified model and the experimental data to check the model accuracy, where HC and Oxy denote hydrocarbons (no including wax), and oxygenates, respectively.

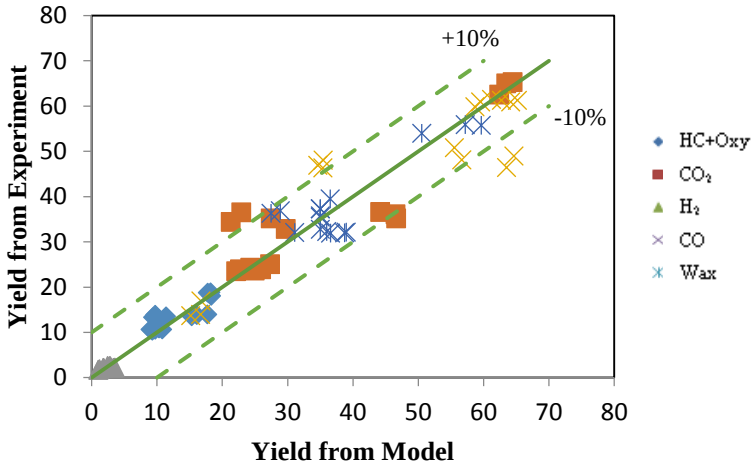

Figure 3-12. Comparison between the model results and experimental data.

Amine-based acid gas removal

Amine-based AGR technology is applied to all CBTL processes to remove CO_2 from medium or low pressure stream, when necessary. In the indirect CBTL plant, the products from the FT reactor, especially when Fe-based FT catalyst is used, can contain high amount of CO_2 that must be removed. In this study, we have considered CCS where the captured CO_2 is sent to the CO_2 compression unit for sequestration. Solvent-based and other technologies, such as high concentration MEA, inhibited MDEA, Benfield hot K_2CO_3, Rectisol, Ryan-Holmes cryogenic distillation, membrane, and PSA, have been compared by Bechtel for post-FT CO_2 removal. (Bechtel, 1992b) It was observed that the chemical absorption and the Ryan-Holmes process were the most likely candidates for FT application because of very little loss of valuable components, such as H_2, CO and light hydrocarbons. The chemical absorption process was selected for the baseline design instead of the Ryan-Homes process because of its lower capital cost. (Bechtel, 1992b) The inhibited MDEA is preferred over the MEA process because of its less corrosiveness and about 13.8% lesser steam consumption. (Bechtel, 1992b)

In direct CBTL plants, the fuel gas released from the liquefaction, product recovery, and upgrading units contains H_2S, which needs to be removed before utilized in the process furnaces or gas turbines. MDEA is considered to be the desired solvent for removing H_2S from fuel gas in presence of CO_2. (Wu et al., 2015) The general configuration of a chemical absorption process is shown in Figure 3-13. The absorber is operated at 38 ^oC and 20 bar, relatively low temperature and high pressure. (Wu et al., 2015) The 'RadFrac' model in Aspen Plus with rate-based calculations is used to simulate the absorber and stripper using the kinetics and thermal model available in the open literature. (Austgen et al., 1991; Rinker et al., 1997) The gas oil and fuel gas produced inside the process are sent to either process furnaces or a gas turbine, which eventually gets converted to CO_2. The major CO_2 emission of the system is from the H_2 production units, process furnaces, and the gas turbine. The H_2-rich syngas stream from the POX/CG unit contains not only a significant amount of CO_2, but also a small amount of H_2S. In order to recover pure H_2, those streams are sent to the AGR unit to selectively remove CO_2 and H_2S, no matter if CCS is considered or not. The removed CO_2 is vented or sent to the CO_2 compression unit, depending on whether CCS is considered and the targeted extent of CCS. If high extent of CCS is considered, additional CO_2 needs to be captured from the gas turbine flue gas by post-combustion CO_2 capture technologies, and the amount is determined by carbon balance. Physical absorption is considered to deal with the streams with high P_{CO_2}, while chemical absorption is considered for capturing CO_2 from the steams with low P_{CO_2}.

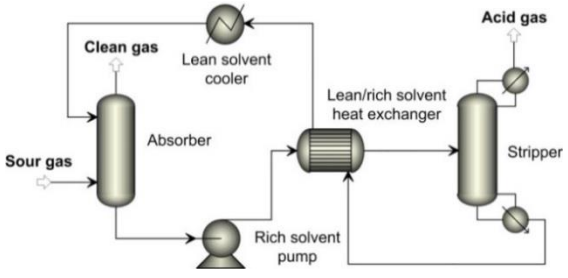

Figure 3-13. Schematic of the amine-based chemical absorption process.

Three chemical solvents are evaluated in this study, MDEA, MDEA/PZ and MEA. The advantages of chemical solvents over physical solvents are that the hydrocarbon loss is very low due to lower selectivity towards hydrocarbons, and the process could be operated at low pressure. In addition, a high level of CO_2 removal can be achieved in order to avoid CO_2 accumulation in downstream equipment. However, the chemical solvents suffer a higher parasitic loss, mainly due to the considerable amount of steam required for solvent regeneration (Bechtel, 1992b), in comparison to the physical solvents. Another disadvantage of most chemical solvents is the relatively lower operating pressure for solvent regeneration than that of the most physical solvents in order to avoid solvent degradation. This results in more power consumption for CO_2 compression section.

The PZ activated MDEA is a chemical solvent with high potential for CO_2 capture at reduced energy consumption in comparison to MEA. The stripper reboiler duty of MDEA/PZ system is expected to be lower than the MEA system (Kohl and Nielsen, 1997; Neveux, et al., 2013) PZ, a cyclic amine, is added to MDEA to improve solvent performance. (Xu et al., 1998; Puxty and Rowland, 2011; Plaza, 2012)

In the indirect CBTL plant, three packed columns are considered in the CO_2 removal unit, one for absorption, two for solvent regeneration, as shown in Figure 3-14. The FT vapor stream enters at the bottom of the absorption column while the recycled lean solvent enters at the top of absorption column. The rich solvent leaving the bottom of the absorber is heated by the lean solvent out of the stripper bottoms and sent to the strippers to remove CO_2. For satisfactory vapor velocity in the stripper, two strippers are used for one absorber. This is also consistent with the open literature. (Bechtel, 1992b; Bechtel, 1992c)

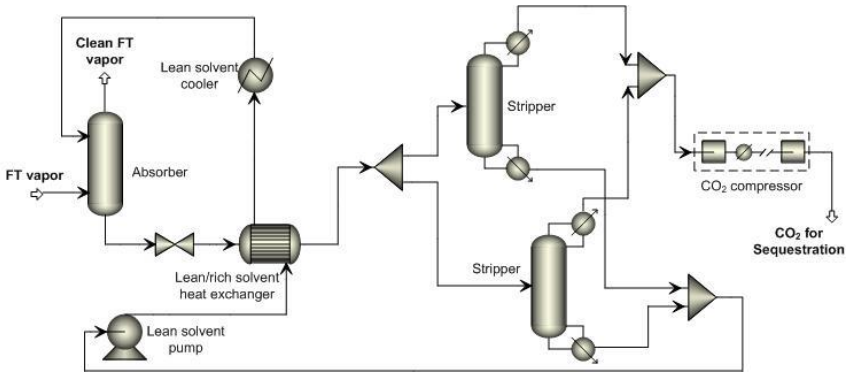

Figure 3-14. Amine-based CO_2 removal unit.

The lean solvent at the base case condition constitutes of 21 wt% MDEA and 5 wt% PZ aqueous solution with loading of 0.06 mol of CO_2/mol of amine group. Reactions considered in the rate-based model of the column are shown below, where reactions 14 a-e are assumed to be at equilibrium. Reactions 14 f-m are modeled using power law kinetics as shown in Eq. (15). The reactions listed, kinetic model, thermodynamic model and related constants are obtained from recent works. (Austgen et al., 1991; Hilliard, 2008; Bishnoi and Rochelle, 2000; Bishnoi and Rochelle, 2002)

$$2H_2O \leftrightarrow H_3O^+ + OH^- \quad (14a)$$

$$HCO_3^- + H_2O \leftrightarrow CO_3^{2-} + H_3O^+ \quad (14b)$$

$$PZH^+ + H_2O \leftrightarrow PZ + H_3O^+ \quad (14c)$$

$$HPZCOO + H_2O \leftrightarrow PZCOO^+ + H_3O^+ \quad (14d)$$

$$MDEAH^+ + H_2O \leftrightarrow MDEA + H_3O^+ \quad (14e)$$

$$CO_2 + OH^- \rightarrow HCO_3^- \quad (14f)$$

$$HCO_3^- \rightarrow CO_2 + OH^- \quad (14g)$$

$$PZ + CO_2 + H_2O \rightarrow PZCOO^- + H_3O^+ \quad (14h)$$

$$PZCOO^- + H_3O^+ \rightarrow PZ + CO_2 + H_2O \quad (14i)$$

$$PZCOO^- + CO_2 + H_2O \rightarrow PZ(COO^-)_2 + H_3O^+ \quad (14j)$$

$$PZ(COO^-)_2 + H_3O^+ \rightarrow PZCOO^- + CO_2 + H_2O \quad (14k)$$

$$MDEA + CO_2 + H_2O \rightarrow MDEAH^+ + HCO_3^- \quad (14l)$$

$$MDEAH^+ + HCO_3^- \rightarrow MDEA + CO_2 + H_2O \quad (14m)$$

$$r = k\left(\frac{T}{T_0}\right)^n \exp\left[-\frac{E}{R}\left(\frac{1}{T}-\frac{1}{T_0}\right)\right]\prod_{i=1}^{N} C_i^{a_i} \quad (15)$$

MEA is another popular chemical solvent for CO_2 capture. Reactions considered are shown below. Reactions 16 a-c are considered to be equilibrium-limited. Reactions 16 d-g are simulated by using power law kinetics as shown in Eq. (15). (Zhang et al., 2009) The kinetic model and the pilot plant data for model validation are available in the open literature. (Dugas, 2006; Hikita et al., 2006) In agreement with existing studies (Bechtel, 1992b; Dugas, 2006), the lean solvent is 30 wt% aqueous solution of MEA with CO_2 loading of 0.27 mol of CO_2/mol of amine group.

$$H_2O + MEAH^+ \leftrightarrow MEA + H_3O^+ \quad (16a)$$

$$2H_2O \leftrightarrow H_3O^+ + OH^- \quad (16b)$$

$$HCO_3^- + H_2O \leftrightarrow CO_3^{2-} + H_3O^+ \quad (16c)$$

$$CO_2 + OH^- \rightarrow HCO_3^- \quad (16d)$$

$$HCO_3^- \rightarrow CO_2 + OH^- \quad (16e)$$

$$MEA + CO_2 + H_2O \rightarrow MEACOO^- + H_3O^+ \quad (16f)$$

$$MEACOO^- + H_3O^+ \rightarrow MEA + CO_2 + H_2O \quad (16g)$$

Intercooling of the solvent in the absorber is considered in the baseline design for decreasing the utility consumptions. In the Aspen Plus environment, the intercooling is modeled by the pumparound option in the RadFrac block. The pumparound flow rate is set to be the lean solvent flow rate. The cooling temperature is set to be 40°C. Removed H_2S stream from the Selexol unit is mixed with the H_2S stream from the MDEA unit and then sent to the Claus unit for conversion to elemental sulfur. The extent of H_2S removal is decided by comparing the gas turbine sulfur tolerance and the SO_2 emission regulation (40 CFR 60.42b) and selecting the lower value. CO_2-rich streams at different pressure levels are vented or sent to different stages in a split-shaft multistage CO_2 compressor, determined by the targeted extent of CCS. Norton IMTP 1.5in, metal packing is used. The electrolyte NRTL properties package in Aspen Plus V7.3 is used. Column design carried out with the following objectives:

(1) The CO_2 stream concentration should meet the recommended design basis for the CO_2-sequestration gas for a remote, deep, geological storage site.
(2) The stripper column temperature should be chosen in a way that prevents solvent degradation.
(3) The CO_2-lean FT product must be free of solvent.

Catalytic two stage liquefaction (CTSL)

The CTSL unit is the core section in the direct CBTL plant to convert coal and biomass directly to syncrude. In the CTSL unit, as shown in Figure 3-15, coal and biomass are mixed with hot recycle solvents in the slurry tank, preheated and then sent to two ebullated bed reactors (EBRs) in a close-coupled mode with recycled and make-up H_2 stream. (Valent and Cronauer, 2005) Because of the heavy oil produced from the second stage is recycled to form feed slurry and fed back to the first stage, the two stages are interrelated and treated as a single unit in this study. (Valent and Cronauer, 2005) A yield model is developed for the CTSL unit fed with coal and small amount of biomass. As mentioned in Section 1, biomass can promote DCL process under mild condition, while the synergistic effect reduced with the increasing temperature and is imapparent at the normal DCL temperature. (Tchapda and Pisupati, 2014; Coughlin and Davoudazdeh, 1986; Shui et al., 2011; Shui et al., 2011; Anderson and Tuntawiroon, 1993; Ai, 2007) Hence, in this study the interaction between coal and biomass is ignored because of the low percentage of biomass in the feedstock and high operating temperature and pressure. The yield of liquids and their hydrocarbon distribution from the coal liquefaction reactors are estimated based on the operating data from the DCL proof-of-concept (POC) facility reported by HTI in 1995. (Comolli et al., 1995) The operating conditions in POC-01 Period 26, shown in Table 3-5, was recommended by HTI's study because of its higher efficiency and better operability, and therefore, are considered in our baseline study. (Comolli et al., 1995; Bechtel and Amoco, 1990) There is limited information in the open literature on direct biomass liquefaction using oil as slurry medium and H_2 as the reduction gas. In this work, the data from the Pittsburgh Energy Research Center (PERC) are used as baseline. In

the process reported by the PERC, wood chips were fed to the reactor with recycle oil serving as the solvent. The oil yield was about 45-55% of the dry wood with about 100% conversion of the wood. (Behrendt et al., 2008; Stevens, 1987; Sofer and Zaborsky, 2012) It is also assumed that the elimination of oxygen from wood can occur by producing H_2O, CO and CO_2. (White et al., 1987) Therefore, the yield of bio-oil and gases can be estimated by atom balance with the elemental analysis of bio-oil to be 81 wt% carbon, 10.2 wt% hydrogen and 8.8 wt% of oxygen as reported in the open literature. (Stevens, 1987; Elliot, 1980) These assumptions result in an estimated oil yield of 47% from the biomass liquefaction, which is consistent with the experimental data. (Stevens, 1987) In order to simplify atom balance calculation in the yield model of coal/biomass co-liquefaction, syncrude is specified as pseudo-components in Aspen Plus, with the elemental composition of each crude cut calculated by a linear combination of the corresponding data of coal liquids reported by HTI and biomass liquids reported by PERC. (Comolli et al., 1995; Stevens, 1987; Elliott, 1980) The yield model of the coal-biomass co-liquefaction process is developed in MS Excel by applying atom balance for calculating H_2 consumption and the yield of gases (i.e. CO, CO_2, NH_3, H_2S, H_2O), since the heteroatoms in the coal and biomass are either converted into gases (i.e. H_2O, H_2S, NH_3, CO, CO_2) or contained in the liquids. For the base case with a coal/biomass weight ratio of 92/8, the calculated elemental composition of syncrude and the results from the reactor model are shown in Table 3-6 and Table 3-7.

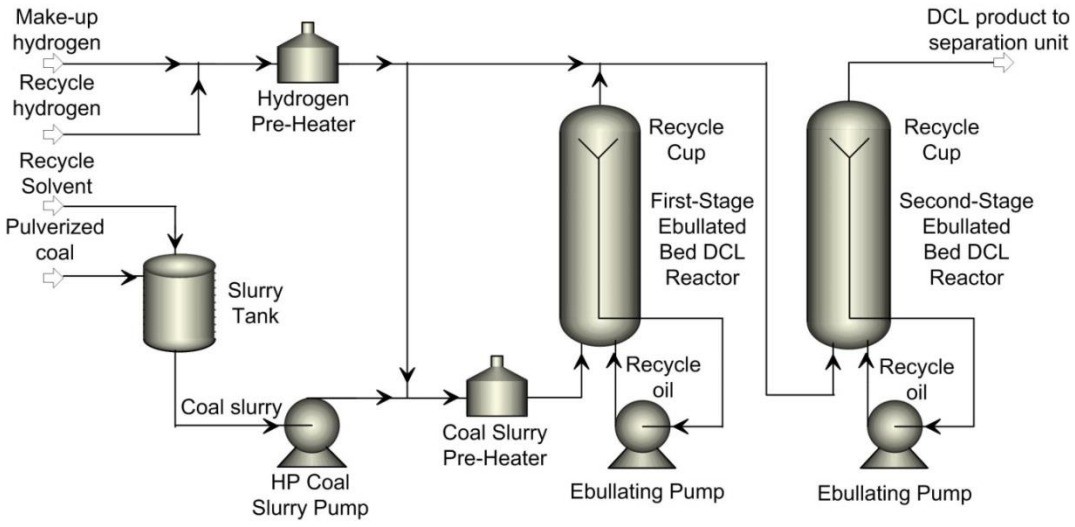

Figure 3-15. Plant configuration of the DCL process.

Table 3-5. Operating conditions of the CTSL unit.

Variable	Value	Variable	Value
Reactor inlet pressure (MPa)	22.1	First stage temperature (°C)	407
Reactor outlet pressure (MPa)	20.7	Second stage temperature (°C)	432
Hydrogen partial pressure (P_{H_2}, MPa)	13.4	Solvent/feed ratio (wt/wt)	1.82

Table 3-6 Element analysis of raw syncrude (base case)

Crude cut	Average NBP (°C)	Specific gravity	Elemental composition (wt%)				
			C	H	O	N	S
IBP-177 °C	93	0.799	84.75	14.09	0.99	0.16	0.01
177-288 °C	232	0.924	86.92	11.33	1.54	0.20	0.02
288 -344 °C	315	0.975	87.89	10.05	1.84	0.20	0.02
344 -454 °C	399	1.012	88.63	9.93	1.17	0.21	0.04
454-FBP	540	1.097	88.78	8.11	1.10	0.52	1.45

Table 3-7. Outlet stream distribution of the coal/biomass CSTL reactors (base case)

Component	wt%	Component	wt%	Component	wt%
Coal	1.14	C_1	0.57	288 - 344 °C	8.86
H_2O	4.06	C_2	0.45	344 - 454 °C	45.92
H_2S	0.94	C_3	0.47	454 °C - FBP	17.36
CO	0.18	C_4	0.76	Char	0.03
CO_2	0.69	IBP - 177 °C	5.57	Ash	3.45
NH_3	0.43	177 - 288 °C	9.1		

Other than the yield model, a mathematical model was developed in Aspen Custom Modeler (ACM) for ebullated-bed direct coal liquefaction (DCL) reactors based on rigorous reaction kinetics, hydrodynamics and mass and heat balances. The EBR is novel gas-liquid-solid three-phase reactors, which have been widely considered for the petroleum residue hydrocracking and hydrodesulphurization processes. (Martinez et al., 2010) The Shenhua DCL plant, the only commercial DCL plant under operating after World War II, also used EBRs for coal hydrogenation. EBRs are preferred in DCL process because of their small axial temperature distribution (backmixing), large reactor volume utilization (small gas holdup) and negligible solid precipitation (large superficial liquid velocity). (Wu et al., 2015; Robinson, 2009) The EBR is basically a slurry bubble column reactor (SBCR) in which the solid particles are held in suspension mostly by the upward movement of the liquid-phase rather than only the gas-phase as in a SBCR. As shown in Figure 3-15, part of the liquid from the reactor top section is collected in the recycle cup and then sent back to the reactor bottom by ebullating pumps to achieve high liquid-phase velocity.

The eight-lump kinetic models, as shown in Eq. (17a) to (17g) proposed by Shan et al. and Jiang et al. are applied for both coal slurry pre-heater and CTSL reactors. (Shan et al., 2015; Jiang et al., 2015) In those models, the dry ash-free (daf) coal was divided into three parts: the easy reactive component (C1), the difficult reactive component (C2) and the nonreactive component (C3). The liquefied product was divided into pre-asphaltene and asphaltene (PAA), oil (Oil), water (H_2O) and gas (Gas). C1 can be converted to PAA, Oil, H_2O and Gas; C2 can only be converted to PAA; C3 does not participate in any reaction. PAA can react with H_2 and produce Oil, H_2O and Gas.

$$\frac{dM_{C1}}{dt} = -(k_1 + k_2 + k_3 + k_4)M_{C1} \qquad (17a)$$

$$\frac{dM_{C2}}{dt} = -k_5 M_{C2} \quad (17b)$$

$$\frac{dM_{PAA}}{dt} = -(k_6 + k_7 + k_8)M_{PAA} + k_1 M_{C1} + k_5 M_{C2} + k_9 M_{PAA} \quad (17c)$$

$$\frac{dM_{Oil}}{dt} = k_2 M_{C1} + k_6 M_{PAA} \quad (17d)$$

$$\frac{dM_{Gas}}{dt} = k_3 M_{C1} + k_7 M_{PAA} \quad (17e)$$

$$\frac{dM_{H_2O}}{dt} = k_4 M_{C1} + k_8 M_{PAA} \quad (17f)$$

$$\frac{dM_{H_2}}{dt} = -k_9 M_{PAA} \quad (17g)$$

Where M_i is the mass fraction of component i using the daf basis of feed coal as benchmark; t is the reaction time and k_i is the reaction rate constant in s^{-1} defined as $k_i = k_{i,0}\exp(-\frac{E_i}{RT})$. The kinetic parameters reported by Shan et al. for the heating stage can be applied for the coal slurry pre-heater by specifying resident time (Shan et al., 2015), while the kinetic parameters reported by Jiang et al. can be applied to the main CTSL reactor (Jiang et al., 2015). It is notice that Eq. (17a) to (17g) is in mass basis and can be converted to molar concentration basis by manipulating with molecular weight. In ACM, Coal, C1, C2, C3 are specified as solids; Ash, H_2 and H_2O are specified as conventional components; Gas, Oil, PAA and Solvent are specified as pseudo-components. Table 3-8 gives the molecular weight and average normal boiling point (NBP) of the pseudo-components, which is required for calculating physical and thermal properties and converting the kinetic model to molar basis. (Anbar and John, 1978; Yan, 2014; Marzec, 2002; Jiang and Bhattacharyya, 2016; Comolli et al., 1995; Ferrance et al., 1996)

Table 3-8. Component specification.

Component	Average NBP (°C)	Molecular weight
Coal	N/A	1500
Gas	-98	28.2
Oil	232	169
PAA	593	450
Solvent	393	317

In this study, the commercial-scale EBRs for DCL process are simulated using an axial dispersion model with recycle as shown in Figure 3-16, where $F_{i,g}^F$ and $F_{i,sl}^F$ are the molar flowrate of component i of gas and slurry in the fresh feed in $kmol/s$; $F_{i,g}^{in}$ and $F_{i,sl}^{in}$ are the molar flowrate of component i of gas and slurry in the reactor inlet in $kmol/s$; $F_{i,g}^{out}$ and $F_{i,sl}^{out}$ are the molar flowrate of component i of gas and slurry in the reactor outlet in $kmol/s$; $F_{i,sl}^R$ is the molar

flowrate of component i of the recycle oil in $kmol/s$; $F_{i,sl}^{N}$and $F_{i,sl}^{N}$ are the molar flowrate of component i of gas and slurry in the reactor net product in $kmol/s$; T^{F}, T^{in}, T^{out}, T^{R} and T^{N} are the temperature of the fresh feed, reactor inlet stream, reactor outlet stream, recycle stream and reactor net product in K; x is the fraction of slurry in the reactor outlet recycled back to the inlet. (Robinson, 2009)

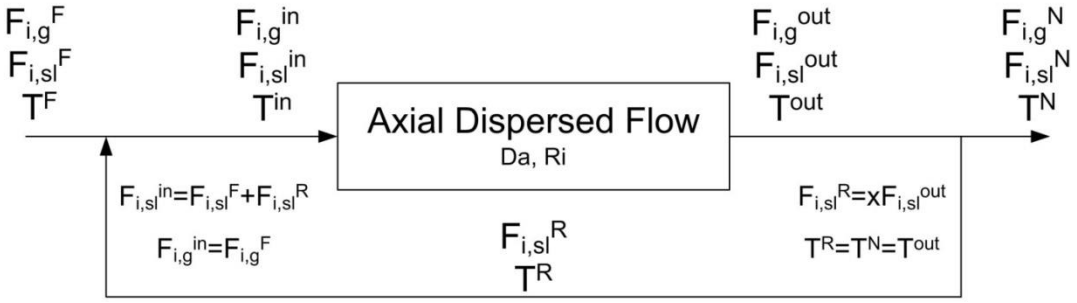

Figure 3-16. Modeling approach of the ebullated bed reactors.

The axial dispersion model (ADM) of the reaction section was built with the following features and assumptions: 1) the EBR is operated in a homogeneous bubble flow regime (Ishibashi et al., 2001); 2) both slurry and gas is moving upward; 3) pseudo-homogeneous condition is assumed for the coal slurry because of the high superficial liquid velocity and small particle size (Wu et al., 2015; Martubez et al., 2010); 4) the superficial velocity of slurry phase is assumed to be constant (Sehabiague et al., 2008); 5) the main reactions are taken place at the slurry phase; 6) The mass transfer resistance is negligible because of the high operating temperature and pressure (Lenoard et al., 2015), and therefore the mass transfer rate between the slurry phase and the gas phase equals to the reaction rate; 7) temperature gradient between phases does not exist; 8) The axial dispersion coefficients of gas phase and slurry phase are assumed to be the same in a homogeneous bubble flow regime (de Swart, 1996; Sehabiague et al., 2008); 9) the reactor is operating in a steady-state.

With the above assumptions, the mass and energy balance equations is listed in Eq. (18a) to (19c) for each component, where values of kinetic constant k_i is reported by Jiang et al. as a function of temperature in s^{-1} (Jiang et al., 2015); $C_{i,sl}$ and $C_{i,g}$ are the molar concentration of component i in the slurry and gas phase in $kmol/m^3$; ε_{sl} and ε_g are the slurry and gas holdup; D_a is the axial dispersion coefficient in m^2/s; U_{sl} and U_g are the superficial velocity of the slurry and gas phase in m/s; MW_i is the molecular weight of component i.

For the slurry phase:

$$\frac{d}{dz}\left(\varepsilon_{sl}D_a\frac{dC_{C1,sl}}{dz}\right)-\frac{d}{dz}\left(U_{sl}C_{C1,sl}\right)-\varepsilon_{sl}(k_1+k_2+k_3+k_4)C_{C1,sl}=0 \qquad (18a)$$

$$\frac{d}{dz}\left(\varepsilon_{sl}D_a\frac{dC_{C2,sl}}{dz}\right)-\frac{d}{dz}\left(U_{sl}C_{C2,sl}\right)-\varepsilon_{sl}k_5C_{C2,sl}=0 \qquad (18b)$$

$$\frac{d}{dz}\left(\varepsilon_{sl}D_a\frac{dC_{Oil,sl}}{dz}\right)-\frac{d}{dz}\left(U_{sl}C_{Oil,sl}\right)+\varepsilon_{sl}\left(k_2C_{C1,sl}\frac{MW_{C1}}{MW_{Oil}}+k_6C_{PAA,sl}\frac{MW_{PAA}}{MW_{Oil}}\right)=0 \quad (18c)$$

$$\frac{d}{dz}\left(\varepsilon_{sl}D_a\frac{dC_{PAA,sl}}{dz}\right)-\frac{d}{dz}\left(U_{sl}C_{PAA,sl}\right)+\varepsilon_{sl}\left((k_9-k_6-k_7-k_8)C_{PAA,sl}+k_1C_{C1,sl}\frac{MW_{C1}}{MW_{PAA}}+k_5C_{C2,sl}\frac{MW_{C2}}{MW_{PAA}}\right)=0 \quad (18d)$$

For the gas phase:

$$\frac{d}{dz}\left(\varepsilon_gD_a\frac{dC_{H_2,g}}{dz}\right)-\frac{d}{dz}\left(U_gC_{H_2,g}\right)-\varepsilon_{sl}k_9C_{PAA,sl}\frac{MW_{PAA}}{MW_{H_2}}=0 \quad (19a)$$

$$\frac{d}{dz}\left(\varepsilon_gD_a\frac{dC_{Gas,g}}{dz}\right)-\frac{d}{dz}\left(U_gC_{Gas,g}\right)-\varepsilon_{sl}\left(k_3C_{C1,sl}\frac{MW_{C1}}{MW_{Gas}}+k_7C_{PAA,sl}\frac{MW_{PAA}}{MW_{Gas}}\right)=0 \quad (19b)$$

$$\frac{d}{dz}\left(\varepsilon_gD_a\frac{dC_{H_2O,g}}{dz}\right)-\frac{d}{dz}\left(U_gC_{H_2O,g}\right)-\varepsilon_{sl}\left(k_4C_{C1,sl}\frac{MW_{C1}}{MW_{H_2O}}+k_8C_{PAA,sl}\frac{MW_{PAA}}{MW_{H_2O}}\right)=0 \quad (19c)$$

The heat balance (Onazaki et al., 2000) and pressure profile (Deckwer, 1992; Sehabiague et al., 2008) is listed in Eq. (20) and (21), where ΔH_r is the reaction heat based on hydrogen conversion in $kJ/kmol\ H_2$ given by Onazaki et al. (Onazaki et al., 2000); H_{mix} is the heat capacity of gas-slurry mixture in $J/(m^3 slurry\ K)$ defined by Eq. (22) (Onazaki et al., 2000); ρ_{sl} and ρ_g are the slurry phase and gas phase density in kg/m^3; $C_{p,sl}$ and $C_{p,g}$ are the heat capacity of the slurry and gas phase in $kJ/(kg\ K)$; g is the acceleration of gravity in m^2/s; T and P are the reactor temperature in K and pressure in Pa.

$$\frac{d}{dz}\left(\varepsilon_{sl}D_aH_{mix}\frac{dT}{dz}\right)-\frac{d}{dz}\left(U_{sl}H_{mix}T\right)+\Delta H_r\varepsilon_{sl}k_9C_{PAA,sl}\frac{MW_{PAA}}{MW_{H_2}}=0 \quad (20)$$

$$\frac{dP}{dz}+\left(\varepsilon_g\rho_g+\varepsilon_{sl}\rho_{sl}\right)g=0 \quad (21)$$

$$H_{mix}=\rho_gC_{p,g}U_g/U_{sl}+\rho_{sl}C_{p,sl} \quad (22)$$

The boundary conditions for the gas and slurry at the inlet (bottom, $z=0$) of the reactor are Danckwerts' type as listed in Eq. (23a) to (23d), in which the inlet condition $C_{i.g}^{in}$ and $C_{i.sl}^{in}$ is evaluated by Eq. (24a) and (24b); T^{in} is evaluated by enthalpy balance as shown in Eq. (24c). In Eq. (24b) and (24c), D_T is the reactor diameter in m; h_l^F, h_l^R, h_l^{in}, h_g^F and h_g^{in} are the specific enthalpy of the liquid and gas phase in the fresh feed, recycle stream and reactor inlet at corresponding temperature in $kJ/kmol$; F_l^F, F_l^R, F_l^{in}, F_g^F and F_g^{in} are the molar flowrate of the liquid and gas phase in the fresh feed, recycle stream and reactor inlet in $kmol/s$; F_s^F, F_s^R and F_s^{in} are the specific enthalpy of solids in the fresh feed, recycle stream and reactor inlet at

corresponding temperature in kJ/kg; F_s^F , $F_s^R$and F_s^{in} are the mass flowrate of solids in the fresh feed, the recycle stream and reactor inlet in kg/s. The boundary conditions at the outlet (top, $z = L$) of the reactor are listed in Equation (25a) to (25c).

$$U_{sl}C_{i,sl} - \varepsilon_{sl}D_a\frac{dC_{i,sl}}{dz} = U_{sl}C_{i.sl}^{in} \quad (23a)$$

$$U_gC_{i,g} - \varepsilon_gD_a\frac{dC_{i,g}}{dz} = U_gC_{i.g}^{in} \quad (23b)$$

$$U_{sl}T - \varepsilon_{sl}D_a\frac{dT}{dz} = U_{sl}T^{in} \quad (23c)$$

$$P = P^{in} \quad (23d)$$

$$C_{i.sl}^{in} = (F_{i,sl}^F + F_{i,sl}^R)/(0.25\pi D_T^2U_{sl}) \quad (24a)$$

$$C_{i.g}^{in} = F_{i,g}^F/\left(0.25\pi D_T^2U_g\right) \quad (24b)$$

$$F_l^Fh_l^F + F_s^Fh_s^F + F_g^Fh_g^F + F_l^Rh_l^R + F_s^Rh_s^R = F_l^{in}h_l^{in} + F_s^{in}h_s^{in} + F_g^{in}h_g^{in} \quad (24c)$$

The boundary conditions at the outlet (top, $z = L$) of the reactor are listed in Equation (25) to (27).

$$\frac{dC_{i,sl}}{dz} = 0 \quad (25a)$$

$$\frac{dC_{i,g}}{dz} = 0 \quad (25b)$$

$$\frac{dT}{dz} = 0 \quad (25c)$$

The axial dispersion coefficient (D_a) in m^2/s and gas holdup (ε_g) of the EBRs are given by Eq. (26) and (27), which were developed based on the data collected or tested for a gas-coal slurry system at the coal liquefaction operating conditions. (Baird and Rice, 1975; Kara et al., 1982; Ishibashi et al., 2001) In the above equations, the specific enthalpy, heat capacity and density of the gas mixture and the liquid mixture are estimated using Peng-Robison equation of state in ACM, while the density and coal was set to be 1346 kg/m^3, and the heat capacity of coal is given by Eq. (28), where T is in ^oC. (Tomeczek and Palugniok, 1996; Richardson, 1993)

$$D_a = 0.35g^{1/3}{D_T}^{4/3}{U_g}^{1/3} \quad (26)$$

$$U_g/\varepsilon_g = \left(U_g + U_{sl}\right) + 0.114\left(1-\varepsilon_g\right)^{1.02} \quad (27)$$

$$C_{p,s} = 1.13 + 3.58\times10^{-3}T + 2.28\times10^{-6}T^2 - 9.81\times10^{-9}T^3 + 4.63\times10^{-12}T^4 \quad (28)$$

Some preliminary specifications and results are listed and compared with data available in the open literature (Wu et al., 2015) as following. Table 3-9 shows with the same feed flowrate and reactor geometry, the superficial velocity and holdups are closed to the industrial data, which indicates that the density model is suitable; the coal conversion and oil yield is closed to the industrial data, which indicates that the reaction kinetics work fine. However, the temperature increasing across the reactors is much lower than the industrial data, which indicates that either enthalpy model or the energy balance equation needs to be updated.

Table 3-9 Model validation.

Variable	Model	Industrial
Reactor Specification		
Reactor diameter (m)	4.8	4.8
Reactor length (m)	60.0	62.5
Coal flowrate (kg/s)	69.44	69.44
Solvent flowrate (kg/s)	78.42	78.42
Furnace outlet temperature (°C)	382.2	382.2
1st Reactor output		
Superficial gas velocity (m/s)	6.13	5.0*
Superficial slurry velocity (m/s)	2.75	2.5*
Gas holdup	0.38	0.35*
Coal conversion (%, daf)	87.3	N/A
Oil yield** (%, daf)	60.5	N/A
Temperature increase (°C)	70.8	72.8
2nd Reactor output		
Superficial gas velocity (m/s)	6.44	5.0*
Superficial slurry velocity (m/s)	2.83	2.5*
Gas holdup	0.40	0.35*
Coal conversion (%, daf)	80.4	90.4
Oil yield (%, daf)	60.7	58.0
Temperature increase (°C)	14.0	39.5

*Approximated data

Product recovery and integrated/inline hydrotreating

In the product upgrading section of the indirect CBTL plants, an integrated hydrotreating approach is proposed, as shown in Figure 3-17, for increasing the thermodynamic efficiency and for making

the plant footprint smaller, in comparison to the conventional separated hydrotreating approach shown in Figure 3-18. It should be noted that the integrated hydrotreating has been considered for upgrading of hydrocracked residuum petroleum crude oil (Cavallo et al., 2008), whole crude oil (Cavallo et al., 2008) and syncrude from coal direct liquefaction (Cavallo et al., 2008). It is, therefore, reasonable to consider that integrated hydrotreating can also be applied to upgrading of the FT syncrude because the type of components, such as paraffin, olefin and oxygenate, carbon number and boiling point range of FT syncrude and the main desired reactions, such as hydrodeoxygenation, hydrodemetallization and hydrogenation of alkenes are similar to those in the applications cited before. (Cavallo et al., 2008; Jarullah et al., 2012; Comolli et al., 1995) In the open literature, some rigorous models have been developed for optimization and scaling up of the integrated hydrotreater based on the hydrodynamics, kinetics, heat and mass balance. (Cavallo et al., 2008) Other studies provide simple correlation for estimating the performance of the conventional separated hydrotreating unit. (Fahim et al., 2010) From the perspective of this work, a simplified yield model of the integrated hydrotreating unit in Excel.

In the conventional separated hydrotreating approach, the crude is first separated into different streams in flash drums and distillation columns. Then naphtha and diesel are sent to two different hydrotreating units, while wax is sent to a hydrocracking unit. In contrast, in the integrated hydrotreating unit, the raw syncrude is first preheated to about 267^{o}C by the hot treated syncrude. It is then heated by a furnace to reach the required temperature before being sent to the reactor. After being cooled, the treated syncrude is sent to a high-pressure flash (HPF) drum followed by a low-pressure flash (LPF) drum to recover the H_2 and light gases (LG). Then it is sent to the main distillation column through a series of heat exchangers.

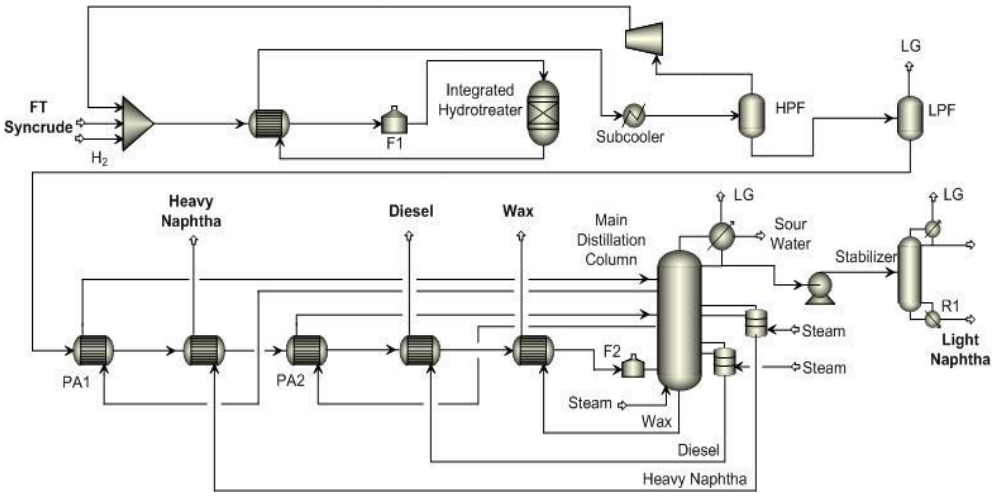

Figure 3-17. Configuration of the novel integrated hydrotreating approach.

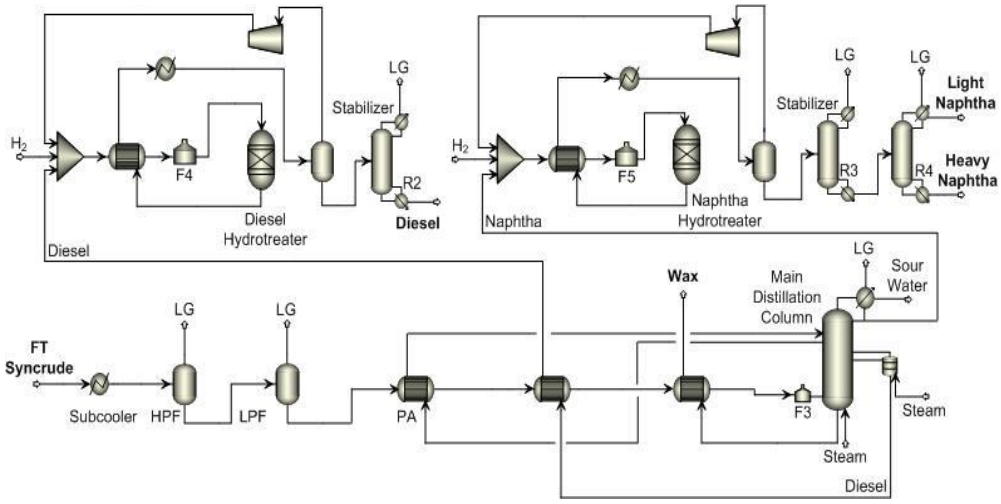

Figure 3-18. Configuration of the conventional separated hydrotreating approach.

In this study, the correlations given by Bechtel (Bechtel, 1993; 1998) are applied for the material and energy balance estimation of the conventional hydrotreating units for naphtha and diesel, while a simple yield model is developed in Excel for the integrated hydrotreater unit for obtaining reasonable estimates of H_2 and utility consumption. To simplify the calculation of H_2 requirement in the novel integrated hydrotreating unit, a number of assumptions have been made. The operating condition is considered to be similar to the conversional diesel hydrotreater (58 bar, 297 ^oC), which is much severe than the operating conditions in the naphtha hydrotreaters. Hence, it is assumed that the naphtha cut gets completely hydrotreated, and the amount of diesel cut that gets hydrotreated depends on the catalyst type and experimental Bromine Number of hydrotreated diesel. Typically, the Bromine Number of the hydrotreated FT diesel is lesser than 6.0 g Br/100g when catalyzed by $NiMo/Al_2O_3$. (Lamprech, 2007) Hence, in the yield model developed, we have considered 5 wt% of unsaturated diesel that corresponds to 6.0 g Br/100g. Because Fe-catalyst FT syncrude contains only small amount of oxygenates and no sulfur and nitrogen, the main reactions considered is hydrogenation of alkenes and hydrodeoxygenation. With the detailed component distribution in the reactor inlet, the H_2 consumption can be estimated by atom balance with the following assumptions: (1) Reacted olefins are converted to the corresponding saturated paraffin compound; (2) Wax remains mainly unreacted in this integrated hydrotreater as wax hydrotreating needs much severe reaction conditions; (3) Yields of light gases produced by the side hydrocracking reaction are assumed to the similar to the conventional hydrotreating units; (4) All oxygenates are hydrotreated and converted to water and corresponding paraffin compound. Most of the heat required for preheating the hydrotreater feed can be recovered by exchanging heat between the feed stream and hydrotreater outlet stream, while the remaining heat is supplied by the feed furnace. Because of the wide variation in the thermodynamic properties of isomers of C_5 to C_8, a statistical model of the isomer distribution of paraffin in the LTFT product developed by Weller and Friedel (Weller and Friedel, 1949) is considered for more accurate energy calculation. The detailed isomer distribution is reported in Table 3-10.

Table 3-10 Isomer distribution of hydrocarbons in LTFT product.

Isomer	Molar fraction	Isomer	Molar fraction
1-Pentene	1	n-Heptane	0.877
n-Pentane	0.95	2-methyl hexane	0.046
i-Pentane	0.05	3-methyl hexane	0.077
1-Hexene	1	1-Octene	1
n-Hexane	0.896	n-Octane	0.845
2-methyl pentane	0.057	2-methyl heptane	0.039
3-methyl pentane	0.047	3-methyl heptane	0.072
1-Heptene	1	4-methyl heptane	0.044

Due to the limited information available on hydrotreating of the FT liquids, the yield model is validated by comparing the calculated product distribution and hydrogen consumed with those reported by Bechtel (Bechtel, 1998) with the same feed composition. The composition of oxygenates in the feed was not specified in the Bechtel report. Hence, for generating the final product distribution we have assumed that oxygenates in naphtha and diesel are represented by $C_{4.78}H_{11.14}O_{1.1}$, and $C_{9.08}H_{18.94}O_{1.1}$, respectively. (Fox and Tam, 1995; Gamba et al., 2010) Table 3-11 lists the results and shows that the errors in yields of major products are within 5 %. It should be noted that the syncrude composition reported by Bechtel (Bechtel, 1993; 1998) is similar to the base case of this study. It is assumed that the hydrocarbon distribution does not change significantly in the range of operating conditions considered in the sensitivity studies conducted in this work.

Table 3-11. Validation of the model of the integrated hydrotreater.

wt%	Bechtel	Model	Error%
H_2 consumption	1.10	1.07	-2.8
Major products			
Light gases	2.97	2.96	0.34
Naphtha	39.27	39.11	0.33
Diesel	57.76	57.93	0.29

In both hydrotreating approaches, the raw or hydrotreated syncrude is cooled to about 40 ^{o}C and sent to the HPF (38 bar) to recover the H_2-rich gas. The remaining portion of the stream is sent to the LPF drum (8 bar) from where the light gases are sent to the fuel gas header. Then a complex distillation column is used to separate the syncrude into products with different boiling point range, as shown in Table 3-12. Stabilizer is used to separate light gases from the light naphtha stream. The ASTM D86 cut points of the hydrocarbons are specified to ensure that the final product pools satisfy the desired gasoline and diesel specs. The cut points of light naphtha are specified for satisfying the gasoline specs. The cut points of heavy naphtha and diesel are specified to satisfy the specs of the gasoline and diesel pools, respectively. PetroFrac model is used to design and simulate the main distillation column, where BK10 EOS is used as the thermodynamic model because the distillation system contains species of wide boiling point range.[52,53] Stabilizer is

simulated via RadFrac model using SRK EOS as the thermodynamic model because the system mainly contains lighter hydrocarbons.

Table 3-12. Product specification of the hydrocarbon recovery system.

Integrated approach		Separated approach	
Product	ASTM D86 cut point	Product	ASTM D86 cut point
Light naphtha	52ºC - 94 ºC	Naphtha	50ºC – 174ºC
Heavy naphtha	104 ºC - 174ºC	Diesel	190ºC - 316 ºC
Diesel	190 ºC- 316 ºC	Wax	327 ºC - FBP
Wax	327 ºC - FBP		

The specifications of the hydrocarbon recovery system is listed in Table 3-13 and Table 3-14, which are obtained based on the traditional crude oil distillation technology (Ji and Bagajewicz, 2002; Bagajewicz and Ji, 2001; Seo et al., 2000) and the multicomponent distillation column used in the Bechtel FT process design[19] with limited information. In the hydrocarbon recovery system, the syncrude passes through a preheating train with several heat exchangers using the pump-around streams and the product streams that need to be cooled before entering the main distillation column. A feed furnace is used for the crude oil distillation tower instead of reboiler, evaporating only a small portion of the wax. The feed furnace is specified by applying a fractional overflash of 3.2 % LV. Stripping stream is used for decreasing the partial pressure of the hydrocarbons in order to prevent decomposition, which occurs at high temperature (about 371 ºC). A commonly-used value for stripping stream to product ratio is about 2.27-4.54 kg/bbl. Pump-arounds are used as main means to obtaining intermediate heat recovery. Liquid is withdrawn from the tray on or above the lower product draw tray, cooled, and returned to a tray, 2-3 trays above, but below the upper product draw. As a result, the size and heat duty of the feed furnace and the overhead condenser could be reduced significantly. Meanwhile, the top reflux and the column diameter could also be reduced. In this study, the outlet temperatures of the two pump-around exchangers are selected to increase the heat recovery as much as possible within operating constraints.

Table 3-13. Column specification.

	Integrated approach	Separated approach
Number of trays		
Main column	30*	23*
Heavy naphtha side stripper	5	NA
Diesel side stripper	5	5
Stabilizer	20	20
Locations		
Feed to main column	26*	19*
Stripping steam to main column	30*	23*
Heavy naphtha product draw and return	15,14	NA
Diesel product draw and return	24,23	17*,16
Pump-around 1 draw and return	15,12	NA
Pump-around 2 draw and return	24,21	17,14
Feed to stabilizer	10	10

Stabilizers are designed using short cut model in Aspen Plus; numbers with * are obtained from the open literature

Table 3-14. Specification of the column operating condition.

	Integrated approach	Separated approach
Main column		
Condenser temperature (ºC) *	37.8	37.8
Overhead pressure (kPa) *	600	600
Pressure drop per tray (kPa) *	1.38	1.38
Feed furnace fractional overflash (%LV)	3.2	3.2
Bottom product to feed ratio (kg/kg)	0.48	0.48
Stripping steam to bottom product ratio (kg/bbl)	4.54	4.54
Side strippers		
Stripping steam to heavy naphtha ratio (kg/bbl)	2.27	NA
Stripping steam to diesel ratio (kg/bbl)	2.27	2.27
Pump-around and preheating train		
Pump-around 1 return temperature (ºC)	82.2	NA
Pump-around 2 return temperature (ºC)	282.2	83.3
Heaby naphtha heat exchanger hot steam temperature drop (ºC)	66.7	NA
Diesel heat exchanger hot stream temperature drop (ºC)	85.6	51.7
Wax heat exchanger hot steam temperature drop (ºC)	193.3	194.4

Numbers with * are obtained from the open literature

Of the direct CBTL plants, the product recovery and inline hydrotreating section is shown in Figure 3-19. The product from the CTSL reactors is first sent to the hot HP separator. The vapor product from the hot HP separator, consisting of H_2-rich light gases, most of the naphtha (IBP-177ºC) and a portion of the gas oil and solvent oil (177-454ºC), is then sent to the inline hydrotreater for stabilization. The hydrotreated syncrude is sent to warm and cold HP flash vessels. The vapor product from the cold HP flash separation contains about 80-85% H_2 and therefore most of this H_2-rich stream is recycled back to the liquefaction reactor, while a portion of it is purged to maintain the P_{H_2} in liquefaction reactors. Liquid products from the warm and cold HP flash vessels are sent to the warm and cold LP flash vessels, respectively. The bottom product from the hot HP separator is de-pressurized and sent to the LP reactor liquid flash vessel where small amount of N_2 is used for stripping. The top product from the LP reactor liquid flash vessel is sent to the warm LP flash vessel while the top product from the warm LP flash vessel is sent to the cold LP flash vessel. Liquid products from the warm and cold LP flash vessels, mainly IBP-454ºC syncrude, are sent to the atmospheric distillation column to be separated into light gases, light naphtha, heavy naphtha, gas oil, and liquefaction solvent. The bottom product from the LP reactor liquid flash vessel, a mixture of heavy oil and solid residues, is sent to the vacuum distillation column and the ROSE-SR unit for solid/liquid separation. The bottom product from the atmospheric distillation column, heavy vacuum gas oil (HVGO) from the vacuum distillation column and the deashed oil (DAO) from the ROSE-SR unit are sent to the recycle solvent tank for preparing coal/biomass slurry. Light naphtha, heavy naphtha, and gas oil from the atmospheric distillation column and light vacuum gas oil (LVGO) from the vacuum distillation column are sent to product upgrading units to produce gasoline, diesel and gas oil column bottom.

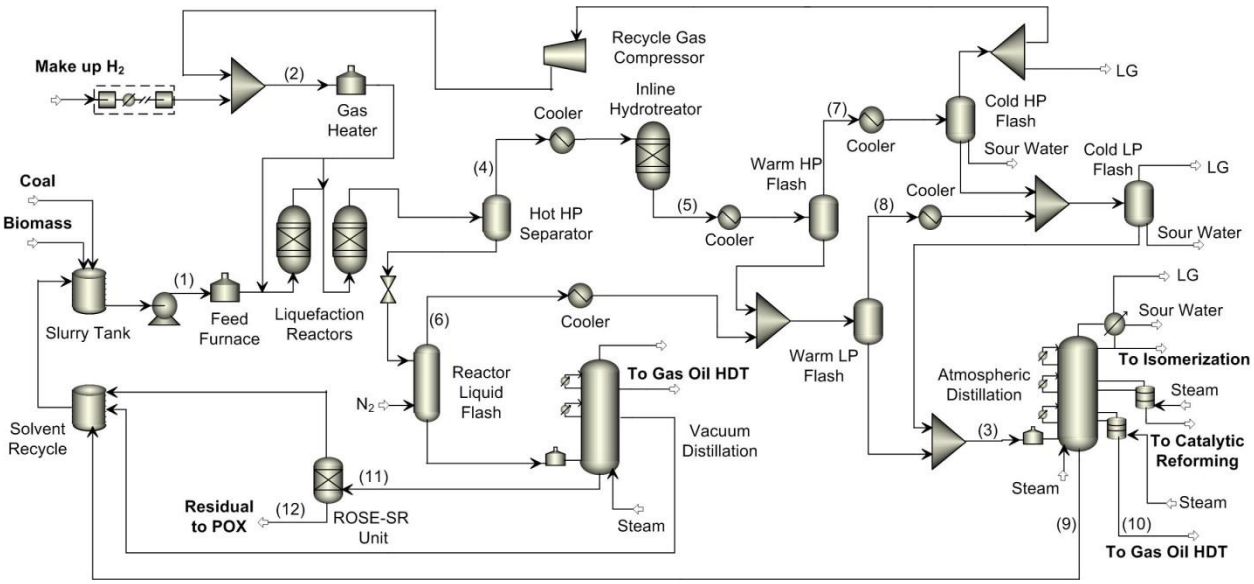

Figure 3-19. Plant configuration of the liquefaction and product recovery section.

The plant configuration of the ROSE-SR unit can be found in Figure 3-20. The deashing solvent, which is considered to be mainly toluene in our study, is mixed with the hot stream from vacuum column bottom and then fed into the 1st stage settler with a solvent to vacuum column bottom weight ratio of 3 (Givens and Kang, 1984; Baldwin and Bills, 1978). The heavy phase from the 1st stage settler, containing 10-20 wt% of the liquefaction liquids along with deashing solvent and essentially all of the solids, is "let down" to the deashing solvent separator operated at atmospheric pressure (Gearhart and Nelson, 1983; Givens et al., 1984). The light phase from the 1st stage settler, which contains 80-90 wt% of the liquefaction liquids and deashing solvent, is heated and sent to the 2nd stage settler. In the 2nd stage settler, most of the solvent is recovered under supercritical condition as the decrease in density and solubility of the supercritical fluid with the increasing temperature is exploited for solvent separation in the 2nd stage settler. The light phase from the 2nd stage settler, containing mainly supercritical solvent, is cooled in a heat exchanger and then sent to the HP solvent tank for preparing recycle solvent. The heavy phase from the 2nd stage, containing mainly deashed oil and small amount of deasing solvent, is "let down" to another deashing solvent separator. A small portion of the deashing solvent is recovered from the two deashing solvent separators, which is cooled and condensed and sent to the deashing solvent feed tank and then pumped to the HP solvent tank. The DAO is recycled to the liquefaction reactor serving as H-donor solvent and is hydrocracked to improve the performance of liquefaction unit, while the residues is partially oxidized to syngas and shifted to hydrogen in order to reduce the external hydrogen demand of the whole liquefaction system.

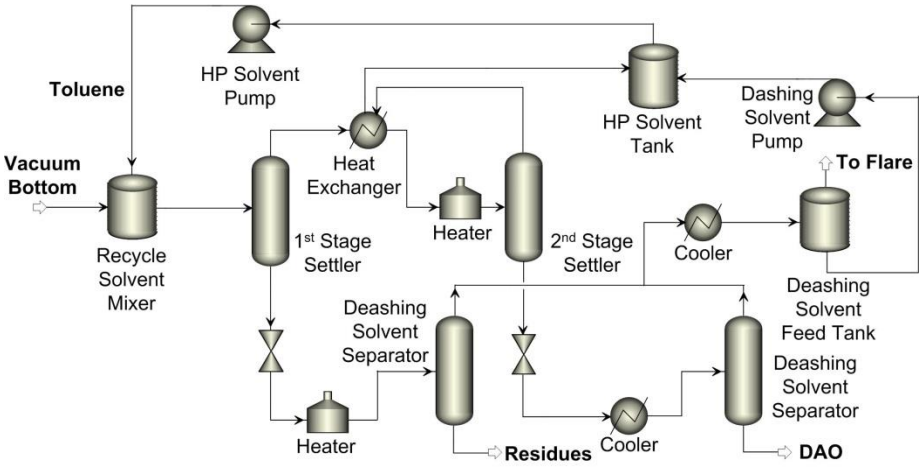

Figure 3-20. Plant configuration of the ROSE-SR unit.

The approach to modeling the inline hydrotreater is the same as the integrated hydrotreating reactor (Jiang and Bhattacharyya, 2015). With the elemental analysis of raw syncrude calculated from Section 2.2.1 and known elemental analysis of hydrotreated syncrude reported by HTI (Comolli et al., 1995; Bechtel and Amoco, 1990), the H_2 consumption of the inline hydrotreater is estimated by atom balance, assuming O, N and S in the syncrude are rejected by producing H_2O, H_2S and NH_3. Table 3-6 lists the elemental analysis of the hydrotreated syncrude obtained from the open literature. (Comolli et al., 1995; Bechtel and Amoco, 1995) For the inline hydrotreater, the syncrude is specified as pseudo-components for the sake of applying atom balance, while syncrude is specified as petroleum assay for other equipment items in the product recovery unit for better estimate of vapor-liquid equilibrium (VLE). For each cut specified in Table 3-6 and Table 3-15, true boiling point distillation curves are available in the open literature (Comolli et al., 1995; Bechtel and Amoco, 1995). Peng-Robinson equation of state (EOS) is used as the thermodynamic model for the system (Fahim et al., 2010). Both atmospheric and vacuum distillation columns are modeled using PetroFrac block in Aspen Plus. The 1st stage and 2nd stage settlers in the ROSE-SR unit are modeled as component separators, using solids rejection efficiency and energy balance reported by HTI and assuming 88% and 80% solvent recovery in the light phases from the 1st and 2nd stage settlers, respectively (Comolli et al., 1995; Rhodes, 1980). Deashing solvent separators are modeled as flash separators. Table 3-16 and Table 3-17 summarize the operating conditions and design specifications of the key equipment items in the product recovery unit. Detailed specifications of the distillation columns can be found in the Table 3-18 to Table 3-21. (Ji and Bagajewicz, 2002; Bagajewicz and Ji, 2001)

Table 3-15. Elemental analysis of hydrotreated syncrude.

wt%	C	H	O	N	S
IBP-177 ºC	85.54	14.05	0.01	0.01	0.00
177-288 ºC	87.90	12.55	0.01	0.01	0.01
288-344 ºC	88.30	11.97	0.01	0.02	0.01
344-454 ºC	88.10	11.28	0.01	0.03	0.05

Table 3-16. Operating conditions of the product recovery unit.

Equipment	Pressure[(1)] (bar)	Temperature[(2)] (°C)	Equipment	Pressure[(1)] (bar)	Temperature[(2)] (°C)
Warm HP flash drum	172	232	Cold HP flash drum	170	40
LP reactor liquid flash drum	7.9	405	Warm LP flash drum	7.8	232
Atmospheric distillation tower	2.8	40/320	Cold LP flash drum	7.6	40
Vacuum distillation tower	0.1	65/305	1st stage settler	55	300
Deashing solvent separator	1.0	325/270	2nd stage settler	54.5	370

(1) Top pressure for all towers
(2) Top/bottom temperature for all towers

Table 3-17. Design specifications of the product recovery unit.

Equipment	Manipulated variable	Target	Value
Hot HP separator	Operating temperature	ASTM D86 FBP of the vapor product	370 °C
LP reactor liquid flash drum	Stripping N_2 flowrate	Recovery of the 288-344°C syncrude in vapor	50%
Atmospheric distillation tower	Bottom flow rate of heavy naphtha stripper	ASTM D86 95vol% temperature of light naphtha	107 °C
	Bottom flow rate of distillate stripper	ASTM D86 95vol% temperature of heavy naphtha	187 °C
	Bottom flow rate of main column	ASTM D86 95vol% temperature of gas oil	376 °C
Vacuum distillation tower	Duty of top pump-around	First stage temperature	65 °C
	Sidestream flow rate of LVGO	ASTM D86 95vol% temperature of LVGO	376 °C
	Sidestream flow rate of HVGO	Recovery of 890-975°F crude in bottom	77.3%
ROSE-SR unit	Operating temperature of deashing solvent separators	Solvent recovery of deashing solvent separators	98%
	Heat duty of the heat exchanger between settlers	Inlet temperature of the first stage settler	300 °C

Table 3-18. Specifications of the atmospheric distillation column.

Specifications	Value
Number of trays	
Main column	29
Heavy naphtha side-stripper	5
Distillate side-stripper	5
Locations	
Feed to main column (Furnace)	26
Stripping steam to main column (Above stage)	30
Heavy naphtha side-stripper draw and return	15, 14
Distillate side-stripper draw and return	24, 23

Table 3-19. Operating conditions of the atmospheric distillation column.

Operating Condition	Value	
Main Column		
Condenser temperature	37.8	ºC
Overhead pressure	240	kPa
Pressure drop per tray	1.38	kPa
Feed furnace fractional overflash	3.2	%LV
Bottom product/feed	0.62	kg/kg
Stripping steam/bottom product	4.54	kg/bbl
Side-strippers		
Stripping steam/heavy naphtha	2.27	kg/bbl
Stripping steam/diesel	2.27	kg/bbl

Table 3-20. Specifications of the vacuum distillation column.

Specification	Value
Total number of trays	6
Feed to main column (Furnace)	6
Stripping steam to main column (Above stage)	7
LVGO sidestream product	2
Top pump-around draw and return	2, 1
HVGO sidestream product	4
HVGO pump-around draw and return	4, 3

Table 3-21. Operating conditions of the vacuum distillation column.

Operating Condition	Value	
Overhead pressure	60	mmHg
Bottom pressure	70	mmHg
Feed furnace fractional overflash	0.6	%LV
Stripping steam/bottom product	2.27	kg/bbl

In the direct CBTL plant, the coal/biomass slurry and recycled H_2 need to be pre-heated to a high temperature before being fed to the CTSL reactors, which results considerable fuel consumption in the pre-heating furnaces. The product from the liquefaction reactor has to be cooled for separation. In the DCL baseline design reported by Bechtel/Amoco (Bechtel and Amoco, 1990), the recycle H_2 is pre-heated by exchanging heat with the hot stream from the top of the hot and warm HP flash vessels. Even though exchange of heat between cold slurry feed and downstream fluid is not considered by Bechtel/Amoco, it is considered to reduce the duty of the preheat furnaces in the SRC-I, SRC-II and NEDOL processes (Morris and Foster, 1983; Thorogood, 1983; Shih, 1995). In this study, a global heat integration analysis is considered for increasing the overall thermal efficiency. Aspen Energy Analyzer is used to design and optimize the heat exchanger

network. The minimum temperature approach is set to be 10 °C. The forbidden matches between streams are specified to avoid operability problem such as that caused by large differential pressure and unexpected leakage during operation.

Temperature changes in the key streams in the liquefaction and product recovery section is shown in Figure 3-21, where the cold streams are in the bars with solid fill and the hot streams are in bars with diamond fill. 25 heat exchangers are designed by Aspen Energy Analyzer using pinch analysis. Table 3-22 lists the forbidden and matched hot and cold streams in the heat exchanger network design. The stream numbers mentioned in Figure 3-21 and Table 3-22 are shown in Figure 3-19. With the new design, the coal/biomass slurry is heated to about 350 °C by HP steam before entering the preheat furnace, while the heat duty of the preheat furnace is reduced by about 52%. These results are similar to the NEDO's DCL experience, where the coal slurry is preheated to 340 °C in the heat exchangers and the heat duty of the furnace is reduced by about 60%. (NEDO, 2006; IEA Coal Research Ltd, 2009)

Table 3-22. Forbidden and matched hot and cold streams in the heat integration.

	4	5	6	7	8	9	10
1	✓	✓	✓	✗	✗	✓	
2			✓	✓	✓	✗	✗
3	✗	✓	✗				✓

✗ - the hot and cold streams are not allowed to exchange heat

✓ - recommended match of hot and cold streams by Aspen Energy Analyzer

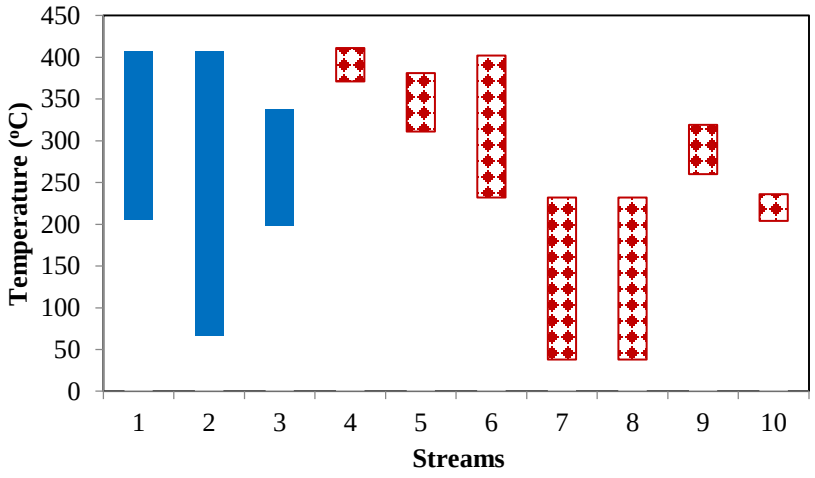

Figure 3-21. Temperature chart of the liquefaction and product recovery section.

Product upgrading (indirect)

In the indirect CBTL plant, the liquid product from the FT reactor is sent to the product upgrading section. In the conventional product upgrading section, as shown in Figure 3-22, syncrude is first

separated into naphtha, diesel and wax and then sent to two different hydrotreating units and hydrocracking unit. Instead, integrated hydrotreating of the syncrude can increase the thermodynamic efficiency and reduce the footprint of the upgrading section. In the integrated hydrotreating unit, as shown in Figure 3-23, the entire syncrude is first hydrotreated and then separated into different products for further upgrading. There is hardly any work in the existing literature on the use of an integrated hydrotreater for upgrading the FT syncrude.

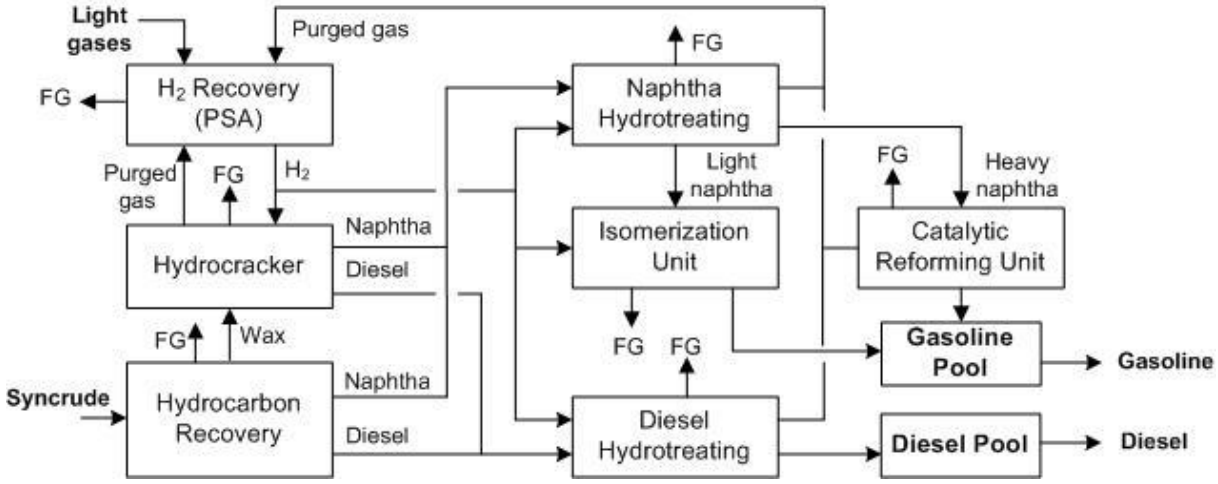

Figure 3-22. BFD of the conventional product upgrading unit with separated hydrotreating process.

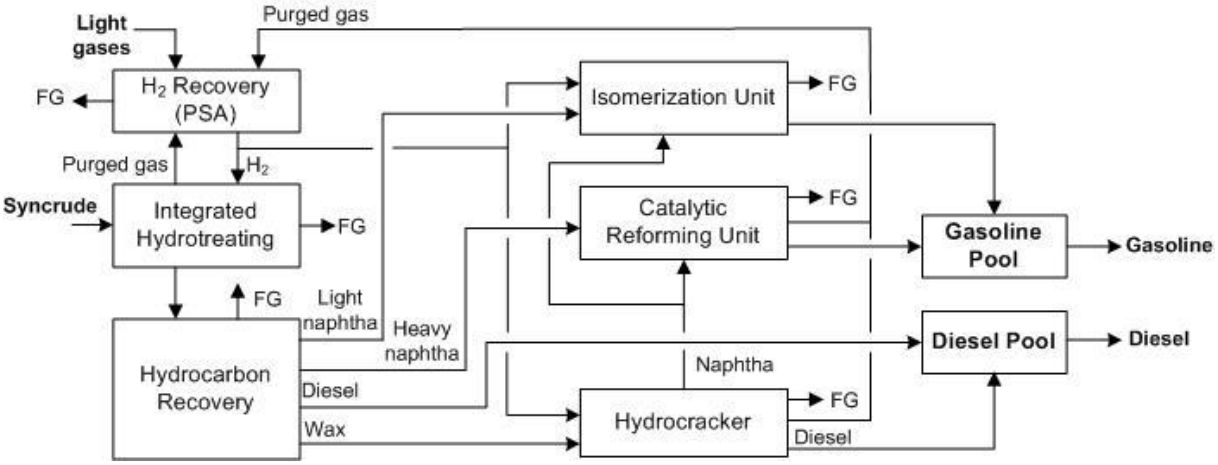

Figure 3-23. BFD of the novel product upgrading unit with integrated hydrotreating process.

In the indirect CBTL plants, the hydrotreated diesel can automatically satisfy most of the property specifications for commercial diesel. However, the straight run FT naphtha mainly contains n-paraffin, resulting in very low octane number, and needs to be further upgraded. The FT naphtha upgrading technology has been well described in the Bechtel reports (Bechtel, 1993; 1998) and has been considered in most of the recent studies on the FT plant. (Liu et al., 2011; Guo et al., 2011) In these designs, the isomerization unit increases the research octane number (RON) of the light naphtha to about 82-85 while the catalytic reforming unit increases the RON of the heavy naphtha to about 95-100. (Bechtel, 1993) Typical selection of technologies in commercial plants can also

be found in the open literature. (Klerk, 2011; Klerk and Furimsky, 2010) However, as the gasoline and diesel specifications continue to change especially with respect to their environmental impacts, suitable technologies should be selected. For example, the designs considered in the Bechtel reports (Bechtel, 1993; 1998) can lead to violation of aromatics content in the gasoline pool (Guo et al., 2011) mainly due to large quantity of high aromatics-containing gasoline from the catalytic reforming unit. One of the alternative approaches is to apply the heavy naphtha isomerization technology that can increase the octane number of the straight run heavy naphtha without producing aromatics. However, as the heavy naphtha is not only active for the isomerization reactions but also for the cracking reactions, the heavy naphtha isomerization technology will produce high amounts of fuel gas and reduce the overall gasoline yield. Previous studies indicate that with tolerable fuel gas production, the isomerization technologies can only increase the octane number to about 80-90. (Liu et al., 2011; Guo et al., 2011; Watanabe et al., 2008; Ramos et al., 2007) Therefore, as the key design parameters such as the H_2/CO ratio in the FT plant are changed, the product upgrading section needs to be appropriately designed in order to satisfy all product specifications. The H_2 required in the product upgrading section is considerable because the technologies, such as hydrotreating and hydrocracking, consume large amount of H_2 and operates under H_2-rich environment. In the indirect CBTL plant, H_2 can be recovered from the unreacted syngas and purged gas from the upgrading section, while the remaining gases can be sent to the combined cycle plant.

In the indirect CBTL plants, the wax stream from the main distillation column is sent to the wax hydrocracking unit to produce shorter-chain hydrocarbons that are then separated into light naphtha, heavy naphtha, and diesel, as shown in Figure 3-24. A simple yield model is developed by multivariable regression using the experimental data reported by UOP for their single-stage HC Unibon process. (Shah et al., 1988) The HC Unibon technology is a fixed-bed catalytic process that uses high activity bifunctional catalyst and has been developed to maximize diesel production for full conversion application. (Shah et al., 1988) The H_2 reacted per barrel of wax (F_{H_2}) depends on the gasoline to diesel ratio if the conversion is the same. Eq. (29) gives an estimation of F_{H_2} of wax hydrocracking unit correlated to the weight percentage of C_{7+} product ($y_{C_{7+}}$), where F_{H_2} is in standard cubic feet per barrel (SCFB) of wax. (Shah et al., 1988) Information on utility consumption is available in the open literature (Shah et al., 1988) and assumed to be proportional to the feed flow rate. It is noted that the wax hydrocracking model does not provide the isomer distribution of the naphtha cut required for modeling the naphtha upgrading units. Hence, a typical composition of naphtha cut from open literature is used in this study. (Gamba et al., 2010; Teles et al., 2007) The yield model developed based on UOP's data is consistent with the experimental data reported by Sasol shown in Table 3-23. (Leckel, 2005; 2007)

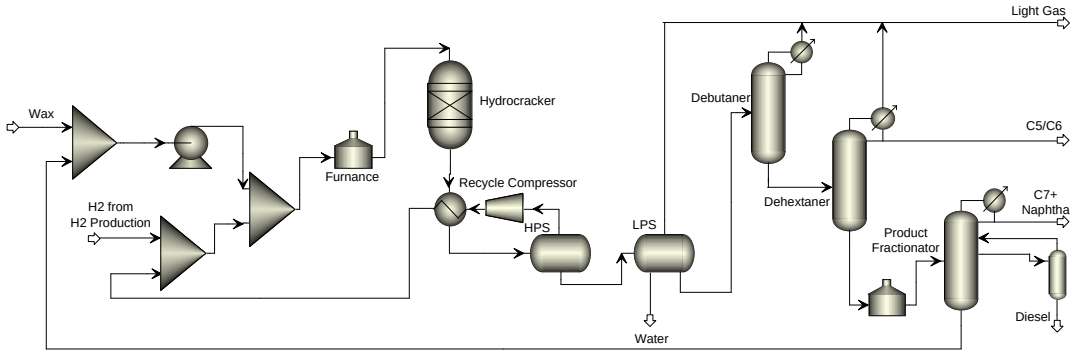

Figure 3-24. Configuration of Hydrocracking Unit.

$$F_{H_2} = 2215 - 15.427 y_{C_{7+}} \tag{29}$$

Table 3-23. Model validation for the FT wax hydrocracking unit.

wt%	Model	Leckel	Error%
C_1-C_4	7.55	7.6	-0.65
C_5-C_9	33.8	34	-0.46
C_{10}-C_{22}	58.6	58	1.05

For naphtha upgrading, the UOP Penex process, as shown in Figure 3-25, for light naphtha isomerization is considered due to its low cost. A simplified yield model has been reported by Bechtel for this process. (Bechtel, 1993) The selectivity of isomer is about 98.3 wt% and the make-up hydrogen rate is about 0.14 wt% of light naphtha feed rate. Utility consumption is assumed to be proportional to the feed flow rate. (Bechtel, 1993; 1998) The UOP CCR Platforming technology, as shown in Figure 3-26, is selected to increase the octane number of FT heavy naphtha by converting them into aromatics. According to the experimental data provided by UOP, this technology for catalytic reforming is able to increase the research octane number (RON) of FT heavy naphtha to about 100. (Bechtel, 1993; Shah, 1990) The Aspen Tech Reformer model under the Aspen One package is used for estimating the process yield and product properties. First, the target RON, the flowrate, and composition of the feed are specified in the Aspen Tech Reformer model. Then the simulation is run and the results are compared with the data provided in Bechtel's report (Bechtel, 1993), as shown in Table 3-24. It shows that the results obtained from the Aspen Tech Reformer are satisfactory.

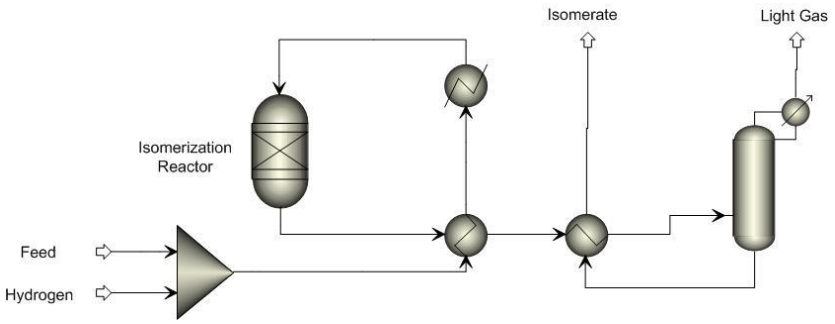

Figure 3-25. Configuration of Isomerization Unit.

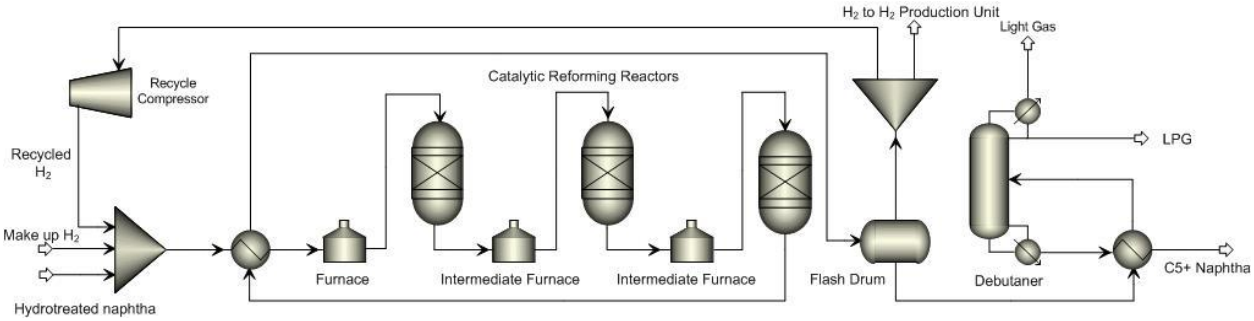

Figure 3-26. Configuration of Catalytic Reforming Unit.

Table 3-24. Comparison between Aspen model and Bechtel data for catalytic reforming.

	Aspen	Bechtel	error %
H_2 wt%	4.14	3.44	
C_1-C_5 wt%	8.68	10.67	
Reformate wt%	87.00	85.89	1.39
Specific gravity	0.80	0.77	3.49
RON	95	95	0
Benzene wt%	0.66	0.70	-5.71
Aromatic wt%	66.14	65.90	0.36

Product upgrading (direct)

One advantage of direct liquefaction process is that the products can be processed as traditional petroleum product without extensive renewal of current infrastructures. (Vasireddy et al., 2011) Compared with typical petroleum oils, the DCL syncrude obtained from the two-stage liquefaction of bituminous coals is usually low in boiling range, low in hydrogen and high in oxygen, low in heteroatom contents and high in contents of cyclic compounds, and mainly composed of paraffins, naphthenes, and aromatics. (Shinn, 1984; Vasireddy et al., 2011; Mochida et al., 2014) On the other hand, the bio-liquids usually contain high amount of oxygenates, such as cyclic ketones, alkyl-phenols, methoxy-phenols, napthols, which can be converted to cyclohexane, alkyl-cyclohexane by hydrotreating. (Stevens, 1987; Elliott, 1980; Behrendt et al., 2008) Despite these differences, the syncrude produced in the direct liquefaction plant with low biomass/coal ratio is very similar to petroleum and can be processed through petroleum refining technologies, where hydroprocessing is a major technology. (Zhou and Rao, 1992)

In the direct liquefaction process, a significant portion of the aromatics and heteroatom in the low boiling range oil is converted in the inline hydrotreating unit. The hydrotreated naphtha cut from the atmospheric distillation column is low in sulfur and nitrogen and has an octane number of about 70, which is an excellent feed for gasoline production. Isomerization and catalytic reforming technologies are applied to increase the octane number of this naphtha cut. Because the gas oil cut (177-370^{o}C) from the CTSL reactors is not completely sent to the inline hydrotreater considering

the operating flexibility and product quality (Zhou and Rao, 1992), the gas oil recovered from the atmospheric distillation column needs to be sent to the gas oil hydrotreating unit for further upgrading. In this study, the yields of the upgrading units are obtained from correlations due to the limited information on the detailed feed composition. Utility consumptions in the isomerization and catalytic reforming units are estimated based on the plant throughput using the correlations available from Bechtel Corp. (Bechtel, 1993), while detailed models of the key equipment items are developed to estimate the utility consumptions in the gas oil hydrotreating unit as shown in Figure 3-27.

In the isomerization unit, n-paraffins in the light straight run naphtha with low octane number are transformed on Pt catalyst into branched chains with the same carbon number but high octane number. The typical yield of isomerization unit used in this study is 0.35 wt% C_3, 2.39 wt% C_4 and 97.26 wt% C_{5+} with a research octane number (RON) of 83. (Fahim et al., 2010) The H_2/oil ratio in the feed is specified to be 0.14 wt% as reported by Bechtel Corp. (Bechtel, 1993) Our study only considers low biomass/coal mix ratio, and most of the oxygenates is hydrotreated and converted to paraffins and naphthenes in the hydrotreater unit. Hence, the distribution of components in the hydrotreated naphtha from biomass/coal co-liquefaction is assumed to be 15 vol% paraffins, 65 vol% naphthenes and 20 vol% aromatics, which are similar to that of DCL naphtha (Bechtel and Amoco, 1995; Vasireddy et al., 2011; Mochida et al., 2014). A yield model, shown in Eq. (30) and (31), is used in this study to estimate the yield of H_2 and C_{5+} reformate from the feed composition $(N+2A)_F$ and severity of catalytic reforming (RON_R), where N, A, and RON_R denote naphthenes (vol%), aromatics (vol%) and reformate RON, respectively. (Fahim et al., 2010; Gary and Handwerk, 2001) Eq. (32) gives the relation between RON_R and aromatic vol% in the reformate (A_R vol%). Table 3-9 shows this model can provide a reasonable estimation of DCL liquid catalytic reforming process. (Smith et al, 1982) The motor octane number (MON) of reformate can be estimated by Eq. (33). (Albahi et al., 2002; Jenkins, 1968)

$$C_{5+}\ (vol\%) = 142.7912 - 0.77033 \times RON_R + 0.219122 \times (N + 2A)_F \quad (30)$$

$$H_2\ (wt\%) = -12.1641 + 0.06134 \times C_{5+}\ (vol\%) + 0.099482 \times RON_R \quad (31)$$

$$A_R(vol\%) = 1.6857 \times RON_R - 92.994 \quad (32)$$

$$MON_R = 22.5 + 0.83RON_R - 20.0SG \quad (33)$$

Table 3-25. Validation of the yield model of the catalytic reforming unit.

Feed composition		Cases	RON_R = 94.2		RON_R = 97.7	
			Experimental	Model	Experimental	Model
N (vol%)	64.4	C_{5+} (vol%)	92.5	91.4	91.1	88.7
A (vol%)	16.0	H_2 (wt%)	2.50	2.81	3.00	3.00
		A_R (vol%)	65.8	65.8	71.7	71.7

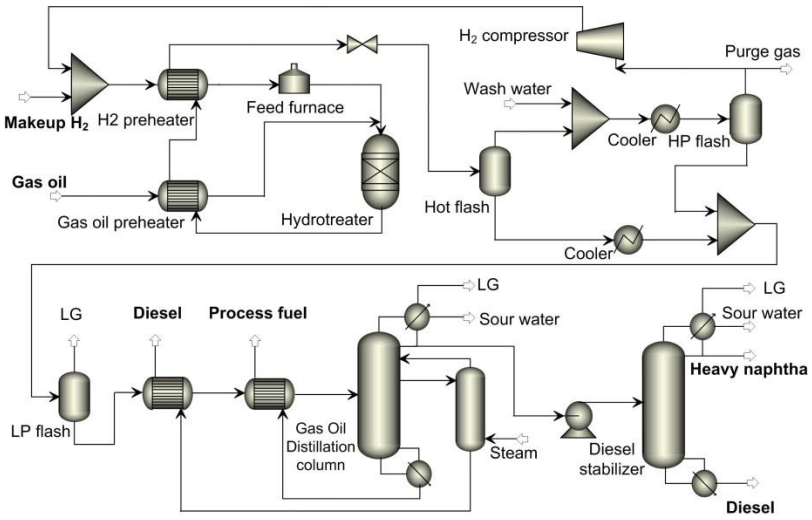

Figure 3-27. Plant configuration of the gas oil hydrotreating unit.

The main purpose of the inline hydrotreater is to stabilize the liquefaction product, while the diesel cut from the inline hydrotreater does not necessarily satisfy the diesel specification. (Wu et al., 2015) Hence, the gas oil hydrotreating unit is required to produce on-spec diesel. In the gas oil hydrotreating unit, the raw gas oil is pre-heated by the hot hydrotreated gas oil and then sent to hydrotreater with heated H_2 stream. H_2-rich stream is recovered from the HP flash drum and recycled back to the reactor. The liquid from the LP flash vessel is sent to a distillation column followed by a diesel stabilizer to separate the hydrotreated product into light gas, heavy naphtha, diesel (177-343^{o}C), and process fuel (343-454^{o}C). The approach to modeling the gas oil hydrotreating reactor is the same as the inline hydrotreating reactor as described in Section 2.2.2. The gas oil hydrotreater is operated at 180 bar and 350 ^{o}C with a pressure drop of 7 bar, a temperature increase of 83 ^{o}C, P_{H_2} of 124 bar, and a liquid hourly space velocity of 1 h^{-1}. It can be noted that these specifications are similar to that reported by Bechtel/Amoco (Bechtel and Amoco, 1995). PetroFrac model in Aspen Plus is used to simulate the distillation column and the diesel stabilizer. Peng-Robinson EOS is used as the thermodynamic model. A 'design spec' in Aspen Plus is set up to satisfy the ASTM D86 90 vol% specification of diesel (ASTM D975) by manipulating the bottom flowrate of the gas oil distillation column.

Product upgrading (hybrid)

Technologies considered for refining different syncrude are listed in Table 3-26 (Jiang and Bhattacharyya, 2015; 2016), while properties and corresponding standard of raw syncrude and refined syncrude are listed in Table 3-27 and Table 3-28. (Klerk and Furimsky, 2010; Wu et al.,2015; Comolli et al, 1995) It is noted that the properties related to restrictions on boiling range are not listed, because those requirements can always be satisfied by manipulating cut point in the distillation columns with different blending ratios. Because the hydrotreated naphtha from the indirect liquefaction route is mainly consists of n-paraffins, it is low in octane number and poor feed to the catalytic reforming unit with low reformate yield about 87%. (Klerk and Furimsky,

2010; Jiang and Bhattacharyya, 2015) On the other hand, straight run naphtha from the direct liquefaction route is rich in naphthenes and aromatics, and therefor high in octane number and becomes an excellent feed to the catalytic reforming unit with high reformate yield of about 93%. (Comolli et al, 1995; Fahim et al., 2010; Gary and Handwerk, 2001; Jiang and Bhattacharyya, 2016) For the diesel pool, the straight run diesel from the indirect liquefaction route is extremely low in sulfur and high in cetant number/index, because most of sulfur in the coal and biomass is removed before being sent to the Fisher-Tropsch synthesis unit, and aromatics yield of the Fisher-Tropsch synthesis unit is negligible, while the straight run diesel from the direct liquefaction route has relatively poor properties and requires further upgrading.

Table 3-26. Syncrude refinery technologies.

	Indirect CBTL	Direct CBTL
whole syncrude	integrated hydrotreating	inline hydrotreating
wax	wax hydrocracking	
light naphtha	isomerization (GTC's Isomalk2)	isomerization (GTC's Isomalk2)
heavy naphtha	catalytic reforming (UOP's CCR)	catalytic reforming (UOP's CCR)
diesel		diesel hydrotreating

Table 3-27. Properties of raw and refined syncrude (gasoline pool).

	Density (kg/m^3)	RON	MON	[R+M]/2	Sulfur (ppm, wt)	Aromatics (vol%)	Olefin (vol%)
Indirect liquefaction							
straight run naphtha*	680	55	50	52.5	trace	trace	
refined light naphtha	625	90	87	88.5	0	0	0
refined heavy naphtha	745	95	87	91	0	61	1.0
straight run heavy naphtha	720	45	40	42.5	0	0	1.0
heavy naphtha from wax hydrocracking unit	725	84	76	80	0	2	40
Direct liquefaction							
straight run naphtha	765	70	64	67	20	19	
refined light naphtha	660	90	87	88.5	20	0	0
refined heavy naphtha	790	95	87	91	20	66	0.2
US standards (ASTM D4814; CA RFG; 40 CFR 80)							
maximum					20	35	
minimum				87			

*After integrated hydrotreating

Table 3-28. Properties of raw and refined syncrude (diesel pool).

	Density (kg/m^3)	Cetane index	Sulfur (ppm, wt)	Aromatics (vol%)
Indirect liquefaction				
straight run diesel	775	73.3	0	0
diesel from wax hydrocracking	789	73	0	2
Direct liquefaction				
straight diesel*	850	33.8	77.5	23.2
refined diesel	880	38.1	10	8.4
US standards (ASTM D975)				
maximum	876		15	35
minimum		40		

Because of the difference in the properties between syncrude from indirect and direct liquefaction routes, it is possible to reduce the penalty of hydrocarbon upgrading units by optimal blending. By blending, less amount of heavy naphtha from indirect liquefaction is required to be sent to the catalytic reforming unit to achieve the gasoline standard, where less amount of diesel from direct liquefaction is required to be sent to the hydrotreating unit to achieve the diesel standard. It is observed from Table 3-2 and Table 3-28 that the octane number ([R+M]/2) of gasoline and sulfur content in diesel are the two hardest specifications to achieve. Hence, in this study, the percentage of heavy naphtha from indirect liquefaction to the catalytic reforming unit (CCR %) is manipulated to satisfy the octane number standard of gasoline, while the percentage of straight run diesel from the direct liquefaction unit to the diesel hydrotreating unit (HDT %) is manipulated to satisfy the sulfur content limitation of diesel. Table 3-29 provides the results of smart blending with different indirect to direct syncrude weight ratio. In Table 3-29, Eq. (34) and Eq. (35) are applied to estimate the research octane number (RON) and motor octane number (MON) of the gasoline pool after blending, where the terms represent volumetric average values of properties as following: R=RON, M=MON, J=RON-MON, RJ=R×J, MJ=M×J, O=Olefins vol%, A=Aromatics vol%, while linear combination is assumed for all other properties. (Maples, 2000) In Table 3-29, the upgrading cost saved of the cases with any blending ratio in between 0/100 and 100/0 is larger than of the pure indirect liquefaction process (100/0) and the pure direct liquefaction process (100/0), which indicates that the hybrid liquefaction process does reduced the cost of downstream syncrude upgrading process.

$$R = \bar{R} + 0.03324[\overline{RJ} - \bar{R} \cdot \bar{J}] + 0.00085\left[\left(\overline{O^2}\right) - (\bar{O})^2\right] \tag{34}$$

$$M = \bar{M} + 0.04285[\overline{MJ} - \bar{M} \cdot \bar{J}] + 0.00066\left[\left(\overline{O^2}\right) - (\bar{O})^2\right] - 0.00632\left[\frac{\left(\overline{A^2}\right) - (\bar{A})^2}{100}\right]^2 \tag{35}$$

Table 3-29. Pmart blending of indirect and direct syncrude.

Indirect/Direct	0/100	10/90	20/80	30/70	40/60	50/50
CCR%	0	22.3	58.0	69.9	75.9	79.5
HDT%	92.8	90.6	88.5	85.4	81.3	75.5
Cost saved* (MM$/yr)	0.23	0.64	0.70	0.76	0.83	0.91
Gasoline pool						
Density (kg/m^3)	725	719	714	710	707	704
[R+M]/2	89.5	87	87	87	87	87
Sulfur (ppm, wt)	20	16.8	14.1	11.8	9.6	7.6
Aromatics (vol%)	33.2	28.9	29.0	29.1	29.2	29.3
Diesel pool						
Density (kg/m^3)	852	846	839	833	826	819
Cetane index	37.8	40.8	44	47.2	50.5	53.9
Sulfur (ppm, wt)	15	15	15	15	15	15
Aromatics (vol%)	9.5	8.9	8.4	7.9	7.3	6.7
Indirect/Direct	60/40	70/30	80/20	90/10	100/0	Standards
CCR%	81.8	83.6	84.8	85.8	86.6	
HDT%	66.9	52.6	23.9	0	0	
Cost saved* (MM$/yr)	0.99	1.10	1.29	1.31	0.56	
Gasoline pool						
Density (kg/m^3)	701	698	696	694	692	
[R+M]/2	87	87	87	87	87	>87
Sulfur (ppm, wt)	5.8	4.2	2.7	1.3	0	<20
Aromatics (vol%)	29.4	29.5	29.5	29.6	29.6	<35
Diesel pool						
Density (kg/m^3)	812	804	797	787	775	<876
Cetane index	57.4	61	64.8	68.9	73.3	>40
Sulfur (ppm, wt)	15	15	15	9.7	0	<15
Aromatics (vol%)	6.1	5.3	4.9	3.2	0.7	<35

*In the base case, all heavy naphtha is sent to the catalytic reforming unit, and entire diesel cut is sent to the diesel hydrotreating unit. Equipment life is assumed to be 10 years to annualize the capital cost. The capital and utility cost of upgrading units are available in the open literature. (Jiang and Bhattacharyya, 2016; Bechtel, 1998)

H_2 network and pressure swing adsorption (PSA)

In the product upgrading section, H_2 produced in the catalytic reforming unit and the purged gases from the hydroprocessing units and the CTSL unit, shown in Figure 3-28, are sent to the H_2 recovery unit, which is a polybed PSA process, to produce a portion of the pure H_2 for hydroprocess ing. The remaining H_2 requirement can be satisfied by sending a portion of the FT vapor to the PSA unit to recover H_2 from the unconverted syngas. In this study, component separator block is used for simulating the PSA unit. (Bechtel, 1993) In should be noted that the

PSA unit is an unsteady state process, where a number of adsorber vessels is cycled in a desired sequence changing their pressure typically between 2620 kPa and 690 kPa for adsorption and desorption, respectively. (Bechtel, 1993) In this study, it is assumed that the number of beds in the PSA unit and the sequence have been appropriately designed so that the H_2 is available continuously at the desired rate. A model of the H_2 network is developed to estimate the flowrate of the make-up H_2 stream and the amount of FT vapor that can be recycled back to the FT reactor. The high H_2 partial pressure in the hydroprocessing reactors is usually maintained by recycling unreacted H_2. The product from the hydroprocessing reactor is cooled and sent to a H_2 recovery flash drum. The majority of the vapor stream is sent back to the reactor and the rest is purged and sent to the PSA H_2 recovery unit to avoid light gas accumulation in the reactor. The purge rate is manipulated to maintain the H_2 partial pressure required by corresponding hydroprocessing unit, while flowrate of the make-up H_2 is manipulated to achieve the required H_2/Oil ratio in the reactor.

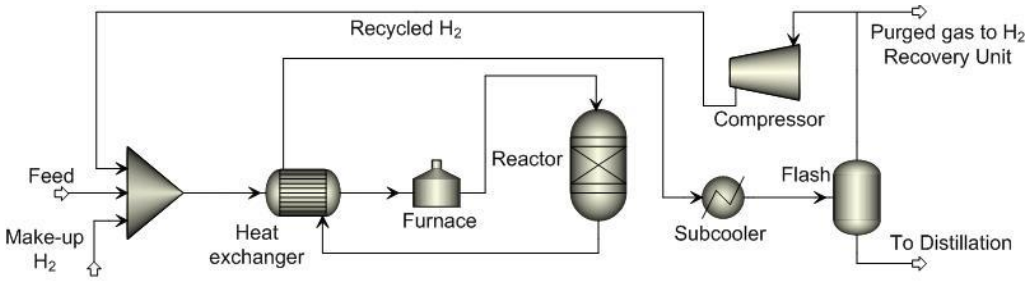

Figure 3-28. General configuration of the hydroprocessing unit.

Shale gas steam methane reforming (SMR)

If shale gas is utilized in the direct CBTL plant for hydrogen production, SMR is one of the promising and widely applied technologies. In the SMR unit, as shown in Figure 3-29, the shale gas is compressed, heated by the steam reformer outlet stream and sent to an adiabatic pre-reformer, where heavier hydrocarbons are converted to methane and syngas through Reactions 8-10. The outlet stream of the pre-reformer is reheated by exchanging heat with the stream reformer outlet stream and then sent to the steam reformer, where most of the methane is converted to syngas by Reaction (36) and (39). The heat required by the highly endothermic in the steam reforming process is produced in the reformer furnace by burning fuel gas taken from the plant fuel gas header. The product of stream reformer is cooled and sent to HTS and LTS reactors. The syngas from the shift reactors is cooled by generating HP, intermediate pressure (IP), and LP steams. The syngas from the LP steam generator is sent to a condenser to remove most of the water. The hot flue gas from the reformer furnace is sent to a series of heat exchangers to generate super-heated HP steam used for steam reforming. In this study, the pre-reformer and steam reformer are modeled as equilibrium reactors. (Molburg and Doctor, 2003) The HTS and LTS reactors are modeled as plug flow reactors (PFRs) with kinetics obtained from the open literature. (Bhattacharyya et al., 2011) The reformer furnace is modeled as 'RStoic' reactor in Aspen Plus with specified combustion reactions. The Peng-Robinson EOS is used as the thermodynamic model of the syngas side, while IAPWS-95 is used for the steam side. The operating conditions of all reactors and heat exchangers can be found in Table 3-30.

$$C_nH_m + nH_2O \rightarrow nCO + \left(n + \frac{m}{2}\right)H_2 - Q \quad (36)$$

$$CO + 3H_2 \leftrightarrow CH_4 + H_2O + Q \quad (37)$$

$$CO + H_2O \leftrightarrow CO_2 + H_2 + Q \quad (38)$$

$$CH_4 + 2H_2O \leftrightarrow CO_2 + 4H_2 - Q \quad (39)$$

Table 3-30. Operating conditions of the shale gas SMR unit.

Flowsheet element	Parameter	Value
Shale gas feed	Temperature/pressure	20 ºC/20 bar
Compressor	Pressure	30 bar
Steam feed	Temperature/pressure	510 ºC/30 bar
Preheaters	Cold stream outlet temperature	510 ºC/650 ºC
Adiabatic pre-reformer	Pressure drop	1.7 bar
Steam reformer	Temperature/pressure drop	815 ºC/1.7 bar
HP/IP/LP steam evaporator	Hot stream outlet temperature	350 ºC/215 ºC/143 ºC
Cooler	Hot stream outlet temperature	40 ºC
Feed water heater/economizer	Cold stream outlet temperature	120 ºC/227 ºC

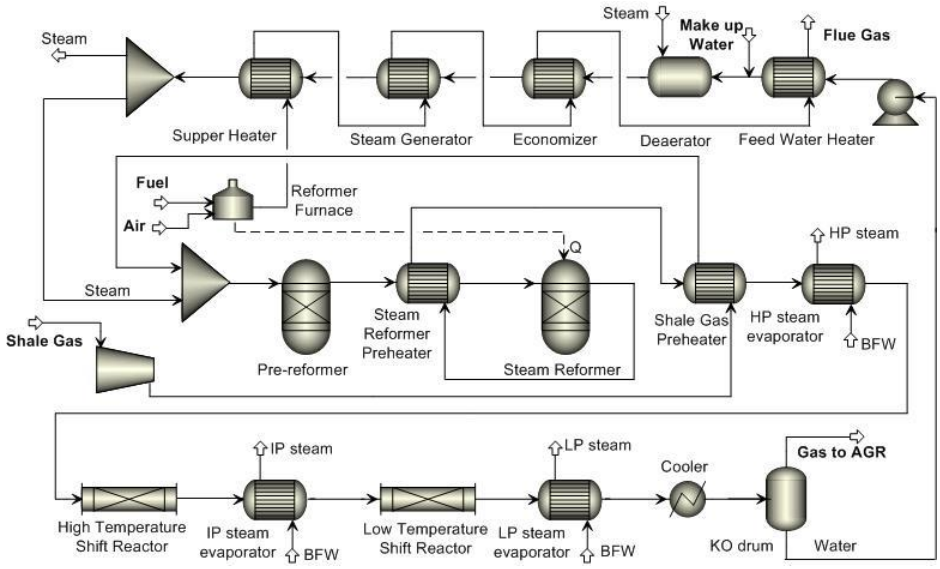

Figure 3-29. Plant configuration of the shale gas SMR unit.

Autothermal reforming (ATR)

In the indirect CBTL plant, light hydrocarbon produced in the FT unit is converted into syngas and fed back to the FT reactor thru ATR reactor for higher overall efficiency. The ATR unit uses a combination of exothermic partial oxidation and endothermic steam reforming reactions while operating under thermally neutral conditions to achieve optimum efficiency with less complicated facilities and less or no external energy in comparison to the steam reforming units. The process can practically approach adiabatic conditions if appropriately designed. Figure 3-30 gives the configuration of the ATR unit, where the ATR reactor is simulated as combination of an RGibbs reactor and a PFR. For modeling purpose, the ATR reactor feed is separated in a dummy component separator, where C_1 and C_{2+} hydrocarbons are separated, and the steam/carbon and O_2/carbon ratios of the two streams are maintained to be the same as in the feed. Availability of information on reforming kinetics of C_{2+} hydrocarbons is scarce in the open literature. However, several studies indicate that reforming of C_{2+} hydrocarbons are faster than methane reforming and results in methane formation. (Ayabe, et al., 2003; Schadel et al., 2009; Schadel and Deutschmann, 2005) Hence, it is assumed that chemical equilibrium is reached for C_{2+} hydrocarbon and therefore, these reactions are modeled by using the RGibbs block. The product of the RGibbs block is mixed with the C_1 stream and sent to a PFR, where the methane reforming reaction is considered. The kinetics of methane reforming on Ni/Al_2O_3 catalysts are shown in Table 3-31 with the kinetic parameters obtained from the open literature. (Rafiq et al., 2012) A high steam/carbon ratio is usually used to increase the H_2 yield. If moderate H_2/CO ratio is required in the syngas, a low steam/carbon ratio can be used in the ATR unit to reduce the utility cost. (Steynberg and Dry, 2004) The steam/carbon ratio is set to be 0.63 for syngas production in this study. The oxygen flowrate is manipulated to achieve a reactor outlet temperature of 982ºC. The SRK EOS is used to calculate the thermodynamic properties.

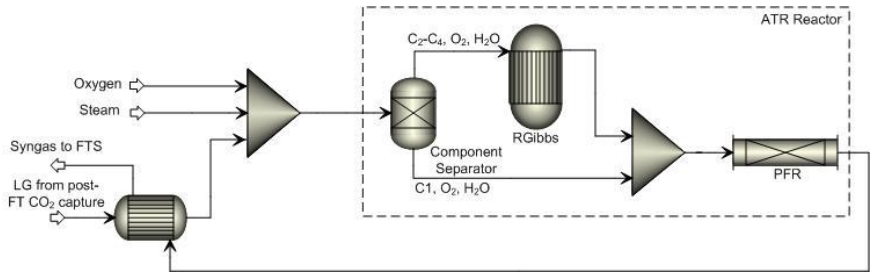

Figure 3-30. Configuration of the ATR unit.

Table 3-31. Reactions considered in the ATR kinetic model.

No.	Name	Reaction	Reaction Heat	Kinetic Equation
1	Oxidation	$CH_4 + 2O_2 \rightarrow CO_2 + 2H_2O$	exothermic	$r_1 = k_1 \cdot P_{CH4} \cdot P_{O2}$
2	Steam Reforming	$CH_4 + H_2O \leftrightarrow CO + 3H_2$	endothermic	$r_2 = k_2 \cdot P_{CH4} \cdot P_{H2O}\left(1 - \frac{P_{CO} \cdot P_{H2}^3}{K_1 \cdot P_{CH4} \cdot P_{H2O}}\right)$
3	Dry Reforming	$CH_4 + CO_2 \leftrightarrow 2CO + 2H_2$	endothermic	$r_3 = k_3 \cdot P_{CH4} \cdot P_{CO2}\left(1 - \frac{P_{co}^2 \cdot P_{H2}^2}{K_2 \cdot P_{CH4} \cdot P_{CO2}}\right)$
4	Water-Gas Shift	$CO + H_2O \leftrightarrow CO_2 + H_2$	slight exothermic	$r_4 = k_4 \cdot P_{CO} \cdot P_{H2O}\left(1 - \frac{P_{CO2} \cdot P_{H2}}{K_3 \cdot P_{CO} \cdot P_{H2O}}\right)$

Figure 3-31 shows that the simulation results agree well with the data available in the open literature for the ATR unit as part of a CTL plant for different feed compositions and operating conditions. (NETL, 2007; Bechtel, 1998) It should be noted that, in the CTL plant, the recycle gas to the ATR unit contains not only light hydrocarbons, but also some unconverted syngas, that strongly impacts the product distribution because of the WGS reaction. The data considered for model validation cover the range of feed compositions and operating conditions listed in Table 3-32. Table 3-33 to Table 3-35 provide detailed stream information for various cases that have been considered for model validation.

Table 3-32. Range of feed composition and operating conditions for ATR model validation.

	Steam/Carbon (mol/mol)	Oxygen/Carbon (mol/mol)	Syngas/Hydrocarbons (mol/mol)	Outlet Temperature (°C)
Minimum	3.76	0.509	3.125	971
Maximum	1.23	0.157	13.15	982

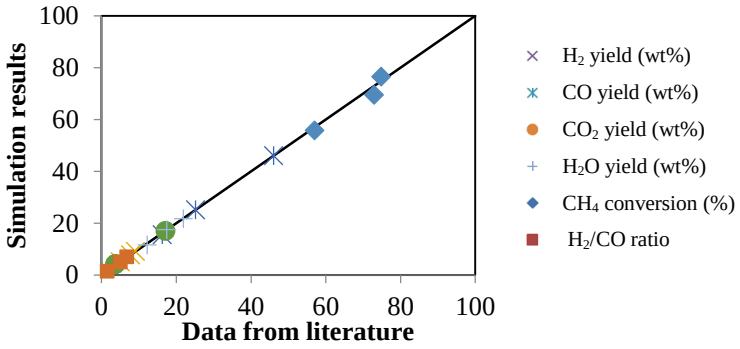

Figure 3-31. ATR model validation.

Table 3-33. Results from the ATR unit model in comparison to the Bechtel data (Bechtel, 1998).

		Feed		Product	
Flowrate (kmol/hr)	Recycle	Steam	Oxygen	Model	Reported
H_2O	0	3068	0	2378	2365
CO_2	38	0	0	944	950
H_2	4507	0	0	6088	6114
CO	4316	0	0	4017	4018
CH_4	465	0	0	205	200
O_2	0	0	415	0	0
N_2	1128	0	2	1128	1128
C_2-C_4	169	0	0	0.44	

Table 3-34. Results from the ATR unit model in comparison to NETL's commercial scale CTL plant (NETL, 2007).

	Feed			Product	
Flowrate (kmol/hr)	Recycle	Steam	Oxygen	Model	Reported
H_2O	0	3367	0	1814	1904
CO_2	38	0	0	269	232
H_2	7289	0	0	12855	12679
CO	576	0	0	2527	2521
CH_4	2344	0	0	548	591
O_2	0	0	430	0	0
N_2	4673	0	8	4673	4673
C_2-C_4	185	0	0	0	

Table 3-35. Results from the ATR unit model in comparison to NETL's small scale CTL plant (NETL, 2007).

	Feed			Product	
Flowrate (kmol/hr)	Recycle	Steam	Oxygen	Model	Reported
H_2O	0	482	0	452	456
CO_2	8	0	0	48	42
H_2	1251	0	0	1454	1455
CO	132	0	0	207	216
CH_4	75	0	0	23	20
O_2	0	0	62	0	0
N_2	644	0	1	642	644
C_2-C_4	30	0	0	0	

CO_2 compression

The CO_2 captured from the CO_2 containing streams is compressed by a split-shaft multistage compressor. The final pressure of the sequestration-ready CO_2 is 15.16 MPa. Impurity limits in the CO_2 to be sequestered (Bhattacharyya et al., 2011) should be satisfied. The limits on H_2S, CH_4, and SO_2 are automatically satisfied, but the H_2O content in the stream out of the LP flash vessel is higher than the limit, i.e. 0.015 vol %. 90% of the incoming water in the CO_2 stream is removed by cooling and flashing. The remaining amount of water that needs to be removed to satisfy the limits is removed in an absorber using triethylene glycol (TEG) as the solvent. The modeling approach for this section can be found in the work of Bhattacharyya et al. (Bhattacharyya et al., 2011)

Combined cycle power plant

In the indirect CBTL plant, the fuel gas from the PSA unit and the hydrocarbon upgrading section provides fuel required in the FT synthesis and the entire hydrocarbon upgrading units. The

remaining portion is sent to the gas turbine (GT) for electricity production, shown in Figure 3-32. The appropriate GT model for this CBTL plant is selected to be GEE MS7001EA, which has a designed power rating of 85 MW, a simple cycle efficiency of 32.7% (natural gas), and could been used for H_2-rich (H_2% >50%) gas. Chiesa et al. have evaluated the possibility of burning H_2-rich gas in large heavy-duty gas turbine designed for natural gas. (Chiesa et al., 2005) If H_2-rich gas is fed into GT, steam or nitrogen dilution is required to controlled NO_x emission, and three strategies, variable guide vane operations, increasing pressure ratio and re-engineered machine, can be considered for proper operation. (Chiesa et al., 2005) In this study, nitrogen dilution is selected for NO_x control, taking advantage of the existing ASU, and machine is assumed to be re-engineered so that GT firing H_2 rich gas can be operated without air extraction (Chiesa et al., 2005; NETL, 2010) and with the same pressure ratio and first rotor inlet temperature as firing natural gas (Chiesa et al., 2005), while the turbine outlet temperature is about 14 K lower. (Chiesa et al., 2005) The same simulation method reported by Bhattacharyya et al. for GT in IGCC plant with CCS is applied to estimate the performance of the GT. (Bhattacharyya et al., 2011) The N_2 to fuel ratio is manipulated to reduce the stoichiometric flame temperature to 2300 K. (Chiesa et al., 2005) The operating conditions of MS7001EA firing natural gas are obtained from the open literature. (GEE) The combustion air is compressed to 12.7 atm in an axial flow compressor. The GT combustor temperature is maintained at 1150ºC with a specified heat loss of 1.5% of the fuel gas LHV by manipulating the combustion air flow. The GT firing temperature is maintained at 1125ºC by manipulating the air flow rate to the combustor outlet gas before the first expansion stage. The exhaust temperature is maintained at 526ºC by manipulating the isentropic efficiency. (Bhattacharyya et al., 2011; Chiesa et al., 2005)

A model of the triple-pressure HRSG with reheat is developed for the indirect CBTL process, with the configuration shown in Figure 3-33 and Table 3-36. The steam for power generation is mainly produced by recovering heat from the gas turbine exhaust flue gas, radiant syngas cooler, heat recovery exchangers and the FT reactor cooling system. Part of the steam produced is sent to other units for operating. The pressure levels and steam turbine inlet conditions are specified based on the studies conducted recently for FT application (Bechtel, 1993; Steynberg and Nel, 2004), while 6% pressure drop is considered for the reheat section. (Spencer et al., 1963) The minimum temperature of flue gas to the stack is set at 120ºC. (Bhattacharyya et al., 2011) For the performance of a three-pressure-level steam turbine with multiple steam addition and extraction points, a simple stage-by-stage calculation is done in Matlab based on the algorithm presented by Lozza. (Lozza, 1990)

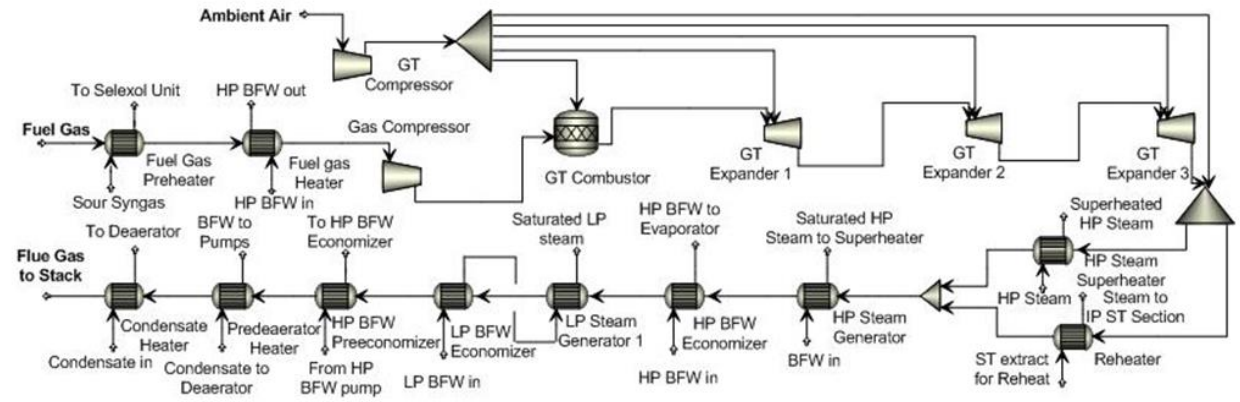

Figure 3-32. Configuration of the combined cycle power plant (fuel side).

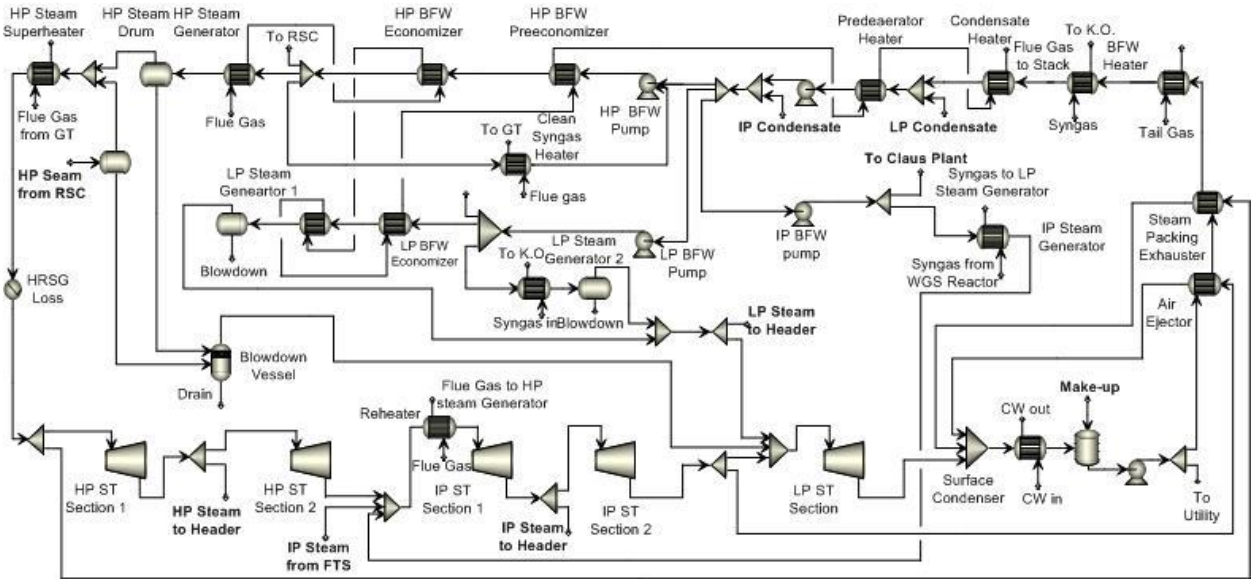

Figure 3-33. Configuration of the combined cycle power plant (steam side).

Table 3-36. Configuration and operating conditions of the HRSG section and steam header.

Steams	Pressure (kPa)	Temperature (ºC)	From	To
HP steam to ST	7419	373.9	SHR, HRSG	ST HP section
IP steam to ST	2172	346.1	SHR, Claus, FT (through reheater)	ST IP section
LP steam to ST	365	141.7	SHR, HRSG	ST LP section
HP steam to header	4137		ST	Upgrading unit, ATR
IP steam to header	931		ST	SWS, Selexol unit
LP steam to header	365		SHR, HRSG	MDEA/PZ unit, upgrading unit

In the model, the steam properties are evaluated by the IAPWS IF97 correlations and coded in Matlab. Given the flowrate, pressure, temperature of the stage inlet, specific speed (N_s), Δh_{is} and the outlet steam condition can be solved by Eq. (40), Eq. (41) and IAPWS IF97 correlations. The stage power output is calculated by Eq. (42), where isentropic efficiency (η_{st}) is a known function of N_s and the average moisture content across the stage given by Lozza.[64] The net power output of the steam turbine is shown in Eq. (43). If no information is available, the exhaust velocity of last stage (v_{ex}) is assumed to be 250 m/s. (Baily et al., 1967)

$$N_s = (RPM/60) \cdot \sqrt{V_{ex}}/(\Delta h_{is})^{0.75} \tag{40}$$

$$\Delta h_{is} = k_{is} \cdot u^2/2 \tag{41}$$

Where V_{ex} is the volumetric flow rate at stage outlet under isentropic condition in m^3/s;

Δh_{is} is the stage isentropic enthalpy drop in J/kg;

u is the mean diameter peripheral velocity of steam turbine in m/s, which is given by a function of stage number;

k_{is} is the stage head coefficient, and correlated with N_s.

$$W_i = \Delta h_i = m_i \cdot \Delta h_{is,i} \cdot \eta_{st,i} \tag{42}$$

$$P_{net} = \eta_g \cdot \eta_m \cdot \eta_l \cdot \left(\sum_i W_i - m_{last\ stage} \cdot \Delta h_{ek}\right) \tag{43}$$

Where, η_g, η_m, η_l are the generator loss, mechanical loss and sealing loss, which is a function of steam turbine power rating; $\Delta h_{ek} = v_{ex}^2/2$ is the energy loss due to axial exhaust velocity.

In the direct CBTL plant, most of the flue gas and waste heat produced in the product recovery and upgrading unit, the POX/CG unit and the SMR unit are utilized in the combined cycle power island. The steam generator in the combined cycle power island operates at three pressure levels and not only produces steam to generate electricity but also provides IP and LP steams needed in the POX/CG, product upgrading, and AGR units, as shown in Table 3-37. The modeling approach of the combined cycle plant and its pressure levels is the same as the indirect CBTL plant.

Table 3-37. Configuration of the HRSG section and steam header.

Steams	Pressure (bar)	Temperature (ºC)	From	To
HP steam to ST	114	510	POX, GT, SMR	ST HP section
IP steam to ST	25	510	POX, SMR, HCR (through reheater)	ST IP section
LP steam to ST	4	140	GTFG, HCR, SMR POX, HCU	ST LP section
HP steam to header	57		ST HP section	POX, HCU
IP steam to header	9		ST IP section	AGR
LP steam to header	4		ST LP section	AGR, HCU

Summary of modeling approach

The modeling approach and operating conditions of the indirect and direct CBTL plant is summarized in Table 3-38 and Table 3-39, while the hybrid CBTL plant is a combination of indirect and direct CBTL plants.

Table 3-38. Summary of the key equipment simulation approach and operating conditions.

Blocks	Highlight of simulation approach	Operating conditions
Gasification	Equilibrium model for coal gasification and yield model for biomass gasification	Fluidized bed reactor at 2380 kPa, 850 °C
WGS	PFR model in Aspen Plus with LHHW kinetics	Adiabatic single stage with inlet temperature of 250 °C
Selexol unit	Dual-stage Selexol unit modeled in Aspen Plus using RadFrac blocks for absorbers	2048 kPa, 2 °C (solvent chilling temperature)
Fischer-Tropsch	Yield model using modified correlation from open literatures and ASF theory for conversion and product distribution	Fe-catalyzed slurry bed reactor at 2000 kPa, 257 °C
Post-FT CO_2 removal	RadFrac with equilibrium stage for physical absorption and rate-based stage for chemical absorption	Absorber at 1965 kPa, 38 °C (MEA or MDEA/PZ) or 2 °C (Selexol)
CO_2 compression	Multistage compressor in Aspen Plus	15.3 MPa for CO_2 pipeline
Autothermal reformer	PFR model in Aspen Plus with power law kinetics	1965 kPa, adiabatic with outlet temperature of 982 °C
Hydrocarbon recovery	PetroFrac for distillation columns	
Hydrogen recovery	A polybed PSA process modeled in Aspen Plus using component separator block	Adsorption at 2620 kPa and desorption at 690 kPa
Hydroprocessing	Yield model developed for reactors; heat exchanger, compressor, distillation column modeled using Aspen Plus library blocks	
Isomerization	Same as above	UOP Penex process
Catalytic reforming	Aspen Tech Reformer under the Aspen One package	UOP CCR Platforming technology
Combined cycle power plant	Stage-by-stage estimation of steam turbine performance in Matlab; Aspen Plus standard models for others	Three pressure level HRSG with reheat, 7419/2172/365 kPa

Table 3-39. Summary of the process model of direct CBTL plants.

Section/Block	Simulation Approach	Property Model/Operating Conditions
Liquefaction and hydrocarbon recovery		Peng-Robinson
Liquefaction	Close-coupled yield model for two ebullated-bed reactors in series	1st stage: 407 °C, 22.1 MPa 2nd stage: 432 °C, 20.7 MPa
Inline hydrotreating	Yield model	370 °C, 17.2 MPa
Distillation columns	PetroFrac	Atmospheric column: 2.8 bar Vacuum column: 0.1 bar
ROSE-SR	Component separator for settlers and flash vessel for deashing solvent separator	Solvent/solid weight ratio: 3 1st stage settler: 300 °C, 55 bar 2nd stage settler: 370 °C, 54.5 bar
Product upgrading		Peng-Robinson
Gas oil hydrotreating	Same as inline hydrotreater	350 °C, 180 bar, LHSV: 1 h^{-1}
Isomerization	Yield model	Hydrogen/oil: 0.14 wt% Targeted RON: 83
Catalytic reforming	Yield model	Targeted RON: 95
Syngas Production		
Pre-reformer	RGibbs model	Adiabatic; Inlet: 510 °C, 27 bar
Steam reformer	RGibbs for reformer and Rstoic with combustion reactions for furnace	Reformer: 815 °C, 25 bar Reformer furnace: 955 °C
Gasification	RGibbs model	1315 °C, 56 bar
Water gas shift	Plug flow reactor	CO conversion: 95%
Acid gas removal and hydrogen recovery		ELECNRTL/PC-SAFT
Chemical absorption	RadFrac model with rate-based stages and reaction kinetics	Absorber: 40 °C Regenerator: 1.7 bar
Physical absorption	RadFrac model with equilibrium stages	Solvent chilling: 2 °C
Hydrogen recovery	Polybed PSA process modeled as component separator	Adsorption: 26.2 bar Desorption: 6.9 bar
CO_2 compression	Multistage compressor	15.3 MPa for CO_2 pipeline
Power island		Ideal/IAPWS-95
Combined cycle	Stage-by-stage estimation of steam turbine and Aspen Plus standard models for others	Triple-pressure HRSG with reheat: 114/25/4 bar

✓ **Process model validation**

Table 3-40 shows a comparison of the material and energy balances of the indirect CBTL plant with CCS (base case) with the data available in the open literature for the indirect CTL plant. (Liu et al., 2011; NETL, 2007; Bechtel, 1998) As shown in Table 3-38, the overall thermal efficiency and the carbon efficiency of the base case analyzed in this project is similar to those of the previous studies. The efficiency obtained in this study is slightly higher than the data reported by other studies with the similar extent of CO_2 capture mainly due to the difference in feedstock, CO_2 capture technology, extent of CO_2 capture, product upgrading technologies and their operating conditions as discussed in the previous sections.

Table 3-40. Material and energy balance of the indirect CBTL plant.

		Bechtel	NETL[a]	Liu et al.	Liu et al.	Base case[b]
Report Year		1993	2007	2011	2011	2014
Feedstock						
Coal (dry)	ton/hr	702.13	908.54	892.02	94.88	153.44
Biomass (dry)	ton/hr	0	0	0	126.83	13.29
Product						
Propane	ton/hr	6.45	0	0	0	0
Butanes[c]	ton/hr	(11.98)	0	0	0	0
Gasoline	bbl/day	23,943	22,173	N/A	N/A	4,050
Diesel	bbl/day	24,686	27,819	N/A	N/A	5,950
Total FT Liquid	bbl/day	48,629	49,992	50,000	9,845	10,000
Electric Power	MW	-54.32	124.25	295	53	12.28
Analysis						
CO_2 Removal Technology		Rectisol MDEA	Selexol, MDEA	Rectisol	Rectisol	Selexol, MDEA/PZ
CCS		No	Yes	Yes	Yes	Yes
C Captured by FTL	%	N/A	35.5	34.1	33.7	36.4
C Captured by CCS	%	0	56.6	51.6	53.7	56.9
Thermal Efficiency[d]	% (HHV)	51.8	42.4	46.0	47.5	46.8

a) Additional refinery is required for producing on-specification gasoline; efficiency is expected to be higher.
b) Data generated in this study
c) In Bechtel's refinery design, purchased n-butane are required for the upgrading section, such as C_4 isomerization and alkylation unit. (Bechtel, 1993; 1998)
d) The HHV of FT derived gasoline and diesel is assumed to be 45,471 kJ/kg and 47,655 kJ/kg.

Given the steady-state process model developed in Aspen Plus, material and energy balances can be computed for all four configurations. Due to the limited information on applications of CCS technologies for DCL processes, simulation results are only validated for the SMR_VT and CG_VT processes. It is generally accepted that the DCL processes without CCS usually have a thermal efficiency between 60% and 70%. (Wu et al., 2015) As shown in Table 3-41, results from our study are in-between the values reported by HTI (73.4%) and Shenhua (59.8%) and seem reasonable. (Williams and Larson, 2003; Comolli et al., 1995; Bechtel and Amoco, 1990; Bauman and Maa, 2014) The differences are mainly due to the different types of coal, whether all utility

consumption is included for efficiency calculation, and different sources for hydrogen and process utility. Detailed material and energy balances for all four configurations can be found in Table 3-42, which indicates that the thermal efficiency of the direct CBTL plant can be significantly increased by producing hydrogen from shale gas. Application of CCS will reduce the thermal efficiency by 2.2% if H_2 is produced from steam reforming or 2.1% if H_2 is produced by gasification.

Table 3-41. Comparison between the simulation results and data in the open literature.

Process	SMR_VT	CG_VT	HTI design(1)	Modified HTI design(2)	Bechtel/ Amoco design(3)	Modified Bechtel/ Amoco design	Shenhua design
Reference		Comolli et al., 1995	Comolli et al., 1995	Comolli et al., 1995	Williams and Larson, 2003	Williams and Larson, 2003	Bauman and Maa, 2014
Biomass (wt %)	8	8	0	0	0	0	0
Hydrogen source	Shale gas	Coal/ biomass	Natural gas	Coal	Coal	Coal	Coal
Power and fuel source	Fuel gas*	Fuel gas*	N/A	N/A	Natural gas	Coal	Coal
Efficiency (HHV, %)	66.5	62.1	73.4	70.9	61.6	59.0	59.8

*Fuel gas is generated insider plant mainly from the liquefaction unit and product upgrading units.
(1) In the original HTI design, utility consumptions are not considered during the efficiency calculation.
(2) It is assumed that the effective thermal efficiency is 57.5% on HHV basis for producing H2 from coal gasification. (Williams and Larson, 2003)
(3) Estimations are based on the HTI technology for liquefaction, while utility consumptions are considered.

Table 3-42. Material and energy balances of the direct CBTL plant (HHV basis(1)).

Process	SMR_CCS	SMR_VT	CG_CCS	CG_VT
Energy inputs				
Coal, tonne/hr (GJ/hr)	100.1 (2962)	100.1 (2962)	151.4 (4479)	151.4 (4479)
Biomass, tonne/hr (GJ/hr)	9.3 (163)	9.3 (163)	14.1 (247)	14.1 (247)
Shale gas, tonne/hr (GJ/hr)	21.6 (1105)	21.6 (1105)	N/A	N/A
Energy outputs				
Gasoline, bbl/day (GJ/hr)	2443 (595)	2443 (595)	2443 (595)	2443 (595)
Diesel, bbl/day (GJ/hr)	7557 (1936)	7557 (1936)	7557 (1936)	7557 (1936)
Net power (MW)	52.4	77.8	84.5	111.9
Thermal efficiency (%)	64.3	66.5	60.0	62.1

(1) HHVs of gasoline and diesel are set to be 5.84 and 6.15 GJ/bbl (Williams and Larson, 2003)

Task 3.2 Equipment Design and Capital Costs

Planned Activities

- ✓ **Capital cost estimation:** Based on process model developed in Aspen Plus, capital cost of all different CBTL plants was estimated using Aspen Process Economic Analyzer.
- ✓ **CAPEX model validation:** The total project costs of the direct and indirect CBTL plants were validated by comparing with the data available in the open literature.

Accomplishments

- ✓ **Capital cost estimation**

Aspen Process Economic Analyzer (APEA) V8.4 is used to perform economic analysis of the direct CBTL plants. Figure 3-34 summarizes the procedure that is followed for techno-economic analysis in this study. Stream information, such as temperature, pressure and flowrate, as well as the basic equipment type is automatically specified by directly 'exporting' the plant-wide models developed in Aspen Plus to APEA. In APEA, the capital investment, denoted as the total project cost (TPC), can be estimated by mapping the equipment items from the Aspen Plus flowsheet to corresponding APEA project component(s), if available. These equipment items are sized using ASTM standards or other correlations available in APEA. Vendor cost obtained from the open literature is used for the equipment items for which there are no suitable APEA project component and also for those for which yield models were used in Aspen Plus (Jiang and Bhattacharyya, 2016). In APEA, economic analysis and sensitivity studies can be conducted by using the Decision Analyzer tool. If plant configuration and/or any key process design parameters changes, a new process model is developed in Aspen Plus and then 'exported' to APEA for economic analysis (Jiang and Bhattacharyya, 2016). Because the hybrid CBTL plant is a synergistic combination of indirect and direct CBTL plant, the focus of this section is on the capital cost estimation of indirect and direct CBTL plant.

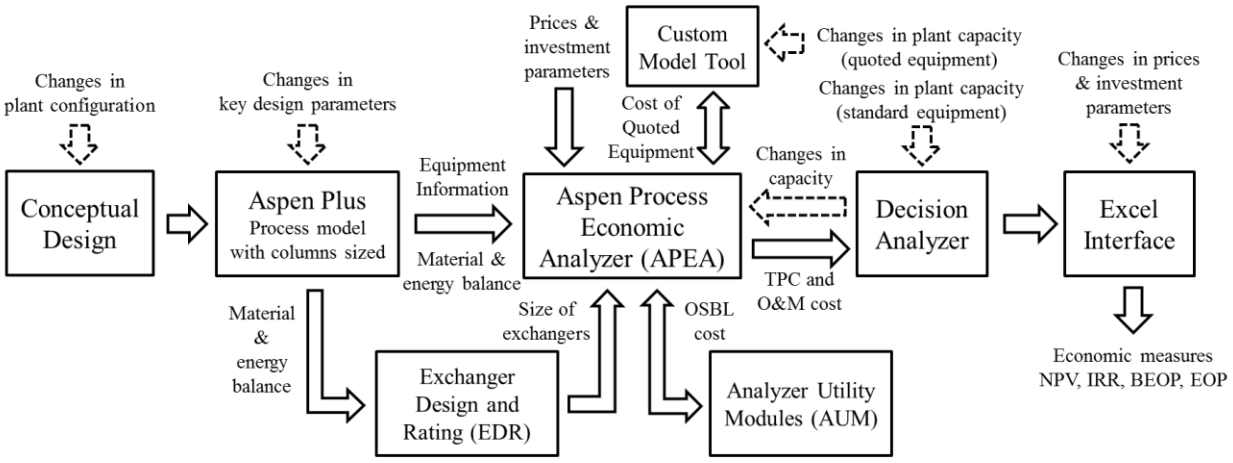

Figure 3-34. Procedure for economic analysis in multi-software environment.

Capital cost estimation of indirect CBTL plants

The economic analysis of indirect CBTL plant was computed with 2014 pricing basis. Table 3-43 lists the price of raw materials and products, labor and product for base case scenario. The prices of coal and crude oil are obtained from the US Energy Information Administration (EIA) website. The type of coal used in this study is Illinois No.6 coal, while the crude oil price (COP) used for comparison is the refiner acquisition cost of crude oil of PADD1 area (the east coast of US). It should be noted that with the current volatile price of crude oil, it is difficult to reach definitive conclusions. Therefore the authors decided to use the 2014 prices of products and raw materials as basis for this study, then conduct some sensitivity study. The delivered biomass price is assumed to be $80/dry ton. (Wu et al., 2012) Table 3-44 lists the specified values of investment parameters in APEA for the estimation of key economic performance measures, such as NPV, payout period, IRR and BEOP. The sale price of FT gasoline and diesel is defined as COP plus refinery margin (RM), where the BEOP is defined as the COP for which the NPV of the plant is zero. The RM used in this study is $0.333/gallon for gasoline and $0.371/gallon for diesel. (Baliban et al., 2011)

Table 3-43. Prices of raw material, labor and product (base case).

	Cost ($/unit)		Cost ($/unit)
Coal[(1)] ($/ton)	44.7	Supervisor ($/hr)	80
Wood chip ($/dry ton)	80.0	Crude oil price[(1)] ($/bbl)	107
Operator ($/hr)	50	Electricity ($/MWh)	50

(1) Last accessed on EIA website on Aug. 20, 2014

Table 3-44. Investment parameters (base case).

Parameter	Value	Parameter	Value
Start date of engineering	2014	Utility escalation (%/year)	1
Contingency percent	18%	Working capital percentage (%/FCI)	12
Number of years for analysis	30	Operating charges (% of labor costs)	25
Tax rate	40%	Plant overhead	50%
Interest rate/desired rate of return	10%	General & administrative expenses	8%
Project capital escalation (%/year)	1	Length of start-up period (weeks)	40
Products escalation (%/year)	1	Operating hours per period	8000
Raw material escalation (%/year)	1	Construction time	2.5 yr

In this study, the key equipment items are designed and their capital costs are estimated in multiple-software environment. Figure 3-35 shows the methodology for estimating the TPC. For process units, of which detailed models are developed for all standard process components, such as heat exchangers, columns, compressors, pumps and vessels, in Aspen Plus, rigorous cost estimations are conducted in APEA using Icarus database. For other units, the equipment items, especially the reactors and process auxiliaries, of which the costs cannot be estimated by simplified process models and Icarus database, are mapped as quoted equipment in APEA using Excel-based Custom Model Tool for cost estimation.

Table 3-45 shows the methodology of sizing and estimating cost of standard process components. Spares are considered for all pumps. All the compressors are mapped as centrifugal compressor without spare except the tail gas compressor, which is mapped as reciprocating compressor with a spare, due to the relatively smaller flow rate. The materials of construction (MOC) for all the equipment items are selected based on the operating temperature, service stream composition, and common industry practice. (NETL, 2010; Kohl and Nielsen, 1997; Tsai, 2010; NREL, 2006) The MOC for most of the equipment items, excluding the quoted equipment, is carbon steel, while the MOC for H_2 compressor, NH_3 compressor, hydrotreating reactor and part of the amine plant is stainless steel (SS316 or SS304) to avoid the corrosion problem. Feed furnace of the hydrotreater is constructed by Cr-Mo alloy (A213F or A213C) for applicability in hydrogen service at high temperature. In the amine-based AGR unit, stainless steel are used as main construction material or cladding material to avoid corrosion for all columns and some of heat exchangers and pumps in this process section, as suggested by Kohl and Nielsen. (Kohl and Nielsen, 1997) The complete equipment list and detailed specifications for all units in the indirect CBTL plant with CCS are provided in Table 3-46 to Table 3-50.

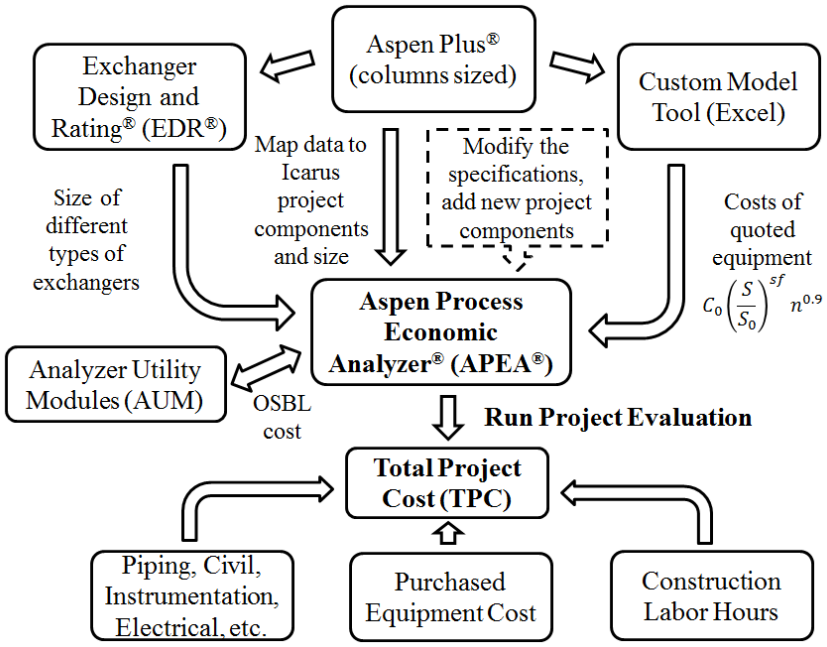

Figure 3-35. Methodology for TPC estimation.

Table 3-45. Sizing and cost estimation of project component.

Equipment	Model	Sizing	Cost
Heat exchanger	HeatX in Aspen Plus	Aspen EDR	APEA with Icarus database
Columns	RadFrac or PetroFrac in Aspen Plus	Aspen Plus tray/packing sizing	APEA with Icarus database
Vessels, pumps, compressors, etc.	Standard model in Aspen Plus	APEA sizing expert using respective ASTM standards	APEA with Icarus database
Others	Simplified models or correlations	N/A	Cost correlation from open literature

Table 3-46. Detailed equipment list for the syngas production section and water treatment units.

Equipment	# Req	# Spares	Model in APEA	Cost source	Material
Biomass handling and drying	1	0	C*	Baliban et al.	N/A
Coal handling and drying	1	0	C*	Baliban et al.	N/A
Air separation unit	1	0	C*	Baliban et al.	N/A
Gasifier (with steam generator)	1	0	C*	Baliban et al.	N/A
Slag separator	1	0	VT CYLINDER	Aspen Icarus	SS304
Scrubber	1	0	VT CYLINDER	Aspen Icarus	CS
Sour water gas shift reactor	1	0	C*	Baliban et al.	N/A
COS hydrolysis	1	0	C*	Baliban et al.	N/A
Medium pressure steam generator	1	0	HE WASTE HEAT	Icarus	CS
Low pressure steam generator	2	0	HE WASTE HEAT	Icarus	CS
Hydrocarbons preheater	1	0	HE FLOAT HEAD	Icarus	A285C, A214
Boiler feed water heater	1	0	HE FLOAT HEAD	Icarus	A285C, A214
K.O. drum	5	0	VT CYLINDER	Icarus	A516
Fuel gas preheater	1	0	HE FLOAT HEAD	Icarus	A285C, A214
Syngas cooler	2	0	HE FLOAT HEAD	Icarus	A285C, A214
Makeup water heater	1	0	HE FLOAT HEAD	Icarus	A285C, A214
Black water treatment	1	0	VT CYLINDER	Icarus	A516
Black water pump	1	1	CP CENTRIF	Icarus	CS casing
Makeup water pump	1	1	CP CENTRIF	Icarus	CS casing
Multi-stage O_2 compressor	1	0	GC CENTRIF	Icarus	CS casing
Slurry tank	1	1	AT MIXER	Icarus	A285C
Slurry water pump	1	1	CP CENTRIF	Icarus	CS casing
SWS - condenser	1	0	HE FIXED T S	Icarus	A285C, A214
SWS - drum	1	0	HT HORIZ DRUM	Icarus	A516
SWS - reboiler	1	0	RB U TUBE	Icarus	A285C, A214
SWS - reflux pump	1	1	CP CENTRIF	Icarus	CS casing
SWS - tower	1	0	TW TRAYED	Icarus	A516, A285C
SWS bottom pump	1	1	CP CENTRIF	Icarus	CS casing
Claus unit	1	0	C*	Baliban et al.[1]	N/A
Scrubber water pump	1	1	CP CENTRIF	Aspen Icarus	CS casing

*Quoted equipment
SWS=sour water stripper

Table 3-47. Detailed equipment list for the Selexol unit and the CO_2 compression unit.

Description	# Req	# Spares	Model in APEA	Cost source	Material
Tail gas compressor	1	1	GC RECIP MOTR	Icarus	CS casing
NH_3 compressor	1	0	GC CENTRIF	Icarus	SS304
CO_2 absorber	1	0	TW TRAYED	Icarus	A516, A285C
Solvent chilling	2	0	HE FLOAT HEAT	Icarus	A285C, A214
Solvent pre-cooler	1	0	HE FLOAT HEAT	Icarus	A285C, A214
Solvent recycle pump	1	1	CP CENTRIF	Icarus	CS casing
H_2 recovery drum	1	0	VT CYLINDER	Icarus	A516
H_2 recovery compressor	1	0	GC CENTRIF	Icarus	SS316 casing
H_2 recovery cooler	1	0	HE FLOAT HEAT	Icarus	A285C, A214
High pressure flash	1	0	VT CYLINDER	Icarus	A516
Medium pressure flash	1	0	VT CYLINDER	Icarus	A516
Low pressure flash	1	0	VT CYLINDER	Icarus	A516
Rich solvent pump	1	1	CP CENTRIF	Icarus	CS casing
H_2S absorber solvent chilling	1	0	HE FLOAT HEAT	Icarus	A285C, A214
H_2S absorber	1	0	TW TRAYED	Icarus	A516, A285C
Lean solvent pre-cooler	1	0	HE FLOAT HEAT	Icarus	A285C, A214
H_2S concentrator	1	0	TW TRAYED	Icarus	A516, A285C
H_2S concentrator cooler	1	0	HE FLOAT HEAT	Icarus	A285C, A214
Acid gas K.O. drum	1	0	VT CYLINDER	Icarus	A516
Strippered gas compressor	1	0	GC CENTRIF	Icarus	CS casing
Selexol stripper - top product pump	1	1	CP CENTRIF	Icarus	CS casing
Selexol stripper - condenser	1	0	HE FIXED T S	Icarus	A285C, A214
Selexol stripper - drum	1	0	HT HORIZ DRUM	Icarus	A516
Selexol stripper - reboiler	1	0	RB U TUBE	Icarus	A516
Selexol stripper - reflux pump	1	1	CP CENTRIF	Icarus	CS casing
Selexol stripper - tower	1	0	TW TRAYED	Icarus	A516, A285C
Lean solvent pump	1	1	CP CENTRIF	Icarus	CS casing
Lean solvent vessel	1	0	VT CYLINDER	Icarus	A516
Makeup solvent pump	1	1	CP CENTRIF	Icarus	CS casing
CO_2 compressor	1	0	C*	NETL[2,3]	N/A

*Quoted equipment

Table 3-48. Detailed equipment list for the synfuel production and upgrading units.

Description	# Req	# Spares	Model in APEA	Cost source	Material
Fischer-Tropsch synthesis	1	0	C*	Bechtel	N/A
Autothermal reformer	1	0	C*	Baliban et al.	N/A
Syncrude pump	1	1	CP CENTRIF	Icarus	CS casing
Hydrotreating feed furnace	1	0	FU BOX	Icarus	A213F
Feed/product heat exchanger	1	0	HE FLOAT HEAD	Icarus	A285C, A214
Hydrotreating reactor	1	0	VT MULTI WALL	Icarus	SS347
Product cooler	1	0	HE FLOAT HEAD	Icarus	A285C, A214
High pressure flash	1	0	VT CYLINDER	Icarus	A516
H_2 recycle compressor	1	0	GC CENTRIF	Icarus	SS316
Low pressure flash	1	0	VT CYLINDER	Icarus	A516
Heavy naphtha pumparoud	1	0	HE FLOAT HEAD	Icarus	A285C, A214
Diesel pumparoud	1	0	HE FLOAT HEAD	Icarus	A285C, A214
Heavy naphtha heat exchanger	1	0	HE FLOAT HEAD	Icarus	A285C, A214
Diesel heat exchanger	1	0	HE FLOAT HEAD	Icarus	A285C, A214
Wax heat exchanger	1	0	HE FLOAT HEAD	Icarus	A285C, A214
Main column - condenser	1	0	HE FIXED T S	Icarus	A285C, A214
Main column - drum	1	0	HT HORIZ DRUM	Icarus	A516
Main column - reflux pump	1	1	CP CENTRIF	Icarus	CS casing
Main column - tower	1	0	TW TRAYED	Icarus	A516, A285C
Main column - feed furnace	1	0	FU BOX	Icarus	A213C
Side stripper - heavy naphtha	1	0	TW TRAYED	Icarus	A516, A285C
Side stripper - diesel	1	0	TW TRAYED	Icarus	A516, A285C
Pump to the stabilizer	1	1	CP CENTRIF	Icarus	CS casing
Stabilizer - condenser	1	0	HE FIXED T S	Icarus	A285C, A214
Stabilizer - drum	1	0	HT HORIZ DRUM	Icarus	A516
Stabilizer - reboiler	1	0	RB U TUBE	Icarus	A285C, A214
stabilizer - reflux pump	1	1	CP CENTRIF	Icarus	CS casing
Stabilizer - tower	1	0	TW TRAYED	Icarus	A516, A285C
Hydrocracking	1	0	C*	Shah et al.	N/A
Isomerization	1	0	C*	Bechtel	N/A
Catalytic reformer	1	0	C*	Bechtel	N/A
H_2 recovery (PSA)	1	0	C*	Bechtel	N/A
Diesel storage tank (30 days)	1	0	VT STORAGE	Icarus	A285C
Gasoline storage tank (30 days)	1	0	VT STORAGE	Icarus	A285C

*Quoted equipment

Table 3-49. Detailed equipment list for the post-FT CO_2 capture unit.

Description	# Req	# Spares	Model in APEA	Cost source	MOC
Treated gas K.O. drum*	1	0	VT CYLINDER	Icarus	A516
Feed gas K.O. drum*	1	0	VT CYLINDER	Icarus	SS304
Activated carbon drum*	1	0	VT CYLINDER	Icarus	A516
Rich amine flash drum*	1	0	HT HORIZ DRUM	Icarus	A516
Absorber	1	0	TW PACKED	Icarus	A516**, M107YC
Absorber intercooling	1	0	HE FLOAT HEAD	Icarus	A285C, A214
Lean/rich heat exchanger	4	0	HE PLAT FRAM	Icarus	SS316
Solvent regeneration - condenser	2	0	HE FIXED T S	Icarus	T150A, SS316
Solvent regeneration - drum	2	0	HT HORIZ DRUM	Icarus	A516
Solvent regeneration - reboiler	8	0	RB U TUBE	Icarus	316LW, SS316
Solvent regeneration - reflux pump	2	2	CP CENTRIF	Icarus	SS316
Solvent regeneration - tower	2	0	TW PACKED	Icarus	304L, M107YC
Solvent cooling	1	0	HE FLOAT HEAD	Icarus	A285C, A214
Solvent recycle pump	1	1	CP CENTRIF	Icarus	SS316
Amine storage tank *	1	0	VT STORAGE	Icarus	A285C

*sizing information available in Bechtel's report[18]

**With 1/8 inch SS304 cladding

Table 3-50. Detailed equipment list for the combined cycle power plant*.

Description	# Req	# Spares	Model in APEA	Cost source	Material
Clean fuel gas heater	1	0	HE FLOAT HEAD	Icarus	A258C, A214
Fuel gas compressor	1	0	GC CENTRIF	Icarus	CS Casing
Gas turbine	1	0	C*	NETL	N/A
Boiler feed water pump	1	1	CP CENTRIF	Icarus	CS Casing
Medium pressure steam reheater	1	0	HE AIR COOLER	Icarus	A214
High pressure steam superheater	1	0	HE AIR COOLER	Icarus	A214
High pressure steam generator	1	0	HE WASTE HEAT	Icarus	CS
High pressure BFW economizer	1	0	HE AIR COOLER	Icarus	A214
High pressure steam blowdown	1	0	VT CYLINDER	Icarus	CS
Low pressure steam generator	1	0	HE WASTE HEAT	Icarus	CS
Low pressure BFW economizer	1	0	HE AIR COOLER	Icarus	A214
High pressure BFW pre-economizer	1	0	HE AIR COOLER	Icarus	A214
Pre-deaerator heater	1	0	HE AIR COOLER	Icarus	A214
Deaerator	1	0	TW TRAYED	Icarus	A516, A285C
Steam packing exhauster	1	0	HE FLOAT HEAD	Icarus	A516, A285C
Air ejector	1	0	HE FLOAT HEAD	Icarus	A516, A285C
Condenser pump	1	1	VP MECH BOOST	Icarus	CS Casing
Surface condenser	1	0	C BAROMETRIC	Icarus	N/A
Steam turbine	1	0	EG TURBO GEN	Icarus	CS Casing
High pressure BFW pump	1	1	CP CENTRIF	Icarus	CS Casing

Medium pressure BFW pump	1	1	CP CENTRIF	Icarus	CS Casing
Low pressure BFW pump	1	1	CP CENTRIF	Icarus	CS Casing

*Quoted equipment

BFW= boiler feed water

For the reactors, product upgrading units and auxiliaries, the parameters for the cost correlations, Eq. (44) and Eq. (45), are shown in Table 3-51, which are directly obtained from the open literature or derived using the data available in the open literature. (Baliban et al., 2011; Bechtel, 1998; NETL, 2007; Shah et al., 1988) In Eq. (44) and (45), *DIP* is the direct permanent investment (includes ISBL cost and OSBL cost), *BOP* is the balance of plant percentage (site preparation, utility plants, etc.), C_0 is the base cost, S_0 is the base capacity, S is the actual capacity, *sf* is the scaling factor, and n is the total number of trains. Multiply trains are considered, if the throughput of a certain unit exceeds the maximum capacity (S_{max}).

$$DIP = (1 + BOP)C_0\left(\frac{S}{S_0}\right)^{sf} n^{0.9} \quad (44)$$

$$ISBL\ cost = C_0\left(\frac{S}{S_0}\right)^{sf} n^{0.9} \quad (45)$$

Table 3-51. Capital cost correlation for quoted equipment items.

Unit name	C_0 (MM$)[1]	S_0	Smax	S_0 Basis	units	*sf*	Eq	Reference
Biomass handling and drying	27.82	2000		dry feed	TPD	0.67	1	Baliban et al.
Coal handling and drying	81.67	2, 64	2616	dry feed	TPD	0.67	1	Baliban et al.
Gasifier	136.30	2464	2616	dry feed	TPD	0.6	1	Baliban et al.
Sour WGS	3.14	2556	2600	output	TPD	0.65	2	Baliban et al.
COS hydrolysis	3.05	4975	7500	output	TPD	0.67	2	Baliban et al.
Claus	24.09	125		sulfur	TPD	0.67	2	Baliban et al.
CO_2 compressor	31.63	11256		CO_2	TPD	0.75	2	NETL
Fischer-Tropsch synthesis	40.71	226669	228029	feed	Nm^3/h	0.75	2	Bechtel Corp.
Autothermal reformer	3.27	430639	9438667	output	Nm^3/h	0.67	1	Baliban et al.
Wax hydrocracking	9.60	97.92	2656	feed	TPD	0.55	2	Shah et al.
Isomerization	0.99	13.06	2720	feed	TPD	0.62	2	Bechtel Corp.
Catalytic reformer	5.36	36.99	8160	feed	TPD	0.6	2	Bechtel Corp.
Hydrogen recovery (PSA)	0.84	944		H_2	Nm^3/h	0.55	2	Bechtel Corp.
Air separation unit (ASU)	57.57	1839	2500	TPD	O_2	0.50	2	Baliban et al.

(1) The costs of quoted equipment are escalated with the Chemical Engineering Plant Cost Index (CEPCI).

It should be noted that two methods are applied to estimate the OSBL cost in this study. For the units with missing design and operating information, Eq. (44) is applied, where BOP includes the cost associated with the utility plants. For the unit with all information available, especially utility consumption, AUM in APEA can be applied to estimate the OSBL cost of the plant. In the indirect CBTL plant, fuels, steam, and electricity required are supplied by the fuel gas header and the

combined cycle plant, which is included in ISBL. (Yuan and Bhattacharyya, 2015) Cooling water system is the major OSBL plant considered in this study, with the design approach in AUM shown in Figure 3-36.

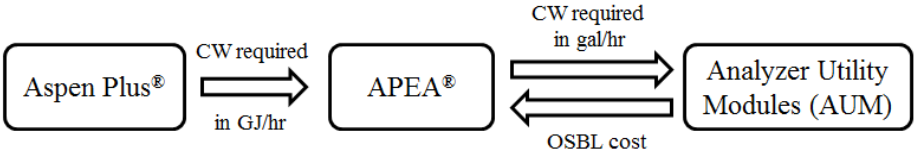

Figure 3-36. Methodology for cooling water system cost estimation using AUM.

Cost of the raw materials is the major contributor to the operating and maintenance (O&M) cost. This is estimated from the material balance obtained from the process model developed in Aspen Plus® and the unit prices listed in Table 3-43. The utility cost usually makes a large contribution to the O&M cost. However, in the indirect CBTL plant with the plant construction shown in Figure 3-1, fuels, steam, electricity are generated internally (Yuan and Bhattacharyya, 2015). As the circulating water system is designed using AUM, process water is the only external utility considered in the economic model. The costs of catalyst and chemicals are estimated based on the data available in the open literature. The initial costs of the catalysts in all reactors, excluding hydrotreater, are included in the ISBL cost. For the hydrotreating catalyst and chemicals like Selexol and amine solvents for CO_2 capture, the cost for initial loading is accounted for by inserting quoted equipment in APEA with specified cost. The cost of catalyst in the catalytic reforming unit is not explicitly considered in this project, because the correlation for the UOP continuous catalyst regeneration (CCR) Platforming technology is considered, where the initial catalyst cost and capital cost of catalyst regeneration facilities are already included in the ISBL cost and the annual cost for catalyst replacement is relatively low and therefore ignored. (Bechtel, 1993; Meyer, 2003) The catalyst replacement rate in the FT process is specified to be 0.5% per day of total catalyst inventory, while a 5-year catalyst life is assumed for other catalysts. (Bechtel, 1993; 1998) The replacement rates of chemicals (Selexol and amine solvent) are assumed to be the same as reported in a NETL study. (NETL, 2007) With the availability of unit costs for replacing catalyst and chemicals included, the replacement cost is annualized, and included in APEA. Table 3-52 lists the initial and replacement costs of major catalysts and chemicals considered in the indirect CBTL plant.

Once all the information required by APEA is specified, profitability analysis and sensitivity studies are conducted by the Decision Analyzer tool available in APEA, which is a user friendly Excel interface that reports the important economic measures. For sensitivity studies, if the key design parameters are changed, the process model in Aspen Plus is updated and a new APEA file is created by importing the updated steady-state simulation results and following the above procedure. If the key design parameters remain the same, sensitivity studies can be conducted in APEA only using the scenario created by the original Aspen Plus model. The sensitivity studies related to investment parameters as well as the raw material, labor, utility and product can be conducted in the Excel file generated by Decision Analyzer. The sensitivity study related to plant capacity is also conducted in Decision Analyzer. The entire plant is rescaled by Decision Analyzer, while most of the standard equipment is resized and evaluated with the new plant capacity. For quoted equipment, the capital cost is estimated by Excel-based Custom Model Tool for the new

plant capacity and multiple train may be considered if the throughput existing the up limit. Figure 3-37 summarizes the general approach for economic analysis and sensitivity studies.

Table 3-52. Costs of catalysts and chemicals in the indirect CBTL plant (base case, 10k bbl/day).

	Unit Cost(1) ($/unit)	Unit	Initial(2) (M$)	Replacement(2) ($/day)	Cost source
Catalyst					
Fischer Trospch	4.80	kg	with equipment	7404	Bechtel Corp.
Sour WGS	16774	m^3	with equipment	710	NETL
COS hydrolysis	2.01	kg	with equipment	65	NETL
Claus unit	4414	m^3	with equipment	395	NETL
Autothermal reformer	37080	m^3	with equipment	510	NETL
Hydrotreating	34.17	kg	1090	582	SRI
Hydrocracking	34.17	kg	with equipment	414	SRI
Isomerization(3)	0.180	bbl FF	with equipment	540	Meyer
Chemicals					
Selexol solvent	3804	m^3	1010	456	NETL
Amine solvent	2.16	kg	218	60	NETL
Total			2318	11136	

(1) Costs listed are the original value published in different years.
(2) The costs of catalyst and chemicals are escalated with the average Producer Price Index.
(3) $0.18/bbl fresh feed is the total replacement cost of catalyst and adsorbent.

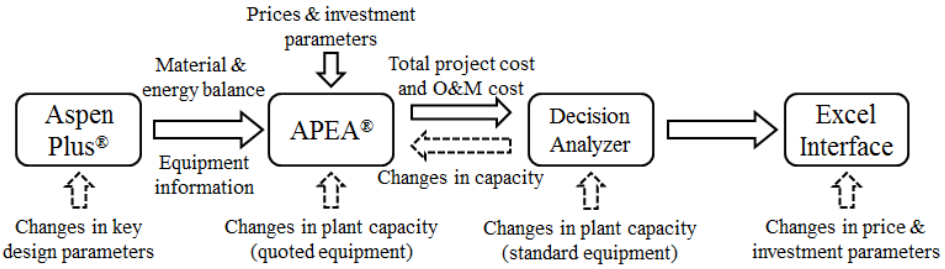

Figure 3-37. Economic analysis and sensitivity studies in multi-software environment.

Capital cost estimation of direct and hybrid CBTL plants

The procedure of capital cost estimation for the direct and hybrid CBTL plant is the same as that for the indirect CBTL plant as discussed above. Table 3-53 lists the prices of raw materials, labor and products in 2015 basis. The prices of raw material and products are mainly obtained from the US EIA website. The COP is the refiner acquisition cost of crude oil in the PADD1 area (the east coast of US). In this study, NPV and IRR are calculated assuming the wholesale prices of gasoline and diesel are COP plus the refinery margin, $0.333/gallon for gasoline and $0.371/gallon for diesel (Yuan and Bhattacharyya, 2016). BEOP is the COP making the process NPV zero, while equivalent oil price (EOP) is defined as the COP making the process IRR be 12%. The carbon credit is defined as carbon in the additional CO_2 captured by the CCS facilities compared with the petroleum baseline. In the PADD1 area, the CO_2 emission from the petroleum refineries is about

45 kg CO_2/bbl crude oil, which is equivalent to about 8.12 kg CO_2/GJ fuel (Karras, 2011). It is assumed that if the CBTL facility is located in a place that is subject to carbon tax and if CO_2 emission of the CBTL plant with CCS is lesser than 8.12 kg CO_2/GJ fuel, then the additional CO_2 that is captured and sequestered can be leveraged to improve the plant economics. In the base case, the price of carbon credit is set to be zero as carbon tax is still fairly uncommon in most locations around the world. Table 3-54 lists the investment parameters for the base case scenario. Here, process contingency is set to be 24% because of the novelty of the direct CBTL plants. The length of start-up period is set to be 40 days because of the process complicity. Parameters in the cost correlations with 2015 pricing basis are obtained from the open literature or derived using the data available in the open literature, as shown in Table 3-55 for direct CBTL plant. Table 3-56 to Table 3-61 list all standard equipment in the direct CBTL process (SMR_CCS) with a capacity of 10000 bbl/day, and their material of construction (MOC), modeling and sizing approach. It is noted that all 'quoted' equipment is not listed in this section. Cost correlation and equipment list of the hybrid CBTL plant are obtained by synergistically combining the indirect and direct CBTL plants and therefore not shown in detail in this report.

Table 3-53. Prices of raw material, labor, and product (base case).

	Cost ($/unit)		Cost ($/unit)
Coal ($/tonne)	34.0	Supervisor ($/hr)	80
Wood chip ($/dry tonne)	61.5	Crude oil price ($/bbl)	60
Shale gas ($/GJ)	2.25	Electricity ($/MWh)	50
Operator ($/hr)	50	Carbon credit ($/tonne)	0

Table 3-54. Investment parameters (base case).

Parameter	Value	Parameter	Value
Start date of engineering	2015	Utility escalation (%/year)	1
Contingency percent	24%	Working capital percentage (%/FCI)	12
Number of years for analysis	30	Operating charges (% of labor costs)	25
Tax rate	40%	Plant overhead	50%
Interest rate/desired rate of return	10%	General & administrative expenses	8%
Project capital escalation (%/year)	1	Length of start-up period (weeks)	40
Products escalation (%/year)	1	Operating hours per period	8000
Raw material escalation (%/year)	1	Construction time	2.5 yr

Table 3-55. Parameters for Eqs. (44) and (45) for quoted equipment items (2015 pricing basis).

Equipment	C_0 (MM$)[1]	S_0	S_{max}	S_0 basis	Units	sf	BOP	Reference
Gasifier	137.09	2464	2616	dry feed	tonne/day	0.67	added	Baliban et al., 2011
WGS reactor	3.16	2556	2600	output	tonne/day	0.65	no	Baliban et al., 2011
Isomerization	1.00	13.06	2720	feed	tonne/day	0.62	no	Bechtel, 1998
Catalytic reforming	5.39	36.99	8160	feed	tonne/day	0.6	no	Bechtel, 1998
Air separation unit	57.90	1839	2500	O_2	tonne/day	0.5	added	Baliban et al., 2011
Coal pre-processing	57.50	2464	2616	dry feed	tonne/day	0.67	added	Baliban et al., 2011
Biomass pre-processing	27.98	2000		dry feed	tonne/day	0.67	added	Baliban et al., 2011
CO_2 compressor	31.81	11256		CO_2	tonne/day	0.75	no	NETL, 2010
PSA H_2 recovery	0.84	944		H_2	Nm3/h	0.55	no	Bechtel, 1998
Claus unit	24.23	125		S	tonne/day	0.67	no	Baliban et al., 2011
Steam methane reformer	62.10	26.1	35	feed	kg/s	0.67	no	NETL, 2013
Shale gas pre reformer	12.30	26.10		feed	kg/s	0.67	no	Baliban et al., 2013
ROSE-SR unit	66.70	50800		feed	bbl/day	0.67	no	Bechtel and Amoco, 1992
Liquefaction reactor	94.79	587.79		feed	tonne/hr	0.67	no	Bechtel and Amoco, 1992

(1) The costs of quoted equipment are escalated using the Chemical Engineering Plant Cost Index (CEPCI).

Table 3-56. Equipment list of the liquefaction and hydrocarbon recovery unit.

Equipment	#Required/Spares	Model in APEA	Sizing	MOC[1]
Reactors & vessels				
Inline hydrotreater	1/0	VT MULTI WALL	APEA	A387D
Slurry tank	2/0	AT MIX	APEA	A516
Slurry surge tank	1/0	VT CYLINDER	APEA	A285C
Slurry surge tank vent scrubber	1/0	VT CYLINDER	APEA	A516
High pressure high temp flash	1/0	VT CYLINDER	APEA	A387F (SS347)
Low pressure oil separator	1/0	TW TRAYED	Aspen Plus	A387D/A387D
High pressure cold flash	1/0	VT CYLINDER	APEA	A387B
Low pressure warm flash	1/0	VT CYLINDER	APEA	A516
Low pressure cold flash	1/0	VT CYLINDER	APEA	CS
High pressure warm flash	1/0	VT CYLINDER	APEA	A387D
Atmosphere still feed separator	1/0	VT CYLINDER	APEA	A387B
Wash water drum	1/0	HT HORIZ DRUM	APEA	CS
Sour water drum	1/0	HT HORIZ DRUM	APEA	CS
Recycle solvent tank	1/0	VT CYLINDER	APEA	A387D
Atmosphere still condenser drum	1/0	HT HORIZ DRUM	APEA	A516
Stabilizer condenser drum	1/0	HT HORIZ DRUM	APEA	A516
Distillation columns				
Atmosphere still tower	1/0	TW TRAYED	Aspen Plus	316L/316L
Atmosphere gas oil stripper	1/0	TW TRAYED	Aspen Plus	316L/316L
Atmosphere naphtha stripper	1/0	TW TRAYED	Aspen Plus	316L/316L
Stabilizer tower	1/0	TW TRAYED	Aspen Plus	A516/A258C

Vacuum still tower	1/0	TW TRAYED	Aspen Plus	SS410/SS410
Compressors, pumps & turbines				
Atmospheric still reflux pump	1/1	CP CENTRIF	APEA	SS casing
Stabilizer reflux pump	1/1	CP CENTRIF	APEA	CS casing
Slurry tank bottom pump	1/1	CP CENTRIF	APEA	SS316 casing
High pressure slurry feed pump	1/1	P RECIP MOTR	APEA	SS316 casing
Make up H_2 compressor	1/1	GC RECIP MOTR	APEA	SS casing
Recycle H_2 compressor	1/0	GC CENTRIF	APEA	SS316 casing
Stabilizer feed pump	1/0	CP CENTRIF	APEA	CS casing
Stabilizer feed compressor	1/1	GC CENTRIF	APEA	CS casing
ROSE-SR unit feed pump	1/1	CP CENTRIF	APEA	SS316 casing
Atmospheric still bottom pump	1/1	CP CENTRIF	APEA	SS316 casing
Atmospheric still feed pump	1/1	CP CENTRIF	APEA	SS316 casing
Gas oil product pump	1/1	CP CENTRIF	APEA	SS casing
Sour water pump	1/1	CP CENTRIF	APEA	SS casing
LVGO pumparound	1/1	CP CENTRIF	APEA	SS casing
HVGO pumparoud	1/1	CP CENTRIF	APEA	SS casing
VGO product pump	1/1	CP CENTRIF	APEA	SS316 casing
Furnaces, boiler & heat exchangers				
Atmosphere still condenser	1/0	HE FIXED T S	EDR	A214/A516
Atmosphere still feed furnace	1/0	FU VERTICAL	APEA	347S
Stabilizer condenser	1/0	HE FIXED T S	EDR	A214/A516
Stabilizer reboiler	1/0	RB U TUBE	EDR	A214/A516
Slurry feed heat exchanger	2/0	HE FLOAT HEAD	EDR	316S/SS316
Slurry feed heat exchanger	4/0	HE FLOAT HEAD	EDR	316S/A387D (SS316)
Slurry feed furnace	1/0	FU BOX	APEA	347S
H_2 pre heating	1/0	HE FLOAT HEAD	EDR	I825/SS304
H_2 pre heating	1/0	HE FLOAT HEAD	EDR	321S/A387D
H_2 feed furnace	1/0	FU BOX	APEA	347S
Recycle H_2 heat exchanger	3/0	HE FLOAT HEAD	EDR	304LS/304L
Product heat exchanger	1/0	HE FLOAT HEAD	EDR	316LS/A387D (SS316)
IP steam generator	1/0	HE WASTE HEAT	EDR	CS
Water cooler	7/0	HE FLOAT HEAD	EDR	A214/A516
Product heat exchanger	1/0	HE FLOAT HEAD	EDR	A213C/A387C
LP steam generator	3/0	HE WASTE HEAT	EDR	CS

(1) ( ) denotes cladding material

Table 3-57. Equipment list of the syngas production unit.

Equipment	#Required/Spares	Model in APEA	Sizing	MOC
Reactors & vessels				
Slag separator	1/0	VT CYLINDER	APEA	SS304
Scrubber	1/0	VT CYLINDER	APEA	SS304
Syngas KO drum	2/0	HT HORIZ DRUM	APEA	A516
flue gas KO drum	2/0	HT HORIZ DRUM	APEA	A516
Compressors, pumps & turbines				
Boiler feed water pump	1/1	CP CENTRIF	APEA	CS casing
Shale gas compressor	1/0	GC CENTRIF	APEA	CS casing
Furnaces, boiler & heat exchangers				
Boiler feed water heater	2/0	HE AIR COOLER	EDR	A214
Low pressure steam generator	2/0	HE WASTE HEAT	EDR	CS
Shale gas pre heater	1/0	HE FLOAT HEAD	EDR	A214/A516
Steam reformer pre heater	1/0	HE FLOAT HEAD	EDR	316S/SS316
Medium pressure steam generator	3/0	HE WASTE HEAT	EDR	CS
High pressure steam generator	2/0	HE WASTE HEAT	EDR	CS
Low pressure steam economizer	1/0	HE AIR COOLER	EDR	A214
High pressure steam economizer	1/0	HE AIR COOLER	EDR	A214
High pressure steam superheater	1/0	HE AIR COOLER	EDR	A214
Other coolers	3/0	HE FLOAT HEAD	EDR	A214/A516

Table 3-58. Equipment list of the Selexol (AGR) unit.

Equipment	#Required/Spares	Model in APEA	Sizing	MOC
Reactors & vessels				
High pressure flash	1/0	VT CYLINDER	APEA	A516
Medium pressure flash	1/0	VT CYLINDER	APEA	A516
Low pressure flash	1/0	VT CYLINDER	APEA	A516
H_2 recovery drum	1/0	VT CYLINDER	APEA	A516
H_2S concentrator	1/0	VT CYLINDER	APEA	A516
H_2S stripper condenser drum	1/0	VT CYLINDER	APEA	A516
Selexol stripper condenser drum	1/0	HT HORIZ DRUM	APEA	A516
Lean solvent vessel	1/0	VT CYLINDER	APEA	A516
Distillation columns				
CO_2 absorber	1/0	TW TRSYED	Aspen Plus	A516/A285C
H_2S absorber	1/0	TW TRSYED	Aspen Plus	A516/A285C
Selexol stripper tower	1/0	TW TRSYED	Aspen Plus	A516/A285C
Compressors, pumps & turbines				
NH_3 compressor	1/0	GC CENTRIF	APEA	SS304 casing
H_2 recovery compressor	1/0	GC CENTRIF	APEA	CS casing
Stripped gas compressor	1/0	GC CENTRIF	APEA	CS casing
Lean solvent pump	2/2	CP CENTRIF	APEA	CS casing
Recycle solvent pump	1/1	CP CENTRIF	APEA	CS casing
Selexol stripper reflux pump	1/1	CP CENTRIF	APEA	CS casing
Rich solvent pump	1/1	CP CENTRIF	APEA	CS casing
Furnaces, boiler & heat exchangers				
Selexol stripper condenser	1/0	HE FIXED T S	EDR	A214/A516
Selexol stripper reboiler	1/0	RB U TUBE	EDR	A214/A516
Recycle solvent cooler	1/0	HE FLOAT HEAD	EDR	A214/A516
H_2S absorber solvent cooler	1/0	HE FLOAT HEAD	EDR	A214/A516
Lean solvent cooler	1/0	HE FLOAT HEAD	EDR	A214/A516
Syngas cooler	1/0	HE FLOAT HEAD	EDR	A214/A516
Other coolers	4/0	HE FLOAT HEAD	EDR	A214/A516

Table 3-59. Equipment list of the amine unit.

Equipment	#Required/Spares	Model in APEA	Sizing	MOC[(1)]
Reactors & vessels				
MDEA/PZ storage tank	1/0	VT CYLINDER	APEA	A516
GT flue gas condenser	1/0	VT CYLINDER	APEA	A516
MDEA storage tank	1/0	VT CYLINDER	APEA	A516
CO_2 Stripper condenser drum	2	HT HORIZ DRUM	APEA	A516
H_2S Stripper condenser drum	1	HT HORIZ DRUM	APEA	A516
Distillation columns				
High pressure absorber	1/0	TW PACKED	Aspen Plus	A516 (SS304)/M107YC
GT flue gas absorber	2/0	TW PACKED	Aspen Plus	A516 (SS304)/M107YC
SMR flue gas absorber	1/0	TW PACKED	Aspen Plus	A516 (SS304)/M107YC
CO_2 Stripper tower	2/0	TW TRSYED	Aspen Plus	304L/M107YC
H_2S Absorber	1/0	TW PACKED	Aspen Plus	A516 (SS304)/1.0PPR
H_2S Stripper tower	1/0	TW TRSYED	Aspen Plus	304L/1.0PPR
Compressors, pumps & turbines				
Flue gas blower	2/0	FN CENTRIF	APEA	CS
CO_2 Stripper reflux pump	2/2	CP CENTRIF	APEA	SS316 casing
H_2S Stripper reflux pump	1/1	CP CENTRIF	APEA	SS316 casing
GT rich solvent pump	2/2	CP CENTRIF	APEA	CS casing
SMR rich solvent pump	1/2	CP CENTRIF	APEA	CS casing
MDEA/PZ lean solvent pump	1/1	CP CENTRIF	APEA	CS casing
MDEA lean solvent pump	1/1	CP CENTRIF	APEA	CS casing
Furnaces, boiler & heat exchangers				
High pressure absorber pumparound	1/0	HE FLOAT HEAD	EDR	A214/A516
GT absorber pumparound	2/0	HE FLOAT HEAD	EDR	A214/A516
SMR absorber pumparound	1/0	HE FLOAT HEAD	EDR	A214/A516
CO_2 Stripper condenser	2/0	HE FIXED T S	EDR	T150A/SS316
CO_2 Stripper reboiler	2/0	RB U TUBE	EDR	316LW/SS316
H_2S Stripper condenser	1/0	HE FIXED T S	EDR	T150A/SS316
H_2S Stripper reboiler	1/0	RB U TUBE	EDR	316LW/SS316
GT flue gas cooler	1/0	HE FLOAT HEAD	EDR	A214/A516
MDEA/PZ lean/rich exchanger	1/0	HE PLAT FRAM	EDR	SS316
Lean solvent cooler	2/0	HE FLOAT HEAD	EDR	A214/A516
MDEA lean/rich exchanger	1/0	HE PLAT FRAM	EDR	SS316

(1) ( ) denotes cladding material

Table 3-60. Equipment list of the hydrocarbon upgrading unit.

Equipment	#Required/Spares	Model in APEA	Sizing	MOC(1)
Reactors & vessels				
Gasoline storage tank	3/0	VT STORAGE	APEA	A516
Diesel storage tank	6/0	VT STORAGE	APEA	A516
Gas oil hydrotreater	2/0	VT MULTI WALL	APEA	A387F (SS347)
Hot high pressure flash	1/0	VT CYLINDER	APEA	A387D
Cold high pressure flash	1/0	VT CYLINDER	APEA	A516
Low pressure flash	1/0	VT CYLINDER	APEA	A516
Stabilizer condenser drum	2/0	HT HORIZ DRUM	APEA	A516
Main distillation condenser drum	1/0	HT HORIZ DRUM	APEA	A516
Distillation columns				
Main distillation tower	1/0	TW TRAYED	Aspen Plus	A516/A285C
Stabilizer tower	1/0	TW TRAYED	Aspen Plus	A516/A258C
Compressors, pumps & turbines				
Main distillation reflux pump	1/1	CP CENTRIF	APEA	CS casing
Stabilizer reflux pump	1/1	CP CENTRIF	APEA	CS casing
Makeup H_2 compressor	1/1	GC RECIP MOTR	APEA	SS casing
Recycle H_2 compressor	1/0	GC CENTRIF	APEA	SS316 casing
Stabilizer feed pump	1/1	CP CENTRIF	APEA	CS casing
Gas oil feed pump	1/1	CP CENTRIF	APEA	CS casing
Furnaces, boiler & heat exchangers				
Diesel pumparound	1/0	HE FLOAT HEAD	EDR	A214/A516
Gas oil pumparound	1/0	HE FLOAT HEAD	EDR	A214/A516
Main distillation condenser	1/0	HE FIXED T S	EDR	A214/A516
Main distillation feed furnace	1/0	FU VERTICAL	APEA	A213C
Stabilizer condenser	1/0	HE FIXED T S	EDA	A214/A516
Stabilizer reboiler	1/0	RB U TUBE	EDA	A214/A516
H_2 pre heater	1/0	HE FLOAT HEAD	APEA	A214/A516
Feed H_2 furnace	1/0	FU BOX	APEA	347S
Gas oil feed pre heater	1/0	HE FLOAT HEAD	EDR	A213D/A387D
Low pressure steam generator	3/0	HE WASTE HEAT	EDA	CS
Heavy diesel cooler	1/0	HE FLOAT HEAD	EDR	A214/A516
Light gas oil cooler	1/0	HE FLOAT HEAD	EDR	A214/A517
Other coolers	4/0	HE FLOAT HEAD	EDR	A214/A516

(1) ( ) denotes cladding material

Table 3-61. Equipment list of the combined cycle power island.

Equipment	#Required/Spares	Model in APEA	Sizing	MOC
Reactors & vessels				
High pressure steam blowdown	1/0	HT HORIZ DRUM	APEA	A516
Compressors, pumps & turbines				
High pressure BFW pump	1/1	CP CENTRIF	APEA	CS casing
Medium pressure BFW pump	1/1	CP CENTRIF	APEA	CS casing
Low pressure BFW pump	1/1	CP CENTRIF	APEA	CS casing
Condenser pump	1/1	VP MECH BOOST	APEA	CS casing
Steam turbine	1/0	EG TURBO GEN	APEA	CS casing
Fuel gas compressor	1/0	GC CENTRIF	APEA	CS casing
Gas turbine	1/0	EG TURBO GEN	APEA	CS casing
Furnaces, boiler & heat exchangers				
High pressure pre economizer	1/0	HE AIR COOLER	EDA	A214
High pressure BFW economizer	1/0	HE AIR COOLER	EDA	A214
High pressure steam superheater	1/0	HE AIR COOLER	EDA	A214
Medium pressure steam reheater	1/0	HE AIR COOLER	EDA	A214
Boiler feed water heater	1/0	HE AIR COOLER	EDA	A214
Air ejector	1/0	HE FLOAT HEAD	EDR	A214/A516
Steam packing exhauster	1/0	HE FLOAT HEAD	EDR	A214/A516
High pressure steam generator	1/0	HE WASTE HEAT	APEA	CS
Low pressure steam generator	1/0	HE WASTE HEAT	APEA	CS
Surface condenser	1/0	C BAROMETRIC	APEA	CS

Other than the raw material costs, costs of utility, operating labor, catalysts and chemicals also have significant contributions on the O&M cost of a chemical plant. In this study, the raw material cost can be easily estimated based on the material and energy balance given steady state simulation. Process fuels, steam and electricity are generated internally from the fuel gas header and the combined cycle power island. As the circulating water system is designed using AUM, process water is the only external utility considered in this economic model. The costs of catalysts and chemicals are listed in Table 3-62 for all four plant configurations. In APEA, the initial loading of catalysts and chemicals is specified as 'quoted' equipment, while costs for replacing catalysts and chemicals are specified under raw materials. For the water gas shift, Claus, isomerization and catalytic reforming units, the initial catalyst cost is included in the equipment cost. The catalyst in the liquefaction unit is replaced continuously/periodically. The catalyst in the catalytic reforming unit is replaced periodically to maintain the desired catalysts activity. (Bechtel, 1998) Other catalysts are replaced every five to ten years, depending on the catalyst life. Replacement costs of those catalysts are amortized when treated as raw materials. The number of operators is calculated based on the economic analysis given by Bechtel and Amoco (Bechtel and Amoco, 1992).

Table 3-62. Cost of catalyst and chemicals in the direct CBTL plants with CCS (10000 bbl/day).

	Unit Cost[(1)]	Initial (k$)/Replacement ($/hr)[(2)]			
	($/unit)	SMR_CCS	SMR_VT	CG_CCS	CG_VT
Catalysts					
Liquefaction	$4.00/kg	661/461	661/461	661/461	661/461
Water gas shift	$16774/$m^3$	0/75	0/75	0/75	0/75
Claus unit	$4414/$m^3$	0/15	0/15	0/15	0/15
Steam reforming	$22930/$m^3$	868/33	868/33	0/0	0/0
Hydrotreating	$34.17/kg	6754/282	6754/282	6754/282	6754/282
Isomerization	$4414/$m^3$	0/4.5	0/4.5	0/4.5	0/4.5
Chemicals					
Selexol solvent	$3804/$m^3$	98/2.0	98/2.0	433/9.2	433/9.2
Amine solvent	$2.16/kg	1355/17	301/3.8	350/4.4	0/0
ROSE-SR solvent	$3/gallon	54/1.6	54/1.6	54/1.6	54/1.6
Total		9790/891	8736/878	8252/853	7902/848

(1) Costs listed are the original value published in different years.
(2) The costs of catalyst and chemicals are escalated with the average Producer Price Index.

✓ Economic model validation

There is scarcity of techno-economic studies on the CBTL plants with CCS in the open literature. As the feed contains only 8 wt% biomass, the effect of biomass on the capital investment is not expected to be significant. Therefore, the capital cost estimates is compared with the previous studies conducted for CTL plants with most similar plant configurations. However those studies have different plant capacities in comparison to this study. Therefore, the base case plant is rescaled using APEA Decision Analyzer. For each case study, the investment parameters, such as plant contingency and working capitals, tax rate, escalation rate and plant contingency, which affect the TPC, are specified to be the same as those in the references for the case studies. In this study, only the economic model of indirect and direct liquefaction process is validated, since no data are available in the open literature for hybrid liquefaction plants. However, since the hybrid CBTL plant is a synergistic combination of the indirect and direct CBTL plants, it is anticipated that the economic analysis of the hybrid CBTL plant is reasonable as well.

Economic model validation of the indirect CBTL plants

Table 3-63 summarizes the results of the comparison of the economic model developed in APEA® with three different case studies -two large scale plants, and one small scale plant. (Bechtel, 1998; NETL, 2007) As seen in Table 3-63, the relative difference in TPC between our estimate and reported data is within 6%. The main difference is due to plant configuration such as the application of CCS technology, the approach of hydrocarbon upgrading, and the key design parameters such as the H_2/CO ratio in the FT inlet stream. Detailed comparison of each breakdown plant section for all three cases is provided in Table 3-64 to Table 3-66. It should be noted that the capital investment given in the original reports (Bechtel, 1998; NETL, 2007) is escalated using CEPCI values for fair comparison.

Table 3-63. Summary of the capital investment comparison.

	Case 1[9]	Case 2[(1)11]	Case 3[(1)12]	Base Case
Capacity (bbl/day)	48629	49992	9609	
Difference in plant construction				
CO_2 capture & storage	No	Yes	No	Yes
Naphtha upgrading	Yes	No	No	Yes
Light gases to gasoline	Yes	No	No	No
Total project cost (TPC, 2014 MM$)				
TPC calculated	4905.6	5137.6	1185.2	
TPC reported[9,11,12]	4748.5	5214.3	1124.1	
Difference in TPC (%)	-3.31	1.47	-5.44	

(1) Additional 25% process contingency is considered for FT process and added to the calculated TPC for Case 2 and Case 3 for fair comparison.

Table 3-64. Comparison with Bechtel studies (Bechtel, 1998).

		Bechtel*	Model	Difference	Notes
		(MM$, 2014)		%	
ISBL cost of each unit					(1)
Unit 100	Syngas production and treatment	2056.6	2280.4	-10.88	
	Pre-processing & gasificaiton	1355.7	1266.8	6.56	
	Syngas treating & cooling	60.8	63.4	-4.26	
	Sour water stripper	5.1	4.9	5.33	
	Acid gas removal	29.9	299.6		(2)
	Sulfur recovery	69.5	70.0	-0.77	
	Syngas wet scrubbing	12.1	13.3	-9.75	
	Air separation unit	523.5	422.3	19.34	
	Ash handling		140.1		(3)
Unit 200	Fischer-Tropsch synthesis loop	800.2	437.3	45.35	(4)
	Fischer-Tropsch synthesis	352.8	326.0	7.61	
	Carbon dioxide removal	226.7	60.6	-6.93**	(5)
	Dehydration and hydrocarbon recovery	114.5	3.0		
	Autothermal reformer	35.1	35.0	-0.35	
	Hydrogen recovery	71.1	15.8		(6)
Unit 300	Product upgrading and refining	243.7	190.5	21.83	(7)
	Wax hydrocracking	69.8	65.9	5.63	
	Hydrotreating	33.0	30.6	7.3	
	Catalytic reforming	50.2	46.4	7.66	
	C_5/C_6 isomerization	11.7	13.4	-14.63	
	C_4 isomerization and alkylation	70.2			
	Others	8.9			(8)
Total ISBL cost		3100.5	2883.0	5.91	
Total project cost***		4748.5	4905.6	-3.31	(9)

*Original data reported in 1998 is escalated to 2014 pricing basis using CEPCI.

**Difference in capital investment for same amount of CO_2 capture

******* TPC includes OSBL, engineering cost, contingency cost.

(1) HRSG section with steam turbine is included in OSBL section in Bechtel's analysis.

(2) In Bechtel's baseline design, CCS is not considered; amine solvent is used in the acid gas removal unit for removing H_2S only in Unit 100.

(3) Ash handling system is considered as OSBL facility in Bechtel's baseline design.

(4) Dehydration unit was considered in Bechtel's design but not in this project. More complicated hydrocarbon recovery unit is considered in Bechtel's design

(5) In Bechtel's baseline design, CCS is not considered. Hence, most of the CO_2 is captured by the post FT CO_2 capture unit in Unit 200. However, in the base case of this study, WGS reactor is used to increase the H_2/CO ratio in the FT inlet. As a result, significant amount of CO_2 is captured in the acid gas removal unit instead of the post-FT CO_2 removal unit.

(6) The capital cost estimate is consistent with the recent data released by NETL for hydrogen production plant.[4]

(7) C_4 isomerization & C_3-C_5 alkylation units are considered in Bechtel's design for upgrading light hydrocarbons to gasoline but these units are not considered in this project.

(8) Saturated gas plant considered by Bechtel is not considered in this project because light gases are used in furnace and gas turbine in this project instead of upgraded into gasoline in Bechtel's design.

(9) The OSBL cost is expected to be higher in this project because more electricity produced.

Table 3-65. Comparison with NETL's study on large scale CTL plant (NETL, 2007).

		NETL*	Model	Difference	Notes
		(MM$, 2014)		%	
Bare erected cost of each unit					
Unit 100	Syngas production and treatment	1562.7	1543.6	1.22	
	Preprocessing	295.2	316.3	-7.13	
	Gasifier & accessories	936.7	857.8	8.42	
	Air separation unit	330.7	369.5	-11.72	
Unit 200	Gas cleanup	420.1	420.9	-0.19	(1)
Unit 300	Fuel production and upgrading	480.9	561.4	-13.91	
	without naphtha upgrading	480.9	466.9	2.91	(2)
Unit 400	OSBL facilities	383.8	441.4	15.03	
	Gas turbine & accessories	84.1	86.3	-2.56	
	HRSG & steam turbine	117.7	87.5	25.68	(3)
	Cooling water system	42.0	75.2		(4)
	Slag disposal	139.9	192.5		
Total bare erected cost		2847.4	2970.8	-4.33	
Total project cost**		5214.3	5137.6	1.47	(5)

*Original data reported in 2007 is escalated to 2014 pricing basis using CEPCI.

****** TPC includes OSBL, engineering cost, contingency cost.

(1) Dual-stage Selexol unit is used for pre-FT CO_2 removal in NETL's design, which is the same as the base case of this project.

(2) Catalytic reforming & C_5/C_6 isomerization units for naphtha upgrading are not considered in NETL's study but these units are considered in this study.

(3) Difference in power output

(4) Cost of the cooling water distribution system is included in APEA model but not in NETL's case study. Relative error is 12.59% if the cooling water distribution is not considered in this case.

(5) Additional 25% of process contingency is considered for FTS in NETL's study.

Table 3-66. Comparison with NETL's study on small scale CTL plant (NETL, 2007).

		NETL*	Model	Difference	Notes
		(MM$, 2014)		%	
Bare erected cost of each unit					
Unit 100	Syngas production and treatment	372.5	377.7	-1.38	
	Preprocessing	60.0	52.4	12.7	
	Gasifier & accessories	234.3	221.0	5.68	
	Air separation unit	78.1	104.2		
Unit 200	Gas cleanup	84.9	173.6		(1)
Unit 300	Fuel production and upgrading	89.4	151.1		(2)
Unit 400	OSBL facilities	79.5	82.4	3.73	
	Gas turbine & accessories	16.7	20.4		(3)
	HRSG & steam turbine	25.7	21.9		
	Cooling water system	8.4	14.8		(4)
	Slag disposal	28.6	25.4	11.38	
Total bare erected cost		658.0	784.7	-24.96	
Total project cost**		1124.1	1185.2	-5.44	(5)

*Original data reported in 2007 is escalated to 2014 pricing basis using CEPCI.

****** TPC includes OSBL, engineering cost, contingency cost.

(1) CCS is not considered in NETL's design; Area 200 is only for H_2S removal in NETL's study on the small-scale plant.

(2) CCS, catalytic reforming and C_5/C_6 isomerization units are not considered in NETL's study but these units are considered in this study.

(3) Difference in power output

(4) Cost of the cooling water distribution system is included in APEA model but not included in NETL's case study.

(5) Additional 25% process contingency is considered for FTS in NETL's study.

Plant profitability measures are compared with the NETL studies for both a large scale plant with CCS and a small scale plant without CCS. (NETL, 2007) For this study, the economic assumptions are the same as the NETL studies, where the prices of coal, operator, naphtha, diesel and electricity were set to be $36.63/ton, $34.78/hr, $1.5/gallon, $1.96/gallon and $52/MWh for the large scale design and $54.77/ton, $32.5/hr, $1.3/gallon, $1.96/gallon and $35/MWh for the small scale design. For both cases, 26%, 30 years, 40%, 3% and 2% were considered for project contingency, number of years for analysis, tax rate, plant outputs escalation and coal price escalation, respectively. (NETL, 2007) Table 3-67 shows that the profitability measures obtained from our study are similar to the large scale NETL studies, rather some improvement in these measures is observed for our study mainly due to changes in plant configuration and differences in the key design parameters. The net present value of the small scale case is lower than the NETL case due to the additional capital and operating cost of CCS, which is not considered in the small scale NETL design.

Table 3-67. Comparison of the profitability with the NETL's indirect CTL case studies.

	Large Scale		Small Scale	
	Estimated	Difference	Estimated	Difference
Plant capacity (bbl/day)	49992	0	9609	0
Total project cost* (MM$, 2006)	4463	-1.4%	980	0.4%
Net present value (MM$, 2006)	1667	8.0%	133	56%
Payback period (year)	5	0	7	0

*The capital cost are escalated with the CEPCI

Economic model validation of the direct CBTL plants

In the limited techno-economic studies conducted for direct liquefaction processes, coal is the only feedstock considered; hydrogen is usually supplied by coal gasification; and no CCS facility is considered. (Robinson, 2009; Bechtel and Amoco, 1992) In this study, the liquefaction reactor feed only contains 8 wt% of biomass in the base case scenario, which is not expected to have significant impact on the TPC estimation. Hence, the capital cost estimation of the CG_VT process is validated by comparing with the estimates available in the open literature for the DCL plant with different capacities. The estimated costs of the SMR unit and CO_2 compression units are compared with the natural gas to liquids plant and the power plant separately and are found to have good match. (NETL, 2007; 2010; 2013; Baliban et al., 2013) The Decision Analyzer tool in APEA is applied to change the plant capacity from our base case model for fair comparison. For some equipment items, parallel trains have to be considered, because of issues such as hardware constraints, high radial variation, etc. Table 3-68 summarizes the results of the comparison, while Table 3-69 provides detailed comparison of each plant section for the large scale case. Our estimations are found to be similar to the data reported by Shenhua (Wu et al., 2015) which is one of the only existing commercial scale DCL plants in the world, but slightly higher than the data reported by Bechtel/Amoco (Bechtel and Amoco, 1992), mainly because the gasification cost estimated by Bechtel/Amoco in 1992 was lower than the data reported by NETL and others (NETL, 2007; 2010; Baliban et al., 2011), even after it is escalated by CEPCI.

Table 3-68. Validation of capital cost estimation.

Process	CG_VT(1)	CG_VT(2)
Reference	Robinson, 2009	Bechtel and Amoco, 1992
Capacity (bbl/day)	16300	61943
Biomass (wt %)	0	0
Total project cost (MM$, 2015)		
Estimated	2024	6853
Reported	2086	6115

(1) The original capital cost is $1.46 billion for a DCL facility in China in 2008. (Robinson, 2009) This value is adjusted by the reported location factor for China and escalated by CEPCI. (Su, 2010; Larson and Ren, 2003)
(2) The original capital cost is $3.87 billion with 1991 pricing basis. The capital investment of the gasification unit reported by Bechtel/Amoco is lower than most recent estimation reported by NETL. (NETL, 2007; 2010; Baliban et al., 2011; Bechtel and Amoco, 1992)

Table 3-69. Detailed comparison of equipment cost estimation (MM$, 61943 bbl/day).

	Estimated	Reported		Estimated	Reported
Feed drying and handling	103.8	115.2	Hydrogen production[3]	250.4	129.3
Liquefaction[1]	416.2	455.2	Air separation unit	138.2	165.0
Product upgrading[2]	92.6	47.6	Sulfur recovery	46.0	24.1
Hydrogen purification	105.3	96.8	Total equipment cost	1178.1	1053.7
ROSE-SR	25.6	20.6	Total project cost	6711.1	6115.0

(1) Required solvent/feed ratio for liquefaction has been reduced since Bechtel/Amoco did their estimation in 1992.
(2) Naphtha upgrading was not considered in Bechtel/Amoco's design but in our design
(3) The equipment cost for gasification estimated by Bechtel/Amoco is lower than the data published in other resources. (NETL, 2007; 2010; Baliban et al., 2011; Bechtel and Amoco, 1992)

Task 3.3 Evaluation of Projects

Planned Activities

- ✓ **Material and energy balance (base case):** material and energy balance is computed for all different CBTL plant with baseline design
- ✓ **Techno-economic analysis (base case):** techno-economic analysis is performed for all different CBTL plants with baseline design

Accomplishments

- ✓ **Material and energy balance (base case)**

Table 3-70 lists the base case values of the key design parameters investigated in this study of the indirect CBTL plant with CCS (FT_CCS). The stream and utility summaries of the base case can be found in Table 3-71 and Table 3-72. Table 3-72 indicates that syngas production and CCS are the two major utility consumers in the indirect CBTL plant, with is consistent with open literature. (Jiang and Bhattacharyya, 2014; Dry, 2002; Kreutz et al., 2008) It should be noted that the process fuel required in the CBTL plant is supplied by the fuel gas header while the steams and electricity are supplied by the combined cycle plant. Table 3-73 provides the overall material and energy balance of the indirect CBTL Plant with CCS.

Table 3-70. Key design parameters (indirect, base case).

Design parameter	Value
Biomass type	Bagasse
Plant capacity (bbl/day)	10,000
Biomass/coal (wt/wt, dry)	8/92
Hydrotreating approach	Integrated
Steam/carbon ratio in the ATR inlet	0.63
H_2/CO in FT inlet stream (mol/mol)	2
CO_2 captured in Selexol unit (%)	90
CO_2 captured in MDEA/PZ unit (%)	98
CO_2 stream to compression section (%)	100

Table 3-71. Summary of stream (indirect, base case).

Steam	1	2	3	4	5	6	7	8	9	10	11	12
Temperature (ºC)	32	16	850	284	258	49	49	261	38	25	38	81
Pressure (kPa)	2380	2380	2380	2289	1999	1965	1965	1999	1965	101	138	15,270
Flowrate (kg/hr)												
Coal		173747										
Biomass		15021										
H_2O			57005	149827	409	109	267	5281	195			30
CO_2			124409	204043	20451	1398	54057	2202	397			229545
O_2	141,184											
N_2	2139		4584	4583								
CH_4			1865	1863	1676	30	3743	721	2751		1130	309
CO			183130	132431	130823	39	11897	22168	8732		3187	4745
COS			208	109								
H_2			12570	16203	16154	7	5509	5594	4043		1474	64
H_2S			45142	4547								
C_2-C_4			177	177		910	6512	14	3479		6853	141
C_5-C_{10}						13933	3251	1531	1531		1725	
C_{11}-C_{20}						12036	7	1	1			
Wax						25632						
Oxygenates						3279	774	553	553			
Gasoline										18391		
Diesel										30579		

(1) Streams numbered in Figure 3-1

Table 3-72. Summary of utility consumption (indirect, base case)*.

Sections	Power	74 bar steam	42 bar steam	21 bar steam	9.3 bar steam	3.7 bar steam	Fuel
	MW	kg/hr	kg/hr	kg/hr	kg/hr	kg/hr	GJ/hr
Syngas Production	59.48	(119895)		(25667)	58340	(119680)	8.31
Syncrude Production	0.88		6784	(186727)			19.97
CO_2 Capture & Storage	42.24				79538	50841	
Product Upgrading	1.16		213			1190	87.31
Fuel Gas Header							(699.51)
Others	12.94			(4266)			
Gas Turbine	(56.52)						583.92
HRSG	(72.44)	119895	(6997)	216660	(137878)	67649	

* ( ) means utility generation

Table 3-73. Key design parameters (indirect, base case).

Plant performance	Flowrate
Coal/biomass (ton/hr, dry)	153.8/13.5
Gasoline/diesel (bbl/day)	4050
Net power output (MW)	2.50
Thermal efficiency (%, HHV basis)	45.9

The material and energy balances for all four configurations of direct CBTL plants can be found in Table 3-74, which indicates that the thermal efficiency of the direct CBTL plant can be significantly increased by producing hydrogen from shale gas. Table 3-75 provides the temperature, pressure and key component flowrates for the main streams in the SMR_CCS process with a capacity of 10000 bbl/day and a biomass/coal weight ratio of 8/92. The streams are numbered in Figure 3-2.

Table 3-74. Material and energy balances of the direct CBTL plant (HHV basis(1)).

Process	SMR_CCS	SMR_VT	CG_CCS	CG_VT
Energy inputs				
Coal, tonne/hr (GJ/hr)	100.1 (2962)	100.1 (2962)	151.4 (4479)	151.4 (4479)
Biomass, tonne/hr (GJ/hr)	9.3 (163)	9.3 (163)	14.1 (247)	14.1 (247)
Shale gas, tonne/hr (GJ/hr)	21.6 (1105)	21.6 (1105)	N/A	N/A
Energy outputs				
Gasoline, bbl/day (GJ/hr)	2443 (595)	2443 (595)	2443 (595)	2443 (595)
Diesel, bbl/day (GJ/hr)	7557 (1936)	7557 (1936)	7557 (1936)	7557 (1936)
Net power (MW)	52.4	77.8	84.5	111.9
Thermal efficiency (%)	64.3	66.5	60.0	62.1

(1) HHVs of gasoline and diesel are set to be 5.84 and 6.15 GJ/bbl (Williams and Larson, 2003)

Table 3-75. Stream summary of the SMR_CCS process.

Stream	1	2	3	4	5	6	7	8	9	10	11
Temperature (°C)	27	21	35	432	267	414	93	302	35	36	36
Pressure (bar)	1	20	22	208	1	208	3	55	55	3	3
Flow rate (kg/s)											
Coal	27.81			1.03				1.03			
Biomass	2.59										
H_2O			0.06	3.18		2.72			0.01		
CO_2		0.14	11.55	1.88		1.77			9.89		
CO			0.12	0.63		0.61			0.30		
H_2			2.04	2.52		2.43			0.74	2.41	0.14
H_2S				2.01		1.85			0.22		
NH_3				0.88		0.81					
CH_4		4.73	1.67	1.89		1.81			0.02		
C_2-C_4		1.09		3.50		3.23					
C_5-177 °C				5.15		4.13	3.56				
177-288 °C				8.24		4.89	6.65				
288-344 °C				8.05	2.59	3.43	6.29				
344-454 °C				41.37	40.62	10.81	1.11				
454 °C +				15.63	13.57	1.09		2.53			
Ash				3.04	0.03			2.88			

✓ Techno-economic analysis (base case)

An early study of NETL claimed that increasing the percentage of biomass in the feedstock would increase capital and operating costs due to the higher raw material cost and reduced economies of scale and recommended that modest biomass percentages in CBTL plant would provide affordable fuels from domestic biomass feedstock and enable considerable reduction in GHG emission. (NETL, 2009) What's more, due to the high transportation cost, low energy density and limited long-term availability of biomass, the capacity of BTL or CBTL are constrained. (Wang and McNeel, 2009) As the concern about economic and environmental sustainability, the biomass to coal mix ratio and plant size are set to be 8/92 and 10k bbl/day for the base case. (NETL, 2009; Liu et al., 2015; Wang and McNeel, 2009) Given the steady-state model developed in Aspen Plus, the key design parameters and process performance measures are shown in Table 3-76 to Table 3-78 for the base case scenario of the indirect, direct and hybrid CBTL plant with CCS.

Table 3-76. Key design parameters and plant performance measures (indirect).

Key design parameters	Value	Plant performance	FT_CCS
Plant capacity (bbl/day)	10000	Coal/biomass (ton/hr, dry)	153.8/13.5
Biomass type	Wood chip	FT gasoline (bbl/day)	4050
Biomass/coal (wt/wt, dry)	8/92	FT diesel (bbl/day)	5950
Hydrotreating approach	Integrated	Net power output (MW)	2.50
Post-FT CO_2 capture technology	MDEA/PZ	Carbon captured by FT liquids (%)	36.3
H_2/CO in FT inlet stream (mol/mol)	2	Carbon captured by CCS (%)	56.9
Extent of CCS (%)	High(1)	Thermal efficiency (%, HHV basis)	45.9

(1)All CO_2 streams removed from pre- and post-FT CO_2 removal units are sent to compression section

Table 3-77. Key design parameters and plant performance measures (direct).

Key design parameters	Value	Plant performance	SMR_CCS	CG_CCS
Plant capacity (bbl/day)	10000	Coal/biomass (tonne/hr)	100/9	151/14
Biomass type	Wood chip	Shale gas (tonne/hr)	22	0
Biomass/coal (wt/wt, dry)	8/92	Gasoline/diesel (bbl/day)	2433/7557	2433/7557
Low pressure CO_2 capture	MDEA/PZ	Net power (MW)	52.4	84.5
Extent of CCS if considered	High(1)	Efficiency (%, HHV)	64.3	60.0

(1) 90% of carbon in the raw materials is either converted to gasoline and diesel or stored in captured CO_2

Table 3-78. Key design parameters and plant performance measures (hybrid).

Key design parameters	Value	Plant performance	HSMR_CCS	HCG_CCS
Plant capacity (bbl/day)	10000	Coal (tonne/hr)	136.3	166.0
Biomass type	Wood chip	Biomass (tonne/hr)	12.7	15.5
Biomass/coal (wt/wt, dry)	8/92	Shale gas (tonne/hr)	14.8	0
Indirect/direct(1) (%/%)	50/50	Gasoline (bbl/day)	2845	2845
H_2/CO in FT inlet stream (mol/mol)	2	Diesel (bbl/day)	7155	7155
Low pressure CO_2 capture	MDEA/PZ	Net power (MW)	84.9	91.5
Extent of CCS if considered	High(2)	Efficiency (%, HHV)	56.5	55.7

(1) Ratio of coal and biomass sent to the gasification unit over that sent to the direct liquefaction unit
(2) 90% of carbon in the raw materials is either converted to gasoline and diesel or stored in captured CO_2

For the base case scenario of indirect CBTL plant (Table 3-76) with economic parameters specified in Table 3-43 and Table 3-44, the NPV, IRR, payback period, and BEOP are \$179 MM, 11.5%, 7 year and \$95.5/bbl, respectively. Table 3-79 lists the economic measures of the CBTL plant with different capacities. It shows that for the current plant design and specified economic parameters, the BEOP of FT liquids can be reduced to about \$77.8/bbl and the IRR can be increased to about 14.0%, if the plant capacity is increased to 50k bbl/day.

Table 3-80 shows the contribution of each unit to the BEOP of the CBTL plant. The results indicate that feedstock cost contributes about half of the BEOP, while the other half of the BEOP is due to the capital cost. The syngas production section contributes about 60% of the total capital investment, which is similar to the data reported in the open literature. (Dry, 2002) The CCS units, including pre- and post- FT CO_2 removal process and CO_2 compression process, also consume a significant amount of utilities and capital

investment. As noted before, the utilities such as fuel gas, steam and electricity are generated inside the plant and therefore utilized in the process. The change in utility consumption is reflected by the change in net power output of the CBTL plant. As seen in Table 3-80, the main consumers of utilities are the syngas production unit and the CCS unit. Therefore selections of the CCS technologies and related design parameters are critical for reducing the BEOP of the CBTL plant with CCS.

Table 3-79. Effect of plant capacity on the economic performance of the CBTL plant with CCS.

Cases	Small scale	Medium scale	Large scale
Plant capacity (bbl/day)	10000	30000	50000
Net present value (MM$)	179	771	2057
Internal rate of return (%)	11.5	12.2	14.0
Payback period (year)	7	6	5
Break-even oil price ($/bbl)	95.5	89.8	77.8

Table 3-80. Contribution to the BEOP of the CBTL plant with CCS (10k bbl/day, Base case). (1)

Percentage	Feedstock	Capital(2)	Electricity	Steam	Fuel
Total	55.18	45.63	(0.81)	0.00	0.00
Process units					
Syngas production(3)		57.5	51.0	(52.9)	1.2
Syncrude production		10.7	0.8	(46.0)	2.9
CO_2 capture & storage(4)		11.5	36.2	35.6	0.0
Product upgrading		10.6	1.0	0.4	12.5
Fuel gas header		0.0	0.0	0.0	(100)
Others		3.0	11.1	(1.1)	0.0
Gas turbine		2.8	(46.7)	0.0	83.5
HRSG & steam turbine		3.9	(55.4)	64.1	0.0

(1) ( ) indicates utility generation
(2) Annualized by assuming 10-year economic life of equipment
(3) ASU is included in the syngas production section
(4) Including pre- and post- CO_2 capture units and CO_2 compression unit

With the economic parameters listed in Table 3-53 and 3-54 as well as the material and energy balance shown in Table 3-77, the major economic measures of the base case are calculated and reported in Table 3-81 for the direct and hybrid CBTL plants with CCS. It can be noted that none of the four investigated configurations of the direct CBTL plants can make profit or have positive NPV due to the current low crude oil price (COP). However, the direct CBTL plants may start to payback once COP surpasses the reported BEOP, and be competitive with traditional petroleum industries once COP surpasses the reported EOP. The results also shows that the capital investments of the CG_CCS and CG_VT processes are much higher than those of the SMR_CCS and SMR_VT processes, because of the high capital cost and low hydrogen production efficiency of the gasification unit in comparison to the shale gas steam reforming unit. (Jiang and Bhattacharyya, 2016; Williams and Larson, 2003) As a result, the BEOP and EOP of the SMR_CCS and SMR_VT processes are higher than those of the CG_CCS and CG_VT processes,

which indicate that the direct CBTL plants will be more profitable if hydrogen is produced from low cost shale gas. Additionally, the relative penalty of CCS based on BEOP is about 10.2% if hydrogen produced from shale gas SMR and residual POX and 8.8% if hydrogen is produced from coal/biomass/residues CG, because CO_2 produced from gasification unit is at higher partial pressure and therefore easier to be captured. (Jiang and Bhattacharyya, 2016)

Table 3-81. Major economic measures (10,000 bbl/day, base case).

Process	SMR_CCS	HSMR_CCS	CG_CCS	HCG_CCS
Total project cost (MM$)	1162	1474	1464	1593
Net present value (MM$)	-408.6	-552.0	-591.7	-636.8
Internal rate of return (%)	6.0	5.6	5.2	5.1
Break-even oil price ($/bbl)	86.1	94.5	97.5	100.6
Equivalent oil price ($/bbl)	101.0	112.0	115.5	120.0

Task 3.4 Sensitivity Studies

Planned Activities

- ✓ **Effect of key design parameters on the indirect CBTL plant performance:** Effect of key design parameters on the plant performance (thermal and carbon efficiency) is studied.
- ✓ **Effect of key design and investment parameters on the indirect CBTL plant economic performance:** Effect of key design and investment parameters on the economic performance (NPV, IRR, BEOP and EOP) is studied.
- ✓ **Effect of key design parameters on the direct CBTL plant performance:** Effect of key design parameters on the plant performance (thermal and carbon efficiency) is studied.
- ✓ **Effect of key design and investment parameters on the direct CBTL plant economic performance:** Effect of key design and investment parameters on the economic performance (NPV, IRR, BEOP and EOP) is studied.
- ✓ **Effect of plant configuration and summary of case studies:** The results generated from the process model are validated by comparing with the data available in the open literature.

Accomplishments

- ✓ **Effect of key design parameters on the indirect CBTL plant performance**

In this section, sensitivity study is conducted for the indirect CBTL plant to analyze the effect of key design parameters and economic measures. First a simplified indirect CBTL plant (once-through, no combined cycle) is studied, as shown in Figure 3-38. Then studies are conducted for the entire indirect CBTL plant with CCS as shown in Figure 3-1.

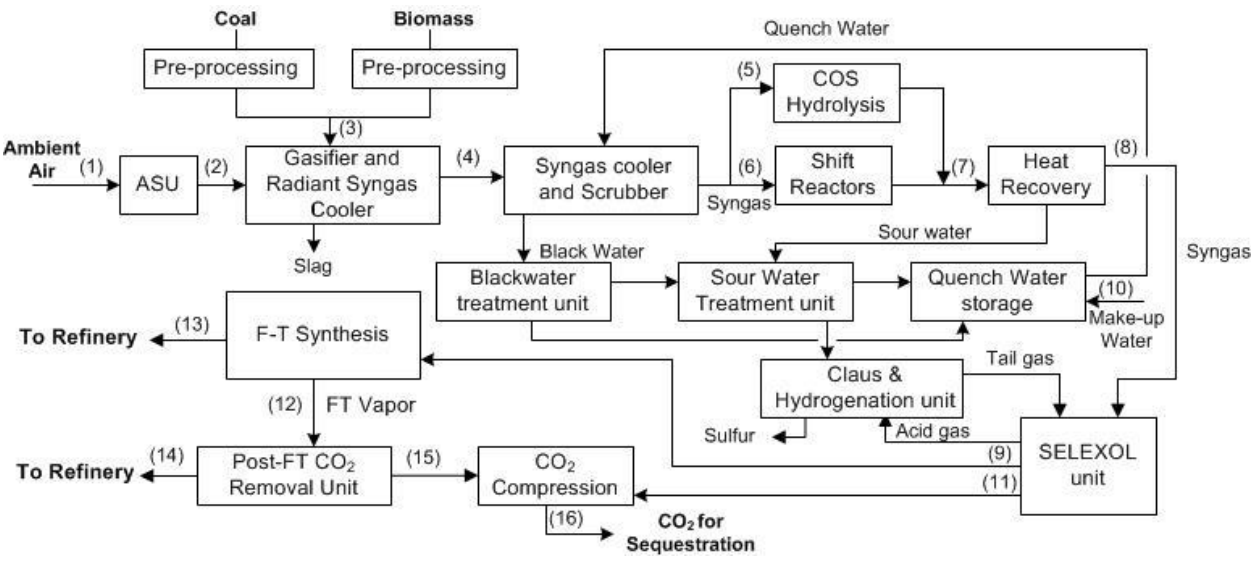

Figure 3-38. BFD of the simplified indirect CBTL plant with CCS (utility streams not shown).

Effect of the lean solvent loading on MDEA/PZ CO_2 removal unit with intercooling

This study is conducted for the simplified indirect CBTL plant. Lean solvent loading is one of the key operating conditions for amine-based CO_2 removal systems. A decrease in the lean solvent loading can reduce the solvent circulation rate required for the same extent of CO_2 removal. However, it can result in an increase in the heat requirement for solvent regeneration. Six values of lean solvent loading are investigated. It should be noted that the solvent circulation rate is manipulated to achieve 98% of CO_2 removal for these studies. In these studies, the lean solvent loading is calculated in terms of moles of CO_2 per moles of amine groups. The costs of cooling water, LP steam, and power are taken as \$0.354/GJ, \$13.28/GJ, and \$16.8/GJ, respectively. (Turton et al., 2012) Table 3-82 shows that the utility cost first decreases as the lean solvent loading is increased. But with further increase in the lean solvent loading, the utility cost increases. The optimum lean solvent loading is found to be about 0.06 mol CO_2/ mol amine group for the FT product. It can be noted that the optimum value of lean loading can change if the gas composition, operating pressure and/or extent of CO_2 removal change. In this study, the utility consumption does not change significantly with the lean solvent loading, which is consistent with the experimental data (Seagraves and Weiland, 2009) and simulation results (Salkuyeh and Mofarahi, 2013) available in the open literature for MDEA-based system and relatively low range of lean solvent loading and high operating pressure. One reason of this insensitivity is that with the decreasing of lean solvent loading, the temperature increasing from the exothermic reaction in the column increases and the CO_2 loading of the rich solvent decreases, which will limit the extent of the increase in the CO_2 capacity of the solvent, a function of the difference in CO_2 loading of the rich and the lean solution. Hence, the solvent circulation rate will not decrease as much as we expected with the decreasing lean solvent loading. Another reason is that the absorber is operated at higher pressure level than the normal post-combustion CO_2 removal system, which increase the effect of physical absorption step. From Salkuyeh and Mofarahi's work (Salkuyeh and Mofarahi, 2013), the effect of lean solvent loading on the utility consumption decreases with the increasing absorption pressure.

Table 3-82. Effect of lean solvent loading in the MDEA/PZ based CO_2 capture unit.

Lean loading (mol CO_2/mol amines)	Solvent/CO_2 (mol/mol)	Cooling Water (GJ/hr)	Reboiler Duty (GJ/hr)	Pumping Power (kW)	Utility Cost ($/hr)
0.03	19.00	118.93	120.33	876.94	1694
0.05	19.47	118.64	120.18	888.87	1692
0.06	19.71	118.56	120.05	895.55	1690
0.08	20.22	118.82	120.27	909.78	1694
0.09	20.49	119.25	120.68	918.17	1700
0.10	20.77	119.30	120.88	924.25	1703

Effect of the operating pressure of the flash drums on the single-stage Selexol unit

This study is conducted for the simplified indirect CBTL plant as shown in Figure 3-38, of which the stream information can be found in Table 3-86. In the single-stage Selexol unit for post-FT CO_2 capture, 93% CO_2 capture is achieved in the absorber and released in a series of flash drums at decreasing pressure levels. The reduction of the power consumption of this unit with the CO_2 compression can be achieved by operating the HP, MP and LP flash drums at optimum pressures. With different operating pressures of the LP flash drum, the CO_2 loading in the lean solvent recycled back to the absorber becomes different, which will significantly affect the solvent circulation rate of the system with the same extent of CO_2 removal. If the operating pressure of the LP flash drum is fixed, the solvent circulation rate does not change much with change in the pressures of MP and HP flash drums, but the relative distribution of CO_2 obtained from the three flash drums will change, which will affect the power consumption of the CO_2 compression system. In this study, first the MP and HP drum pressures are fixed at 414 kPa and 690 kPa, respectively to study the effect of the operating pressure of the LP flash drum. Once the optimum LP drum pressure is obtained, the effect of the MP and HP flash drum pressures are obtained.

Figure 3-39 shows, as expected, that the solvent circulation rate increases with the increasing pressure of the LP flash vessel. With the increasing solvent circulation rate, the total power consumption increases mainly due to the increase in the refrigeration load and power consumption by the solvent circulation pump. An increase in the solvent circulation rate also results in higher loss of hydrocarbons. The optimal pressure of the LP drum is found to be 138 kPa. Once this pressure is fixed, Figure 3-40 shows the effect of the change in the pressure of the MP and HP flash drums. From Figure 3-40, the optimal pressures of the MP and HP flash drums are 310 kPa and 621 kPa, respectively. Figure 3-40 shows that the total power consumption does not change significantly in the pressure range studied. It should be noted that the pressures of the HP and MP drums were not changed widely as these pressures are constrained by the operating pressure of the H_2 flash drum (1.1 MPa). Furthermore, the CO_2 compressor consumes about 33% power in the Selexol unit, while the remaining power is consumed for solvent chilling and circulation.

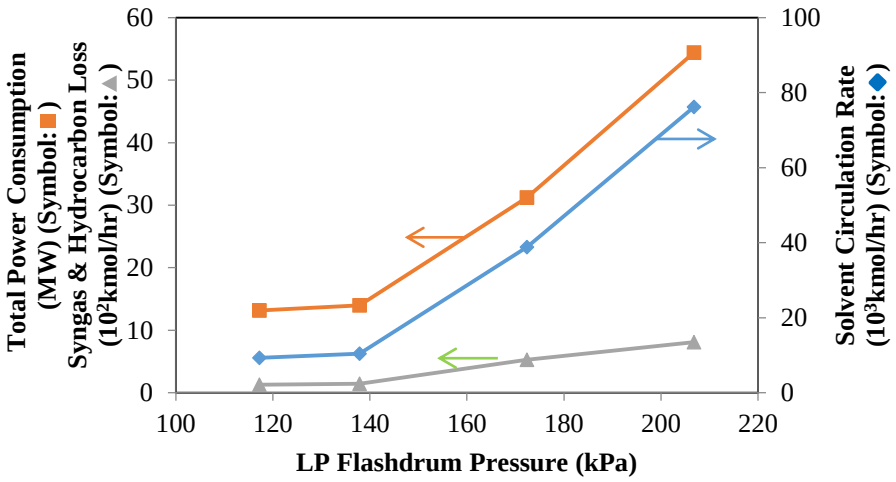

Figure 3-39. Effect of LP Flash drum Pressure.

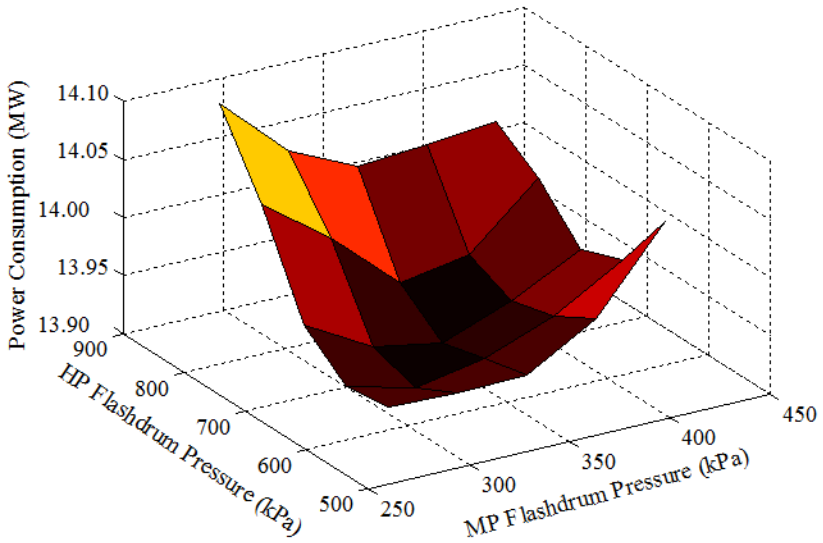

Figure 3-40. Effect of Pressures of MP and HP Flash drums.

Selection of the post- FT CO_2 removal technology

This study is conducted for the simplified indirect CBTL plant. In this section, three solvents, MEA, MDEA/PZ, and Selexol, are evaluated for removing CO_2 from the FT hydrocarbons. As mentioned before, the selectivity of Selexol, a physical solvent, is poor, and as a result significant amount of hydrocarbons can be lost. The lower heating value (LHV) of total hydrocarbon lost in the Selexol unit is calculated and converted to equivalent utility consumption for a fair comparison with the amine-based CO_2 removal technologies. The hydrocarbon loss and corresponding LHV loss in the Selexol unit are shown in Table 3-83. The loss is found to be about 15 wt% of total hydrocarbon produced. Table 3-84 indicates that the Selexol technology is not suitable for removing CO_2 from the FT product because of the considerable hydrocarbon loss. It also shows

that the intercooling can significantly reduce the total utility cost of MEA and MDEA/PZ based CO_2 removal units. The MDEA/PZ CO_2 removal unit with intercooling gives the lowest utility cost and is therefore considered to be the desired technology for all following base case studies. It is also noted that the steam consumption of MDEA/PZ system is 14.4% less than that the MEA system, which might be more economic than the inhibited MDEA system (13.8% less than the MEA system) selected by Bechtel (Bechtel, 1992) as their base case. Additionally, it can be noted that the MDEA/PZ as a solvent is also advantageous due to its lower corrosion and lower vapor pressure in comparison to MEA.

Table 3-83. Hydrocarbon loss in the single-stage Selexol unit.

	HC Loss (kg/hr)	Heat Loss (GJ/hr)
C_1	267	13.3
$C_{2=}$	1393	66.5
C_2	533	25.1
$C_{3=}$	1825	83.4
C_3	396	18.2
$C_{4=}$	1544	69.7
C_4	581	27.0
$C_{5=}$	1156	52.3
C_5	414	18.6
$C_{6=}$	630	28.1
C_6	217	9.6
Total		411.8

Table 3-84. Comparison of the three CO_2 removal technologies (including CO_2 compressing)*.

	Selexol	MEA w/o*	MEA w/*	MDEA/PZ w/o	MDEA/PZ w/**
Power (MW)	13.92	6.20	6.13	6.03	5.88
Cooling Water (GJ/hr)	30.84	175.65	167.32	164.81	147.33
Reboiler Duty (GJ/hr)		146.23	137.94	136.81	120.05
Heat Lost (GJ/hr)	411.8				
Utility Cost ($/hr)	6322	2379	2262	2240	2001

* w/o denotes without intercooling, and w/ denotes with intercooling; the lean solvent loading of MEA units is 0.27 mol CO_2/ mol amine (Dugas, 2006).
** the technology selected for all following base case studies

Material and utility summaries of the simplified indirect CBTL plant with CCS

This study is conducted for the simplified indirect CBTL plant. In the base case of the simplified indirect CBTL plant, the H_2/CO ratio and the biomass/coal weight ratio are set to 2 and 8/92 (dry); the total feed flowrate of coal and biomass is 246.6 ton/hr and the MDEA/PZ with intercooling process is used for post-FT CO_2 removal. Table 3-85 lists the operating condition of key units. Considering the valid range for the available correlations and the economic analysis available in the open literature (Bechtel, 1992a; Kou, 1985; Fox and Tam, 1995), the operating condition of

the FT reactor for the base case is decided to be 257°C and 2 MPa. In our base case design, the inlet H_2/CO ratio is set to 2 to decrease the selectivity of main byproduct CO_2 and the utilities consumption in the CCS facilities. After the operating pressure of the FT unit is decided, the operating pressure of other units is calculated by considering pressure drop in all equipment. The operating temperature of each unit is decided based on the optimization studies available in the open literature (Bhattacharyya et al., 2011; Bechtel, 1992a; Bain, 1992).

Table 3-85. Summary of the operating condition of key units.

	Pressure (kPa)	Temperature (°C)
Syngas Production		
ASU Air Compressor	1310	
Oxygen Compressor	2400	
Gasifier	2380	850
Fischer-Tropsch		
FT Reactor	2000	257
Selexol		
H_2S Absorber	2048	2
CO_2 Absorber	2013	2
H_2S Concentrator	1930	117
Selexol Stripper*	600	41/153
H_2 Recovery Drum	1620	
LP Flash Vessel	241	
Post-FT CO_2 Removal		
Absorber	1965	38
Stripper*	172	38/116

*For strippers, the temperatures of condensers and reboilers are listed.

Table 3-86 lists the flow rate of the key species in the main streams numbered in Figure 3-38 for the base case conditions. In the base case, 6% of carbon in the coal and biomass is vented to the atmosphere in form of CO_2, 53% of carbon is stored in the captured CO_2, while the remaining carbon is converted to the FT syncrude and fuel gas. To simplify the results and discussion of the plant utility consumptions, the plant shown in Fig. 1 is divided into four sections for showing the results and discussion. They are syngas production section, CO_2 capture and storage (CCS) section, FT synthesis section and others. Table 3-87 lists the main utility consumptions for the base case. The syngas production and the CCS sections are the two main consumers of the electric power, consuming about 54% and 36%, respectively, of total power demand. The production of purified syngas has been reported to cost 60-70% of the total capital and running cost in conventional CTL plants without CCS facilities. (Dry, 2002) The HP, IP and LP steam are generated from the syngas production and cleanup section, Claus unit, and the FTS section. The strippers and heaters in the CBTL plant consume IP and LP steam. It can be noted that the HP steam generated in the radiant syngas cooler can be used to produce electricity. The power consumptions in the remaining units are calculated based on the utility summary available in the open literature (Reed et al., 2007; NETL, 2010; Bechtel, 1998) by scaling up with respect to the coal and biomass flowrate (dry).

Table 3-86. Stream summary of the CBTL plant with CCS.

Stream	1	2	3	4	5	6	7	8
Name	Air	O_2	Coal & Biomass	Raw syngas	Raw syngas	Raw syngas	Shifted syngas	Cooled syngas
Temperature (°C)	15	32	16	850	208	208	301	21
Pressure (kPa)	103	2,380	2,380	2,380	2,324	2,324	2,289	2,082
Flowrate (kg/hr)								
H_2O	5,792			74,468	105,675	132,678	186,570	467
CO_2	386			162,520	72,014	90,412	288,921	288,830
O_2	197,602	184,434						
N_2	643,327	2,794		5,988				
CH_4				2,436	1,080	1,356	2,436	2,431
CO				239,229	106,056	133,159	158,774	158,769
COS				272	118	150	14	14
H_2				16,402	7,271	9,131	22,190	22,190
H_2S				5,897	2,604	3,266	5,947	5,919
Coal			226,972					
Biomass			19,623					
Slag				24,916				
C_2-C_4				231	104	127	231	231
C_5-C_{10}								
C_{11}-C_{20}								
Wax								
Oxygenates								

Stream	9	10	11	12	13	14	15	16
	Clean syngas	Make-up water	CO_2	FT vapor	FT liquid	Light gases	CO_2	CO_2
Temperature (°C)	3	16	37	38	38	39	38	89
Pressure (kPa)	2,013	1,014	203	1,979	1,979	1,965	172	15,272
Flow Rate (kg/hr)								
H_2O	535	173,089	5	272	109	272	73	78
CO_2	28,550		260,280	58,846	1,538	1,175	57,671	317,951
O_2								
N_2								
CH_4	2,350		73	3,211	27	3,211		73
CO	153,834		4,940	12,211	41	12,193	18	4,958
COS								
H_2	22,136		64	5,135	5	5,126	9	73

H_2S							
Coal							
Biomass							
Slag							
C_2-C_4	27		204	6,446	1,021	6,446	204
C_5-C_{10}				3,012	13,531	3,012	
C_{11}-C_{20}				9	12,760	9	
Wax					27,189		
Oxygenates				689		689	

Table 3-87. Summary of the utilities in the CBTL plant with CCS.

Power Consumptions (MW)		%	Steam Generation (GJ/hr)	
Syngas Production	88.2	53.58	Syngas Production	
Syngas Generation	77.1	46.84	Radiant Syngas Cooler (HPSTM)	-240.6
Steam Generation	0.5	0.3	Heat Recovery (IPSTM)	-113.2
Black and Sour Water Treatment	10.6	6.44	Heat Recovery (LPSTM)	-348.1
CO_2 Capture and Storage	59.5	36.15	SWS Reboiler (IPSTM)	79.6
Selexol	33.1	20.11	Fischer-Tropsch Synthesis	
MDEA/PZ	0.9	0.55	IP Steam Generator (IPSTM)	-369.1
CO_2 Compression	25.5	15.49	CO_2 Capture and Storage	
Fischer-Tropsch Synthesis	0.9	0.55	Selexol Striper Reboiler (IPSTM)	197.9
Others	16	9.72	MDEA/PZ Striper Reboiler (LPSTM)	120.1
Total	164.6	100	Others (IPSTM)	4.5

Effect of biomass/coal ratio in the feedstock

This study is conducted for the simplified indirect CBTL plant. As mentioned before, an increase in the biomass content in the gasifier feed can significantly decrease the carbon footprint of the indirect CBTL plant. In this study, impact of the biomass content on the syngas composition and the utility generation in the syngas production and cleanup sections is investigated. Four biomass concentrations are studied here, 5 wt%, 8 wt%, 15 wt%, and 20 wt% (dry), with the same dry feed flowrate. The results are listed in Table 3-88. When the biomass content in the feedstock is increased, the H_2/CO ratio of the raw syngas from the gasifier increases. This results in a decrease in the extent of the WGS reaction in the WGS reactors. Therefore, the heat that can be recovered after the WGS reactor also decreases because the WGS reaction is exothermic. Considering the total energy balance, this would be expected as the heating value of biomass is lower than the coal.

Table 3-88 Effect of biomass/coal ratio on the syngas composition and steam generation.

	Syngas Composition (mol %)							Heat to HRSG (GJ/hr)	
Biomass/Coal	H_2	CO	CO_2	H_2O	Others	H_2/CO	$\frac{\text{Syngas to WGS}}{\text{Syngas produced}}$	RSC	Heat Recovery
5/95	32	33.8	14.2	15.5	4.5	0.947	0.447	240.9	541.0
8/92	31.7	33.2	14.4	16.1	4.6	0.955	0.443	240.6	532.8
15/85	30.9	31.9	14.7	17.6	4.9	0.969	0.433	239.9	513.8
20/80	30.3	30.9	15	18.7	5.1	0.981	0.429	239.5	500.5

Effect of the H_2/CO ratio at the FT inlet on the utility consumption of CCS facilities

This study is conducted for the simplified indirect CBTL plant. H_2/CO ratio in the coal derived syngas is always lower than the stoichiometric ratio needed in the FT reactor. However, the H_2/CO ratio in the coal derived syngas can be increased in the WGS unit. The effect of the H_2/CO ratio on the utility consumption in the CBTL process with CCS is evaluated. From Table 3-87, it can be noted that the units for CCS, i.e. the Selexol unit for pre-FT CO_2 capture, the MEDEA/PZ unit for post-FT CO_2 capture, and the CO_2 compression unit, use about 36% of the total electricity consumed in the plant. The range of H_2/CO ratio investigated is from 1 to 2. The lower bound is decided based on the composition of the raw syngas that is generated from the gasifier assuming that the WGS reactor is not available. The upper bound is set to match with the stoichiometric ratio of the FTS reaction. Table 3-89 presents the results from this study. With the increase in the H_2/CO ratio from 1 to 2 at the FT reactor inlet, the utility consumption keeps decreasing; however, the net heat recovery does not change appreciably. The decrease in power, IP steam and LP steam consumption results from the decrease in solvent circulation rates in both the Selexol and MDEA/PZ units as shown in Table 3-90. In summary, the power consumption in the CCS section (the Selexol, MDEA/PZ, and CO_2 compression units) and the entire CBTL plant (excluding the product upgrading section) can be reduced by 8.5% and 3.6% if the inlet H_2/CO ratio increases from 1 to 2. Figure 3-41 shows that about $3800/hr in utility costs can be saved using the H_2/CO ratio of 2 in comparison to the H_2/CO ratio of 1.

Table 3-89. Effect of H_2/CO ratio on the plant utility.

H_2/CO	2	1.7	1.5	1.3	1
Total Power Consumption (MW)	164.6	165.9	167.0	169.0	170.8
Syngas Production (MW)	88.2	88.4	88.5	88.5	88.7
CO_2 Capture and Storage (MW)	59.5	60.6	61.6	63.5	65.0
FTS & Others (MW)	16.9	16.9	16.9	17.0	17.1
Heat Recovery (HPSTM) (GJ/hr)	-240.6	-240.6	-240.6	-240.6	-240.6
Heat Recovery (IPSTM) (GJ/hr)	-482.3	-499.4	-496.9	-493.5	-487.6
Heat Recovery (LPSTM) (GJ/hr)	-348.1	-354.3	-377.8	-405.7	-453.3
IPSTM Consumption (GJ/hr)	282.0	329.2	390.4	426.1	517.9
LPSTM Consumption (GJ/hr)	120.1	142.2	156.9	176.1	227.0

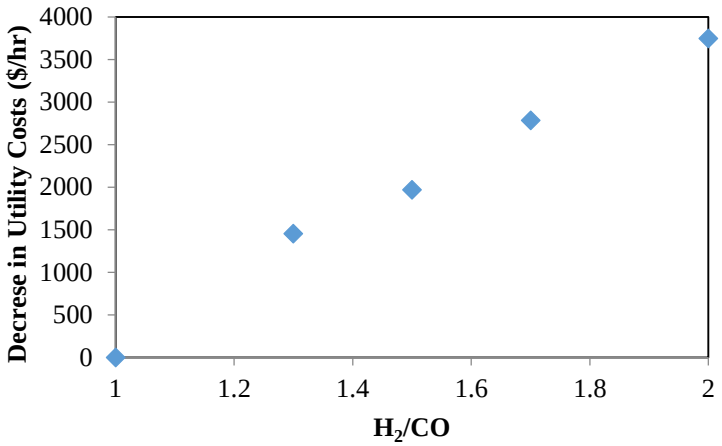

Figure 3-41. Decrease in utility costs due to change in the H_2/CO ratio.

Table 3-90. Effect of the H_2/CO ratio on the solvent circulation rates.

H_2/CO	2	1.7	1.5	1.3	1
SELEXOL					
CO_2 Captured (kmol/hr)	5914	5328	4865	4317	3380
Partial Pressure of CO_2 (kPa)	564	523	488	445	366
Solvent Circulation Rate (kmol/hr)	9979	11340	12474	13971	16556
Solvent/CO_2 (kmol/kmol)	1.69	2.13	2.56	3.24	4.90
MDEA/PZ					
CO_2 Captured (kmol/hr)	1311	1678	1967	2320	2954
Solvent Circulation Rate (kmol/hr)	25998	32487	37588	43587	54266
Solvent/CO_2 (kmol/kmol)	19.83	19.36	19.11	18.79	18.37

In the Selexol process, the main power consumption is due to the compressors in the NH_3 vapor-compression cycle. This is a strong function of the solvent circulation rate. The partial pressure of the acid gases is the main driving force for mass transfer as Selexol is a physical solvent. The higher the CO_2 partial pressure (P_{CO_2}) is, the more efficient the Selexol process will be. In the CBTL plant, the operating pressure of the absorbers in the Selexol unit is constrained by the pressure of the gasification section. Hence, the only way to increase the inlet P_{CO_2} is to increase the H_2/CO ratio in the syngas sent to the Selexol unit. Obviously, as the higher mole fraction of H_2 is achieved by converting CO to CO_2 through the WGS reaction, the mole fraction of CO_2 increases. Figure 3-42 shows that the circulation rates of Selexol decreases considerably as the H_2/CO ratio is increased, even though the amount of CO_2 that needs to be captured increases simultaneously. Figure 3-43 shows that an increase in the H_2/CO ratio decreases the power consumption in the Selexol unit significantly mainly due to the lower solvent circulation rate.

Another effect of the H_2/CO ratio on the Selexol unit is in the loss of syngas. The solubility of CO_2 in Selexol is about 36 times of the solubility of CO. (Kohl and Nielsen, 1997) Since CO partial

pressure is still high in the syngas to the Selexol unit, still a considerable CO loss occurs. Table 3-91 shows that the CO loss decreases from 5.29% to 3.21% when the H_2/CO ratio increases from 1 to 2.

Since MDEA/PZ is a chemical solvent, its performance does not get affected by the pressure significantly. High H_2/CO ratio in the Fe-catalyzed FTS unit decreases the formation of CO_2. The solvent required in the MDEA/PZ unit decreases with an increase in the H_2/CO ratio because of the decrease in the CO_2 selectivity in the FTS unit as shown in Figure 3-44.

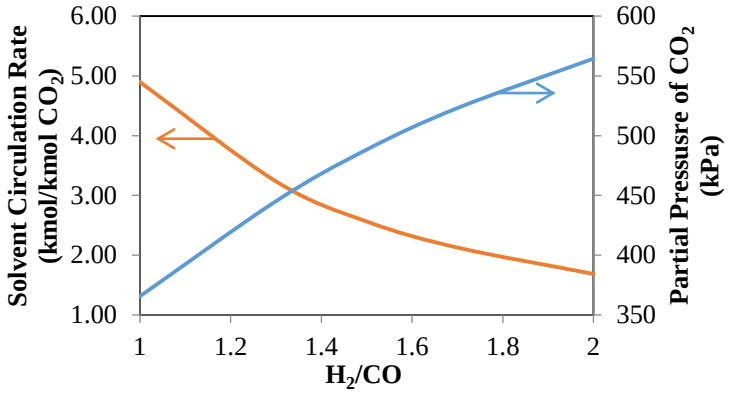

Figure 3-42. Effect of H_2/CO on the solvent circulation rate in the Selexol unit.

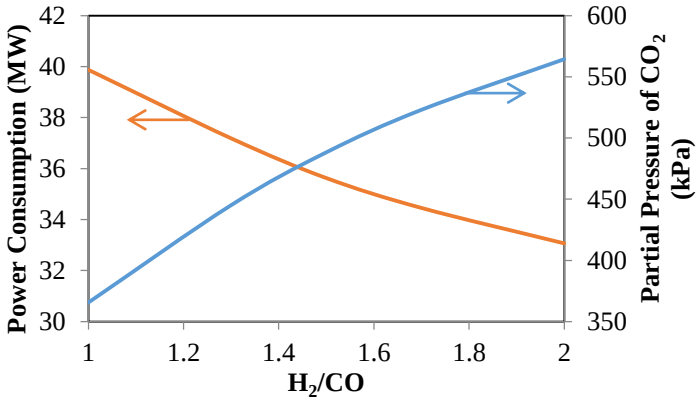

Figure 3-43. Effect of the H_2/CO ratio on power consumption in the Selexol unit.

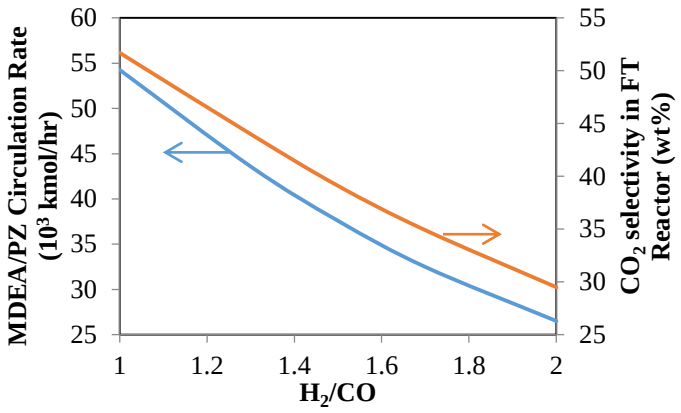

Figure 3-44. Effect of the H_2/CO ratio in the post-FT CO_2 capture unit.

Table 3-91. Effect of the H_2/CO ratio on CO loss in the Selexol unit.

H_2/CO	2	1.7	1.5	1.3	1
CO loss (kg/hr)	4940	6518	7852	9512	2555
CO loss%	3.21	3.69	4.11	4.57	5.29

Effect of the H_2/CO ratio at the FT inlet on the carbon efficiency and product selectivity

This study is conducted for the simplified indirect CBTL plant. As shown before, the high H_2/CO ratio results in a decrease in the utilities consumption in the CCS units. However, an increase in the H_2/CO ratio raises the light gas selectivity and reduces the fuel yield of the CBTL plant. Figure 3-45 shows the carbon number distribution in light hydrocarbons from C_1 to C_{20} (weight basis) for different H_2/CO ratios. The summary of product selectivity and carbon efficiency of the entire CBTL plant can be found in Table 3-92.The figure shows a high yield of CH_4 in comparison to other hydrocarbons, which is consistent with the experimental results available in the open literature. (Bechtel, 1992a; Kuo, 1985; Kuo, 1983; Steynberg and Dry, 2004) The higher the H_2/CO ratio is, the higher the selectivity of light hydrocarbons is. However, the H_2/CO ratio is not expected to affect the overall syngas conversion significantly. According to Figure 3-44, the CO_2 selectivity increases with a decrease in the inlet H_2/CO ratio. However, when H_2/CO ratio increases, more CO in the raw syngas is converted to CO_2 in the WGS unit and captured in the Selexol unit. As a result, lower amount of syngas enters the FTS unit. In summary, the overall carbon efficiency, defined as fraction of carbon in feed converted to hydrocarbon, of the CBTL plant does not change much with the change in the H_2/CO ratio, but the utilities consumption in the CCS unit and CH_4 production does. This study suggests that an optimal H_2/CO ratio exists. The optimum can be determined by conducting a techno-economic analysis. To evaluate the impact of the H_2/CO ratio on the plant economics, the product upgrading section needs to be considered.

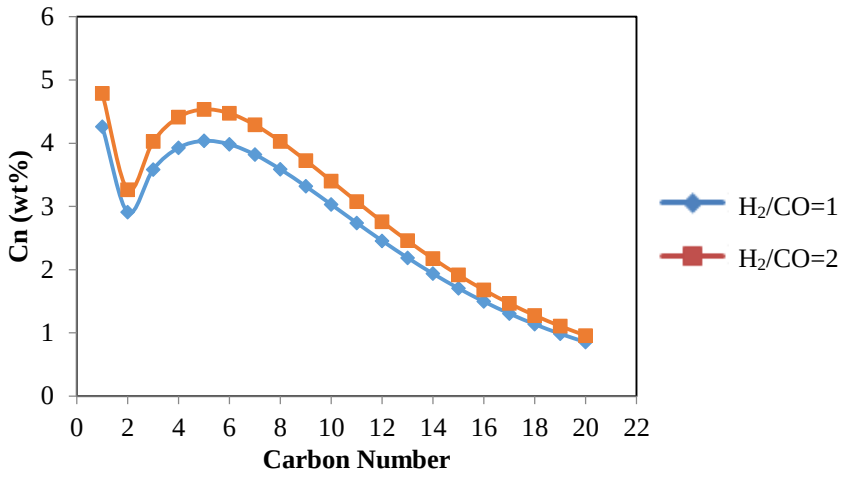

Figure 3-45. Carbon number distribution.

Table 3-92. Effect of the H_2/CO ratio on the product selectivity and carbon efficiency.

H_2/CO	2	1.7	1.5	1.3	1
Carbon Efficiency (%)	34.7	35.1	35.4	35.5	35.6
C_1-C_4 (wt%)	16.48	16.16	15.88	15.51	14.68
C_5-C_{10} (wt%)	27.53	27.00	26.52	25.91	24.51
C_{11}-C_{20} (wt%)	15.80	15.49	15.22	14.86	14.07
Wax (wt%)	40.19	41.35	42.38	43.72	46.74

Effect of steam to carbon ratio at the ATR inlet

This study is conducted for the indirect CBTL plant with CCS, shown in Figure 3-1. The effect of steam/carbon ratio in the ATR unit is evaluated by fixing the H_2/CO ratio in the FT inlet to 2, the same as the base case condition. As seen in Table 3-93, the results indicate that the H_2/CO ratio in the ATR outlet and the utility consumptions increase with the increase in the steam/carbon ratio. As the H2 demand should be satisfied, a higher H_2/CO ratio in the ATR outlet would require a lower extent of reactions in the WGS reactor and therefore the percent of CO_2 captured by physical solvent in the Selexol unit decreases with the increasing steam/carbon ratio. As a results, the penalty of CCS increases as the steam/carbon ratio is increased. Furthermore, the FT reactor is usually operated with an inlet H_2/CO ratio less than 2.1. Therefore, a low steam/carbon ratio is recommended at the ATR inlet for FT application. (Steynbreg and Dry, 2004) In order to prevent coking, the steam/carbon ratio is set to be 0.63 for the base case. (Steynbreg and Dry, 2004)

Table 3-93. Effect of steam to carbon ratio on the performance of ATR unit.

Steam/Carbon (mol/mol)	0.5	1.0	2.0	3.0
Performance				
H_2 produced (kmol/hr)	759	791	822	857
CO produced (kmol/hr)	486	454	394	359
H_2 produced/CO produced (mol/mol)	1.6	1.7	2.1	2.4

H_2/CO in ATR outlet (mol/mol)	3.4	3.6	4.1	4.8
Utilities				
O_2 consumed (kg/hr)	7335	7947	9075	10598
Steam consumed (kg/hr)	5460	10729	21368	33440
CO_2 captured by Selexol unit (%)	79.3	78.8	77.5	75.1

Advantage of the integrated hydrotreating unit

This study is conducted for the indirect CBTL plant with CCS, shown in Figure 3-1. By comparing configuration of the integrated hydrotreating approach with the conventional separated hydrotreating approach, it clearly shows that the integrated hydrotreating approach can reduce the plant footprint and make the plant more compact. In the integrated hydrotreating approach, the entire hydrotreated syncrude is sent to the main distillation column to separate the product to light naphtha, heavy naphtha, diesel and wax, which is similar to the main distillation column in the separated hydrotreating approach design. The only difference in the main distillation columns is that the heavy naphtha side-stripper is not considered in the separated approach, because the entire naphtha cut is sent to the naphtha hydrotreating unit together and then separated in another distillation column. One advantages of the integrated hydrotreating approach is to eliminate some distillation columns from the conventional approach, which are required to remove light gases from the products and separate light naphtha from heavy naphtha, thus consuming considerable amount of plant fuel because of the large reboiler duty. The disadvantage of the integrated hydrotreating approach is that the wax, which does not necessarily need to be hydrotreated, is also sent to the hydrotreating unit, resulting in the increase in the preheat furnace duty and the hydrotreater reactor size. However, the temperature increase in the furnace is very low, just about 20ºC and the wax remains in liquid phase. Therefore the increase in the heat duty and the volumetric flowrate to the reactor is not very large. For the separated hydrotreating approach, the utility consumptions in and capital investment for naphtha and diesel hydrotreating units are given by Bechtel (Bechtel, 1998; 1993), and then the capital investment is escalated with the CEPCI. (Bechtel, 1998; 1993; Turton et al., 2012) For the remaining units, the utility consumptions and capital investment are estimated using Aspen Plus and APEA, respectively. Detailed specifications of the APEA model for capital investment estimation can be found in Table 3-94. Table 3-95 and 96 show the comparison of heat consumption and capital investment between the two hydrotreating approaches. It is observed that the integrated hydrotreating approach can reduce the heat consumption by about 30% and the capital investment by about 25%.

Table 3-94. Specifications of project components of the integrated hydrotreating unit in APEA.

Description	# Req	# Spares	Model in APEA	Sizing	MOC	10^3 $ (2013)
syncrude pump to hydrotreator	1	1	CP CENTRIF	Icarus	CS casing	334
hydrotreator feed furnace	1	0	FU BOX	Icarus	A213F	662
feed/product heat exchanger	1	0	HE FLOAT HEAD	EDR	A285C, A214	489
hydrotreating reactor*	1	0	VT MULTI WALL	Correlation	SS347	3370
product cooler	1	0	HE FLOAT HEAD	EDR	A285C, A214	129
high pressure flash	1	0	VT CYLINDER	Icarus	A516	188
H_2 recycle compressor	1	0	GC CENTRIF	Icarus	SS316	1745
catalyst	1	1	C	NA	NA	11598
low pressure flash	1	0	VT CYLINDER	Icarus	A516	144
pumparound 1	1	0	HE FLOAT HEAD	EDR	A285C, A214	88
pumparound 2	1	0	HE FLOAT HEAD	EDR	A285C, A214	102
heavy naphtha heat exchanger	1	0	HE FLOAT HEAD	EDR	A285C, A214	78
diesel heat exchanger	1	0	HE FLOAT HEAD	EDR	A285C, A214	84
wax heat exchanger	1	0	HE FLOAT HEAD	EDR	A285C, A214	121
main column - condenser	1	0	HE FIXED T S	EDR	A285C, A214	120
main column - drum	1	0	HT HORIZ DRUM	Icarus	A516	105
main column - reflux pump	1	1	CP CENTRIF	Icarus	CS casing	103
main column - tower	1	0	TW TRAYED	Aspen Plus	A516, A285C	693
side stripper - diesel	1	0	TW TRAYED	Aspen Plus	A516, A285C	167
side stripper - heavy naphtha	1	0	TW TRAYED	Aspen Plus	A516, A285C	162
main distillation - feed furnace	1	0	FU BOX	Icarus	A213C	765
pump to the stabilizer	1	1	CP CENTRIF	Icarus	CS casing	87
stabilizer - condenser	1	0	HE FIXED T S	EDR	A285C, A214	75
stabilizer - drum	1	0	HT HORIZ DRUM	Icarus	A516	73
stabilizer - reboiler	1	0	RB U TUBE	EDR	A285C, A214	92
stabilizer - reflux pump	1	1	CP CENTRIF	Icarus	CS casing	97
stabilizer - tower	1	0	TW TRAYED	Aspen Plus	A516, A285C	275

*The hydrotreater is sized by assuming the same space velocity and L/D ratio as reported in the open literature. (Jarullah et al., 2012)

Table 3-95. Major utility consumptions of the two hydrotreating approaches.

Integrated hydrotreating			Separated hydrotreating		
Unit	Description	GJ/hr	Unit	Description	GJ/hr
F_1	Hydrotreating preheater	4.26	F_3	Furnace of main column	24.75
F_2	Furnace of main column	23.70	F_5+R_3+R_4	Naphtha hydrotreating	19.83
R_1	Reboiler of stabilizer	3.67	F_4+R_2	Diesel hydrotreating	3.44
STM	Stripping steam	2.51	STM	Stripping steam	2.18
COM	Hydrogen compressor	3.87	COM	Hydrogen compressor	3.87
Total		38.01	Total		54.07

Table 3-96. Capital investment of the two hydrotreating approaches.

Integrated hydrotreating		Separated hydrotreating	
Section	MM$	Section	MM$
Integrated hydrotreating loop	8.17	Hydrocarbon recovery	2.56
Hydrocarbon recovery	3.43	Naphtha hydrotreating	4.70
		Diesel hydrotreating	9.45
Total	11.60	Total	16.71

Effect of H_2/CO ratio in the FT inlet stream

This study is conducted for the indirect CBTL plant with CCS (FT_CCS), shown in Figure 3-1. In the indirect CBTL plant, the H_2/CO ratio in the syngas can be adjusted in the WGS reactor before sending to the Selexol unit, as shown in Figure 3-1. Studies indicate that the H_2/CO ratio in the FT inlet stream not only affects the penalty of CCS but also the fuel product yield and distribution. (Jiang and Bhattacharyya, 2014; Steynverg and Dry, 2004) Hence, in this study, a sensitivy study is conducted by changing the H_2/CO ratio from 1 to 2.25 and keeping the raw materaial flowrate and other design parameters the same as the base case.

Previous study from our group indicates that with an increase in the H_2/CO ratio in the FT inlet stream, the penalty of CCS keeps reducing in a once-through indirect CBTL plant without product upgrading. (Jiang and Bhattacharyya, 2014) Similar trend, shown in Figure 3-46, can be found in the CBTL plant producing on-spec gasoline and diesel. For the Selexol unit, the solvent circulation rate reduces with increasing H_2/CO ratio because of the higher partial pressure of CO_2, which can provide more driving force for the physical absorption process. For the MDEA/PZ unit, the solvent circulation rate decreases because the CO_2 selectivity in the FT reactor decreases with the increasing H_2/CO ratio. (Jiang and Bhattacharyya, 2014) The CO_2 can be recovered from the Selexol unit at different pressure levels, usually higher than the pressure of the CO_2 released in the chemical absorption unit, which indicates that the penalty of CO_2 compression section can be reduced as larger potion of CO_2 is captured in the Selexol unit.

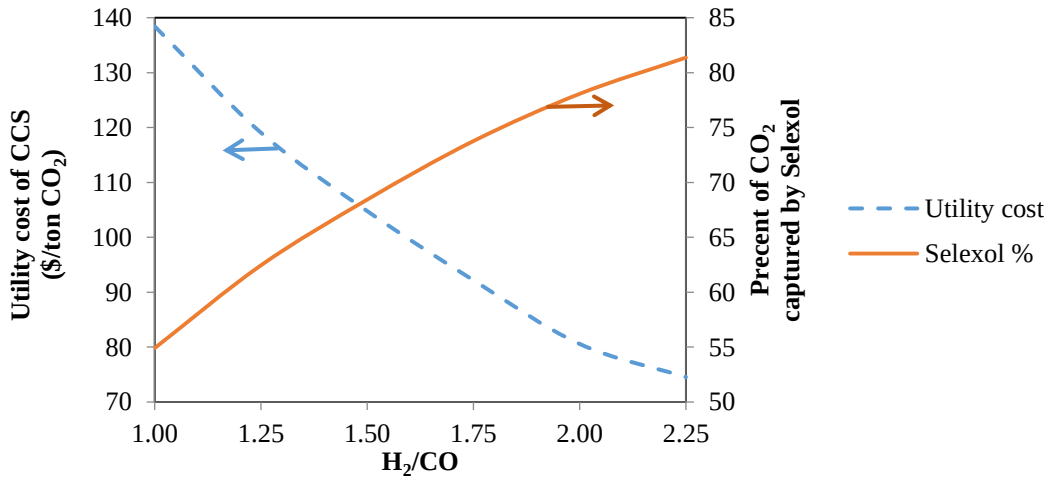

Figure 3-46. Effect of H_2/CO ratio on the penalty of CCS.

Because the H_2/CO ratio in the FT inlet has a strong impact on the hydrocarbon selectivity in the FT reactor (Jiang and Bhattacharyya, 2014; Steynberg and Dry, 2004; Dry, 1981), the product distribution and the fuel yield of the indirect CBTL plant highly depend on the H_2/CO ratio in the FT inlet. Figure 3-11 indicates that the gasoline to diesel ratio keeps increasing with increasing H_2/CO ratio, because the FT reaction produces lighter hydrocarbon with higher H_2/CO ratio in the inlet. (Jiang and Bhattacharyya, 2014; Steynberg and Dry, 2004; Dry, 1981) Figure 3-47 to Figure 3-50 also show that the fuel yield, overall plant efficiency and plant profit increase with the increasing H_2/CO ratio but with decreasing slope. That is because with a higher H_2/CO ratio, the H_2 conversion decreases in the FT reactor. As a result, the recycled light gases from the post-FT CO_2 capture unit has a higher H_2 percentage, and a smaller portion is needed to be sent to the H_2 plant to produce the H_2 required for the product upgrading section. A larger portion can be sent back to the FT unit through the ATR to produce more syncrude. In the meanwhile, less amount of light gases is purged from the H_2 unit, which is then sent to the combined cycle plant for power production, where no CO_2 capture facilities are considered for the flue gas. Hence, with the same extent of CO_2 removal in the Selexol unit and the MDEA/PZ unit, the electricity production and overall CO_2 emission in plant also decrease with the increase in the H_2/CO ratio. However, it is expected that with a very high H_2/CO ratio, the fuel yield will decrease as more amount of carbon in the feedstock gets converted to CO_2 and removed by the Selexol unit before being sent to the FT unit for fuel production. In this study, H_2/CO ratio larger than 2.25 is not considered because of the absence of the experimental data of FT reactor operated at very high H_2/CO ratio. It should be noted that in Figure 3-49, the thermal efficiency is defined as energy output (fuels and electricity) to input (coal and biomass) ratio in HHV basis, while the carbon efficiency is defined as percent of carbon in the feedstock converted into fuels. The profit function in Figure 3-50 is defined as Eq. (46).

$$PF = \sum_{prod} C_p F_p - \sum_{feed} C_f F_f - \sum_{utility} C_u F_u \tag{46}$$

Where C_i is the unit cost of i^{th} item listed in Table 3-13; F_i is the material or energy flow rate of the i^{th} item.

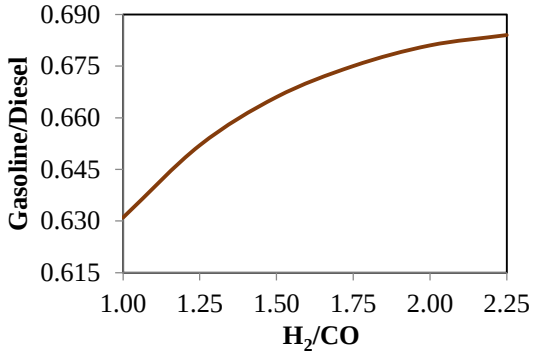

Figure 3-47. Effect of H_2/CO ratio on the product distribution.

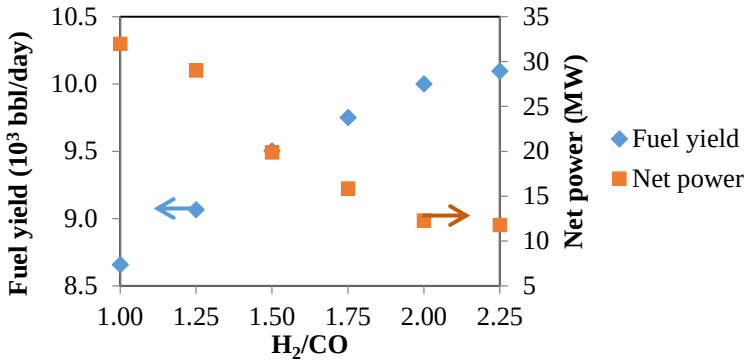

Figure 3-48. Effect of H_2/CO ratio on the fuel yield.

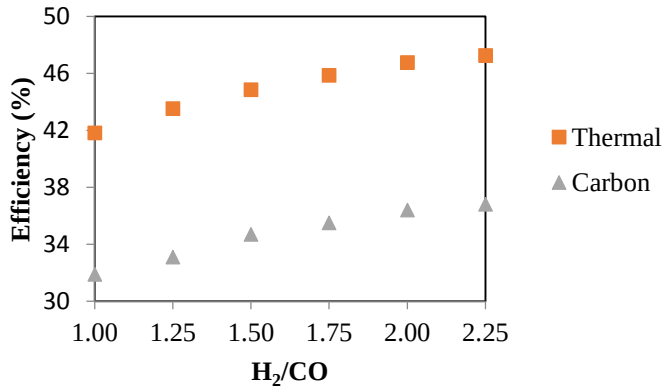

Figure 3-49. Effect of H_2/CO ratio on the plant efficiency.

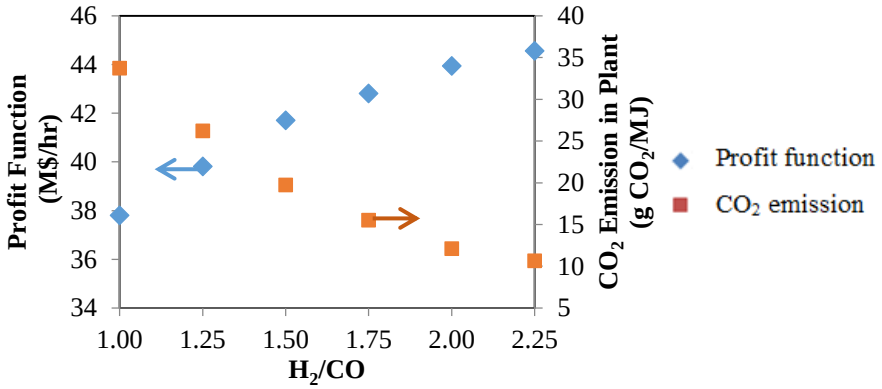

Figure 3-50. Effect of H_2/CO ratio on the plant profit and CO_2 emission.

Effect of biomass/coal ratio

This study is conducted for the indirect CBTL plant with CCS (FT_CCS), shown in Figure 3-1. As mentioned before, the carbon footprint of the indirect CBTL plant can be decreased by increasing the biomass content in the feedstock. In this study, a sensitivity analysis is conducted

for biomass/coal weight ratios of 8/92, 15/85, 20/80 (dry) to estimate the effect of feedstock composition on the plant performance, especially product yield and the plant efficiency. Relatively low biomass content is considered in this study mainly considering sustainability of the plant. (Wang and McNeel, 2009) For the alternative cases, the total amount of dry feed, and other design parameters are fixed to be the same as the base case. The simulation results are presented in Table 3-97. It shows that as the biomass content keeps increasing, the overall fuel production and the plant thermal efficiency decreases, mainly because of the relatively high oxygen content in the biomass. Our previous study has shown that an increase in the biomass/coal ratio results in an increase in the H_2/CO ratio in the raw syngas (Stream 3 in Figure1). (Jiang and Bhattacharyya, 2014) As a consequence, the extent of the WGS reaction and the heat recovery decreases if the H_2/CO ratio keeps increasing in the raw syngas while the H_2/CO ratio at the WGS outlet (Stream 4 in Figure1) remains constant. (Jiang and Bhattacharyya, 2014)

Table 3-97. Effect of biomass/coal ratio in the indirect CBTL plant.

Biomass/coal	dry weight	8/92	15/85	20/80
Feedstock				
Coal (dry)	ton/hr	153.44	141.80	133.49
Biomass (dry)	ton/hr	13.29	24.93	33.24
Product				
Gasoline	bbl/hr	4,050	3,848	3,721
Diesel	bbl/hr	5,950	5,656	5,465
Total FT liquid	bbl/hr	10,000	9,504	9,186
Net Electricity	MW	12.28	9.81	7.62
Thermal Efficiency	HHV			
FT liquid	%	45.9	44.7	44.0
Net Electricity	%	0.9	0.7	0.6
Total	%	46.8	45.4	44.6

Effect of the extent of CO_2 capture and storage (CCS)

For all case studies, the acid gases, CO_2 and H_2S, are removed from the syngas and FT vapor product by the same extent as the base case. CO_2 removal is required to improve the kinetics and economics of the downstream synthesis and upgrading process. (Kreutz et al., 2008) H_2S removal is required to avoid catalyst poisoning. (Kreutz et al., 2008) In this study, the extent of CCS is manipulated by changing the fraction of the CO_2 streams sent to the CO_2 compression section, not by the extent of CO_2 captured. The results are shown in Table 3-98. In the base case, all CO_2 steams removed from the system are sent to the CO_2 compression section. If CCS technology is not considered (i.e. no compression), all CO_2 stream is vented to the atmosphere. With an increase in the extent of CCS, CO_2 streams that are sent to the CO_2 compression section depend on their pressure levels. The underlying philosophy is that if one would like to vent a portion of CO_2, then this portion will be bled off from the lowest pressure CO_2 stream available. For example, in the low CCS case, CO_2 streams released from the HP and MP flash drums in the Selexol unit and portion of the CO_2 stream released from the LP flash drum are sent to the compression section, while CO_2 streams released from the MDEA/PZ unit and the remaining portion of the CO_2 stream from the LP flash drum in the Selexol unit are vented. It is noticed that in the case without CCS,

the CO_2 emission from the plant is about 25 g CO_2/MJ less than the data reported in the work of Edwards et al. (Edwards, 2011), which is reasonable because the WGS technology is not considered in that work. (Edwards, 2011) Figure 3-50 indicates that the CO_2 emission from the plant can be reduced by about 22 g CO_2/MJ when the H_2/CO ratio in the FT inlet is increased from 1 to 2. Table 3-98 also indicates that the CO_2 emission from the plant can be reduced from 67.37 to 12.14 g CO_2/MJ at the cost of 1.4 % decrease in the overall thermal efficiency. The penalty due to capital investment for CCS is not discussed in this paper, but will be considered in a separate study focusing on techno-economic analysis.

Table 3-98. Effect of the extent of CCS (i.e. amount of CO_2 that is compressed).

Cases	High	Intermediate	Low	No CCS
CO_2 stream to compression section (%)	100	75	50	0
Net electric power (MW)	12.01	16.44	21.33	30.59
CO_2 emission from plant (g CO_2/MJ)	12.14	25.95	39.76	67.37
Thermal efficiency (%, HHV)	46.8	47.2	47.5	48.2

Impact of biomass type

This study is conducted for the indirect CBTL plant with CCS (FT_CCS), shown in Figure 3-1. Impact of biomass type on the performance of the CBTL process is shown in Table 3-99. The results indicate that the thermal efficiency of wood chips is lower than bagasse due to the higher oxygen content and lower hydrogen/carbon ratio in wood chips. The carbon efficiency remains similar because all the other key design parameters remain the same and the biomass/coal ratio is small in the feedstock.

Table 3-99. Alternative biomass as feed stock.

Biomass type		Wood chips	Bagasse
Feedstock			
Coal (dry)	ton/hr	153.8	153.4
Biomass (dry)	ton/hr	13.5	13.3
Product			
Gasoline	bbl/day	4050	4050
Diesel	bbl/day	5950	5950
Electric Power	MW	5.09	12.28
Analysis			
C Captured by FTL	%	36.3	36.4
Thermal Efficiency	% (HHV)	46.1	46.8

Properties of the gasoline and diesel product

With the simplified refinery design shown in Figure 3-2, the required specifications of gasoline and diesel can be achieved by adjusting the D86 95 vol% cut point of the light and heavy naphtha stream of the main distillation column. In the base case, the D86 95 vol% cut point of the light and

heavy naphtha stream is set to be 94℃ and 174℃, respectively. Table 3-100 shows the values of the final gasoline blends properties and the selected USA standard of gasoline. (ASTM, 2014; CARB, 2012; ECFR, 2015) Table 3-101 shows that the conceptual design developed in this study can produce on-specification diesel (ASTM, 2014); and the estimated properties from our model are consistent with the industrial data. (Leckel, 2010)

Table 3-100. Estimated properties of the gasoline pool and specifications of US gasoline.

		USA Specification		
Fuel property	Product	min	max	Source
Restrictions on boiling range				
D86 50 vol% (ºC)	92.8	76.7	121	ASTM D4814
D86 90 vol% (ºC)	139.4		190	ASTM D4814
RVP (kPa)	47.9		54	ASTM D4814
Restrictions on composition				
Aromatics (vol%)	34.1		35	CA RFG*
Benzene (vol%)	0.4		1	40 CFR 80
Sulfur (ppm, wt)	0		20	40 CFR 80
Road Octane Number ([R+M]/2)	87.2	87		

* Flat limit of small refinery from California RFG, Phase 3

Table 3-101. Estimated properties of the diesel pool and specifications of No.2 Diesel.

	Sasol (Leckel, 2010)		USA Specification		
Fuel property	Product	LTFT	Min	Max	Source
Restrictions on boiling range					
Density at 15 ºC (kg/m^3)	769	772		876	ASTM D975
Flash Point (ºC)	60	60	52		ASTM D975
Restrictions on composition					
Aromatic (vol%)	0	0.7		35	ASTM D975
Sulfur (ppm, wt)	0	<5		15	ASTM D975
Cetane Number	>70	>70	40		ASTM D975
Cetane Index	>70		40		

✓ **Effect of key design and investment parameters on the indirect CBTL plant economic performance**

Figures 51 and 52 show the sensitivities for ±25% changes in the major plant economic inputs for both small scale and large scale plants. The results show that the BEOP is between $88/bbl and $106/bbl for a small scale operation and between $72/bbl to $86/bbl for a large scale operation. 7% increase in BEOP is observed, if high project contingency (26%) is considered due to the novelty of the indirect CBTL plant with CCS. Table 3-102 shows the contribution of each unit to the BEOP of the CBTL plant. The results indicate that feedstock cost contributes about half of the BEOP, while the other half of the BEOP is due to the capital cost. The syngas production section contributes about 60% of the total capital investment, which is similar to the data reported in the open literature. (Dry, 2002) The CCS units, including pre- and post- FT CO_2 removal process and CO_2 compression process, also consume a significant amount of utilities and capital investment. As noted before, the utilities such as fuel gas, steam and electricity are generated inside the plant and therefore utilized in the process. The change in utility consumption is reflected by the change in net power output of the CBTL plant. As seen in Table 3-102, the main consumers of utilities are the syngas production unit and the CCS unit. Therefore selections of the CCS technologies and related design parameters are critical for reducing the BEOP of the CBTL plant with CCS.

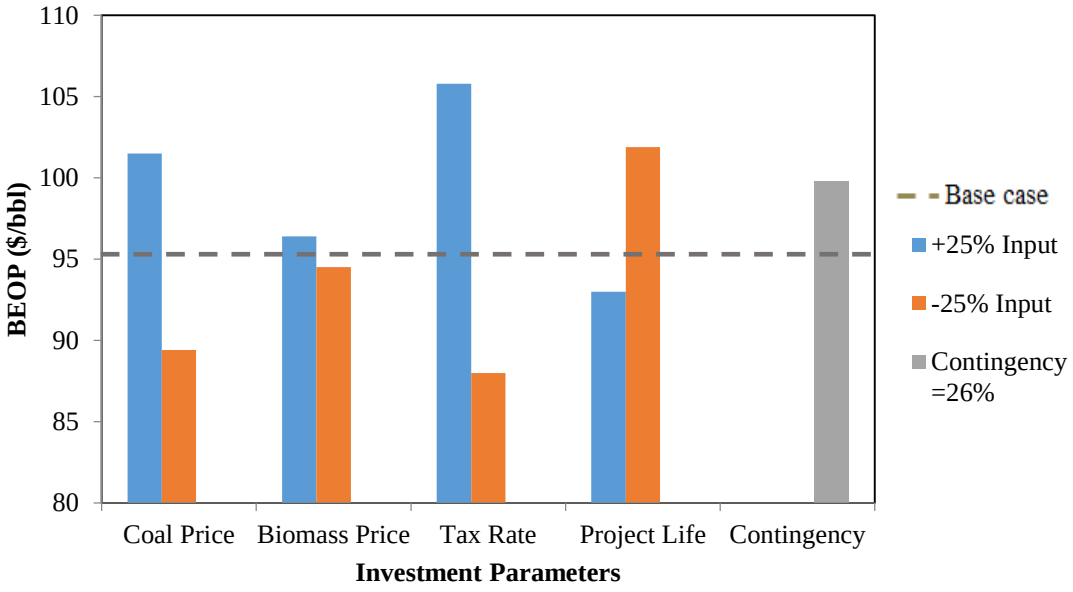

Figure 3-51. Sensitivity studies of the small scale CBTL plant with CCS (10k bbl/day).

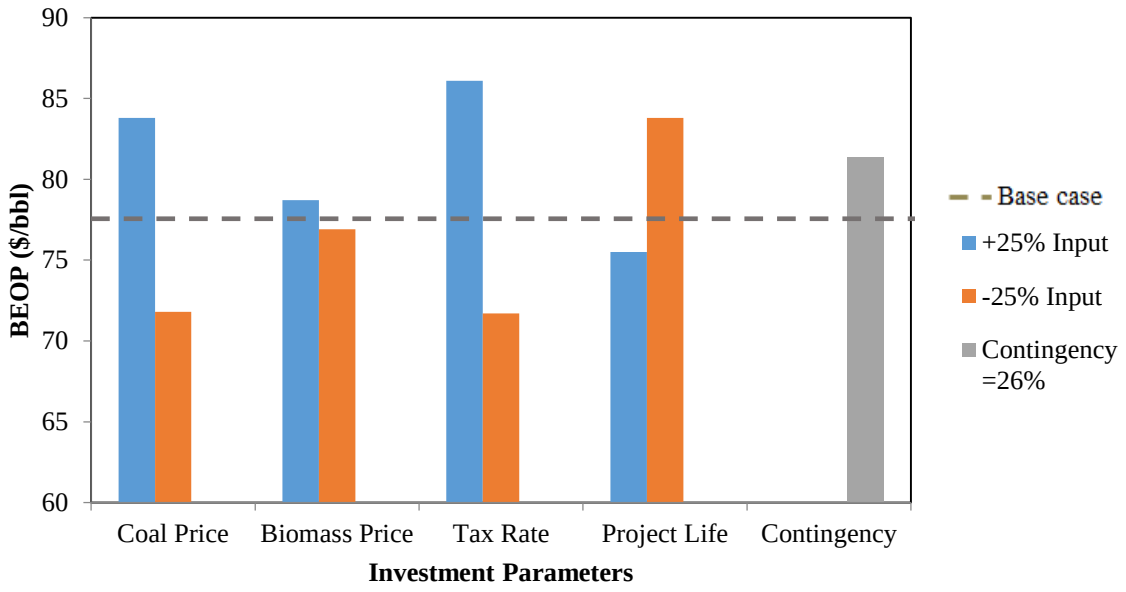

Figure 3-52. Sensitivity studies of the large scale CBTL plant with CCS (50k bbl/day).

Table 3-102. Contribution to the BEOP of the CBTL plant with CCS (10k bbl/day, Base case) [(1)]

Percentage	Feedstock	Capital[(2)]	Electricity	Steam	Fuel
Total	55.18	45.63	(0.81)	0.00	0.00
Process units					
Syngas production[(3)]		57.5	51.0	(52.9)	1.2
Syncrude production		10.7	0.8	(46.0)	2.9
CO_2 capture & storage[(4)]		11.5	36.2	35.6	0.0
Product upgrading		10.6	1.0	0.4	12.5
Fuel gas header		0.0	0.0	0.0	(100)
Others		3.0	11.1	(1.1)	0.0
Gas turbine		2.8	(46.7)	0.0	83.5
HRSG & steam turbine		3.9	(55.4)	64.1	0.0

(1) ( ) indicates utility generation
(2) Annualized by assuming 10-year economic life of equipment
(3) ASU is included in the syngas production section
(4) Including pre- and post- CO_2 capture units and CO_2 compression unit

Different CCS technologies

As mentioned earlier, a dual-stage Selexol process is selected for selectively removing CO_2 and H_2S produced in the gasifier. The Selexol technology is widely considered for acid gas capture because of its relatively low capital and operating costs when the partial pressure of CO_2 is relatively high. (Jiang and Bhattacharyya, 2014; 2015; Doctor et al., 1994; Mohammed et al., 2014) Three different carbon capture technologies are considered in our earlier study for post-FT CO_2 capture-single-stage Selexol unit, MEA absorption unit and MDEA/PZ absorption unit.

(Jiang and Bhattacharyya, 2015) That study indicated that the MDEA/PZ unit has the lowest utility consumption among these three technologies. Table 3-103 gives the economic analysis for all three technologies considering both utility consumption and capital investment. The result shows that the BEOP for the MDEA/PZ unit is slightly lower than the BEOP for the MEA unit because of the lower utility consumption in the MDEA/PZ unit while the capital investment are similar and overall thermal efficiency of the CBTL process remains relatively unchanged for both of these technologies. A considerable increase in BEOP is observed for the single-stage Selexol unit due to the loss of light hydrocarbons in the physical absorption process, which results in higher feed flowrate and larger throughput of each section for achieving the same fuel production rate. Hence, the MDEA/PZ technology is selected for the base case and other sensitivity studies.

Table 3-103. Effect of different CCS technologies for post-FT CO_2 capture (10k bbl/day).

	Single-stage Selexol	MEA	MDEA/PZ
Thermal efficiency (%, HHV basis)	40.8	45.7	45.9
Total project cost (MM$)	1332	1280	1281
Net present value (MM$)	54	175	179
Internal rate of return (%)	10.4	11.4	11.5
Payback period (year)	9	7	7
Break-even oil price ($/bbl)	103.6	95.7	95.5

Integrated hydrotreating versus separated hydrotreating

In this study, two hydrotreating routes, namely novel integrated hydrotreating and conventional separated hydrotreating, are considered for upgrading FT liquids. (Jiang and Bhattacharyya, 2015) In the novel integrated hydrotreating approach, the syncrude is hydrotreated before sent to a separation unit for further upgrading, while the syncrude is first separated and then sent to several separated hydrotreating units in the conventional process. The integrated hydrotreating approach has the potential to reduce the utility consumption and capital investment of the hydrotreating units by about 30%, because of higher thermal efficiency and smaller plant footprint. (Jiang and Bhattacharyya, 2015) For detailed technical discussion on these units, interested readers are referred to Section 2.3 and 3.2 of our previous work. (Jiang and Bhattacharyya, 2015) The techno-economic analysis, reported in Table 3-104, shows that the integrated hydrotreating approach can reduce the BEOP of FT liquids by about 0.5%. It should be noted that the changes in the overall thermal efficiency and economic performance due to the change in the hydrotreating approach are not significant because the total utility and capital cost of the entire product upgrading section contribute only about 10% of the entire indirect CBTL plant, as shown in Table 3-12.

Table 3-104. Effect of different hydrotreating approaches (10k bbl/day).

	Integrated	Separated
Thermal efficiency (%,HHV)	45.9	45.9
Net present value (MM$)	179	171
Internal rate of return (%)	11.5	11.4
Payback period (year)	7	7
Break-even oil price ($/bbl)	95.5	96.0

H_2/CO ratio in the FT inlet stream

Previous study from our group indicated that with an increase in the H_2/CO ratio in the FT inlet stream, the utility consumption in the CCS units keep reducing and the overall thermal efficiency of the CBTL plant keeps increasing . (Jiang and Bhattacharyya, 2015) With an increasing H_2/CO ratio, the partial pressure of CO_2 in the Selexol unit inlet increases as more CO_2 generated in the WGS reactor, which accelerates physical absorption and reduces the solvent circulation rate. At the meanwhile, CO_2 selectivity decreases with the increasing H_2/CO ratio in the FT unit using Fe-based catalyst. (Jiang and Bhattacharyya, 2014; 2015; James et al., 2013) As a consequence, the amount of CO_2 needs to be removed in the post-FT CO_2 removal unit decreases. Table 3-15 shows the effect of the H_2/CO ratio on the profitability of the CBTL plant. It is observed that the BEOP of the indirect CBTL plant with CCS can be reduced by about 10% if the H_2/CO ratio in the FT inlet stream is increased to 2.0, which is the stoichiometric ratio of the FT reaction. The process becomes more profitable with higher H_2/CO ratio not only because of the increasing thermal efficiency, which leads to smaller equipment size, but also because of the reduction in the solvent circulation rate in the CCS units, which leads to lesser capital investment. (Jiang and Bhattacharyya, 2015) Table 3-105 shows that the rate of decrease in the BEOP is lesser when H_2/CO ratio is increased from 1.5 to 2 in comparison to when it is increased from 1.0 to 1.5. Under current conceptual design, as the H_2/CO ratio keeps increasing, larger portion of carbon in the feedstock is converted to CO_2 in the WGS reactor and removed from the system in the pre-FT CO_2 removal unit before being sent to the FT unit. (Jiang and Bhattacharyya, 2015) Thus, amount of clean syngas sent to the downstream FT reactors decreases with the increasing H_2/CO ratio. Therefore the relative improvement in the capital and operating costs becomes smaller with the increase in the H_2/CO ratio. Higher H_2/CO ratio beyond H_2/CO ratio of 2 is not considered in this study due to lack of operational or experimental data for FT reactor beyond H_2/CO ratio of 2.

Table 3-105. Effect of the H_2/CO ratio in the FT inlet stream (10k bbl/day).

H_2/CO ratio (mol/mol)	1.0	1.5	2.0
Thermal efficiency (%,HHV)	40.8	43.9	45.9
Total project cost (MM$)	1439	1312	1281
Net present value (MM$)	9	139	179
Internal rate of return (%)	10.1	11.1	11.5
Payback period (year)	9	8	7
Break-even oil price ($/bbl)	106.5	98.1	95.5

Extent of CCS

Applying CCS technologies to the indirect CBTL will obeviously increase both operating and capital costs and considerably affect the profitability of the plant. The CCS section contributes about 11.5% of total capital investment and 35% of utility consumption, as shown in Table 3-106. It is noted that CO_2 removal units are still required in a FT plant, even though CCS is not considered. (Liu et al., 2011; Bechtel, 1998; Kreutz et al., 2008) The difference between the cases with and without CCS is whether removed CO_2 being sent to a CO_2 compression section for

pipeline transportation and sequestraion or direct vent to the atmosphere. Hence, the penalty of CCS in an indirect liquefaction plant is not expected to be as significant as coal-fired power plant. For a FT plant with recycle stream, Liu et al. reported a CCS penalty of \$12.4/ton CO_2, including CO_2 compression, pipeline and sequestration. (Liu et al., 2011) If only considering the capital and operating cost of the CO_2 comprssion section reported by Liu et al. (Liu et al., 2011), the penalty is about \$6.2/ton CO_2, corresponding to a utility consumption of 91kWh/ton CO_2 and a capital investment of 67 million 2007 US dollar for capturing 29039 ton CO_2 per day. (Liu et al., 2011) With the proposed plant configuration and modeling approach in this paper, the penaly of CCS is about \$6.1/ton CO_2 for the base case, considering the captial and operating cost of CO_2 compression section and assuming 10-year economic life of equipment and a electricity cost of \$0.06/kWh from grid, which is closed to the data reported by Liu et al. (Liu et al., 2011; Turton et al., 2012) Our previous study showed that the thermal efficiency of the indirect CBTL plant will be 1.4% less than that of a CBTL plant without CCS, if 90% and 98% CO_2 in the inlet streams are removed in the pre- and post-FT CO_2 capture units for both cases, corresponding to 56.9% of carbon in the feedstock. (Jiang and Bhattacharyya, et al., 2015) The techno-economic studies shown in Table 3-16 indicate that the BEOP of the FT liquids will increase by about 5% due to CCS. This value is lower than what reported by Liu et al. (10%) (Liu et al., 2011), because downstream CO_2 pipeline and sequestration facility is not included in our analysis.

Table 3-106. Effect of the extent of CCS (10k bbl/day).

Extent of CCS	High	Intermediate	Low	No CCS
CO_2 stream to compression unit (%)	100	75	50	0
Thermal efficiency (%,HHV)	45.9	46.3	46.6	47.3
Net present value (MM\$)	179	192	208	245
Internal rate of return (%)	11.5	11.6	11.7	12.0
Payback period (year)	7	7	7	7
Break-even oil price (\$/bbl)	95.5	94.6	93.6	91.3

Biomass/coal ratio in the feedstock

Our previous study showed that as the biomass content is increased (keeping the biomass content as high as 20%), overall fuel production and the plant thermal efficiency slightly decrease, mainly because of the relatively high oxygen content in the biomass. (Jiang and Bhattacharyya, 2015) From Table 3-102, it is noted that the raw material cost contributes more than half of the BEOP of the indirect CBTL plant. Table 3-107 indicates that when the biomass content increases from 8% to 20% with the same extent of CCS (not considering the carbon credit of biomass), the BEOP increases by about 4% due to lower plant efficiency, larger equipment size, higher feedstock price of biomass, less net electricity produced as by product and reletively more expensive biomass preprocessing unit. If carbon credit for biomass is considered, less CO_2 needs to be captured and stored. The results show that the BEOP increases by about 3% even when carbon credit of biomass is taken into account.

Table 3-107. Effect of the coal biomass mix ratio (10k bbl/day).

Biomass/Coal (wt/wt)	8/92	15/85		20/80	
Carbon credit	Base case	No	Yes	No	Yes
Thermal efficiency (%, HHV)	45.9	44.5	44.7	43.7	43.9
Net present value (MM$)	179	135	140	119	129
Internal rate of return (%)	11.5	11.1	11.1	11.0	11.0
Payback period (year)	7	8	8	8	8
Break-even oil price ($/bbl)	95.5	98.6	98.3	99.5	98.9

Impact of biomass type

Bagasse is selected as an alternative biomass input to the indirect CBTL plant, which has a higher thermal efficiency (Jiang and Bhattacharyya, 2015) but higher price than wood chips (Bain, 2007; IRENA, 2012; Gonzales et al., 2011) The thermal efficiency of the CBTL plant using bagasse is slightly higher than that using wood chips with the same biomass to coal ratio and all other key design parameters because of lower oxygen content and higher hydrogen/carbon ratio in the bagasse. (Jiang and Bhattacharyya, 2015) For economic analysis, the bagasse price is set to be $108/ dry ton, 35% higher than that of wood chips in dry basis. (IRENA, 2012; Gonzales, 2011) Table 3-108 shows that wood chip is a more economic option for the indirect liquefaction process.

Table 3-108. Effect of the biomass type (10k bbl/day).

	Wood chip	Bagasse
Thermal efficiency (%,HHV)	45.9	46.6
Net present value (MM$)	179	172
Internal rate of return (%)	11.5	11.4
Payback period (year)	7	7
Break-even oil price ($/bbl)	95.5	95.9

Economic feasibility of the indirect CBTL plant at low crude oil price.

Since the end of 2014, the crude oil price has dropped considerably. In this section, August, 2015 prices of gasoline, diesel and coal is considered in order to evaluate the impact of the current low price of crude oil. The results are shown in Table 3-109. As expected, both small scale and large scale CBTL plants are not competitive with the traditional petroleum refineries when the crude oil price is so low. In particular, the small scale CBTL plant does not seem to be economically viable even with significant decrease in coal and biomass prices. For the large scale CBTL plant, the price of coal and biomass would have to decrease to about 57% of the current price for making the CBTL plant at par with the typical petroleum refinery.

Table 3-109. Economic feasibility with 2015 pricing basis.

Plant capacity (bbl/day)	10000		50000	
Coal ($/ton)	34.0	0	34.0	19.3
Biomass ($/dry ton)	61.5	0	61.5	35.0
Crude oil ($/bbl)	62	62	62	62
Net present value (MM$)	-427	-84	-650	0
Internal rate of return (%)	6.1	9.3	8.5	9.7
Payback period (year)	N/A	N/A	N/A	N/A
Break-even oil price ($/bbl)	88.7	88.7	71.1	71.1

✓ Effect of key design parameters on the direct CBTL plant performance

For the base case conditions, the biomass/coal weight ratio, the plant capacity and the extent of CCS are set to be 8/92 (dry basis), 10000 bbl/day, and 90% (for SMR_CCS and CG_CCS). Following studies are conducted for analyzing the feasibility of applying CCS and introducing shale gas and biomass into the traditional DCL processes. First, the CCS system is optimal designed. Then based on the validated process model and heat integration, sensitivity studies are conducted by changing the biomass/coal ratio, CCS solvent and the extent of CCS with different hydrogen sources. Finally, the direct CBTL process is compared with the indirect CBTL processes.

Carbon balance and design of the CO_2 removal system

Based on the models developed for the liquefaction and product recovery section and the syngas production section, the carbon balances of the direct CBTL plants are computed and shown in Table 3-110. In the SMR_CCS and SMR_VT processes, 53.9 % of the carbon in the feedstock is converted to gasoline and diesel. In the CG_CCS and CG_VT processes, it is only 43.5 % because the H/C ratio in coal and biomass is less than that in shale gas or natural gas, resulting in less efficiency in the H_2 plant. In order to achieve 90% carbon capture, another 36.1 % of carbon in the feedstock (78.3 % of CO_2 generated) needs to be captured by the CO_2 capture process in the SMR_CCS process, and another 46.5 % of carbon in the feedstock (82.3 % of CO_2 generated) needs to be captured in the CG_CCS process. Based on the design procedure discussed in Section 3.2, Table 3-111 through Table 3-113 list the main CO_2 sources ordered by P_{CO_2} and flowrate, preliminary selection of absorption technologies, operating condition and targeted extent of CO_2 removal of each stream.

Table 3-110. Carbon balance of the direct CBTL plants(1)

Carbon in (%)	SMR	CG	Carbon out (w/o utility, %)	SMR	CG	Carbon out (w/ utility, %)	SMR	CG
Coal	77.4	94.6	Gasoline	11.4	9.4	Fuel	53.9	43.5
Biomass	4.6	5.4	Diesel	41.2	34.1	POX/CG	10.7	38.8
Shale gas	18.0		Gas oil	7.0	5.8	SMR	19.2	
			Fuel gas	10.5	11.9	Gas turbine	9.5	12.1
			H_2 plants	29.9	38.8	Others	6.7	5.6

(1) Fuel gas and gas oil combustion as utility is considered in the case with (w/) utility, but not in the case without (w/o) utility

Table 3-111. CO_2 emission and sources in the SMR_CCS and SMR_VT processes.

Source	Carbon (%)	CO_2 (mol%)	P_{CO_2} (bar)	CO_2 removal	SO_2 removal	Technology	CO_2 removal (%)
POX (syngas)	11	36	18.5	Yes	Yes	Selexol, Amine	83.6 98.3
SMR (syngas)	12	19	3.9	Yes	No	Amine	98.3
SMR furnace (flue gas)	7	7	0.07	Yes	No	Amine	86.3
Gas turbine (flue gas)	9	3	0.03	Yes(1)	No	Amine	66.5
Others (flue gas)	8			No	No	N/A	

(1) Not considered in the SMR_VT processes

Table 3-112. CO_2 emission and sources in the CG_CCS and CG_VT processes.

Source	Carbon (%)	CO_2 (mol%)	P_{CO_2} (bar)	CO_2 removal	SO_2 removal	Technology	CO_2 removal (%)
CG (syngas)	39	40	21.6	Yes	Yes	Selexol	95.0
Gas turbine (flue gas)	12	3	0.03	Yes(1)	No	Amine	69.8
Others (flue gas)	6			No	No	N/A	

(1) Not considered in the CG_VT processes

Table 3-113. Configurations and operating conditions of the AGR units.

Column	Pressure (bar)	Sour gas from	Clean gas to
HP CO_2 absorber	50.5	POX/CG (syngas)	H_2 recovery
IP absorber(1)	20.7	SMR (syngas) and/or Selexol CO_2 absorber (syngas)	H_2 recovery
LP absorber(2)	1.0	Gas turbine (flue gas) and/or SMR furnace (flue gas)	Stack

(1) Not considered in the CG_CCS and CG_VT processes
(2) Not considered in the SMR_VT and CG_VT processes

Based on the process model developed in Aspen Plus, the utility consumption and cost of the CO_2 removal and compression units are calculated and shown in Table 3-114 for all four configurations for a plant capacity of 10000 bbl/day. For the SMR_CCS (base case) process, two different amine solvent are considered- MEA and MDEA/PZ. The utility consumptions in the Selexol unit, the amine unit and the CO_2 compression unit are similar to the data available in the open literature. (Bhattacharyya et al., 2011; NETL, 2010; Jiang and Bhattacharyya, 2014; Bechtel, 1992; Liu et al., 2011) The reboiler duty of the solvent stripper is 3590 kJ/kg if MEA is used as a solvent in the SMR_CCS process. This duty can be reduced by 14% if using MDEA/PZ as the solvent. (Jiang and Bhattacharyya, 2014) Hence, MDEA/PZ is selected for removing CO_2 from IP and LP CO_2-contianing streams in all case studies and sensitivity studies. Table 3-114 also indicates that the utility costs for the CG_CCS and SMR_CCS processes are similar. The CCS utility cost for the CG_VT process is lower than the SMR_VT process, even though more CO_2 needs to be captured in the CG_CCS process due to the lower carbon efficiency. The reason is that P_{CO_2} of most CO_2-

containing streams to be sent to the AGR unit is higher in the CG_CCS and CG_VT processes than that in the SMR_CCS and SMR_VT processes. As a result, in the CG_CCS and CG_VT processes, most of the CO_2 is captured by the Selexol unit instead of the amine unit resulting in lesser utility penalty for CO_2 capture.

Table 3-114. Utility consumptions in and costs for the CCS units.

Process	SMR_CCS	SMR_CCS	SMR_VT	CG_CCS	CG_VT
CO_2 captured (kmol/hr)	2660	2660	1733	4245	3367
Amine solvent	MEA	MDEA/PZ	MDEA/PZ	MDEA/PZ	N/A
Utility consumptions (electricity (MW)/IP steam (GJ/hr)/LP steam (GJ/hr)/cooling water (GJ/hr))					
Selexol unit	1.98/3/0/57	1.98/3/0/57	1.98/3/0/57	8.32/29/0/255	8.32/29/0/255
Amine unit(1)	0.94/0/309/389	0.92/0/297/377	0.34/0/78/77	0.46/0/229/343	0/0/0/0
Compression	9.59/0/0/48	9.59/0/0/48	0/0/0/0	11.58/0/0/61	0/0/0/0
Total	12.5/3/309/494	12.5/3/297/482	2.3/3/78/134	20.4/29/229/659	8.3/29/0/255
Cost(2) ($/h)	5077	4913	1265	4919	993

(1) If high extent of CCS is considered, flue gas needs to be cooled before sending it to the amine system. The extra cooler is included in the amine unit.
(2) Costs of electricity, IP steam, LP steam and cooling water are assumed to be $16.8, $14.19, $13.28 and $0.354 per GJ (Turton et al., 2010)

Effects of the biomass to coal mix ratio

In this study, three biomass/coal weight ratios are investigated. Table 3-115 and Table 3-116 show that the thermal efficiency and carbon efficiency of the direct CBTL plant keep increasing for both SMR_CCS and CG_CCS processes, as more biomass is added into the liquefaction reactor. Even though H_2 consumption in the hydrotreating processes increases with the biomass/coal ratio due to the higher oxygenates contents, overall H_2 consumption in the direct CBTL plant decreases with the biomass/coal ratio, because the higher H/C ratio in the biomass reduces the H_2 consumption in the main liquefaction reactor more significantly. As a consequence, the increasing biomass/coal ratio decreases the amount of shale gas required for H_2 production, leading to an increase in the overall carbon efficiency and a decrease in the amount of CO_2 needed to be captured to achieve overall 90% carbon capture. With less CO_2 captured, less steam and electricity are consumed by the CCS facilities. Hence, the overall thermal efficiency of the CBTL plants is increasing with the biomass/coal ratio for both SMR_CCS and CG_CCS processes.

Table 3-115. Effects of the coal biomass mix ratio (SMR_CCS, 10k bbl/day).

Biomass/coal (wt/wt)	8/92	15/85	20/80
Coal (tonne/hr)	100.1	90.1	84.2
Biomass (tonne/hr)	9.3	17.6	22.7
Shale gas (tonne/hr)	21.6	20.7	20.3
Thermal efficiency (%, HHV)	64.3	66.5	67.6
Total H_2 consumption (% daf feed)	8.61	8.24	8.05
Liquefaction H_2 consumption (% daf feed)	6.70	6.20	6.00
Carbon efficiency (%)	53.9	56.4	57.6
CO_2 captured (kmol/hr)	2660	2366	2240

Table 3-116. Effects of the coal biomass mix ratio (CG_CCS, 10k bbl/day).

Biomass/coal (wt/wt)	8/92	15/85	20/80
Coal (tonne/hr)	151.4	138.8	132.0
Biomass (tonne/hr)	14.1	26.8	35.4
Thermal efficiency (%, HHV)	60.0	61.5	62.1
Total H_2 consumption (% daf feed)	8.61	8.24	8.05
Liquefaction H_2 consumption (% daf feed)	6.70	6.20	6.00
Carbon efficiency (%)	43.5	45.1	45.6
CO_2 captured (kmol/hr)	4245	3959	3852

Effects of the extent of CCS

As mentioned earlier, CCS is not considered in the SMR_VT and CG_VT processes, where CO_2 is removed from the syngas for hydrogen purification and directly vented to the atmosphere. For the SMR_CCS and CG_CCS processes, effects of low and high extent of CCS are studied. If low extent of CCS is considered, the removed CO_2 from the syngas is sent to the CO_2 compressor for sequestration, and no additional CO_2 needs to be removed from flue gas. On the other hand, high extent of CCS is considered in the SMR_CCS and CG_CCS processes, where additional CO_2 is captured from the flue gas and sent to the CO_2 compressor along with the CO_2 captured from the syngas preparing for CO_2 pipeline. Table 3-117 and 118 show the effect of the extent of CCS on the thermal efficiency and CO_2 emission with different biomass/coal ratio and hydrogen sources. It is observed that the CO_2 emission of the direct CBTL plant with the hydrogen produced from the shale gas can be reduced by more than half with the thermal efficiency reduced by only 0.5%, if low extent of CCS is considered. On the other hand, high extent of CCS will reduce the thermal efficiency by another 1-1.5% because of the higher penalty of post-combustion CO_2 capture facilities. The difference between low and high extent of CCS is higher in the direct CBTL plants with hydrogen produced from gasification, because most of the CO_2 is generated in the gasification unit with higher partial pressure, and therefore the Selexol technology that has lower penalty than the amine-based technologies can be applied for CO_2 capture. It is also noticed that with the

increasing biomass/coal ratio for both cases, the CCS penalty is reduced, because less CO_2 needs to be captured.

Table 3-117. Effects of the extent of CCS (SMR_CCS and SMR_VT).

Biomass/coal (wt/wt)		8/92			20/80	
Extent of CCS	High	Low	No	High	Low	No
CO_2 emission (kg CO_2/GJ product)	12.0	26.3	53.2	11.5	21.9	47.2
Thermal efficiency (HHV, %)	64.3	66.0	66.5	67.6	68.7	69.2

Table 3-118. Effects of the extent of CCS (CG_CCS and CG_VT).

Biomass/coal (wt/wt)		8/92			20/80	
Extent of CCS	High	Low	No	High	Low	No
CO_2 emission (kg CO_2/GJ product)	14.3	27.3	77.4	13.8	23.5	72.7[(1)]
Thermal efficiency (HHV, %)	60.0	61.2	62.1	62.1	63.1	63.6

(1)The CO_2 emission from the CG_VT process with low biomass/coal ratio is 72.7 kg CO_2 per GJ product, about 0.5 tonne/bbl oil, which is similar to the data reported by Shenhua. (Vasireddy et al., 2011)

Direct CBTL plants vs indirect CBTL plants

ICL and DCL are two commercially proven but very different approaches to produce transportation fuels from coal. The performance of the direct and indirect CBTL plants with a biomass/coal weight ratio of 8/92 is compared in this section, with detailed plant-wide model developed in this study and our previous studies. (Jiang and Bhattacharyya, 2014; 2015) Table 3-119 shows that the CO_2 emission from the indirect CBTL plant is much higher than the direct CBTL plant, while the thermal efficiency is much lower. That is because more carbon in the feedstock is converted to fuels instead of CO_2 in the direct liquefaction processes. Table 3-119 also indicates that the CCS penalty is less in the indirect CBTL plant with high extent of CCS, because most of CO_2 is produced in either gasification or Fisher-Tropsch unit and available at higher partial pressure and no CO_2 needs to be removed from low pressure flue gas in the indirect approach. Even though the direct CBTL plant surpasses the indirect CBTL plant in terms of carbon and thermal efficiency, it should be noted that a detailed techno-economic analysis is required for fair comparison.

Table 3-119. Performance of the direct and indirect CBTL plants.

Process	Indirect		Direct			
Hydrogen source	N/A		Shale gas		Coal/biomass	
Carbon efficiency (%)	36.4		53.9		43.5	
Extent of CCS	High	No	High	No	High	No
Thermal efficiency (HHV, %)	46.6	48.0	64.3	66.0	60.0	62.1
CO_2 emission (kg CO_2/GJ product)	18.9	118.6	12.0	53.3	14.3	77.4

- ✓ **Effect of key design and investment parameters on the direct CBTL plant economic performance**

In this section, sensitivity study is conducted for the direct CBTL plant to analyze the effect of key design parameters and economic measures on the plant economic performance, such as net present value, internal rate of return, break-even oil price and equivalent oil price.

Effect of the economic parameters and plant capacities

The major economic measures of the base case are calculated and reported in Table 3-120. It is noticed that none of the four investigated configurations of the direct CBTL plants can make profit or have positive NPV due to the current low crude oil price (COP). However, the direct CBTL plants may start to payback once COP surpasses the reported BEOP, and be competitive with traditional petroleum industries once COP surpasses the reported EOP. The results also shows that the capital investments of the CG_CCS and CG_VT processes are much higher than those of the SMR_CCS and SMR_VT processes, because of the high capital cost and low hydrogen production efficiency of the gasification unit in comparison to the shale gas steam reforming unit. (Jiang and Bhattacharyya, 2016; Williams and Larson, 2003) As a result, the BEOP and EOP of the SMR_CCS and SMR_VT processes are higher than those of the CG_CCS and CG_VT processes, which indicate that the direct CBTL plants will be more profitable if hydrogen is produced from low cost shale gas. Additionally, the relative penalty of CCS based on BEOP is about 10.2% if hydrogen produced from shale gas SMR and residual POX and 8.8% if hydrogen is produced from coal/biomass/residues CG, because CO_2 produced from gasification unit is at higher partial pressure and therefore easier to be captured. (Jiang and Bhattacharyya, 2016)

Table 3-120. Major economic measures (10,000 bbl/day, base case).

Process	SMR_CCS	SMR_VT	CG_CCS	CG_VT
Total project cost (MM$)	1162	1080	1464	1387
Net present value (MM$)	-408.6	-263.8	-591.7	-453.0
Internal rate of return (%)	6.0	7.3	5.2	6.2
Break-even oil price ($/bbl)	86.1	77.3	97.5	88.9
Equivalent oil price ($/bbl)	101.0	91.5	115.5	107.0

Figure 3-53 to Figure 3-56 provide the results due to $\pm$25% changes in the major plant economic inputs for all four configurations of the direct CBTL plant with a 10,000 bbl/day capacity. The results shows that the BEOP is between $83.4/bbl to $92.2/bbl for the SMR_CCS process, between $74.5/bbl to $82.9/bbl for the SMR_VT process, between $93.4/bbl to $104.7/bbl for the CG_CCS process, and between $84.7/bbl to $96.0/bbl for the CG_VT process. Figure 3-57 shows the effect of plant capacity in comparison between the small-scale operation (10,000 bbl/day, base case) and the large-scale operation (50,000 bbl/day) for all four configurations. As the plant capacity increases, multiple trains may be required for different process sections. For example, three parallel trains are required by the liquefaction and hydrocarbon recovery section, when the plant capacity reaches 50,000 bbl/day. The results indicate that the BEOP of the SMR_VT process decreases to $56.9/bbl with high capacity, which is less than the COP of the second quarter of 2015. However, the BEOP of the CG_CCS and the CG_VT processes is still much higher than the

COP even with a high plant capacity, because multiple trains are required by the gasification unit, one of the most expensive process sections.

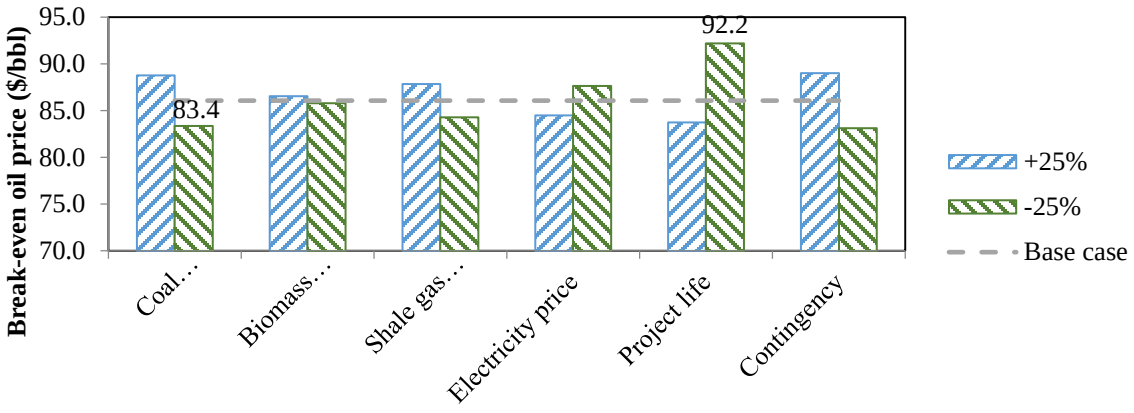

Figure 3-53. Sensitivity studies of the SMR_CCS process (10,000 bbl/day).

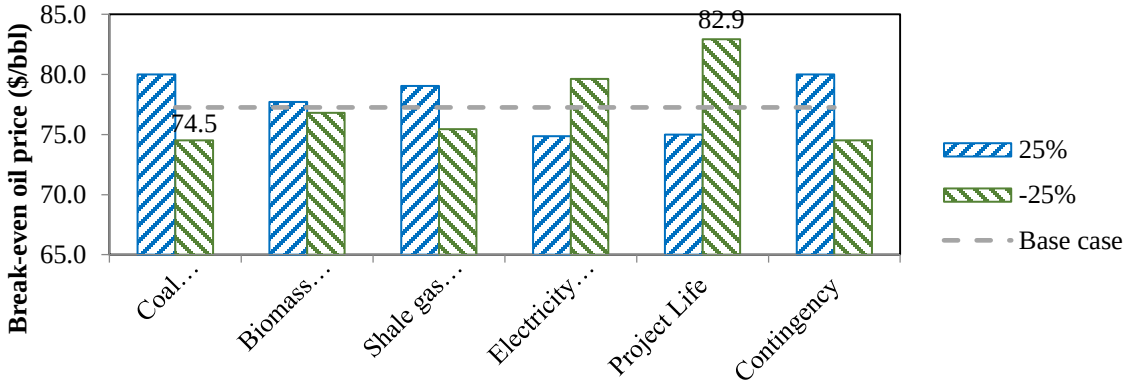

Figure 3-54. Sensitivity studies for the SMR_VT process (10,000 bbl/day).

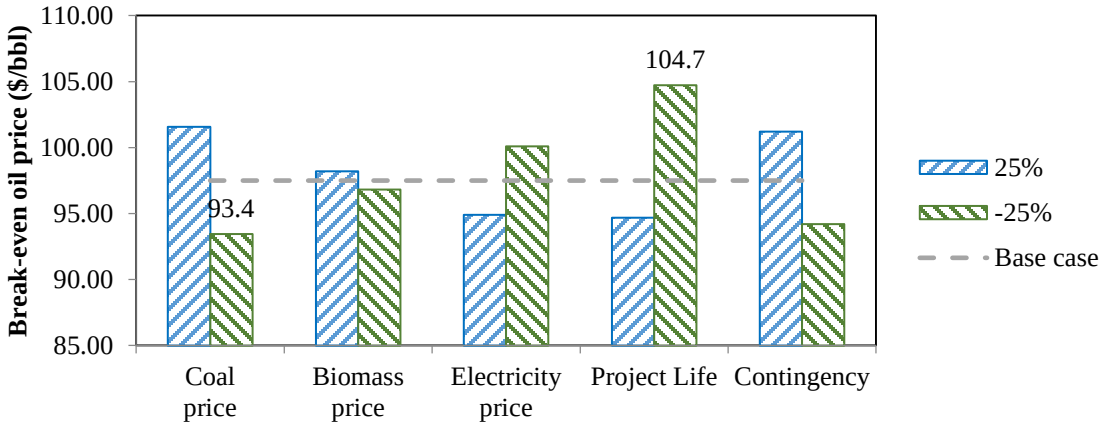

Figure 3-55. Sensitivity studies of the CG_CCS process (10,000 bbl/day).

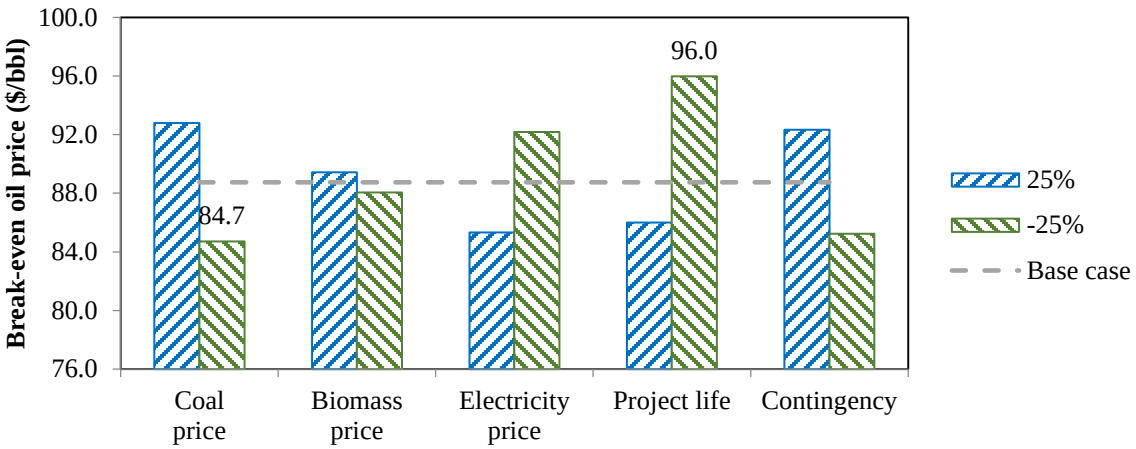

Figure 3-56. Sensitivity studies of the CG_VT process (10,000 bbl/day).

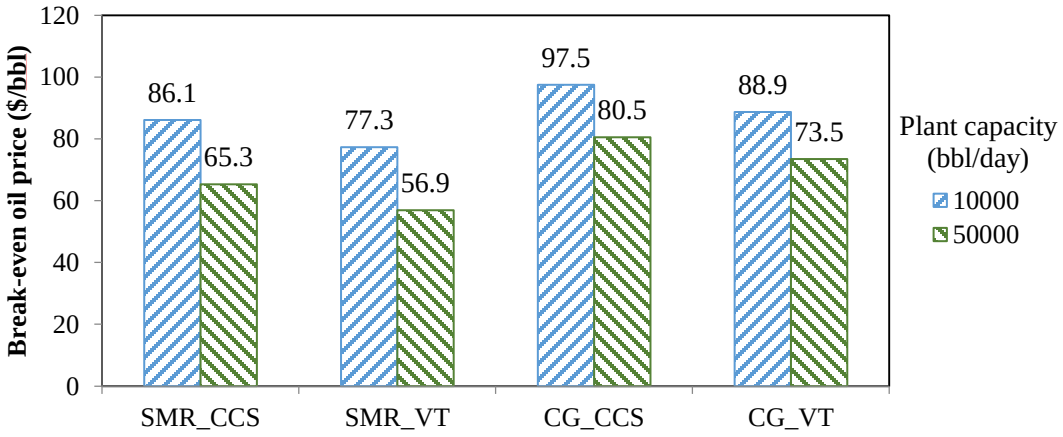

Figure 3-57. Effect of the plant capacity (10,000 and 50,000 bbl/day).

Effect of the biomass to coal ratio and the extent of CCS

In this study, two levels of biomass to coal weight ratio, 8/92 and 20/80, and two levels of CCS are considered and compared with the direct CBTL cases without CCS. For the case with low extent of CCS, all CO_2 removed in the hydrogen production and purification unit is sent to the CO_2 compression section preparing for CO_2 pipeline. For the case with high extent of CCS, additional CO_2 is captured from the low pressure sources, such as flue gas, and sent to the CO_2 compression section with the CO_2 captured from the hydrogen plant. The results are shown in Figure 3-58 and Table 3-121. Figure 3-58 indicates that the penalty of CCS increases with the increase in the extent of CCS and decrease in the biomass to coal ratio. Table 3-121 indicates that the CO_2 emission can be significantly reduced even with the low extent of CCS, where no additional CO_2 capture is required. As a result, the BEOP and TPC do not increase considerably if only low extent of CCS is considered. On the other hand, the penalty of CCS per unit of CO_2 capture in the cases with high extent of CCS is higher than that in the cases with low extent of CCS, because not only additional CO_2 needs to be captured but that the additional CO_2 needs to be captured from the low pressure

sources significantly increasing the operating cost and capital investment. The results also indicate that the overall cost and the penalty due to CCS decrease with the increase in the biomass content in the feedstock. Due to the higher H/C ratio in the biomass than coal, the hydrogen requirement in the liquefaction reactors gets reduced. As a consequence, the throughput of the hydrogen plant and associated CO_2 emission also gets reduced with the increase in the biomass content. To summarize, addition of more biomass and application of the CCS technology will increase the BEOP of the two processes by about $8.8/bbl (SMR_CCS) and $8.6/bbl (CG_CCS).

It is noticed that even with the high extent of CCS and even after taking into account the CO_2 credit due to use of biomass, the SMR_CCS and CG_CCS processes with a biomass to coal ratio of 8/92 still have a higher carbon footprint than the petroleum refineries (about 8.12 kg CO_2/GJ product). However, if the biomass to coal ratio increases to 20/80, the CO_2 emission from both SMR_CCS and CG_CCS process with high extent of CCS is lower than the petroleum refinery.

Table 3-121. Performance and economics of the direct CBTL plants with different extent of CCS.

Biomass/coal (wt/wt)		8/92			20/80	
Extent of CCS	High	Low	No	High	Low	No
Hydrogen produced from shale gas steam reforming and residues partial oxidation (SMR)						
Total project cost (MM$)	1162	1112	1080	1123	1044	1024
Internal rate of return (%)	6.0	7.0	7.3	5.9	6.9	7.3
CO_2 emission (kg CO_2/GJ product)	12.0	26.3	53.2	11.5	21.9	47.2
CO_2 emission with biomass credit(1) (kg CO_2/GJ product)	9.4	23.7	50.6	5.6	16.0	41.3
Thermal efficiency (HHV, %)	64.3	66.0	66.5	67.6	68.7	69.2
Hydrogen produced from coal/biomass/residues co-gasification (CG)						
Total project cost (MM$)	1464	1409	1387	1411	1366	1343
Internal rate of return (%)	5.2	5.9	6.2	5.1	5.9	6.1
CO_2 emission (kg CO_2/GJ product)	14.3	27.3	77.4	13.8	23.5	72.7
CO_2 emission with biomass credit(1) (kg CO_2/GJ product)	9.9	22.9	73.0	3.2	12.9	62.1
Thermal efficiency (HHC, %)	60.0	61.2	62.1	62.1	63.1	63.6

(1) When biomass credit is accounted, CO_2 produced from biomass is deducted from CO_2 emission, which is the molar flowrate of carbon in the biomass × (1- carbon efficiency of the process) × the molecular weight of CO_2.

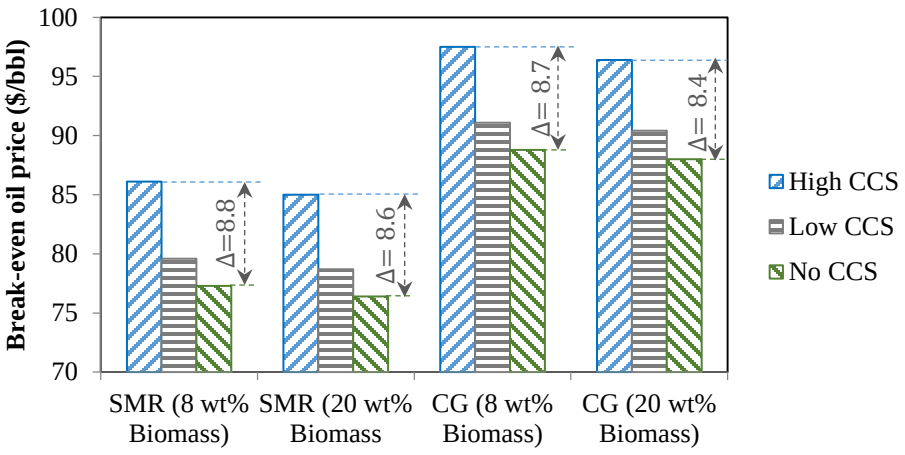

Figure 3-58. Effect of the extent of CCS.

Effect of potential environmental credits

In this section, three potential environmental credits are discussed for the SMR_CCS and CG_CCS processes with high-level CCS and a biomass to coal ratio of 20/80. For each potential environmental credit, two levels are considered, as shown in Table 3-122. Here, carbon credit is defined as the additional CO_2 captured from the processes with the baseline of petroleum refineries, which can be traded as a product in a carbon-constrained market. If the renewable/alternative energy certification is considered, the electricity can be sold at a premium. Here, we assume that the electric power generated from biomass qualifies for this credit, which is defined as the total power generated in the combined cycle island multiplied by the biomass HHV percentage in the feedstock. In addition, the federal government may apply lower tax rate to promote the development of renewable or alternative fuel related technologies, denoted as government-subsidized tax credit. The results in Table 3-13 show that the maximum reduction in BEOP is about $7.1/bbl for the SMR_CCS process and $8.8/bbl for the CG_CCS process if the proposed environmental credits are considered for the cases with a biomass to coal ratio of 20/80 while considering the value of all design and economic parameters the same as the base case. Combined with the sensitivity study shown in Section 4.3 and 4.4, the BEOP of the SMR_CCS and CG_CCS can be reduced to $75.5/bbl and $83.5/bbl at the best case scenario. It is observed that the contribution from the carbon credit and renewable energy certification is not significant because the relatively low biomass percentage in the feed and also due to very high capital and operating costs of the DCL technology. Due to the same reason, the contribution of these two credits is smaller in the SMR_CCS process than that in the CG_CCS process.

Table 3-122. Potential environmental credits.

Potential environmental credits	Description	High	Low	No
Carbon credit ($/tonne carbon)	Additional CO_2 captured	30	15	0
Renewable energy certification ($/MWh)	Electricity from biomass	60	55	50
Government-subsidized tax credit (%)	Incentive tax rate for alternative fuel	30	35	40

Table 3-123. Potential environmental credits for the direct CBTL plants (10,000 bbl/day).

Difference in BEOP ($/bbl)	SMR_CCS		CG_CCS	
Level of the credits	High	Low	High	Low
Carbon credit	-0.2	-0.1	-0.3	-0.2
Renewable energy certification	-0.2	-0.1	-0.5	-0.3
Government-subsidized tax credit	-6.7	-3.1	-8.0	-3.7

Direct versus indirect CBTL plant

A detailed process and economic model of the indirect CBTL plant based on the Fischer-Tropsch (FT) technology was developed in our previous studies using 2014 pricing basis. (Jiang and Bhattacharyya, 2014; 2015; 2016) For fair comparison, previous economic model developed for indirect CBTL plant with CCS (FT_CCS) and without CCS (FT_VT) is updated to the 2015 pricing basis. It is noted that 8% of biomass and 10,000 bbl/day capacity are considered for all cases. Because of the difference in sources of CO_2 and their partial pressure, the extent of CO_2 capture is different between the indirect and direct technologies for the cases with the low extent of CCS. (Jiang and Bhattacharyya, 2016) Hence, only the cases with the high extent of CCS and the cases without CCS are considered in this section for fair comparison. For the indirect CBTL plants, the plant contingency is set to be 18%, because the technology is more proven and there are more industrial operating experiences than the direct CBTL plants. Additionally, the TPC estimation of indirect CBTL plants matches well with the industrial data, once 18% plant contingency is applied.

The results are shown in Figure 3-59. The BEOP and EOP of the CG_CCS and CG_VT processes are slightly higher than those of the FT_CCS and FT_VT processes, while those of the SMR_CCS and SMR_VT processes are much lower than the FT_CCS and FT_VT processes. It indicates that the direct CBTL plants are comparatively less competitive than the indirect CBTL plants even with a higher thermal efficiency, if required hydrogen in the direct CBTL plants is all produced from gasification. If hydrogen is produced from more efficient and less expensive process, for example shale gas steam reforming, the direct CBTL plants are more competitive than the indirect CBTL plants. It is noticed that if the shale gas price is higher, the economic performance of the SMR_CCS and SMR_VT processes may be worse than that of the FT_CCS and FT_VT processes. Table 3-124 shows that the BEOP for the SMR_CCS and SMR_VT processes becomes the same as the FT_CCS and FT_VT processes when the price of shale gas increases to $3.70/GJ or $5.38/GJ, respectively.

The results also show that the penalty of indirect CBTL plants is lower than both direct CBTL plants, because additional CO_2 needs to be captured in the direct CBTL plant to achieve high level of CCS (Jiang and Bhattacharyya, 2016), while the difference between the FT_CCS and FT_VT processes is only in the CO_2 compression unit. (Jiang and Bhattacharyya, 2014; 2015; 2016) As mentioned before, the plant contingency is specified to be 24% because the limited commercial experience of the direct CBTL plant. If the plant contingency is set to be 18%, the same as the indirect CBTL plant, the BEOP of the CG_VT processes reduced to $85.2/bbl lower than that of the FT_VT process as shown in Fig. 6, because of reduced capital investment. However, the BEOP of the CG_CCS is still higher than that of the FT_CCS process, because of the higher CCS penalty.

Table 3-124 SMR processes versus FT processes (10,000 bbl/day).

	SMR_CCS		FT_CCS	SMR_VT		FT_VT
Shale gas price ($/GJ)	2.25	3.70		2.25	5.38	
Break-even oil price ($/bbl)	86.1	90.7	90.7	77.3	86.4	86.4

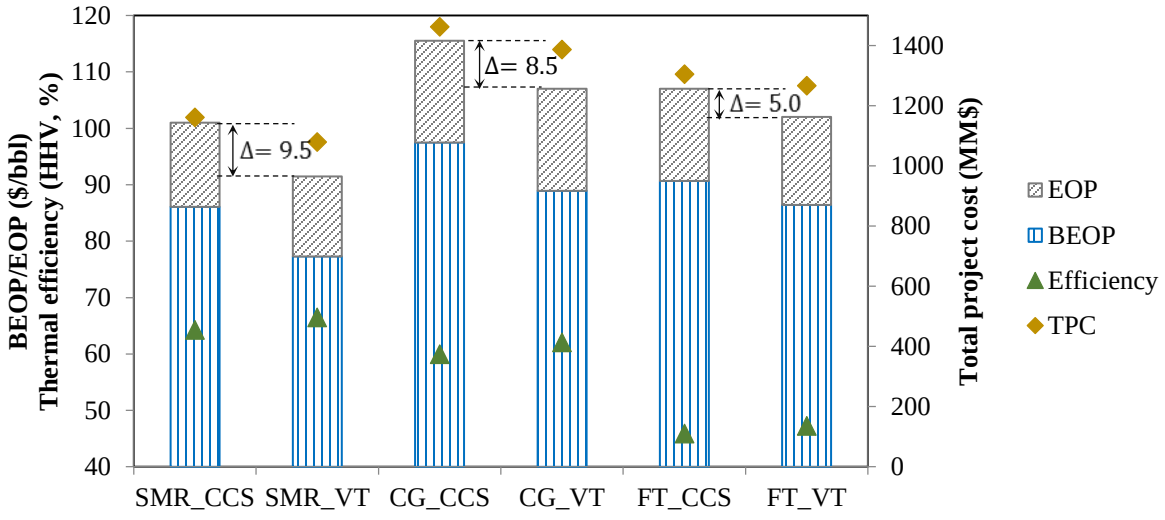

Figure 3-59. Indirect and direct CBTL plants (10,000 bbl/day)

✓ **Effect of plant configuration and summary of case studies**

All case studies conducted for indirect, direct and hybrid CBTL plants are summarized in Table 3-125 including sensitivity studies for different biomass types, coal/biomass ratio and other key design parameters. To summarize, even though the hybrid CBTL plant can reduce the capital and operating costs of upgrading processes, the BEOP for the hybrid plant is the highest because of the complexity of the syncrude production unit. The direct CBTL plant has the best economic performance, if shale gas is utilized as hydrogen source. Comparing case 15 with case 17, it is noticed that utilizing torrefied wood will decrease the BEOP of indirect by about $1/bbl, because of higher thermal efficiency and low gasification cost, even though the price of torrefied wood, $140/dry ton at this study, is almost twice of the wood chips.

Table 3-125. Summary of case studies.

Cases	1	2	3	4	5	6	7
Configuration	indirect	indirect	indirect	indirect	indirect	indirect	indirect
Pricing basis	2014	2014	2014	2014	2014	2014	2014
Capacity (bbl/day)	10000	10000	10000	10000	10000	10000	10000
Biomass type	wood	wood	wood	wood	wood	wood	bagasse
Biomass/coal	8/92	8/92	8/92	8/92	8/92	8/92	8/92
Shale gas utilization	N/A	N/A	N/A	N/A	N/A	N/A	N/A
H_2/CO in FT inlet	2.0	2.0	2.0	2.0	1.5	1.0	2.0
Hydrotreating	integrated	integrated	integrated	separated	integrated	integrated	integrated
Extent of CCS	high	high	high	high	high	high	high
MP/LP solvent	Selexol	MEA	MDEA/PZ	MDEA/PZ	MDEA/PZ	MDEA/PZ	MDEA/PZ
Efficiency (HHV, %)	40.8	45.7	45.9	59.5	43.9	40.8	46.6
BEOP ($/bbl)	103.6	95.7	95.5	96.0	98.1	106.5	95.9
Cases	8	9	10	11	12	13	14
Configuration	indirect	indirect	indirect	indirect	indirect	indirect	indirect
Pricing basis	2014	2014	2014	2014	2014	2014	2014
Capacity (bbl/day)	30000	50000	10000	10000	10000	10000	10000
Biomass type	wood	wood	wood	wood	wood	wood	wood
Biomass/coal	8/92	8/92	8/92	8/92	8/92	15/85	20/80
Shale gas utilization	N/A	N/A	N/A	N/A	N/A	N/A	N/A
H_2/CO in FT inlet	2.0	2.0	2.0	2.0	2.0	2.0	2.0
Hydrotreating	integrated	integrated	integrated	integrated	integrated	integrated	integrated
Extent of CCS	high	high	medium	low	no	high	high
MP/LP solvent	MDEA/PZ	MDEA/PZ	MDEA/PZ	MDEA/PZ	MDEA/PZ	MDEA/PZ	MDEA/PZ
Efficiency (HHV, %)	45.9	45.9	46.3	46.6	47.3	44.5	43.7
BEOP ($/bbl)	89.8	77.8	94.6	93.6	91.3	98.6	99.5
Cases	15	16	17	18	19	20	21
Configuration	indirect	indirect	indirect	direct	direct	direct	direct
Pricing basis	2015	2015	2015	2015	2015	2015	2015
Capacity (bbl/day)	10000	50000	10000	10000	50000	10000	10000

Biomass type	wood	wood	torrefied	wood	wood	wood	wood
Biomass/coal	8/92	8/92	8/92	8/92	8/92	8/92	8/92
Shale gas utilization	N/A	N/A	N/A	yes	yes	no	no
H_2/CO in FT inlet	2.0	2.0	2.0	N/A	N/A	N/A	N/A
Hydrotreating	integrated	integrated	integrated	N/A	N/A	N/A	N/A
Extent of CCS	high	high	high	high	no	high	no
MP/LP solvent	MDEA/PZ	MDEA/PZ	MDEA/PZ	MDEA/PZ	MDEA/PZ	MDEA/PZ	MDEA/PZ
Efficiency (HHV, %)	45.9	45.9	47.5	64.3	66.5	60.0	62.1
BEOP ($/bbl)	90.7	71.1	89.8	86.1	77.3	97.5	88.9
Cases	22	23	24	25	26	27	28
Configuration	direct	direct	direct	direct	direct	direct	direct
Pricing basis	2015	2015	2015	2015	2015	2015	2015
Capacity (bbl/day)	50000	50000	50000	50000	10000	10000	10000
Biomass type	wood	wood	wood	wood	wood	wood	wood
Biomass/coal	8/92	8/92	8/92	8/92	8/92	20/80	20/80
Shale gas utilization	yes	yes	no	no	yes	yes	yes
H_2/CO in FT inlet	N/A	N/A	N/A	N/A	N/A	N/A	N/A
Hydrotreating	N/A	N/A	N/A	N/A	N/A	N/A	N/A
Extent of CCS	high	no	high	no	low	high	low
MP/LP solvent	MDEA/PZ	MDEA/PZ	MDEA/PZ	MDEA/PZ	MDEA/PZ	MDEA/PZ	MDEA/PZ
Efficiency (HHV, %)	64.3	66.5	60.0	62.1	66.0	67.6	68.7
BEOP ($/bbl)	65.3	56.9	80.5	73.5	86.1	85.0	78.7
Cases	29	30	31	32	33	34	35
Configuration	direct	direct	direct	direct	direct	hybrid	hybrid
Pricing basis	2015	2015	2015	2015	2015	2015	2015
Capacity (bbl/day)	10000	10000	10000	10000	10000	10000	10000
Biomass type	wood	wood	wood	wood	wood	wood	wood
Biomass/coal	20/80	8/92	20/80	20/80	20/80	8/92	8/92
Shale gas utilization	yes	no	no	no	no	yes	no
H_2/CO in FT inlet	N/A	N/A	N/A	N/A	N/A	N/A	N/A
Hydrotreating	N/A	N/A	N/A	N/A	N/A	N/A	N/A

Extent of CCS	no	low	high	low	no	high	high
MP/LP solvent	MDEA/PZ	MDEA/PZ	MDEA/PZ	MDEA/PZ	MDEA/PZ	MDEA/PZ	MDEA/PZ
Efficiency (HHV, %)	69.2	61.2	62.1	63.1	63.6	56.5	55.7
BEOP ($/bbl)	76.4	91.1	96.4	90.4	88.0	94.5	100.6

Reference

1) Y. Jiang, D. Bhattacharyya, Modeling and analysis of an indirect coal biomass to liquids plant integrated with a combined cycle plant and CO_2 capture and storage, Energy Fuels, 29, 5434-5451, 2015.
2) Y. Jiang, D. Bhattacharyya, Modeling of Direct Coal-Biomass to Liquids (CBTL) Plants with Shale Gas Utilization and CO_2 Capture and Storage (CCS), Applied Energy, 183, 1616-1663, 2016.
3) Y. Jiang, D. Bhattacharyya, Techno-Economic Analysis of a Novel Indirect Coal-Biomass to Liquids Plant Integrated with a Combined Cycle Plant and CO_2 Capture and Storage, Industrial & Engineering Chemistry Research, 55, 1677-1689, 2016.
4) R. Ibrahim, L. Darvell, J. Jones, A. Williams, Physicochemical characterization of torrefied biomass, Journal of Analytical and Applied Pyrolysis, 103, 21-30, 2013.
5) R.N. Andre, F. Pinto, C. Franco, M. Dias, I. Gulyurtlu, M.A.A. Matos, I. Cabrita, Fluidized bed co-gasification of coal and olive oil industry wastes, Fuel, 84, 1635-1644, 2005.
6) D.Bhattacharyya, R. Turton, S.E. Zitney, Steady-state simulation and optimization of an integrated gasification combined cycle power plant with CO_2 capture, Industrial & Engineering Chemistry Research, 50, 1674-1690, 2011.
7) J.S. Kasule, R. Turton, D. Bhattacharyya, S.E. Zitney, Mathematical modeling of a single-Stage, downward-firing, entrained-flow gasifier, Industrial & Engineering Chemistry Research, 51, 6429−6440, 2012.
8) R.L. Bain, Material and Energy Balances for Methanol from Biomass Using Biomass Gasifiers. National Renewable Energy Laboratory, DE-AC36-83CH10093, 1992.
9) A.D. Overstreet, A screening study of a new water-gas shift catalyst. M. S. Thesis, Virginia Polytechnic Institute and State University, Blacksburg, VA, 1974.
10) V. Berispek, Studies of an alkali impregnated Cobalt-Molybdate catalyst for the water-gas shift and the methanation reactions. M. S. Thesis, Virginia Polytechnic Institute and State University, Blacksburg, VA, 1975
11) B.P., Williams, N.C. Young, J. West, C. Rhodes, G.J. Hutchings, Carbonyl Sulphide hydrolysis using alumina catalysts. Catalysis Today 49, 99-104, 1999.
12) P.D.N. Svoronos, T. Bruno, Carbonyl Sulfide: a review of its chemistry and properties. Industrial & Engineering Chemistry Research 41, 5321, 2002.
13) Gasification of residual material from coal liquefaction, Final Report, Texaco Inc., Montebello Research Laboratory; 1984.
14) A.M. Robin, Gasification of residual material from coal liquefaction, Quarterly Report, Texaco Inc., Montebello Research Laboratory, 1977.
15) A.M. Robin, Hydrogen production from coal liquefaction residues, Final Report, Texaco Inc., Montebello Research Laboratory, December 1976.

16) S.S. Penner, Assessment of long-term research needs for coal-liquefaction technologies, University of California, San Diego, March 1980.
17) F.J. Debyshire, P. Varghese, D.D., Whitehurst Integration of short-contact-time liquefaction and critical solvent deashing with gasification through methanol-to gasoline. Patent US4440622, 1984.
18) J. Gao, Coal liquefaction residue and coal water slurry combined gasification nozzle and application thereof. Chinese Patent CN102268300 B, 2014.
19) A.G. Comolli, L.K. Lee, V.R. Pradhan, T.H. Stalzer, E.C. Harris, D.M. Mountainland et al. Direct Liquefaction Proof-of-Concept Facility, Technical Progress Report POC Run 01, Contract No. AC22-92PC92148, Hydrocarbon Research Inc., 1995.
20) M.E. Dry, The Fischer-Tropsch process: 1950-2000. Catalysis Today 71, 227-241, 2002.
21) M.E. Dry, The Fischer-Torpsch Synthesis. In: Anderson, J.R., Boudart, M. (Eds.), Catalysis Science and Technology, vol. 1. Springer, Berlin, pp. 209-233, 1981.
22) R.L. Espinoza, A.P. Steynberg, B. Jager, A.C. Vosloo, Low temperature Fischer-Tropsch synthesis from a Sasol perspective. Applied Catalysis A: General 186, 13-26, 1999.
23) Bechtel, The Slurry Phase Fischer-Tropsch Reactor a Comparison of Slurry versus Fixed-Bed Reactor Designs for Fischer-Tropsch Distillate Production. Bechtel Corp., DE-AC22-89PC89867, Final Report, June 1990.
24) Bechtel, Baseline Design/Economics for Advanced Fischer-Tropsch Technology. Bechtel Corp., DE-AC22-91PC90027, Final Report, April 1998.
25) Bechtel, Baseline Design/Economics for Advanced Fischer-Tropsch Technology. Bechtel Corp., DE-AC22-91PC90027, Quarterly Report, January-March 1992.
26) Bechtel, Baseline Design/Economics for Advanced Fischer-Tropsch Technology. Bechtel Corp., DE-AC22-91PC90027, Quarterly Report, April-June 1992.
27) Bechtel, Baseline Design/Economics for Advanced Fischer-Tropsch technology. Bechtel Corp., DE-AC22-91PC90027, Quarterly Report, July-September 1992.
28) J.C. Kuo, Two-Stage Process for Conversion of Synthesis Gas to High Quality Transportation Fuels. Mobil R&D Corp., DE-AC22-83PC 60019, Final Report, October 1985.
29) J.C. Kuo, Slurry Fischer-Tropsch/Mobil Two-Stage Process of Converting Syngas to High Octane Gasoline. Mobil R&D Corp., DE-AC22-80PC30022, Final Report, June 1983.
30) E.D. Larson, G. Fiorese, G. Liu, R. H. Williams, T.G. Kreutz, S. Consonni, Co-production of decarbonized synfuels and electricity from coal and biomass with CO_2 capture and storage: an Illinois case study, Energy & Environmental Science 3, 28-42, 2010.
31) E.D. Larson, H. Jin, Biomass conversion to Fischer-Tropsch liquids: preliminary energy balance. In: Proceeding of the 4th Biomass Conference of the Americas, Oakland, CA, USA, 1999.
32) J.M. Fox, S.S. Tam, Correlation of slurry reactor Fischer-Tropsch yield data. Topics in Catalysis 2, 285-300, 1995.
33) L. Bai, H.W. Xiang, Y.W. Li, Y.Z. Han, B. Zhong, Slurry phase Fischer-Tropsch synthesis over manganese-promoted iron ultrafine particle catalyst. Fuel 81, 1577-1581, 2002.
34) R.L. Espinoza, A.P. Steynberg, B. Jager, A.C. Vosloo, Low temperature Fischer-Tropsch synthesis from a Sasol perspective. Applied Catalysis A: General 186, 13-26, 1999.
35) A.P. Steynberg, M.E. Dry, Fischer-Tropsch Technology. Elsevier Science, San Diego, pp. 237-244, 2004.

36) X. Wu, G. Shu, K. Li, S. Xie, Technology and Engineering of Direct Coal Liquefaction Process. Beijing: Science Press; 2015.
37) D.M. Austgen, G.T. Rochelle, C. Chen, Model of vapor-liquid equilibria for aqueous acid gas-alkanolamine systems 2 representation of H_2S and CO_2 solubility in Aqueous MDEA and CO_2 solubility in aqueous mixtures of MDEA with MEA and DEA, Industrial & Engineering Chemistry Research,, 30, 543-555,1991
38) E.B. Rinker, S.S. Ashour, O.C. Sandall, Experimental absorption rate measurements and reaction kinetics for H2S and CO2 in aqueous DEA, MDEA and blends of DEA and MDEA, GPA Research Report, No. 159, 1997.
39) A. Kohl, R. Nielsen, Gas Purification, 5th ed. Gulf Professional Publishing, Houston, TX, pp.40-73, 1997.
40) T. Neveux, Y. Moullec, J.P. Corriou, E. Favre, Energy performance of CO_2 capture processes: interaction between process design and solvent. Chemical Engineering Transactions 35, 337-342, 2013.
41) G. Xu, C. Zhang, S. Qin, W. Gao, H. Liu, Gas-liquid equilibrium in a CO_2-MDEA-H_2O system and the effect of piperazine on it. Industrial & Engineering Chemistry Research 37, 1473-1477, 1998.
42) G. Puxty, R. Rowland, Modeling CO_2 mass transfer in amine mixture: PZ-AMP and PZ-MDEA. Environmental Science and Technology 45, 2398-2406, 2011.
43) J.M. Plaza, Modeling of carbon dioxide absorption using aqueous monoethanolamine, piparazine and promoted potassium carbonate. PhD Dissertation, University of Texas at Austin: Austin, TX, 2012.
44) M.D. Hilliard, A predictive thermodynamic model for an aqueous blend of potassium carbonate, piperazine, and monoethanolamine for carbon dioxide capture from flue gas. Ph.D. Dissertation, University of Texas at Austin: Austin, TX, 2008.
45) S. Bishnoi, G. Rochelle, Absorption of carbon dioxide into aqueous piperazine: reaction kinetics, mass transfer and solubility, Chemical Engineering Science 55, 5531-5543, 2000.
46) S. Bishnoi, G. Rochelle, Absorption of carbon dioxide into aqueous piperazine/ methyldiethanolamine, AIChE Journal, 48, 2788-2799, 2002.
47) Y. Zhang, H. Chen, C. Chen, J.M. P laza, R. Dugas, G.T. Rochelle, Rate-based process modeling study of CO_2 capture with aqueous monoethanolamine solution. Industrial & Engineering Chemistry Research 48, 9233-9246, 2009.
48) R.E. Dugas, Pilot plant study of carbon dioxide capture by aqueous monoethanolamine, M.S. thesis, University of Texas at Austin: Austin, TX, 2006.
49) H. Hikita, S. Asai, Ishikawa H., M. Honda, The kinetics of reactions of carbon dioxide with monoethanolamine, diethanolamine, and triethanolamine by a rapid mixing method, Chemical Engineering Journal 13, 7-12, 1977.
50) A.M. Valente, D.C. Cronauer, Analyses of Illinois No.6 coal liquefaction results generated in the Wilsonville, Alabama Unit. Energy Fuels, 19, 489-498, 2005.
51) A.H. Tchapda, S.V. Pisupati, A review of thermal co-conversion of coal and biomass/waste, Energies, 7, 1098-1148, 2014.
52) R.W. Coughlin, Davoudzadeh F. Coliquefaction of lignin and bituminous coal, Fuel, 65, 95-106, 1986.
53) H. Shui, C. Shan, Z. Cai, Z. Wang, Z. Lei, S. Ren et al. Co-liquefaction behavior of a sub-bituminous coal and sawdust, Energy, 36(11), 6645-6650, 2011.
54) H. Shui, Z. Cai, C. Xu, Recent advances in direct coal liquefaction, Energies, 3:155-70, 2010.

55) L.L. Anderson, W. Tuntawiro, Coliquefaction of Coal and Polymers to Liquid Fuels, Amer Chem Soc Div Fuel Chem Preprints, 38(4), 810-815, 1993.
56) Bechtel and Amoco, Direct coal liquefaction baseline design and system analysis, Quarterly Report, DEAC2290PC89857, September 1990.
57) F. Behrendt, Y. Neubauer, M. Oevermann, B. Wilmes, N. Zobel, Direct Liquefaction of Biomass, Chemical Engineering & Technology, 31, 667-677, 2008.
58) D.J. Stevens, An overview of biomass thermochemical liquefaction research sponsored by the U.S. Department of Energy, Amer Chem Soc Div Fuel Chem Prepr, 32(2), 223–228, 1987.
59) S.S. Sofer, O.R. Zaborsky, Biomass conversion processes for energy and fuels. New York: Springer Science & Business Media, 2012.
60) D.H. White, D. Wolf, Y. Zhao, Biomass liquefaction utilizing extruder-feeder reactor systems. Amer Chem Soc Div Fuel Chem Prepr, 32(2): 106-16, 1987.
61) D.C. Elliott, Process development for biomass liquefaction, Amer Chem Soc Div Fuel Chem Prepr, 25(4), 257-63, 1980.
62) K.K. Robinson, Reaction engineering of direct coal liquefaction, Energies, 2: 976-1006, 2009.
63) X. Shan, K. Li, X. Zhang, H. Jiang, H. Weng, Reaction kinetics study on the heating stage of the Shenhua direct coal liquefaction process, Energy Fuels, 29, 2244-2249, 2015.
64) H. Jiang, X. Wang, Z. Shan, K. Li, X. Zhang, X. Cao, H. Weng, Isothermal stage kinetics of direct coal liquefaction for Shenhua Shendong bituminous coal. Energy Fuels 2015; 29: 7526-31.
65) J. Martinez, J.J. Sanchez, J. Ancheyta, R.S. Ruiz, A review of process aspects and modeling of ebullated bed reactors for hydrocracking of heavy oil, Catalysis Reviews, 52, 60-105, 2010.
66) X. Shan, K. Li, X. Zhang, H. Jiang, H. Weng, Reaction kinetics study on the heating stage of the Shenhua direct coal liquefaction process, Energy Fuels, 29, 2244-2249, 2015.
67) A. Marzec, Towards an understanding of the coal structure: a review, Fuel Processing Technology, 77-78, 25-32, 2002.
68) M. Anbar, G.A. St John, Characterization of coal-liquefaction products by molecular-weight profiles produced by field-ionization mass spectrometry, Fuel, 57, 105-110, 1978.
69) W.U. Yan, Precision of NEDOL method for coal-derived relative molecular weight calculation, Clean Coal Technology, 20(2), 51-54, 2014.
70) J.P. Ferrance, Development of a general model for coal liquefaction, University of Pittsburgh: Pittsburgh, PA, 1996.
71) L. Sehabiague, R. Lemoine, A. Behkish, Y.J. Heintz, M. Sanoja, R. Oukaci, B.I. Morsi, Modeling and optimization of a large-scale slurry bubble column reactor for producing 10,000 bbl/day of Fischer-Tropsch liquid hydrocarbons, Journal of the Chinese Institute of Chemical Engineering, 39, 169-179, 2008.
72) H. Ishibashi, M. Onozaki, M. Kobayash, J. Hayashi, H. Itoh, T. Chiba, Gas holdup in slurry bubble column reactors of a 150t/d coal liquefaction pilot process, Fuel, 80, 655-664, 2001.
73) M.H.I. Baird, R.G. Rice, Axial dispersion in large unbaffled columns, the Chemical Engineering Journal, 9, 171-174, 1975.
74) J.W.A. de Swart, Scale-up of a Fischer-Tropsch slurry reactor, PhD thesis, University of Amsterdam, Amsterdam, Netherlands, 1996.

75) M. Onozaki, Y. Namiki, H. Ishibashi, T. Takagi, M. Kobayashi, S. Morooka, Steady-State thermal behavior of coal liquefaction reactors based on NEDOL process, Energy Fuels, 14, 355-363, 2000.
76) W.D. Deckwer, Bubble column reactors, John Wiley & Sons, New York, 1992.
77) S. Kara, B.G. Kelkar, Y.T. Shah, Hydrodynamics and axial mixing in a three-phase bubble column, Ind. Eng. Chem. Process Des. Dev., 21, 584-594, 1982.
78) J. Tomeczek, H. Palugniok, Specific heat capacity and enthalpy of coal pyrolysis at elevated temperatures, Fuel, 75(9), 1089-1093, 1996.
79) M.J. Richardson, The specific heats of coals, cokes and their ashes, Fuel, 72(7), 1047-1053, 1993.
80) E. Cavallo, D. Januszweski, S. Putek, Upgrade hydrocracked resid through integrated hydrotreating, Hydrocarbon Processing, 87(9), 83-92, 2008.
81) A.T. Jarullah, I.M. Mujtaba, A.S. Wood, Whole Crude Oil Hydrotreating from Small-Scale Laboratory Pilot Plant to Large-Scale trickle-Bed Reactor: Analysis of Operational Issues through Modeling, Energy Fuels, 26, 629–641, 2012.
82) M.A. Fahim, T.A. Al-Sahhaf, A. Elkilani, Fundamentals of Petroleum Refining, 1st ed., Elsevier Science: Oxford, UK, pp 170-179, 2010.
83) D. Lamprecht, Hydrogenation of Fischer-Tropsch synthetic crude, Energy Fuels, 21, 2509-2513, 2007.
84) S. Weller, R.A. Friedel, Isomer distribution in hydrocarbons from the Fischer-Tropsch process, Journal of Chemical Physics, 17(9), 801-803, 1949.
85) S. Gamba, L.A. Pellegrini, V. Calemma, C. Gambaro, Liquid fuels from Fischer–Tropsch wax hydrocracking: Isomer distribution, Catalysis Today, 156, 58–64, 2010.
86) S. Ji, and M. Bagajewicz, Design of crude distillation plants with vacuum units I targeting, Industrial & Engineering Chemistry Research, 41, 6094-6099, 2002.
87) M. Bagajewicz, S. Ji, Rigorous procedure for the design of conventional atmospheric crude fractionation units. 1, Targeting, Industrial & Engineering Chemistry Research, 40, 617-626, 2001.
88) M. Bagajewicz, J. Soto, Rigorous procedure for the design of conventional atmospheric crude fractionation units. 2. Heat exchanger network, Industrial & Engineering Chemistry Research, 40, 627-634, 2001.
89) J.W. Seo, M. Oh, T.H. Lee, Design optimization of crude oil distillation, Chemical Engineering & Technology, 23 (2), 157-164, 2000.
90) E.N. Givens, D. Kang, Coal liquefaction process with enhanced process solvent. Patent US4461694, 1984.
91) R.A. Baldwin, J.L. Bills, Processes for the production of deashed coal. Patent US4119523, 1978.
92) J.A. Gearhart, S.R. Nelson, ROSE process offers energy savings for solvent extraction. In: Proceedings of the 5th Industrial Energy Technology Conference Volume II, Houston, TX, 1983.
93) D.E. Rhodes, Process for improving soluble coal yield in a coal deashing process. Patent US4225420, 1980.
94) S.M. Morris, E.P. Foster, The SRC-I Coal Refining Demonstration Plant. International Coal Refining Company, http://www.fischer-tropsch.org, 1983 [accessed 16.05.31].
95) R.M. Thorogood, Solvent refined coal reactor quench system. Patent US4414094 A, 1983.

96) C.T. Shih, Experimental hydrodynamic study of the slurry distribution in a vertical slurry heat exchanger, PhD dissertation, University of Nevada, Las Vegas; 1995.
97) Clean coal technologies in Japan, New Energy and Industrial Technology Development Organization, Kawasaki, Japan, 2006.
98) Review of worldwide coal to liquids R, D&D activities and the need for further initiatives within Europe, IEA Coal Research Ltd., RFC2-CT-2008-00006, http://www.iea-coal.org.uk; June 2009 [accessed 05.01.16].
99) G. Liu, R.H. Williams, E. Larson, T. Kreutz, Making Fischer-Tropsch fuels and electricity from coal and biomass: performance and cost analysis, Energy Fuels, 25, 415-437, 2011.
100) X. Guo, G. Liu, E.D. Larson, High-octane gasoline production by upgrading low-temperature Fischer-Tropsch syncrude. Industrial & Engineering Chemistry Research, 50, 9743-9747, 2011.
101) A. Klerk, Fischer-Tropsch fuels refinery design. Energy Environ. Sci. 2011, 4, 1177-1205.
102) A. Klerk, E. Furimsky, Catalysis in the Refining of Fischer-Tropsch Syncrude, 1st ed., Royal Society of Chemistry: Cambridge, UK, 2010.
103) K. Watanabe, N. Chiyoda, T. Kawakami, Development of new isomerization process for petrochemical by-products, Processing 18th Saudi Arabia-Japan Joint Symposium, Dhahran, Saudi Arabia, Nov, 2008.
104) M.J. Ramos, J.P. Gomez, F. Dorado, P. Sanchez, J.L. Valverde, Hydroisomerization of a refinery naphtha stream over platinum zeolite-based catalysts, Chemical Engineering Journal, 126, 13-21, 2007.
105) P.P. Shah, G.C. Sturtevant, J.H. Gregor, M.J. Humbach, F.G. Padtra,; K.Z. Steigleder, Fischer-Tropsch Wax Characterization and Upgrading, Final Report; DE-AC22-85PC80017; UOP Inc., June 1988; http://www.fischer-tropsch.org.
106) U.M. Teles, F.A.N. Fernandes, Hydrocracking of Fischer-Tropsch products, Thermal Engineering, 6(2), 14-18, 2007.
107) D. Leckel, Hydrocracking of iron-catalyzed Fischer-Tropsch waxes, Energy Fuels, 19, 1795-1803, 2005.
108) D. Leckel, Low-pressure hydrocracking of coal-derived Fischer-Tropsch waxes to diesel. Energy Fuel, 21, 1425-1431, 2007.
109) P.P. Shah, Upgrading of Light Fischer-Tropsch Products, Final Report; DE-AC22-86PC-90014; UOP Inc., November, 1990; http://www.fischer-tropsch.org.
110) S. Vasireddy, B. Morreale, A. Cugini, C. Song, J.J. Spivey, Clean liquid fuels from direct coal liquefaction: chemistry catalysis technological status and challenges, Energy & Environmental Science, 4, 311-345, 2011.
111) J.H. Shinn, From coal to single-stage and two-stage products: a reactive model of coal structure, Fuel, 63, 1187-1195, 1984.
112) I. Mochida, O. Okuma, S. Yoon, Chemicals from Direct Coal Liquefaction, Chemical Reviews, 114(3), 1637-72, 2014.
113) P. Zhou, S.N. Rao, Assessment of coal liquids as refinery feedstocks, Prepared for DOE Pittsburgh Energy Technology Center, February 1992.
114) J.H. Gary, G.E. Handwerk, Petroleum Refining Technology and Economics. 4th ed. New York: Marcel Dekker Inc., 2001.
115) M.R. Smith, D.A. Hubbard, C.C. Yang, Logic, technology and effect of coal liquefaction condition on final up-graded product slate. In: Proceedings of the 9th Annual International Conference on Coal Gasification, Liquefaction, and Conversion to Electricity, 1982.

116) T.A. Albahri, M.R. Riazi, A.A. Alqattan, Octane number and aniline point of petroleum fuels. Amer Chem Soc Div Fuel Chem Prepr, 47(2), 710-711, 2002.
117) G.I. Jenkins, Journal of Institute of Petroleum, 54, 14, 1968.
118) R.E. Maples, Petroleum Refinery Process Economics, 2nd ed.; PenneWell Corp.: Tulsa, OK, 2000.
119) J.C. Molburg, R.D. Doctor, Hydrogen from steam-methane reforming with CO_2 capture. In: Proceedings of the 20th Annual International Pittsburgh Coal Conference, Pittsburgh, USA, September 15-19, 2003.
120) S. Ayabe, H. Omoto, T. Utaka, R. Kikuchi, K. Sasaki, Teraoka Y., K. Eguchi, Catalytic autothermal reforming of methane and propane over supported metal catalysts, Appl. Catal. A: General, 241(1-2), 261-269, 2003.
121) B.T. Schadel, M. Duisberg, O. Deutschmann, Steam reforming of methane, ethane, propane, butane and natural gas over a rhodium-based catalyst, Catalysis Today, 142, 42-51, 2009.
122) B.T. Schadel, R. Schwiedernoch, L. Maier, O. Deutschmann, Reforming of methane with nickel and rhodium- catalysts: An experimental and modelling study. 4th International Conference on Environmental Catalysis, Heidelberg, 2005
123) I. Rafiqul, B. Lugang, Y. Yan, T. Li, Study on co-liquefaction of coal and bagasse by factorial experiment design method. Fuel Processing Technology, 68, 3-12, 2000.
124) A.P. Steynberg, M.E. Dry, Fischer-Tropsch Technology, 1st ed.; Elsevier Science: San Diego, 2004.
125) NETL, Technical and economic assessment of small-scale Fischer-Tropsch liquids facilities, DOE/NETL-2007/1253, Final Report, February, 2007; http://www.netl.doe.gov
126) NETL, Technical and economic assessment of small-scale Fischer-Tropsch liquids facilities, DOE/NETL-2007/1253, Final Report, February, 2007; http://www.netl.doe.gov
127) P. Chiesa, G. Lozza, L. Mazzocchi, Using hydrogen as gas turbine fuel. Journal of Engineering for Gas Turbines and Power, 127, 73-80, 2005
128) A.P. Steynberg, H.G. Nel, Clean coal conversion options using Fischer-Tropsch technology, Fuel, 83, 765-770, 2004.
129) R.C. Spencer, K.C. Cotton, C.N. Cannon, A method for prediction the performance of steam turbine-generators…: 16,500 kW and larger. ASEM J. ENG. Power, 85, 249-298, 1963.
130) G. Lozza, Bottoming steam cycles for combined steam gas power plants: A theoretical estimation of steam turbines performances and cycle analysis. Proceedings of the 1990 ASME Cogen-Turbo symposium, New Orleans, USA, 83-92, 1990.
131) F.C. Baily, K.C. Cotton, R.C. Spencer, Predicting the Performance of Large Steam Turbine-Generators Operating with Saturated and Low Superheat Steam Conditions. Proceeding 28th Annual Meeting of American Power Conference, General Electric Report 2454-A, Schenectady, NY, 1967.
132) R.H. Williams, E.D. Larson, A comparison of direct and indirect liquefaction technologies for making fluid fuels from coal. Energy Sustain. Dev, 7(4), 103-129, 2003.
133) R.F. Bauman, P.S. Maa, Direct coal liquefaction process, Patent CN104937077A, 2014.
134) Y. Jiang, D. Bhattacharyya, Modeling of Direct Coal-Biomass to Liquids (CBTL) Plants with Shale Gas Utilization and CO_2 Capture and Storage (CCS), Applied Energy, 183, 1616-1663, 2016.
135) R.C. Baliban, J.A. Elia, C.A. Floudas, Optimization framework for the simultaneous process synthesis, heat and power integration of a thermochemical hybrid biomass, coal and natural gas facility, Computers & Chemical Engineering, 35, 1647-1690, 2011.

136) Cost and Performance Baseline for Fossil Energy Plant Volumn 1: Bituminous Coal and Natural Gas to Electricity, National Energy Technology Laboratory, DOE/NETL - 2010/1397, November 2010.
137) R.E. Tsai, Mass Transfer Area of Structured Packing, PhD Dissertation. The University of Texas at Austin, TX, 2010.
138) Equipment Design and Cost Estimation for Small Modular Biomass Systems, Synthesis Gas Cleanup, and Oxygen Separation Equipment; NREL/SR-510-39945; National Renewable Energy Laboratory, 2006.
139) R.C. Baliban, J.A. Elia, C.A. Floudas, Novel natural gas to liquids processes: process synthesis and global optimization strategies, AIChE J, 59(2), 505-31, 2013.
140) H. Su, Economics of geological sequestration and carbon management: a case study of Shenhua's direct coal liquefaction plant in China, PhD thesis, West Virginia University, Morgantown, WV, 2010.
141) T.G. Kreutz, E.D. Larson, G. Liu, R.H. Williams, Fischer-Tropsch fuels from coal and biomass. Proceeding of the 25th International Pittsburg Coal Conference, Pittsburgh, PA, Sep 29 - Oct 2, 2008.
142) J. Wang, J. McNeel, Assessments of Coal/Biomass to Liquid Fuels in West Virginia, Biomaterials and Wood Utilization Research Center, West Virginia University, July 10, 2009.
143) G. Liu, E. Larson, R. Williams, X. Guo, Gasoline from coal and/or biomass with CO_2 capture and storage. 1. Process designs and performance analysis, Energy Fuels 29(3) (2015) 1830-44.
144) R. Turton, R.C. Bailie, W.B. Whiting, J.A. Shaeiwitz, D. Bhattacharyya, Analysis, Synthesis, and Design of Chemical Process, 4th ed. Pearson Education, Boston, pp. 206, 2012..
145) J. Seagraves, R.H. Weiland, Treating high CO_2 gases with MDEA, Optimized Gas Treating Inc. http://www.eptq.com , 2009
146) Y.K. Salkuyeh, M. Mofarahi, Reduction of CO_2 capture plant energy requirement by selecting a suitable solvent and analyzing the operating parameters. International Journal of Energy Research 37, 973-981, 2013.
147) M. Reed, L.V. Bibber, E. Shuster, J. Haslbeck, M. Rutkowski, S. Olson, S. Kramer, Baseline Technical and Economic Assessment of a Commercial Scale Fischer-Tropsch Liquids Facility. National Energy Technology Laboratory, DOE/NETL-2007/1260, Final Report, 2007.
148) A.T. Jarullah, I.M. Mujtaba, A.S. Wood, Whole Crude Oil Hydrotreating from Small-Scale Laboratory Pilot Plant to Large-Scale trickle-Bed Reactor: Analysis of Operational Issues through Modeling, Energy Fuels, 26, 629–641, 2012.
149) R. Edwards, Well-to-wheels Analysis of Future Automotive Fuels and Powertrains in the European Context, WELL-to-TANK Report, Version 3c, July 2011.
150) ASTM D4814-14b, Standard Specification for Automotive Spark-Ignition Engine Fuel; ASTM International, West Conshohocken, PA, 2014; http://www.astm.org.
151) CARB, CARB Phase 3 Gasoline Specifications and Test Methods; California Air Resources Board, 2012; http://www.arb.ca.gov/enf/fuels/gasspecs.pdf.
152) ASTM, US Reformulated Spark-Ignition Engine Fuel and the US Renewable Fuel Standard, Research Report; ASTM International, West Conshohocken, PA, 2014; http://www.astm.org.

153) Code of Federal Regulation, Title 40: Protection of Environment, Part 80: Regulation of Fuels and Fuel Additives; http://www.ecfr.gov; latest access on Feb, 5th, 2015.
154) ASTM D975-14b, Standard Specification for Diesel Fuel Oils; ASTM International, West Conshohocken, PA, 2014; http://www.astm.org.
155) R.D. Doctor, J.C. Molburg, P.R. Thimmapuram, G.F. Betty, C.D. Livengood, Energy System Division, Argonne National Laboratory, Argonne, Illinois, Gasification combined cycle: carbon dioxide recovery, transport and disposal, ANL/ESD-24, work sponsored by United States Department of Energy, September 1994.
156) I.Y. Mohammed, M. Samah, A. Mohamed, G. Sabina, Comparison of Selexol and Rectisol technologies in an integrated gasification combined cycle (IGCC) plant for clean energy production, International Journal of engineering research 2014, 3(12), 742-744.
157) O.O. James, B. Chowdhury, A. Auroux, S. Maity, Low CO_2 selective iron based Fischer-Tropsch catalysts for coal based polygeneration, Applied Energy, 107, 377-383, 2013.
158) IRENA, Renewable energy technologies: cost analysis series biomass for power generation; IRENA, working paper; the International Renewable Energy Agency, June 2012; http://www. irena.org/publications.
159) R. Gonzales, R. Phillips, D. Saloni, H. Jameel, R. Abt, A. Pirraglia, J. Wright, Biomass to energy in the southern United States: supply chain and delivered cost, BioResources, 6(3), 2954-2976, 2011.

Task 4 Market Feasibility

Task 4.1 Develop a marketing plan for the proposed CBTL facility

- Expanded Integrated Model of Marketing Plan
- Market/Industry Summary, Demographics, Needs, Competition, and Buyer Analysis
- SWOT and PESTE Analysis
- Competitive Market Strategies

Task 4.2 Evaluate risks related to the marketing of CBTL fuels

- Determination of Break Even Certainty
- Evaluation of Risk Reduction Strategies

Research Products:

Presentations

Estep, G.D., D. DeVallance, and J. Wang. 2013. Market feasibility of a coal-biomass to liquid fuel facility in the southern West Virginia region. Poster presentation at the Forest Products Society 67th International Convention, Austin, Texas. June 9.

Task 4.1 Develop a marketing plan for the proposed CBTL facility

Market Plan Summary

The subject of this marketing plan is a proposed Coal Biomass to Liquid (CBTL) fuel facility in southern West Virginia, where raw materials are readily available. The primary function of this facility will be to produce liquid fuels such as gasoline and diesel from a mixture of coal (92%) and biomass (8%) using various liquefaction production methods along with a novel tri-reforming process to reduce energy demands as well as production process emissions. Research has been conducted to explore the possible market opportunities of the finished products: gasoline and diesel.

Based on the results of a survey focused on bulk fuel terminals, the economically feasible transportation distances of the CBTL derived product are approximately 150 miles from the proposed plant location of Glade Creek, West Virginia. To penetrate a larger overall market, it is advised to consider bulk fuel terminals within 150 miles as the facilities target market. Advantages of pursuing this market include: the ability to mix additives such as ethanol for gasoline, lubricity for diesel, and undisclosed additives for "branded" gasoline mixtures; the ability to store bulk quantities of mixed and unmixed fuels, expand the demand region for gasoline and diesel fuels to that of the bulk fuel terminals.

At a production rate of 10,000 barrels of crude-oil-equivalent per day, the CBTL facility could supply the immediate 150 mile market with 3.5% and 3.2% of its gasoline and diesel needs, respectively. Moreover, the supply capabilities of the CBTL facility are 0.6% and 0.6% of the total demand for gasoline and diesel, respectively for the expanded markets of the bulk fuel terminals.

There are expected barriers to entering this industry do to inter-firm rivalry, initial capital costs, and pressures from substitute products such as natural gas and other technologies such as coal biomass gas to liquid fuel. However, the closest existing gasoline and diesel production facility in 100 miles away resulting in relatively low local competition and the inherent advantage of lower transportation distances to some markets.

Further results from the survey indicate an interest in purchasing CBTL derived gasoline and diesel at prices lower than petroleum based fuels. Results also determined that price was the driving influence when comparing CBTL derived fuels and petroleum derived fuels. No preference was indicated for the use of raw material used to produce fuels (petroleum vs. coal and biomass), locally sourced raw materials (foreign and domestic vs. West Virginia, and environmental impact of production (crude oil refining emissions vs. CBTL refining emissions).

The recent economic recovery is resulting in a lower unemployment rate and possibly a higher amount of disposable income. These factors coupled with the predicted increase in population for states surrounding and including WV, could increase demand for liquid fuels in the study region. As petroleum prices increase, the price of gasoline and diesel also increase to compensate for the rise in raw material cost and could allow CBTL products to more effectively compete for market share in the region.

Situational Analysis

The company - Description of company and business definition

The subject of this marketing plan is a proposed Coal Biomass to Liquid (CBTL) fuel facility in southern West Virginia. The primary function of this facility will be to produce liquid fuels such as gasoline and diesel. Locating the facility in southern West Virginia will allow the use of locally sourced feed stock materials such as coal and woody biomass for the refinery process. West Virginia is the nation's second largest coal-producing state (National Mining Association 2011) and the nation's third most heavily forested state (Wang et al. 2006). The raw material availability in the local region makes West Virginia a prime candidate for a CBTL plant location.

Utilizing novel technologies in coal biomass to liquid fuels production, the environmental impact, specifically greenhouse gas (GHG) emissions, of the finished product will be less than similar, petroleum-derived products. The production methods used in this facility will incorporate direct and indirect liquefaction as well as a hybrid approach to further the efficiency of the process. Additionally, a tri-reforming process is proposed for this facility to reduce the energy demands compared to other reforming processes and reuse a portion of the CO_2 produced to increase yields while reducing GHG emissions.

Market/Industry Summary

Market Structure

The market structure for the CBTL plant's raw material and product distribution can be seen in Figure 4-1. Two feed stocks are proposed for this facility, coal and woody biomass. These will be transported to the CBTL plant via barge, rail, or truck and combined in a mixture of 92% coal and 8% woody biomass for the refining process. Upon production of the fuel products, there are two major choices for distribution: 1) maintain on-site storage for later distribution to retail fueling

stations, or 2) transport the fuel products to a bulk fuel terminal. Transportation methods to retail fueling stations are limited to truck distribution. However transporting the fuels to bulk fuel terminals can be achieved by truck as well as barge and rail, depending on each bulk terminals receiving capabilities. There are additional advantages in distributing fuels to bulk fuel terminals that include: 1) increased sales area and 2) opportunity to penetrate branded fuel markets. The economically feasible transportation distance of the bulk fuels terminals is generally 100 – 150 miles from their location. Therefore, by selling the CBTL fuel products to bulk fuel terminals, an additional 100 – 150 mile radius of market region could be reached. Also, by selling unbranded fuels to a bulk fuel terminal that mixes and distributes branded fuel products, the CBTL fuels could be used to help satisfy unbranded fuel demand as well as branded fuel demand in the region.

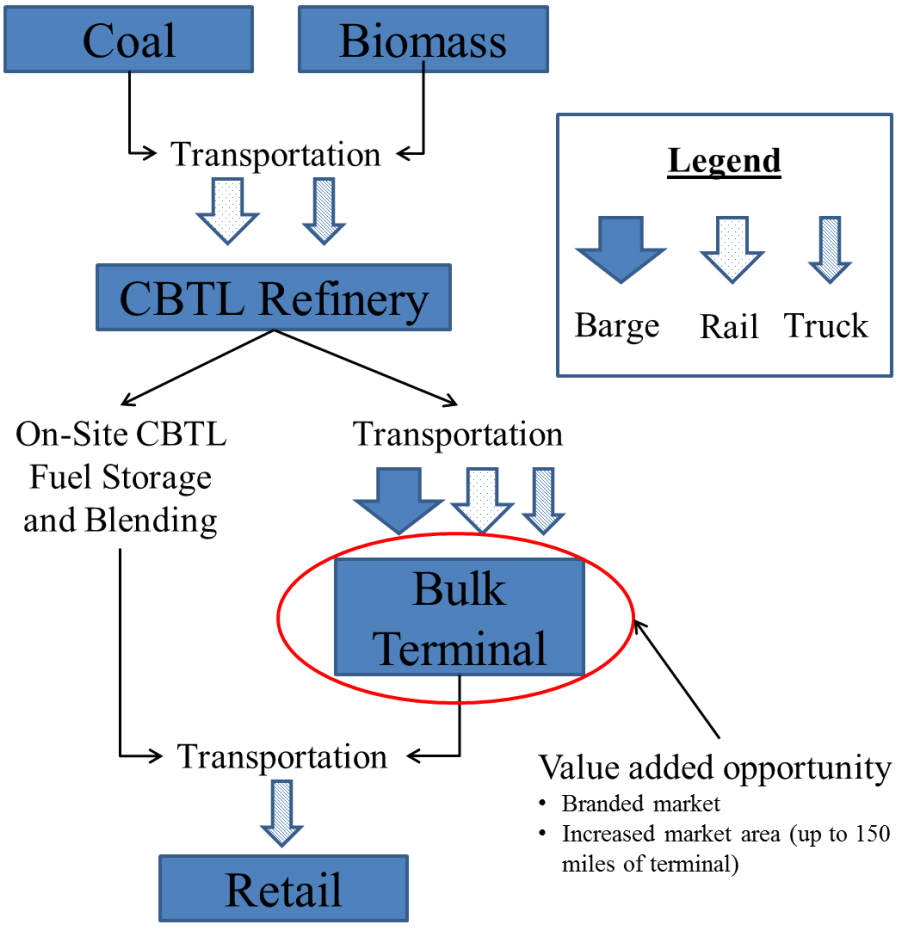

Figure 4-1. Market structure for CBTL fuel products.

Market demographics

The defined sales market encompasses the region within 150 miles of the proposed facility location. This distance is chosen due to the financial constrictions of economically transporting the finished products throughout the sales region. However, to adequately determine the current

demand of liquid fuel products such as gasoline and diesel, extended areas have been considered as the products could be transported further through secondary sales to serve extended markets.

Market needs

Using data from the Energy Information Administration (EIA) website (EIA 2013a, EIA 2013b), previous consumption volumes have been determined for the following states: West Virginia (WV), Pennsylvania (PA), North Carolina (NC), Ohio (OH), Maryland (MD), Kentucky (KY), Virginia (VA), Tennessee (TN), and Indiana (IN). Table 4-1 summarizes the general demand of this area by volume for gasoline and diesel. In instances where data was missing for a state for the indicated year, the most current volume reported was used

Table 4-1. Annual fuel sales in the WV, PA, NC, OH, MD, KY, VA, TN, and IN region.

	Gasoline (2012*)	Diesel (2011)
Annual sales (thousand gallons)	23,932,685	12,698,202

* rates for NC, MD, KY, TN, and IN were approximated based on previous sales due to missing data

To further understand the market needs of this area, the volume of crude oil supplied from this region was evaluated to indicate the amount of "locally sourced", petroleum-derived liquid fuels contributing to the overall supply that is needed. EIA information was used to determine the volume of crude oil supply in the region (Table 4-2) (EIA 2013c). Crude oil is refined and processed into gasoline and diesel, therefore, a conversion was applied to determine actual fuel volumes.

Table 4-2. Annual fuel supply in the WV, PA, NC, OH, MD, KY, VA, TN, and IN region (values derived from EIA crude oil conversion rates).

	Gasoline (2012)	Diesel (2012)	BioDiesel (2013 capacity)
Annual supply (thousand gallons)	326,114	188,833	350,000

According to EIA (2013d), approximately 19 gallons of gasoline and 11 gallons of diesel fuel can be derived from a 42 gallon barrel of crude oil. Additionally, biodiesel production capacities found in this region have also been added as a locally sourced fuel product (EIA 2013e). Yearly sales and supply of distillates (Figure 4-2) and gasoline (Figure 4-3) within the study region have shown constant inadequacies in the region's ability to produce enough gasoline and diesel, from local raw materials, to cover demand. The addition of the CBTL plant production will aid in supplying this region's demand from locally sourced raw materials.

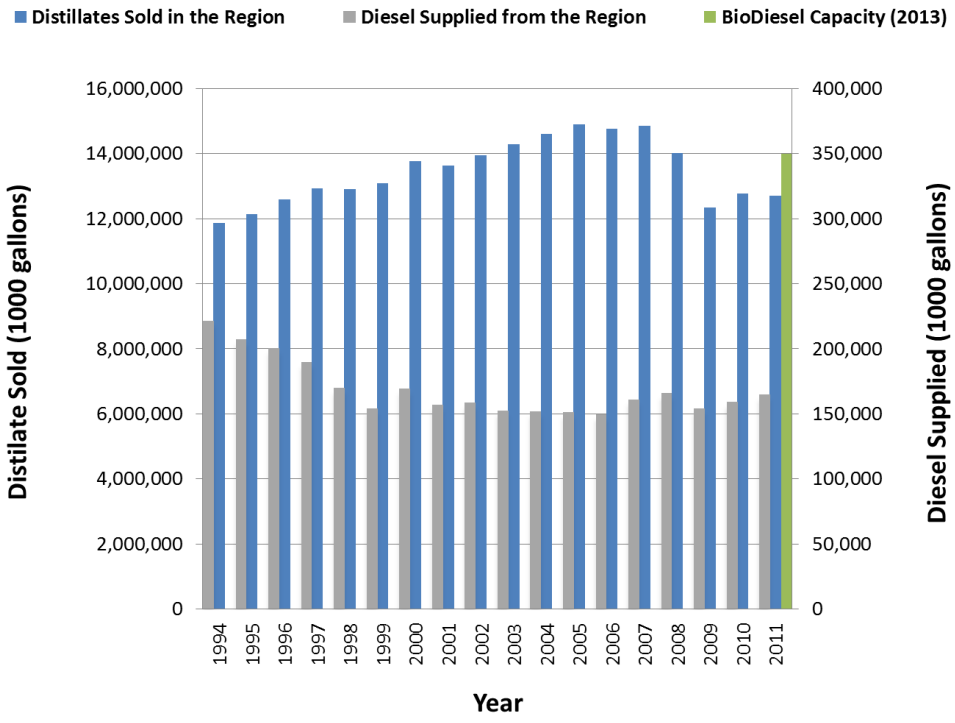

Figure 4-2. Total adjusted distillate sales and supply in the study region. Data obtained from Energy Information Administration (EIA).

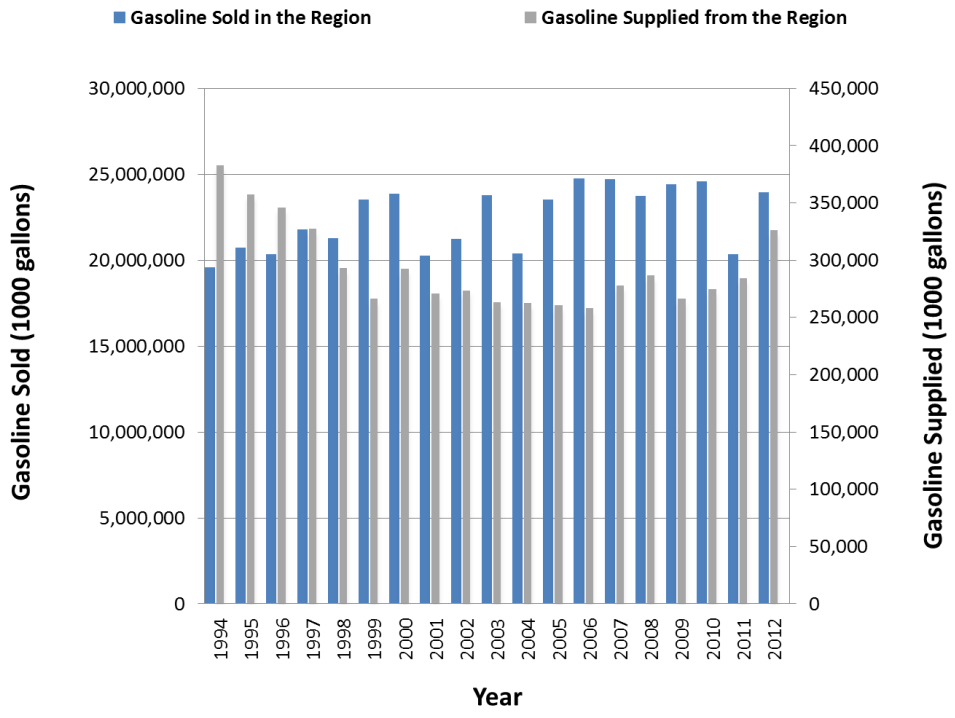

Figure 4-3. Total gasoline retail and wholesale sales and supply in the study region. Data obtained from Energy Information Administration (EIA).

Additionally, statewide liquid fuel usage for both gasoline and diesel were normalized on the county level by population percentage of that county with respect to total state population. It is assumed that population in an area correlates positively with fuel use. Fuel usage by county was summed within a 150 radius of the proposed CBTL facility. Demand on a per year basis in this region (167 counties) totaled 1.3 billion gallons (Figure 4) for diesel fuel and 2 billion gallons (Figure 4-5) for gasoline. To incorporate the expanded distribution of bulk fuel terminals, areas within 150 miles of the terminals, located within 150 miles of the CBTL location, were also summed to represent the broader range of populations that may indirectly receive products from the CBTL facility. Demand on a per year basis in this region (422 counties) totaled 6.2 billion gallons (Figure 4-6) for diesel fuel and 11.6 billion gallons (Figure 4-7) for gasoline.

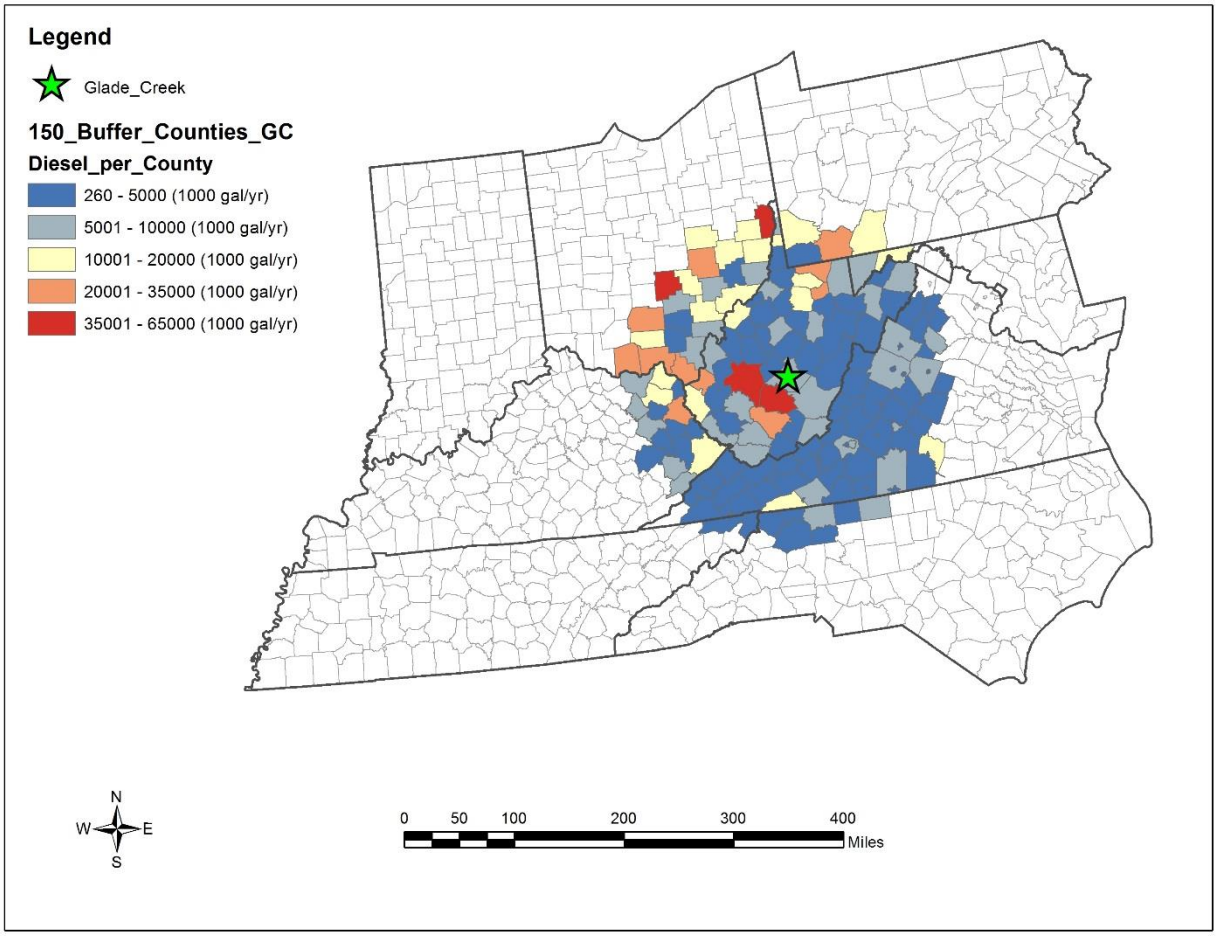

Figure 4-4. County level diesel demand (1,254,106,013 gal/yr) within 150 miles (167 counties) of CBTL location.

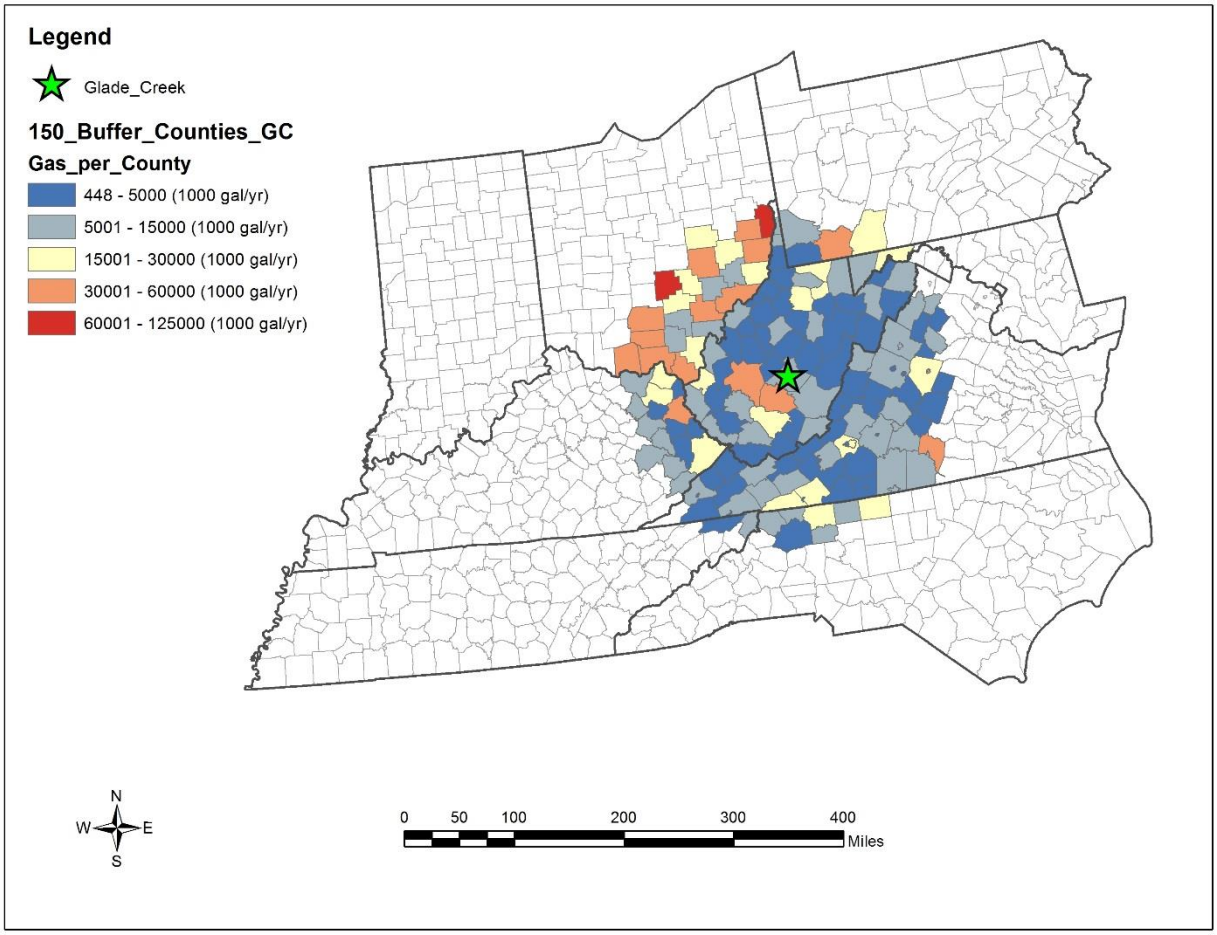

Figure 4-5. County level gasoline demand (1,969,669,811 gal/yr) within 150 miles (167 counties) of CBTL location.

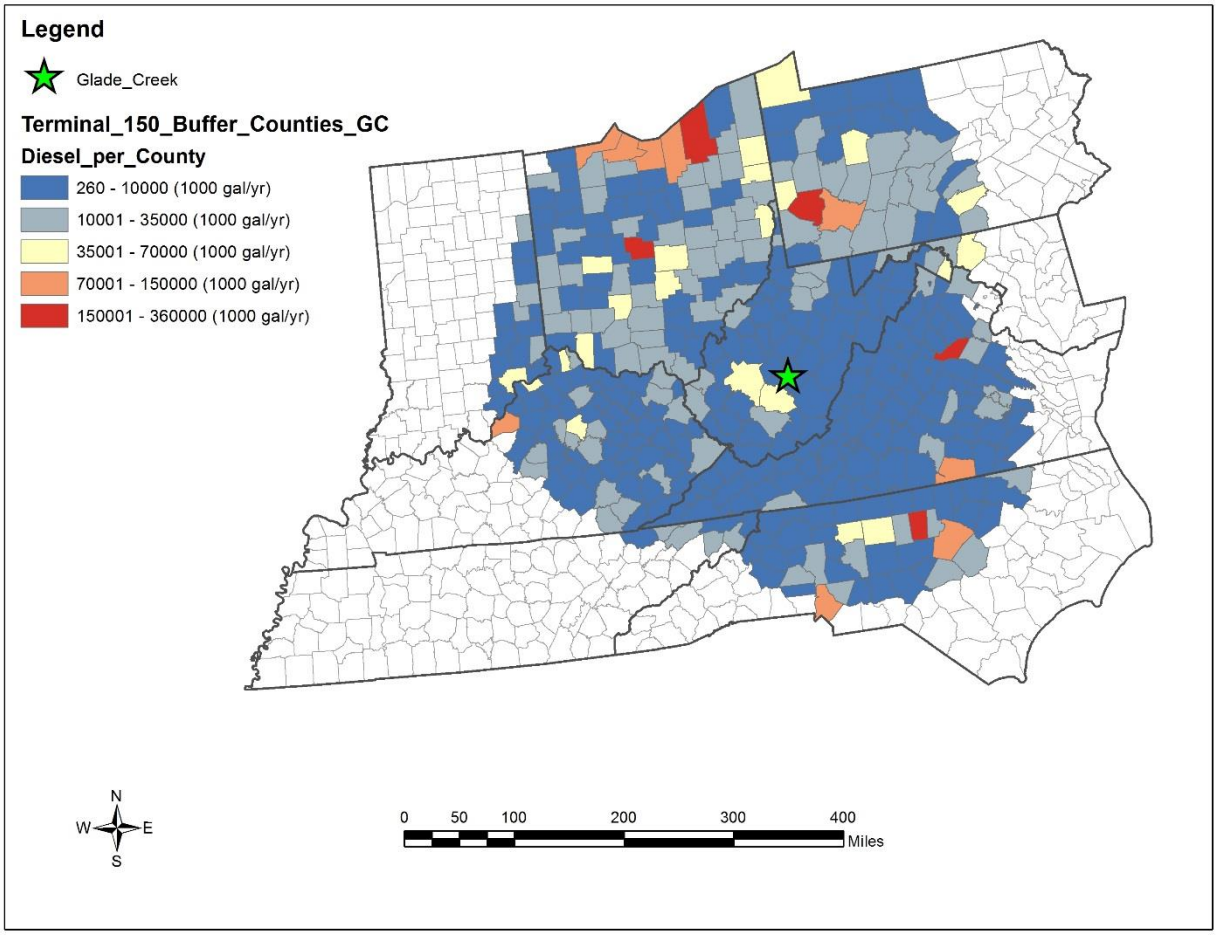

Figure 4-6. County level diesel demand (6,225,663,269 gal/yr) within 150 miles of bulk fuel terminals located within 150 miles of CBTL location (422 counties).

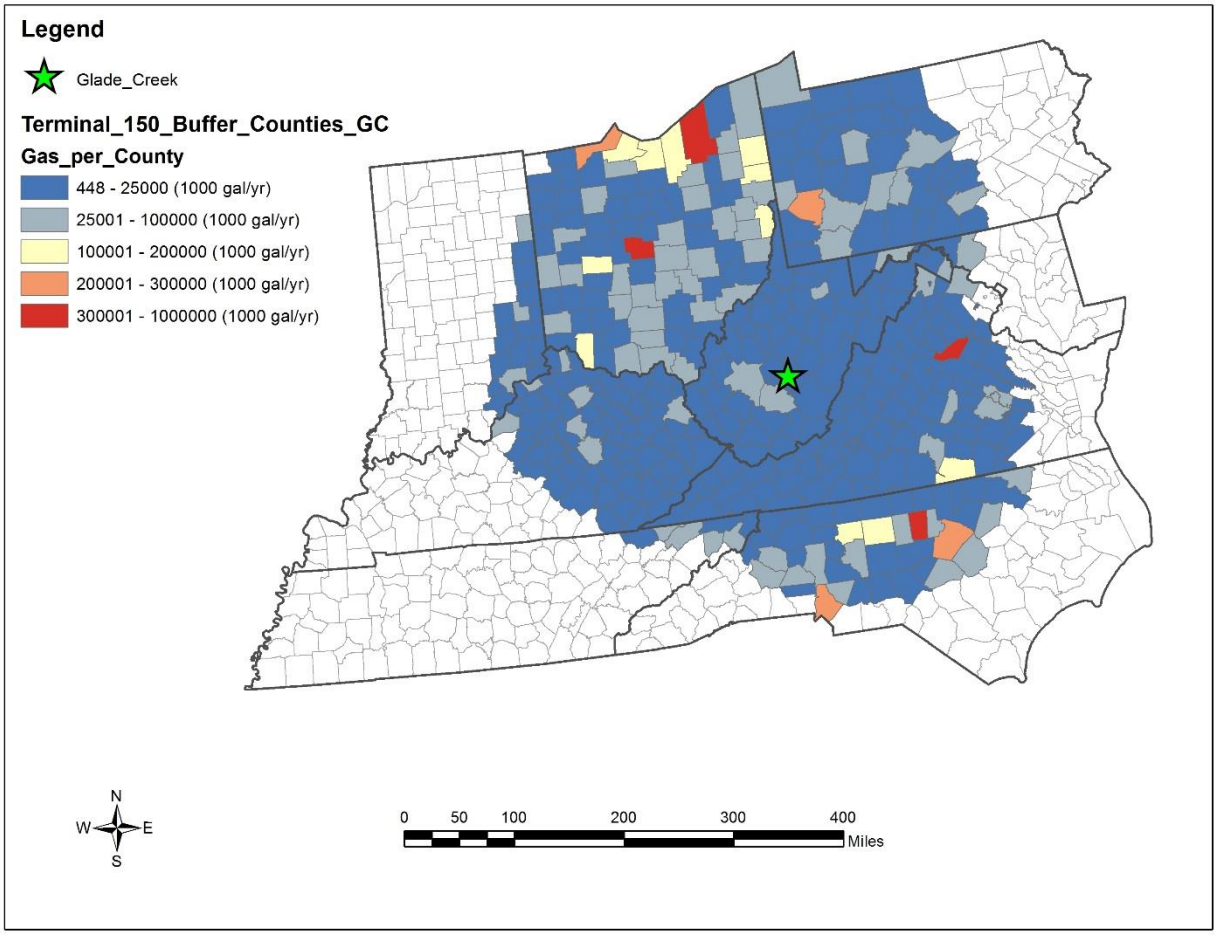

Figure 4-7. County level gasoline demand (11,575,973,366 gal/yr) within 150 miles of bulk fuel terminals located within 150 miles of CBTL location (422 counties).

Competition

Competitor's location: There are 17 Biodiesel facilities and 9 crude oil refineries located within the expanded sales region that may be direct competitors in the liquid fuels market (Table 4-3). Other liquid fuels producers have been located for reference as potential competition (Figure 4-5). Geographically, the proposed CBTL facility is in an area of little gasoline or diesel production. Marathon Petroleum, located in Catlettsburg, KY, is the only gasoline, diesel, or biodiesel production facility within 100 miles of the proposed CBTL location.

Table 4-3. Competition within 150 miles of terminals located within 150 miles of CBTL plant.

Type	Company	City	State
BioDiesel	Bluegrass BioDiesel	Falmouth	KY
BioDiesel	Center Alternative Energy Company	Cleveland	OH
BioDiesel	Chesapeake Green Fuels, LLC Adamstown	Adamstown	MD
BioDiesel	FELDA IFFCO, LLC	Cincinnati	OH
BioDiesel	Foothills Bio-Energies, LLC	Lenoir	NC
BioDiesel	Griffin Industries	Butler	KY
BioDiesel	Jatrodiesel Inc.	Miamisburg	OH
BioDiesel	Kristopher Kelley Ventures, LLC dba Kelley Green	Goshen	KY
BioDiesel	Lake Erie Biofuels dba HERO BX	Erie	PA
BioDiesel	Patriot Biodiesel, LLC	Greensboro	NC
BioDiesel	Piedmont Biofuels	Pittsboro	NC
BioDiesel	RECO Biodiesel, LLC	Richmond	VA
BioDiesel	Red Birch Energy, Inc.	Bassett	VA
BioDiesel	Shenandoah Agricultural Products	Clearbrook	VA
BioDiesel	Synergy Biofuels, LLC	Pennington Gap	VA
BioDiesel	United Oil Company	Pittsburgh	PA
BioDiesel	US Alternative Fuels Corp.	Johnstown	PA
Crude Oil	American Refining Group Inc	Bradford	PA
Crude Oil	BP-Husky Refining LLC	Toledo	OH
Crude Oil	Continental Refining Co. LLC	Somerset	KY
Crude Oil	Ergon West Virginia Inc.	Newell	WV
Crude Oil	Lima Refining Co.	Lima	OH
Crude Oil	Marathon Petroleum Co. LLC	Catlettsburg	KY
Crude Oil	Marathon Petroleum Co. LLC	Canton	OH
Crude Oil	Toledo Refining Co. LLC	Toledo	OH
Crude Oil	United Refining Co.	Warren	PA

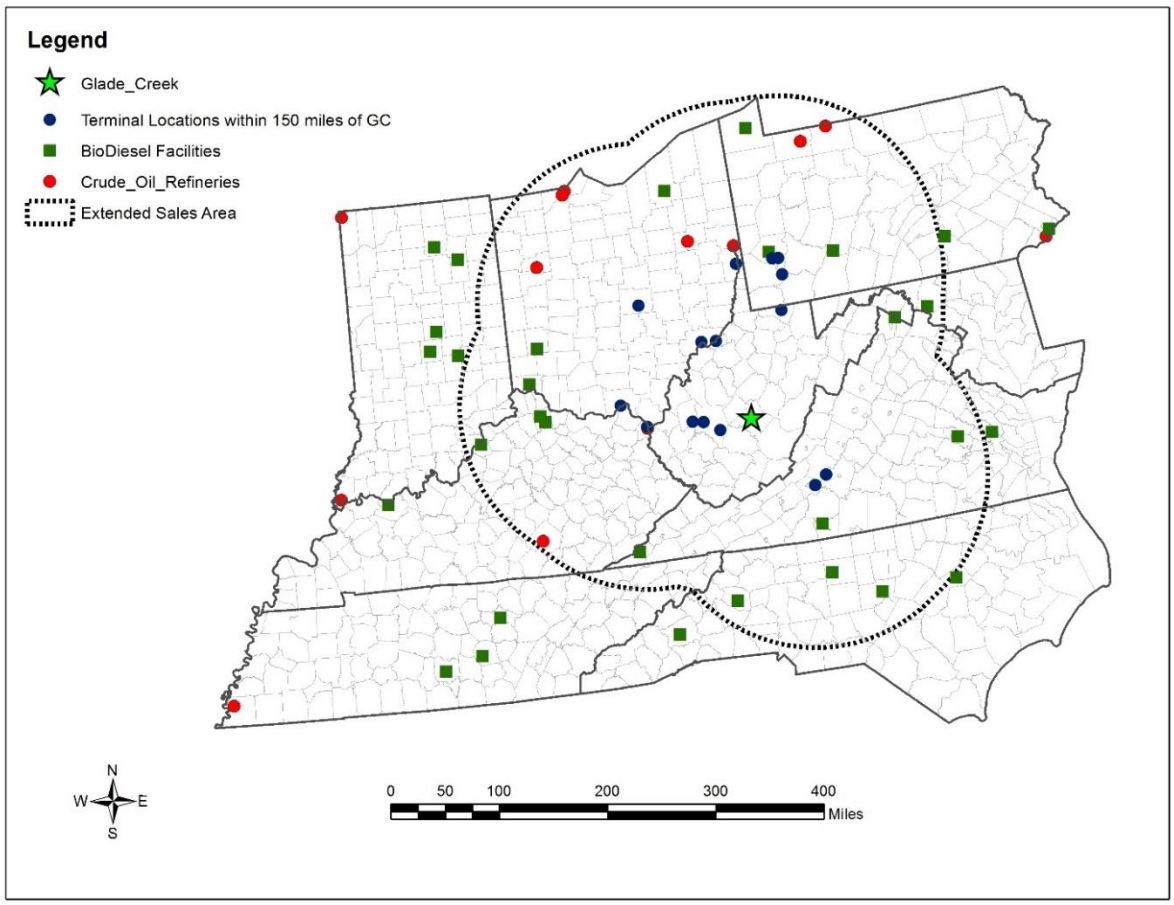

Figure 4-8. Competition, bulk fuel terminals, and extended sales region for CBTL study area.

Competitor Products and Prices

Competitors in the study area have the ability to produce similar liquid fuel products. Given that liquid fuel products such as gasoline and distillates are commodity items and are price-regulated by the government, values found through the EIA (2013f, 2013g, 2013h, 2013i, 2013j, 2013k, 2013l, 2013m, 2013n, 2013o, 2013p, 2013q) are used to indicate the price of these commodities. Although each individual facility will have different productions costs, Table 4 shows wholesale and retail prices obtained by U.S. refineries.

Table 4-4. June 2013 U.S. retail and wholesale prices for gasoline and distillates by refineries.

Regular Gasoline		Midgrade Gasoline		Premium Gasoline		Distillate*	
Retail	Wholesale	Retail	Wholesale	Retail	Wholesale	Retail	Wholesale
$3.105	$2.909	$3.307	$2.948	$3.407	$3.218	$3.18	$3.024

* Distillate prices were derived from averaging U.S. No1, 2, and 4 distillate values.

Market Share Estimates

A sales market was determined based on a maximum economically feasible transportation distance of 150 miles. By selling liquid fuel products to bulk storage terminals for further sales/distribution, the entire area where the CBTL products may be sold, either directly or indirectly, was used to determine the current liquid fuels market. Since county level data for fuel sales was not available, state level data was distributed to the county level based on population percentage of that county in its state. It is assumed that fuel sales will positively correlate with population.

At a production rate of 10,000 barrels of crude-oil-equivalent per day, the impact of CBTL derived fuel products will be minimal in regards to the current supply in this region. Assuming similar conversion rates as oil derived fuel products, 45% of the 10,000 barrel/day production will be processed to gasoline and 26% to diesel. Given the current demand rates shown in Figure 3 through Figure 4-6 above, a CBTL facility producing 10,000 barrels/day at 365 days/year can supply the immediate 150 mile market with 3.5% and 3.2% of its gasoline and diesel needs, respectively. Moreover, as this market is expanded to contain the distribution and sales areas of the bulk fuel terminals within 150 miles of the CBTL facility, the supply capabilities of the CBTL facility are 0.6% and 0.6% of the total demand for gasoline and diesel, respectively.

Industry Attractiveness (Porters 5 forces)

Threat of Entry

Entry in to this industry is relatively high. Tto compete in a commodity market, production cost is one of the key factors that can give competitive advantage over other producers. Therefore, the need to enter this market on a large scale in order to produce liquid fuels at a competitive price is necessary. An additional obstacle to entering this market will be overcoming the brand loyalty held by potential clients. Although a 10,000 barrel/day CBTL facility may only be capable of meeting a small amount of the current demand, brand loyalty to long term providers of gasoline and diesel fuels may inhibit even a small amount of "new entrants" products to be accepted. Fear of strained business relationships with long-time suppliers may result in rejection of new entrant's products for some potential CBTL facility clients.

Inter-Firm Rivalry

Inter-firm rivalry exists within the liquid fuel products industry. Direct competition exists between firms as a result to supply the same customers with the demanded commodity. This high inter-firm rivalry also requires firms to maintain production at full capacity to lower product costs and compete. Consequently, major shifts toward higher production of gasoline and diesel fuels will necessitate high capital investments. Additionally, these large investments coupled with the specialized equipment needed to convert biomass and coal to liquid fuel products such as gasoline and diesel could result in high exit barriers for the facility.

Pressure from substitutes

Pressures from substitute fuel sources are increasing not only in the liquid fuels market but also in the energy sector where liquid fuel products are being used. Potential substitute materials such as Coal to Liquid (CTL) fuels and Coal Biomass Gas to Liquid (CBGTL) fuels are being considered, while ethanol and biodiesel are currently competing for gasoline and diesel markets. Additionally,

energy producers using gasoline or diesel as a raw material feedstock may potentially use natural gas, solar, wind, etc. for energy production. An advantage CBTL fuels hold over oil derived fuels is a lower environmental impact in the form of reduced combustion emissions. However, other technologies such as the Coal Biomass Gas to Liquid (CBGTL) process may have the potential to further reduce environmental impacts as well - all while utilizing a locally sourced natural gas.

Bargaining power of customers

Customer bargaining power could exist in the marketplace of the CBTL facility in that there only a few large buyers (bulk fuel terminals) within 150 miles of the plant. These few clients would have more bargaining power over the CBTL products than if the supply was spread to a larger number of smaller clients. Additionally the bargaining power of customers would be high if the marketing structure of the CBTL facility was to sell large quantities to only a couple of bulk fuel terminals. Buyers in a commodity market such as gasoline and diesel will have very low switching costs between suppliers (assuming unbranded products) and likely purchase the lowest priced product.

Bargaining power of suppliers

The bargaining power of the CBTL facility may exist as a result of plant location, changes in environmental regulations, and/or state regulations. The location of the plant will influence transportation costs that could be a bargaining benefit. Additionally, stricter environmental laws could render current processing techniques of oil deriving refineries inadequate and give a process such as CBTL competitive advantage. Lastly, state regulations benefiting the use of locally sourced gasoline and diesel may increase the bargaining power of the CBTL facility.

Buyer Analysis and Information on Potential Customers

Background and Survey Methods

An email survey was conducted to acquire information from potential buyers of products produced at the proposed Coal Biomass to Liquids (CBTL) facility. These potential buyers were selected due to their geographic proximity to the proposed CBTL location, specifically, based on economically feasible transportation distances. All bulk fuel terminals found in the Internal Revenue Service (IRS) database and located within 150 miles (Euclidean distance) of the CBTL facility were selected as potential respondents to the survey.

The survey was designed to include both closed and semi-closed questions as well as ranking questions. Designing the survey in this manner allowed for direct comparison between groups of survey respondents and provided numerical and categorical data that could be further analyzed to identify trends. The survey was reviewed by industry experts for subject clarity and industry validity prior to distribution. Additionally, this survey was reviewed and approved for distribution by the WVU IRB prior to disbursement.

The target population consisted of all currently operating IRS registered bulk fuel terminals within 150 miles of Glade Creek, WV. Based on these criteria, we identified a total of 23 facilities as potential survey respondents. Each of the 23 facilities was directly contacted in an attempt to obtain the name and email address of the plant manager, regional manager, or owner for direct survey distribution. In 17 instances, direct contact was made with the potential survey respondent. In six

instances, the email address for the potential respondent was given by an employee. However, in six other instances, we were unable to establish contact with the potential respondent. One potential respondent was contacted directly, but declined to participate for either of the two facilities under his management. Additionally, there were two instances where one person was responsible for the management of multiple bulk fuel terminal facilities. These potential survey respondents were instructed to fill out one survey for each of the facilities in which they were responsible. Contact information for individuals (potential survey respondents) responsible for the management of bulk fuel facility(s) was compiled.

An initial contact email was sent to the potential survey respondents introducing the study, the researchers, and the announcement of future emails. Three days later, a second contact email was sent that contained a link to the online survey and directions for completing the survey. Additionally, individuals who were responsible for multiple facilities were supplied a list of physical addresses for each facility and were asked to fill out a new survey for each of the locations provided. After two weeks, a reminder email was sent to the potential survey respondents, thanking those individuals that had completed the survey and to encourage the participation of those who had not yet completed the survey. After two more weeks, a thank you email was sent to all potential respondents and the survey was closed.

The survey response was determined using Equation 4-1. Of the 23 potential survey respondents (i.e., facilities), two potential respondent facilities declined (i.e., refusals) to participate in the survey. In six cases, we were unable to obtain contact information of the potential survey respondent. Five total surveys were completed for a response rate of 33%. During the first two weeks of the survey being open, four surveys were completed, while the final survey was completed after the two week reminder email.

$$rs = \frac{cs}{cu - iu - r} \qquad \text{Equation 4-1}$$

Where:

rs = response rate

cs = number of completed surveys

cu = contacted units

iu = ineligible units

r = refusals

Results and Discussion

Gasoline Storage

Sixty percent of survey respondents reported gasoline storage at their facility. On average, the gasoline storage capacity was reported to be 4.8 million gallons. All survey respondents reported diesel storage at their facility. On average, the diesel storage capacity was reported to be 1.5 million gallons. All respondents indicated zero storage capacity for methanol.

Product Diversification

In terms of gasoline, 60% of the respondents indicated that they received suboctane unleaded 85 gasoline at their facility (Table 4-1). Furthermore, 40% of the respondents indicated that they received unleaded 91 gasoline and 20% received unleaded 93 gasoline. A total of 60% of the respondents indicated that they received ethanol. All (100%) of the respondents that reported receiving suboctane gasoline, also received ethanol at their facility. These facilities may be incorporating the use of ethanol to increase the octane of the unleaded 85 gasoline to meet market demands of commonly purchased 87, 89, and or 91 octane gasoline. Interestingly, all the respondents receiving suboctane 85 gasoline mix liquid fuels with additives in order to produce branded gasoline products.

In terms of diesel fuel, all respondents (100%) indicated receiving ultra-low sulfur diesel. Additionally, mixing of diesel fuel with lubrication additives was being performed at all of the respondent's facilities (Table 4-2). In terms of other additives for non-lubricating purposes, 60% of respondents indicated mixing of red dye for off-road diesel production.

Table 4-5. Typically received fuel products

Product Type	Percentage of respondents that received product
Suboctane Unleaded 85	60%
Unleaded 87	0%
Unleaded 89	0%
Unleaded 91	40%
Unleaded 93	20%
Ultra-Low Sulfur Diesel	100%
K-1 Kerosene	0%
Methanol	0%
Ethanol	60%

Table 4-6. Additives typically mixed at the facility

Product Type	Percentage of respondents that mixed the additive
No mixing occurs at this facility	0%
Ethanol	60%
Methanol	0%
Red dye (for off-road diesel)	60%
Lubricity additive (for diesel fuels)	100%
Branded additives (for branded gasoline)	60%

Overall findings from respondents suggest wide geographic market spread for ultra-low sulfur diesel and a better dispersed market for sub octane unleaded 85 gasoline. These findings may indicate potential product diversification needs in this region. Potentially, the product types and volumes reported by the survey respondents could indicate the market environment for the CBTL sales area. Diesel sales may be common at the majority of bulk fuel terminals and therefore increase the number of potential clients. An increase in potential clients could make penetrating this market easier. Conversely, a lower number of potential clients for gasoline (as compared to diesel) could make penetrating that market slightly more difficult. Volumes of gasoline and diesel reported by the respondents indicate that capacities are 3:1 in favor of gasoline. This ratio may indicate to the CBTL facility, the optimal production mixture of gasoline and diesel, given sales are comparable to potential client capacities.

Sales Area

Sales areas for the respondents ranged from up to 100 miles to up to 150 miles. Sixty percent of the respondents indicated the typical sales area of their facility was up to 100 miles while the remaining 40% of respondents indicated the typical sales area of their facility was up to 150 miles. These findings were similar to primary discussions held with liquid fuel transportation contractors in this industry and indicate the validity of our 150 mile sales radius assumed for the CBTL plant as well as the bulk fuel terminals located within the CBTL sales region.

Transportation System

Respondents report 3 different transportation methods they received fuels: pipeline, barge, and by truck. Sixty percent of respondents were able to receive liquid fuel products by pipeline, 40% by barge, and 60% by truck (some facilities were capable of receiving liquid fuels by multiple transportation types) (Table 4-3). Additionally, in order to determine the number of suppliers currently supplying the bulk fuel terminals in this region, respondents were asked to indicate the number of companies currently supplying their gasoline, diesel, and or methanol. Eighty percent of respondents received at least one fuel type from multiple sources. Twenty percent of respondents used only one company to provide its gasoline products and one company to provide its diesel products. This same 20% indicated the distribution of branded fuel products. This particular type of facility could be an indication that some of the bulk fuel terminals originally anticipated as being a potential sales market may be an affiliate of a liquid fuel producing company and therefore only accept products from the affiliate source. This could consequently reduce the initial market size/area presumed for the CBTL plant.

Table 4-7. Product transportation types received at terminals

Transportation Type	Percentage of Respondents receiving transportation type
Pipeline	60%
Waterway (Barge)	40%
Rail	0%
Road (Truck)	60%

Interest in CBTL Derived Fuels

Lastly, respondents were asked to indicate their interest in purchasing CBTL derived liquid fuel products, at various price points, based on three different factors: 1) raw material feedstock (coal and biomass instead of oil); 2) environmental impact of liquid fuel production (coal and biomass raw materials instead of oil); and 3) locally (WV) sourced raw materials for liquid fuel production. Responses were recorded on a Likert scale and assigned a numerical value for statistical analysis. For example, the survey answers included: No interest (-1 value), neutral interest (0 value), little interest (1 value), some interest (2 value), and high interest (3 value). Additionally, multiple price points were also proposed with each of the three questions: 1) costs of coal and biomass sourced liquid fuels are lower (than oil derived fuels), 2) costs equal, 3) cost is up to 2% higher, 4) costs is 2.1% - 4% higher, 5) cost is 4.1% - 6% higher, and 6) cost is greater than 6% higher. It is important to note that respondents were asked to assume that the quality of CBTL liquid fuel products would meet or exceed that of oil derived fuels products.

Respondents indicated identical interest trends in all three different factor scenarios (Table 4). In all instances, respondents indicated an interest (mean > 0) for CBTL derived liquid fuel products at prices lower than those of oil derived liquid fuels. Neutral (neither positive nor negative) interest (mean = 0) was shown at price levels equal to and up to 4% higher than oil derived fuel products. Disinterest was found at price levels higher than 4% (mean = -0.25) of oil derived fuels. These results indicate interest in bulk fuel terminal facilities for CBTL liquid fuel products to replace a portion of the oil derived liquid fuels market, given the CBTL products are lower in price. Additionally, there may be tolerance for products produced by the CBTL process, at price levels between "equal to" and "4% higher" the oil derived product prices; to compete against oil derived liquid fuel products as neutral interest was reported. However, at prices greater than 4% of oil derived products, a negative interest to purchase CBTL derived fuels was indicated. These results indicate interest for CBTL derived fuels based on the three previously mentioned factors. There is also an indication that, unlike many commodity markets, there may be the opportunity to sell CBTL fuels for a premium price (up to 4% higher than oil derived fuels).

Table 4-8. Interest levels of respondents for 3 different product factors at various pricing levels

Compared to oil derived fuels, the cost would be	Preferential factors based on differences between CBTL derived liquid fuel products and oil derived liquid fuel products		
	feedstock type	environmental impact	locally sourced feedstock
lower	0.5	0.5	0.5
equal	0	0	0
up to 2% higher	0	0	0
2.1%-4%	0	0	0
4.1% - 6% higher	-0.25	-0.25	-0.25
> than 6% higher	-0.25	-0.25	-0.25
*0 indicates neither interested or disinterested, >0 indicates interest, < indicates disinterest			

Interestingly, responses for individual respondents were identical for each of the three different factors: 1) raw material feedstock (coal and biomass instead of oil); 2) environmental impact of liquid fuel production (coal and biomass raw materials instead of oil); and 3) locally (WV) sourced raw materials for liquid fuel production. These results could be the indication of indifferent respondent perception between the three factors, i.e. each of the three factors was of equal importance. From a marketing perspective, this result may indicate that additional perceptions and interests of the market may need to be identified in order to reveal factors of interest. Identifying particular factors of interest that complement the CBTL derived fuel products may allow competitive advantage over oil derived fuel products.

Organization performance - Market Share Predictions

EIA projections indicate a stable market share (23%) for crude oil production in the coming decades (EIA 2013r). However, there are slight increases (5%) indicated in the production of tight oil as well as natural gas liquids (3%). One major shift that is expected is the decrease in petroleum and biofuel imports (8%). The decreased consumption of imported fuels will strengthen the

domestic supply market. An increased demand for domestically produced fuels coupled with the reduced environmental impacts of the CBTL process should favor the increased incorporation of CBTL products for future growth. However, EIA projections also indicate a stable increase in liquid fuel consumption in the U.S. until about year 2020, reflecting the anticipated results of a 4.1% average annual increase in fuel economy standards for newly produced light duty vehicles between the years 2017 and 2025 (EIA 2013r).

SWOT

Internal strengths

An important strength the CBTL facility has is the opportunity of locally sourced raw materials: biomass and coal. The ability to have fuel feedstock in local proximity of the plant may give an advantage in lowering transportation costs as well as no dependence on foreign sourced supplies. Additionally, the CBTL process utilizes direct and indirect (and hybrid) liquefaction, lowering the environmental impact of the production of liquid fuels such as diesel and gasoline. Core competencies such as utilization of a renewable feedstock material, carbon capture during the production process, and a tri-reforming process may all be advantages over crude-oil based gasoline and diesel products

Weaknesses

A weakness the CBTL facility has is the implementation of a new technology. Although converting coal and biomass to liquid fuels is a feasible production method, the learning curve of a start-up facility will likely result in lower-than-normal production volumes. Additionally, the completion in the liquid fuels industry is well established not only in production processes but also in business relationships within the final product supply chain.

External Opportunities

External opportunities exist for the CBTL plant in a variety of forms. Continued population growth in the CBTL sales region will likely increase demand for gasoline and diesel. In addition to demographic changes, social preferences are likely to evolve to less environmentally impactful product choices. Offering a less environmentally impactful alternative while maintaining price and quality could be an opportunity for CBTL products. Also, government influences in the form of tax breaks, subsidies, or mandatory purchasing could benefit the CBTL facility. As products produced in the facility are locally sourced and environmentally less impactful, and the facility creates local jobs – local governments may initiate laws that directly or indirectly present opportunities for the CBTL plant.

Threats to Company

Threats in new as well as established fuel production technologies do exist for the CBTL facility. Existing technologies in oil-derived fuel production are well established with large capital investments that are continually evolving. Advancements in this industry are likely if pressured by government policy or significant outside competition. Additionally, other forms of alternative liquid fuel production as well as alternative fuel consuming products are gaining interest. CTL Fuel technology and CBGTL Fuel technology are two prominent production techniques that may compete directly with CBTL and oil-derived produced liquid fuels. Specifically, CTL and CBGTL techniques may compete directly with CBTL techniques on environmental impacts as well as

through the use of locally sourced feedstock. With recent developments in natural gas recovery techniques, the availability of natural gas has increased significantly. The large supply of this local fuel source may increase in use as an alternative for gasoline or diesel

PESTE

Political

Political influence can have a direct impact on the success of the CBTL facility. The renewable fuels standard in the U.S. has increased the use of renewable fuels in transportation fuels through incremental production requirements in each of the four renewable fuel categories: conventional biofuel, biomass-based diesel, cellulosic biofuel, and other advanced biofuel. The fuel products currently projected for production by the CBTL facility do not meet any of these four renewable fuels categories (EIA 2014). However, in the study region, the following state laws and incentives are present and could influence the adoption of a CBTL fuel product in that state.

Ohio – Alternative Fuel And Fueling Infrastructure Incentives – "*The Alternative Fuel Transportation Grant Program (Program) provides grants and loans for up to 80% of the cost of purchasing and installing fueling facilities offering E85, fuel blends containing at least 20% biodiesel (B20), natural gas; liquefied petroleum gas or propane; hydrogen; electricity; or any fuel that the U.S. Department of Energy determines, by final rule, to be substantially not petroleum. The Program also provides funding for up to 80% of the incremental cost of purchasing and using alternative fuel for businesses, nonprofit organizations, public school systems, and local governments.*" http://www.afdc.energy.gov/laws/6024

Alternative Fuel Signage – "*The Ohio Turnpike Commission allows businesses to place their logos on directional signs within the right-of-way of state turnpikes. An alternative fuel retailer may include a marking or symbol within their logo indicating that it sells one or more types of alternative fuel. Alternative fuels are defined as E85, fuel blends containing at least 20% biodiesel (B20), natural gas, propane, hydrogen, or any fuel that the U.S. Department of Energy determines, by final rule, to be substantially not petroleum."*

http://www.afdc.energy.gov/laws/8980

Kentucky - Clean Transportation Fuels for School Buses – "*The Kentucky Department of Education (Department) must consider the use of clean transportation fuels in school buses as part of its regular procedure for establishing and updating school bus standards and specifications. If the Department determines that school buses may operate using clean transportation fuels while maintaining the same or a higher degree of safety as fuels currently allowed, it must update the standards and specifications to allow for such use.*"

http://www.afdc.energy.gov/laws/law/KY/10743

Vehicle Acquisition Priorities and Alternative Fuel Use Requirements – "*The Kentucky Finance and Administration Cabinet (Cabinet) must develop a strategy to replace at least 50% of commonwealth motor fleet light-duty vehicles with energy-efficient vehicles including hybrid electric, advanced lean burn, fuel cell, and alternative fuel vehicles. The Cabinet must also develop a strategy to increase the use of ethanol (including cellulosic ethanol), biodiesel, and other alternative fuels in commonwealth motor vehicle fleets. The Cabinet must report targeted vehicle and fuel usage amounts annually*." http://www.afdc.energy.gov/laws/law/KY/6297

West Virginia - Alternative Fuel Production Subsidy Prohibition – "*Incentives or subsidies from political subdivisions for the production of alternative fuels are prohibited by law, with exceptions for certain coal-based liquid fuels*." http://www.afdc.energy.gov/laws/law/WV/4823

Tennessee - Supply of Petroleum Products for Blending with Biofuels – "*Petroleum product refiners and suppliers must make all grades of gasoline and diesel fuel available to any wholesaler in a condition that allows for the fuel to be blended with ethanol or other biobased products and sold in Tennessee. In addition, gasoline products must be available with detergent additives in sufficient concentrations such that after the addition of ethanol, the final product meets or exceeds the lowest additive concentrations that the U.S. Environmental Protection Agency requires.*" http://www.afdc.energy.gov/laws/law/TN/6574

North Carolina - Ethanol Blend Requirement – "*Suppliers that import gasoline for sale in North Carolina must offer fuel that is not pre-blended with fuel alcohol but that is suitable for future blending. Future contract provisions that restrict distributors or retailers from blending gasoline with fuel alcohol are void."* http://www.afdc.energy.gov/laws/law/NC/6477

Economic

Sources of Funding and investment: See results from Task 5 – Financial Feasibility of CBTL Plant Feasibility Study for more information

Market growth

The U.S. is recovering from economic disruptions and will likely continue the economic recovery, resulting in a lower unemployment rate and possibly a higher amount of disposable income. These factors, coupled with the predicted increase in population for states surrounding WV (Table 4-9), could increase demand for liquid fuels in the study region (WPS 2014). Additionally, increased competition for the feedstock sources coal and woody biomass, could increase raw material prices. Currently, when petroleum prices increase, the price of gasoline and diesel also increase to compensate for the rise in production cost. However, the CBTL derived products may not follow petroleum trends and could be beneficial or damaging to the profitability of the plant, depending on the situation.

Table 4-9. Population change by year 2020 for states within the study region.

WV	OH	PA	VA	NC	IN	MD	KY	TN
2.3%	0.2%	(0.93%)	7.6%	9%	4.8%	5.8%	N/A*	6.3%

* - data unavailable for Kentucky

Social

The proposed CBTL plant also has large social benefits in the way of job creation. According to a recent study (NETL 2009) domestic job creation of CTL/CBTL plants are estimated at 150,000 jobs per million bbls of production per day. For the proposed CBLT plant in Glade Creek, WV (10,000 bbls/day) – these estimates would equate to approximately 150 jobs being created. Given the continued loss of coal industry-related jobs in this region (USA 2014), skilled workers are likely available.

In addition to job creation, an additional social benefit for the CBTL plant would be the reduced greenhouse gas emissions as compared to petroleum derived fuels. For example, petroleum-derived diesel emits 98.8 kg CO_2 equivalent (Keesom and Unasch 2009) whereas the CBLT derived diesel fuel is projected at 87.17 kg CO_2 equivalent (see Task 1 – Environmental Impact Analysis of CBTL Plant Feasibility Study for more information).

Technological

Technological developments for alternative fuel sources could have implications for the CBTL plant. Increased explorations and new recovery methods in the natural gas industry have resulted in large supply bases for consumer withdraw. The popularity of natural gas has drawn the attention of many producers and consequently driven down price with abundant supply.

Other alternative fuel production methods are also being researched. One CTL plant has been proposed in the southern WV area. Although this plant's construction has been delayed, the technological feasibility exists and could directly compete with the CBTL facility not only in market share but also in raw material resources. Another novel approach to liquid fuel production is the CBGTL process. This is a relatively new technology that mimics the raw material feed stocks of the CBTL process but with the additional natural gas. It is undetermined, however, the difference in environmental impact between the CBGTL process and the CBTL process proposed at this facility.

Environmental

The varieties of seasons experienced by the sales region for the proposed CBTL plant require liquid fuel products to accommodate the changes in temperature. Therefore, "summer" and "winter" blends for gasoline products are needed to insure the stability of the fuel in the different climates. Gasoline mixtures will need to have lower volatility in the summer months to reduce evaporative emissions (EIA, 2013s).

Marketing Strategies

Products/services

Liquid fuel products including gasoline and diesel will be produced by a CBTL process utilizing coal and woody biomass as raw material feed stocks. By implementing liquefaction techniques as well as a tri-reforming process, fuels produced will have a lower environmental impact than

comparable petroleum-derived products. These fuel products will achieve or surpass regulated, liquid fuel quality standards (Summer Gasoline = Reid Vapor Pressure (RVP) for that area (9 for WV)) Winter Gasoline (oxygenated) - Diesel = 15ppm sulfur specifications (ultra-Low Sulfur) (EIA 2013t).

Promotion

Promotional activities will begin by building strong relationships with the bulk fuel terminals located within the 150 radius of the CBTL plant. Assurance in high and consistent product quality, reliable supply capabilities, and long-term, value-chain partnerships will be addressed. Continuing efforts to promote the lower environmental impacts of the CBTL-derived products along with utilizing locally sourced raw materials must be maintained, especially toward local and state governing boards. Initializing markets for more environmentally conscious fuel products through law and regulation could have an incredible impact in the use of CBTL products.

Distribution

The CBTL products will be supplied to bulk fuel terminals with in a 150 mile radius of the CBTL plant location for further sales and distribution. Competing liquid fuel suppliers follow the same regulated quality standards. Most competitors distribute directly to bulk fuel terminals for further distribution and sales. However, some larger competitors have taken the distribution of their products further in two methods: 1) ownership of bulk fuel terminals, and 2) direct sale to fueling stations. Each method provides additional capture of revenue and therefore increased profits. However, the volume of fuels produced by these competitors as well as the inclusion of branded products can help to justify the large capital investment of fuel terminals as the increased risk of distributing directly to fueling stations. These strategies may be an option for the CBTL facility on a smaller scale and should be considered in future planning.

Task 4.2 Evaluate risks related to the marketing of CBTL fuels

Risk analysis was performed to determine the probability that each technology would break-even given the historical prices of oil and the estimated break-even price for each base case and sensitivity evaluated technology in this project. Additionally, for the base case analysis, the influence on risk was evaluated when including the consumer's willingness to pay an extra percent for fuel from these processes and for a potential carbon offset market.

To evaluate the risk of each technology, Oracle Crystal Ball software was used to determine the probability that each technology would, at a minimum, break-even under various what-if scenarios. The first scenario evaluated break-even probabilities when by varying the unknown variable of oil prices. The second scenario evaluated break-even probabilities when by varying the unknown variable of oil prices and adding in a consumer willingness to pay 4% more for this type of product (based on Task 4.1 results). The third scenario evaluated break-even probabilities when by varying the unknown variable of oil prices and adding in a potential carbon offset credit market. The fourth scenario evaluated break-even probabilities when by combing all these factors, specifically by varying the unknown variable of oil prices and adding in both consumer willingness and a potential carbon offset market.

Using historical oil price data and Monte Carlo Simulation, random oil prices (based on historical prices and a fitted distribution) were included in the model to forecast break-even probabilities under each scenario. The value evaluated was the estimated break-even price for a technology minus the varied oil price. Break-even technology prices were used that included a 4% improvement for consumer willingness and a variable carbon credit market price (based on the scenario evaluated). Given this, whenever the estimated value was zero or less, the technology broke-even or made a profit. Returned values over zero indicated that the technology did not break even and resulted in a loss. The simulation was run for 10,000 trials and the probability from – infinity to zero was determined (i.e., probability that a technology at a minimum broke-even given the unknown/variable oil market). Oil was used as a basis, since data was not readily available on gasoline and diesel without additives, refinement, and tax costs included.

Monthly historic oil prices (in today's dollar) from January, 2006 to June, 2016 were the basis of the simulated current oil prices. The oil price data was fitted using Oracle Crystal Ball as a Minimum Extreme type distribution. This distribution was applied to the varied oil price value. The break-even prices and CO_2 emissions for each technology were obtained from the results presented under Task 3. The offset CO_2 emissions for each base case technology was determined as the CO_2 emissions reduced by each technology when biomass was added in the system. Data for CTL emissions was taken from published literature values that was 100, 81, and 64 kg CO_2/GJ product for ICLT, DCTL, and DCGTL, respectively (Williams and Larson 2003, Edwards et al 2011). The carbon offset prices were from October 2011 to August 2016 as reported by the California Carbon Dashboard. The carbon offset prices were fitted using Oracle Crystal Ball as a log-normal distribution. The distribution was applied to the varied carbon offset market price used during the simulation and risk analysis.

Table 4-10 provides the results of the risk assessment for the base case technology. In each of the four different scenarios, both the probability of at least breaking even and the mean value of the estimated current market price (i.e., mean from break-even) is provided. Based on the risk analysis, the maximum probability for breaking even when considering only current oils prices was 52.1 percent for the D-CBGTL-CCS technology. In all cases, the addition of a consumer premium and carbon credits greatly reduced the market risk (i.e., improved the break-even probability) associated with each technology (Table 4-10 and Figure 4-9).

The potential carbon offset credit market has a larger influence on the break-even probability as compared to the consumer willingness to pay more for a premium product from a process that reduced emissions and included locally sourced biomass. Of all the technologies, the H-CBTL-CCS had the highest associated market risk, which would be expected given the high initial break-even oil price value. The inclusion of natural gas in the CBTL system was found to reduce the market risk associated with both the direct (D) and hybrid (H) technologies.

Table 4-10. Risk analysis for base case scenarios based on historical oil prices, consumer willingness to pay a premium, and potential carbon offset markets.

		Process Technology				
Basis	Values/Results	I-CBTL-CCS	D-CBTL-CCS	D-CBGTL-CCS	H-CBGTL-CCS	H-CBTL-CCS
	Break-even oil price ($/bbl)	90.7	97.5	86.1	94.5	100.6
Historical Oil Price Only	Probability of at least breaking even (%)	44.4	33.0	52.1	39.0	28.4
	Mean from break-even ($)	8.04	14.8	3.46	11.52	18.29
Historical Oil Price + Consumer Premium	Probability of at least breaking even (%)	50.3	38.8	57.1	43.4	35.0
	Mean from break-even ($)	4.68	11.87	0.12	8.52	14.47
Historical Oil Price and Carbon Credit Market	Probability of at least breaking even (%)	54.7	41.8	58.2	44.2	37.1
	Mean from break-even ($)	1.66	9.59	-5.59	8.33	12.78
Historical Oil Price, Consumer Premium, and Carbon Credit Market	Probability of at least breaking even (%)	59.1	48.7	63.3	51.7	42.4
	Mean from break-even ($)	-1.81	5.77	-4.38	3.56	9.66

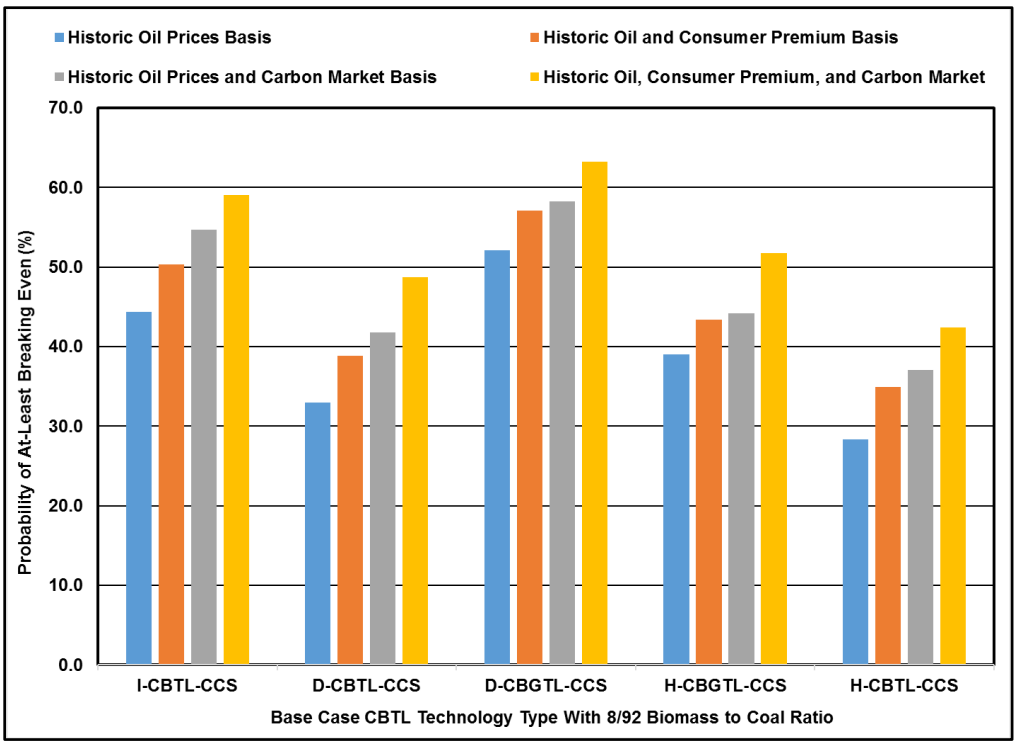

Figure 4-9. Probability for break-even or better scenario for each base case technology.

Table 4-11 provides the results of the risk assessment for the evaluate technology when production is increased to 50,000 bbl/day and when the biomass percentage is increased to a 20/80 biomass/coal ratio. Based on the risk analysis, the maximum probability for breaking even when considering only current oils prices was 76.7 percent for the D-CBGTL-CCS technology.

Table 4-11. Risk analysis for sensitivity analyzed cases with increased production and increased biomass percentage.

	Process Technology at 8/92 Biomass Ratio and 50,000 bbl/day			Process Technology at 20/80 Biomass Ratio and 10,000 bbl/day		
Results	I-CBTL-CCS	D-CBTL-CCS	D-CBGTL-CCS	I-CBTL-CCS	D-CBTL-CCS	D-CBGTL-CCS
Break-even oil price ($/bbl)	73.1	73.5	65.3	92.7	96.4	85.3
Probability of at least breaking even (%)	69.6	67.9	76.7	41.2	38.2	52.8
Mean from break-even ($)	-9.08	-8.59	-16.98	10.36	12.39	2.9

The increase in production rate to 50,000 bbl/day as compared to 10,000 bbl/day substantially reduced the market risk, in terms of the probability of breaking even (Figure 4-10). In all technology types (indirect, direct, and direct with natural gas), the increase in production reduced the risk. The increase in biomass percentage from 8/92 to 20/80 had a minimal influence on the risk. For the indirect system, the increase in biomass percentage slightly lowered the probability to break even. For the direct method (without natural gas), the increase in biomass percentage

resulted in the biggest change in reducing risk, while when natural gas was included there was not significant change in market risk.

Based on the risk analysis, to reduce the market risk, a mandated carbon offset market would be the most beneficial to all the technologies. In terms of marketing, increasing the consumer willingness to pay even more than the 4% analyzed value should be a focus to convince the consumers to pay a high premium for a locally sourced, partially renewable fuel with lower CO2 emissions, as compared to gasoline and diesel from petroleum. To further develop this risk assessment in future studies, greatly varying the gasoline and diesel percentages would allow for a more robust analysis, given that historical data on these fuels without refinement and taxes included is available.

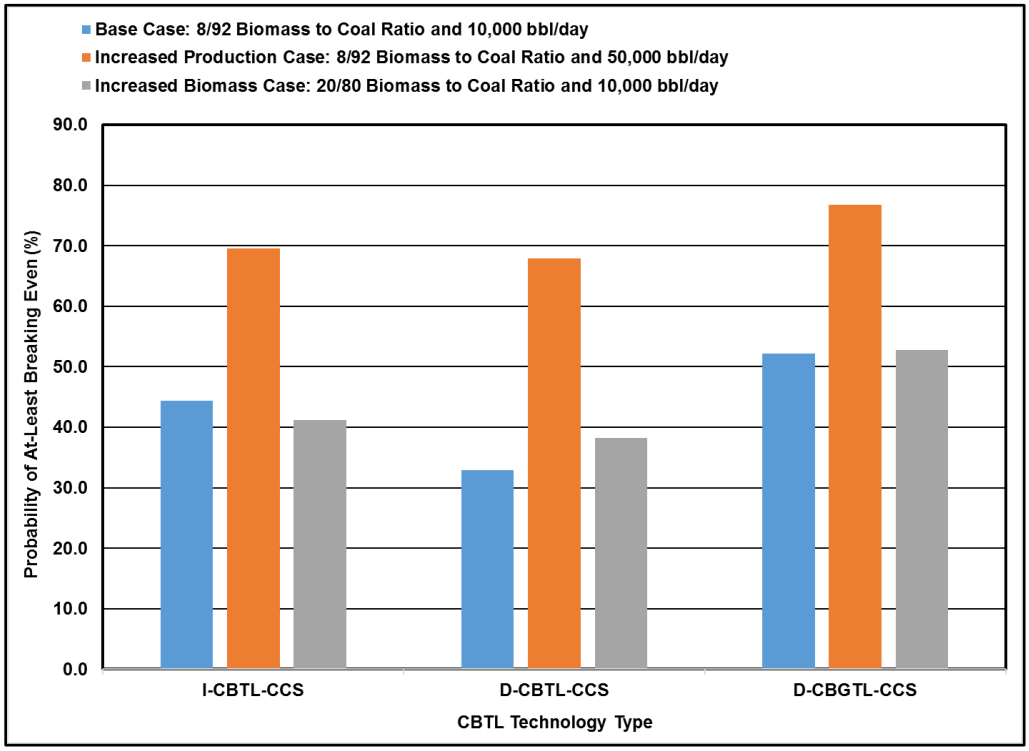

Figure 4-10. Probability for break-even or better scenario comparison between base case and increased production or increased biomass amount.

References

Edwards R, Larive JF, Beziat JC. 2011. Well-to-wheels Analysis of Future Automotive Fuels and Powertrains in the European Context, EUR 24952 RN-2011, JRC Scientific and Technical Reports.

EIA. 2013a. U.S. Energy Information Administration Refiner Motor Gasoline Sales Volumes. Available at: http://www.eia.gov/dnav/pet/pet_cons_refmg_a_EPM0_VTC_mgalpd_m.htm

EIA. 2013b. U.S. Energy Information Administration Adjusted Sales of Distillate Fuel Oil by End Use. Available at: http://www.eia.gov/dnav/pet/pet_cons_821dsta_a_EPD0_VAA_Mgal_a.htm

EIA. 2013e. U.S. Energy Information Administration Monthly Biodiesel Production Report. Available at: http://www.eia.gov/biofuels/biodiesel/production/

EIA. 2013c. U.S. Energy Information Administration Crude Oil Production. Available at: http://www.eia.gov/dnav/pet/pet_crd_crpdn_adc_mbbl_a.htm

EIA. 2013d. U.S. Energy Information Administration Oil Crude and Petroleum Products Explained. Refining Crude Oil. Available at: http://www.eia.gov/energyexplained/index.cfm?page=oil_refining.

EIA. 2013f. U.S. Energy Information Administration U.S. Regular Gasoline Retail Sales by Refiner. Available at: http://www.eia.gov/dnav/pet/hist/LeafHandler.ashx?n=PET&s=EMA_EPMR_PTG_NUS_DPG&f=M.

EIA. 2013g. U.S. Energy Information Administration U.S. Midgrade Gasoline Retail Sales by Refiner. Available at: http://www.eia.gov/dnav/pet/hist/LeafHandler.ashx?n=PET&s=EMA_EPMM_PTG_NUS_DPG&f=M.

EIA. 2013h. U.S. Energy Information Administration U.S. Premium Gasoline Retail Sales by Refiner. Available at: http://www.eia.gov/dnav/pet/hist/LeafHandler.ashx?n=PET&s=EMA_EPMP_PTG_NUS_DPG&f=M.

EIA. 2013i. U.S. Energy Information Administration U.S. Regular Gasoline Wholesale/Resale Price by Refiner. Available at: http://www.eia.gov/dnav/pet/hist/LeafHandler.ashx?n=PET&s=EMA_EPMR_PWG_NUS_DPG&f=M.

EIA. 2013j. U.S. Energy Information Administration U.S. Midgrade Gasoline Wholesale/Resale Price by Refiner. Available at: http://www.eia.gov/dnav/pet/hist/LeafHandler.ashx?n=PET&s=EMA_EPMM_PWG_NUS_DPG&f=M.

EIA. 2013k. U.S. Energy Information Administration U.S. Premium Gasoline Wholesale/Resale Price by Refiner. Available at: http://www.eia.gov/dnav/pet/hist/LeafHandler.ashx?n=PET&s=EMA_EPMP_PWG_NUS_DPG&f=M.

EIA. 2013l. U.S. Energy Information Administration U.S. No 1 Distillate Retail Sales by Refiners. Available at: http://www.eia.gov/dnav/pet/hist/LeafHandler.ashx?n=PET&s=EMA_EPD1_PTG_NUS_DPG&f=M.

EIA. 2013m. U.S. Energy Information Administration U.S. No 2 Distillate Retail Sales by Refiners. Available at:

http://www.eia.gov/dnav/pet/hist/LeafHandler.ashx?n=PET&s=EMA_EPD2_PTG_NUS_DPG&f=M.

EIA. 2013n. U.S. Energy Information Administration U.S. No 4 Distillate Retail Sales by Refiners. Available at: http://www.eia.gov/dnav/pet/hist/LeafHandler.ashx?n=PET&s=EMA_EPD4_PTG_NUS_DPG&f=M

EIA. 2013o. U.S. Energy Information Administration U.S. No 1 Distillate Wholesale/Resale Price by Refiners. Available at: http://www.eia.gov/dnav/pet/hist/LeafHandler.ashx?n=PET&s=EMA_EPD1_PWG_NUS_DPG&f=M.

EIA. 2013p. U.S. Energy Information Administration U.S. No 2 Distillate Wholesale/Resale Price by Refiners. Available at: http://www.eia.gov/dnav/pet/hist/LeafHandler.ashx?n=PET&s=EMA_EPD2_PWG_NUS_DPG&f=M.

EIA. 2013q. U.S. Energy Information Administration U.S. No 4 Distillate Wholesale/Resale Price by Refiners. Available at: http://www.eia.gov/dnav/pet/hist/LeafHandler.ashx?n=PET&s=EMA_EPD4_PWG_NUS_DPG&f=M.

EIA. 2013r. U.S. Energy Information Administration. AEO2014 Early release Overview. Available at: http://www.eia.gov/forecasts/aeo/er/executive_summary.cfm.

EIA. 2013s. U.S. Energy and Information Administration. Guide on Federal and State Summer RVP Standards for Conventional Gasoline Only. Available at: http://www.epa.gov/otaq/fuels/gasolinefuels/volatility/standards.htm

EIA. 2013t. U.S. Energy and Information Administration. Diesel Fuels. Available at: http://www.epa.gov/otaq/fuels/dieselfuels/index.htm.

EIA. 2014. U.S. Energy and Information Administration. Alternative Fuels Data Center. Available at: http://www.afdc.energy.gov/laws/RFS

Keesom, W.; Unnasch, S.; Moretta, J. 2009. Life Cycle Assessment comparison of North American and imported crudes. Jacobs Consultancy: Chicago, Illinois, U.S.

National Mining Association.2011.U.S. Coal Production and Number of Mines by State and Coal Type 2010. http://www.nma.org/pdf/c_production_mines_state_type.pdf. Accessed 5/24/2012.

NBB. 2013. National Biodiesel Board. NBB Member Plant Lists. Available at: http://www.nbb.org/about-us/member-plants/nbb-member-plant-lists.

NETL 2007. Baseline Technical and Economic Assessment of a Small-Scale Fischer-Tropsch Liquids Facility; DOE/NETL-2007/1260; National Energy Technology Laboratory, 2007; http://www.netl.doe.gov.

NETL 2009. National Energy Technology Laboratory. Affordable, Low-Carbon Diesel Fuel from Domestic Coal and Biomass. DOE/NETL-2009/1349

Wang, J., Grushecky, S., and McNeel, J. 2006. Biomass Resources, Uses, and Opportunities in West Virginia. West Virginia University, Biomaterials Center, Morgantown, WV.

Williams, R.H. and Larson E.D. 2003. A comparison of direct and indirect liquefaction technologies for making fluid fuels from coal. Energy Sustain Dev; 7(4): 103-29.

WPS. 2014. World Population Statistics – United States of America. Available at: http://www.worldpopulationstatistics.com/category/regions/united-states-of-america/.

USA. 2014. USA Today – 1,100 layoffs planned at Alpha coal mines in W.Va. Accessed 9-29-2014. Available at: http://www.usatoday.com/story/money/business/2014/07/31/1100-layoffs-planned-at-alpha-coal-mines-in-wva/13428945/

Task 5 Financial Feasibility

Production of biofuel solely from cellulosic feedstock has large barriers related to processing technology (e.g., high cost) and future market uncertainty. These factors have the potential to impact future investment in this technology. To determine the financial feasibility of such projects, a financial analysis including pro forma financial statements have been developed along with an investor prospectus. In addition, the sensitivity of the financial projections to changes in the cost structure and project scenarios have been analyzed and documented.

Task 5.1 Cash flow and Income Statement Development

Accomplishments:

- ✓ The project team has reviewed and completed the financial statements for the indirect, direct, and hybrid CBTL cases, and now has prepared final versions of all documents.

Indirect CBTL pro forma financial models

Financial models for the indirect CBTL model plant were prepared from estimates using APEA V8.4 as detailed in the section for Task 3. Capital expenditures were estimated at approximately $1.43 billion as illustrated in Figure 5.1 below.

Capital Expenditures

Summary for Project

Phase	Weeks	Periods
EPC	119.57	2.29
Construction Delay	0.00	0.00
Start-up	40.00	0.77
Production	1414	27.10

	PV of Escalated Total	Escalated Total	Base, Brought to Start of Calendar
	Cashflows in Millions of USD		
Capital Expenditure	1,219.98	1,436.87	1,434.77
Decision Engineering Studies	-	-	-
Owner's Engineering	-	-	-
Fixed Capital Investment	1,100.98	1,278.49	1,281.05
Engineering, Procurement	23.65	26.31	26.00
Materials	694.51	770.80	785.15
Equipment	477.75	525.52	520.32
Bulk Materials	216.77	245.28	264.83
Construction	382.82	481.38	469.90
Working Capital	119.00	158.38	153.73
Start-Up Costs	-	-	-
Catalyst and Chemicals: Initial Charge	-	-	-
Royalties, Initial Fee	-	-	-
Demolition E&C	-	-	-
Land	-	-	-
Return of Working Capital and Salvage Value	31.66	552.53	409.94
Working Capital	11.87	207.20	153.73
Salvage Value: FCI	19.79	345.33	256.21
Salvage Value: Catalyst	-	-	-
Salvage Value: Land	-	-	-

Figure 5-1. Summary of pro forma capital expenditures, indirect CBTL model plant.

Pro forma income statements were prepared assuming a plant life of thirty (30) years as shown in Figure 5-2(a) through Figure 5.2(c):

Date of First Day in Period	1-Mar-13	1-Mar-14	1-Mar-15	1-Mar-16	1-Mar-17	1-Mar-18	1-Mar-19	1-Mar-20	1-Mar-21	1-Mar-22
Year	2013	2014	2015	2016	2017	2018	2019	2020	2021	2022
Calendar Period	1	2	3	4	5	6	7	8	9	10
Year, from Start of EPC	1	2	3	4	5	6	7	8	9	10
Period of Operation			1	2	3	4	5	6	7	8
	Period Values					Millions of USD				
Production of diesel, Millions of LB per Year	-	-	-	504.7	535.4	535.4	535.4	535.4	535.4	535.4
Domestic	-	-	-	504.7	535.4	535.4	535.4	535.4	535.4	535.4
Export	-	-	-	-	-	-	-	-	-	-
Production, as a % of Design Capacity	-	-	-	94.3%	100.0%	100.0%	100.0%	100.0%	100.0%	100.0%
Product Revenue	-	-	-	397.06	425.44	429.69	433.99	438.33	442.71	447.14
Product diesel	-	-	-	236.87	253.80	256.34	258.91	261.49	264.11	266.75
Domestic	-	-	-	236.87	253.80	256.34	258.91	261.49	264.11	266.75
Export	-	-	-	-	-	-	-	-	-	-
By-Product Credit	-	-	-	160.19	171.63	173.35	175.08	176.84	178.60	180.39
Manufacturing Costs	-	-	186.26	317.63	298.91	280.21	261.52	242.85	224.19	205.54
Operating Costs	-	-	62.54	114.54	115.69	116.85	118.01	119.19	120.39	121.59
Annual Expenses	-	-	-	-	-	-	-	-	-	-
Raw Material	-	-	42.49	85.89	86.75	87.62	88.49	89.38	90.27	91.17
Utilities	-	-	-	-	-	-	-	-	-	-
Operating Labor and Supervision	-	-	14.91	21.31	21.52	21.74	21.96	22.18	22.40	22.62
Maintenance	-	-	2.15	3.07	3.10	3.13	3.16	3.19	3.23	3.26
Operating Supplies	-	-	0.57	0.81	0.82	0.82	0.83	0.84	0.85	0.86
Laboratory Charges	-	-	2.42	3.46	3.50	3.53	3.57	3.60	3.64	3.68
Patents and Royalties (on Production)	-	-	-	-	-	-	-	-	-	-
Fixed Charges	-	-	101.39	167.37	148.77	130.17	111.58	92.98	74.38	55.79
Depreciation	-	-	101.39	167.37	148.77	130.17	111.58	92.98	74.38	55.79
Property Tax	-	-	-	-	-	-	-	-	-	-
Rent	-	-	-	-	-	-	-	-	-	-
Insurance	-	-	-	-	-	-	-	-	-	-
Plant Overhead	-	-	8.53	12.19	12.31	12.44	12.56	12.69	12.81	12.94
General and Administrative	-	-	13.80	23.53	22.14	20.76	19.37	17.99	16.61	15.23
EBIT (Earning before Interest, Taxes)	-	-	(186.26)	79.43	126.53	149.48	172.47	195.48	218.52	241.60
Taxes	-	-	-	31.77	50.61	59.79	68.99	78.19	87.41	96.64
Net Income	-	-	(186.26)	47.66	75.92	89.69	103.48	117.29	131.11	144.96

Figure 5.2(a). Pro forma income statements, indirect CBTL model plant, first 10 years.

Date of First Day in Period	1-Mar-23	1-Mar-24	1-Mar-25	1-Mar-26	1-Mar-27	1-Mar-28	1-Mar-29	1-Mar-30	1-Mar-31	1-Mar-32
Year	2023	2024	2025	2026	2027	2028	2029	2030	2031	2032
Calendar Period	11	12	13	14	15	16	17	18	19	20
Year, from Start of EPC	11	12	13	14	15	16	17	18	19	20
Period of Operation	9	10	11	12	13	14	15	16	17	18
	Period Values					Millions of USD				
Production of diesel, Millions of LB per Year	535.4	535.4	535.4	535.4	535.4	535.4	535.4	535.4	535.4	535.4
Domestic	535.4	535.4	535.4	535.4	535.4	535.4	535.4	535.4	535.4	535.4
Export	-	-	-	-	-	-	-	-	-	-
Production, as a % of Design Capacity	100.0%	100.0%	100.0%	100.0%	100.0%	100.0%	100.0%	100.0%	100.0%	100.0%
Product Revenue	451.61	456.13	460.69	465.30	469.95	474.65	479.40	484.19	489.03	493.92
Product diesel	269.42	272.11	274.83	277.58	280.36	283.16	285.99	288.85	291.74	294.66
Domestic	269.42	272.11	274.83	277.58	280.36	283.16	285.99	288.85	291.74	294.66
Export	-	-	-	-	-	-	-	-	-	-
By-Product Credit	182.19	184.02	185.86	187.71	189.59	191.49	193.40	195.34	197.29	199.26
Manufacturing Costs	186.91	168.30	149.70	151.19	152.70	154.23	155.77	157.33	158.90	160.49
Operating Costs	122.81	124.03	125.27	126.53	127.79	129.07	130.36	131.66	132.98	134.31
Annual Expenses	-	-	-	-	-	-	-	-	-	-
Raw Material	92.09	93.01	93.94	94.88	95.82	96.78	97.75	98.73	99.72	100.71
Utilities	-	-	-	-	-	-	-	-	-	-
Operating Labor and Supervision	22.85	23.08	23.31	23.54	23.78	24.01	24.25	24.50	24.74	24.99
Maintenance	3.29	3.32	3.36	3.39	3.42	3.46	3.49	3.53	3.56	3.60
Operating Supplies	0.87	0.88	0.88	0.89	0.90	0.91	0.92	0.93	0.94	0.95
Laboratory Charges	3.71	3.75	3.79	3.83	3.86	3.90	3.94	3.98	4.02	4.06
Patents and Royalties (on Production)	-	-	-	-	-	-	-	-	-	-
Fixed Charges	37.19	18.60	-	-	-	-	-	-	-	-
Depreciation	37.19	18.60	-	-	-	-	-	-	-	-
Property Tax	-	-	-	-	-	-	-	-	-	-
Rent	-	-	-	-	-	-	-	-	-	-
Insurance	-	-	-	-	-	-	-	-	-	-
Plant Overhead	13.07	13.20	13.33	13.47	13.60	13.74	13.87	14.01	14.15	14.29
General and Administrative	13.85	12.47	11.09	11.20	11.31	11.42	11.54	11.65	11.77	11.89
EBIT (Earning before Interest, Taxes)	264.70	287.83	310.99	314.10	317.25	320.42	323.62	326.86	330.13	333.43
Taxes	105.88	115.13	124.40	125.64	126.90	128.17	129.45	130.74	132.05	133.37
Net Income	158.82	172.70	186.60	188.46	190.35	192.25	194.17	196.12	198.08	200.06

Figure 5.2(b). Pro forma income statements, indirect CBTL model plant, years 11 through 20.

Date of First Day in Period	1-Mar-33	1-Mar-34	1-Mar-35	1-Mar-36	1-Mar-37	1-Mar-38	1-Mar-39	1-Mar-40	1-Mar-41	1-Mar-42
Year	2033	2034	2035	2036	2037	2038	2039	2040	2041	2042
Calendar Period	21	22	23	24	25	26	27	28	29	30
Year, from Start of EPC	21	22	23	24	25	26	27	28	29	30
Period of Operation	19	20	21	22	23	24	25	26	27	28
	Period Values					Millions of USD				
Production of diesel, Millions of LB per Year	535.4	535.4	535.4	535.4	535.4	535.4	535.4	535.4	535.4	534.0
Domestic	535.4	535.4	535.4	535.4	535.4	535.4	535.4	535.4	535.4	534.0
Export	-	-	-	-	-	-	-	-	-	-
Production, as a % of Design Capacity	100.0%	100.0%	100.0%	100.0%	100.0%	100.0%	100.0%	100.0%	100.0%	99.7%
Product Revenue	498.86	503.85	508.89	513.98	519.12	524.31	529.55	534.85	540.20	544.10
Product diesel	297.61	300.58	303.59	306.62	309.69	312.79	315.91	319.07	322.26	324.60
Domestic	297.61	300.58	303.59	306.62	309.69	312.79	315.91	319.07	322.26	324.60
Export	-	-	-	-	-	-	-	-	-	-
By-Product Credit	201.26	203.27	205.30	207.35	209.43	211.52	213.64	215.77	217.93	219.51
Manufacturing Costs	162.10	163.72	165.36	167.01	168.68	170.37	172.07	173.79	175.53	176.47
Operating Costs	135.65	137.01	138.38	139.76	141.16	142.57	144.00	145.44	146.89	147.65
Annual Expenses	-	-	-	-	-	-	-	-	-	-
Raw Material	101.72	102.74	103.76	104.80	105.85	106.91	107.98	109.06	110.15	110.64
Utilities	-	-	-	-	-	-	-	-	-	-
Operating Labor and Supervision	25.24	25.49	25.75	26.00	26.26	26.53	26.79	27.06	27.33	27.53
Maintenance	3.64	3.67	3.71	3.75	3.78	3.82	3.86	3.90	3.94	3.97
Operating Supplies	0.96	0.97	0.98	0.99	1.00	1.01	1.02	1.03	1.04	1.04
Laboratory Charges	4.10	4.14	4.18	4.23	4.27	4.31	4.35	4.40	4.44	4.47
Patents and Royalties (on Production)	-	-	-	-	-	-	-	-	-	-
Fixed Charges	-	-	-	-	-	-	-	-	-	-
Depreciation	-	-	-	-	-	-	-	-	-	-
Property Tax	-	-	-	-	-	-	-	-	-	-
Rent	-	-	-	-	-	-	-	-	-	-
Insurance	-	-	-	-	-	-	-	-	-	-
Plant Overhead	14.44	14.58	14.73	14.87	15.02	15.17	15.33	15.48	15.63	15.75
General and Administrative	12.01	12.13	12.25	12.37	12.49	12.62	12.75	12.87	13.00	13.07
EBIT (Earning before Interest, Taxes)	336.76	340.13	343.53	346.97	350.44	353.94	357.48	361.06	364.67	367.63
Taxes	134.71	136.05	137.41	138.79	140.17	141.58	142.99	144.42	145.87	147.05
Net Income	202.06	204.08	206.12	208.18	210.26	212.36	214.49	216.63	218.80	220.58

Figure 5.2(c). Pro forma income statements, indirect CBTL model plant, years 21 through 30.

Pro forma cash flow projections were also prepared. Figure 5.3 shows the net present value of cash flow over the first twenty-five (25) years, showing a break even by the 22nd year, based on the assumptions of the model as specified in the section regarding Task 3.

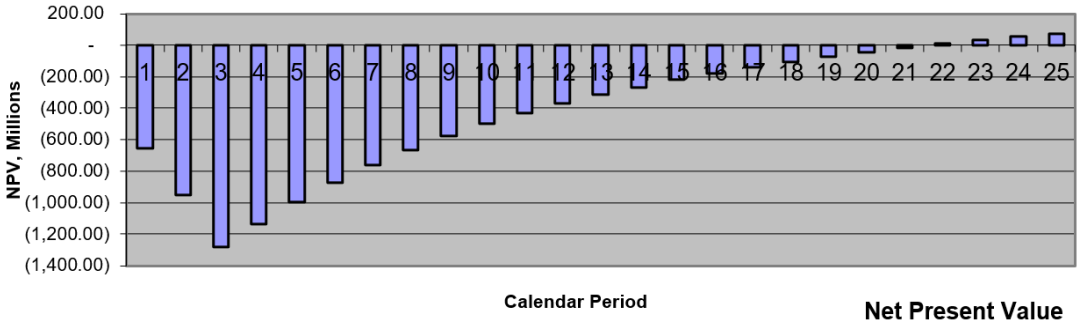

Figure 5.3. Cash flow summary over initial 25 years, indirect CBTL model plant.

Direct CBTL pro forma financial models

Capital expenditures for the direct CBTL model plant (without shale gas) were estimated at approximately $1.6 billion as illustrated in Figure 5.4.

Capital Expenditures

Summary for Project

Phase	Weeks	Periods
EPC	129.86	2.49
Construction Delay	0.00	0.00
Start-up	40.00	0.77
Production	1408	26.99

	PV of Escalated Total	Escalated Total	Base, Brought to Start of Calendar
	Cashflows in Millions of USD		
Capital Expenditure	1,388.32	1,655.61	1,639.42
Decision Engineering Studies	-	-	-
Owner's Engineering	-	-	-
Fixed Capital Investment	1,252.35	1,474.64	1,463.77
Engineering, Procurement	30.89	34.40	33.68
Materials	750.41	835.60	841.16
Equipment	461.86	508.05	503.02
Bulk Materials	288.55	327.55	338.14
Construction	471.05	604.63	588.93
Working Capital	135.97	180.97	175.65
Start-Up Costs	-	-	-
Catalyst and Chemicals: Initial Charge	-	-	-
Royalties, Initial Fee	-	-	-
Demolition E&C	-	-	-
Land	-	-	-
Return of Working Capital and Salvage Value	36.18	631.34	468.41
Working Capital	13.57	236.75	175.65
Salvage Value: FCI	22.61	394.59	292.75
Salvage Value: Catalyst	-	-	-
Salvage Value: Land	-	-	-

Figure 5-4. Summary of pro forma capital expenditures, direct CBTL model plant.

Pro forma income statements were prepared assuming a plant life of thirty (30) years as shown in Figure 5-5(a) through Figure 5.5(c):

Date of First Day in Period	1-Jan-15	1-Jan-16	1-Jan-17	1-Jan-18	1-Jan-19	1-Jan-20	1-Jan-21	1-Jan-22	1-Jan-23	1-Jan-24
Year	2015	2016	2017	2018	2019	2020	2021	2022	2023	2024
Calendar Period	1	2	3	4	5	6	7	8	9	10
Year, from Start of EPC	1	2	3	4	5	6	7	8	9	10
Period of Operation			1	2	3	4	5	6	7	8
	Period Values					Millions of USD				
Production of DIESEL, Millions of LB per Year	-	-	-	560.1	751.6	751.6	751.6	751.6	751.6	751.6
Domestic	-	-	-	560.1	751.6	751.6	751.6	751.6	751.6	751.6
Export	-	-	-	-	-	-	-	-	-	-
Production, as a % of Design Capacity	-	-	-	74.5%	100.0%	100.0%	100.0%	100.0%	100.0%	100.0%
Product Revenue	-	-	-	352.67	477.98	482.76	487.59	492.46	497.39	502.36
Product DIESEL	-	-	-	252.95	342.83	346.26	349.72	353.22	356.75	360.32
Domestic	-	-	-	252.95	342.83	346.26	349.72	353.22	356.75	360.32
Export	-	-	-	-	-	-	-	-	-	-
By-Product Credit	-	-	-	99.72	135.15	136.50	137.87	139.25	140.64	142.04
Manufacturing Costs	-	-	169.67	342.30	320.47	298.66	276.86	255.07	233.30	211.54
Operating Costs	-	-	37.78	105.20	106.26	107.32	108.39	109.48	110.57	111.68
Annual Expenses	-	-	-	-	-	-	-	-	-	-
Raw Material	-	-	15.90	61.84	62.46	63.08	63.71	64.35	64.99	65.64
Utilities	-	-	-	-	-	-	-	-	-	-
Operating Labor and Supervision	-	-	15.37	30.47	30.77	31.08	31.39	31.71	32.02	32.34
Maintenance	-	-	3.49	6.92	6.99	7.06	7.13	7.20	7.27	7.35
Operating Supplies	-	-	0.52	1.03	1.04	1.05	1.06	1.07	1.08	1.09
Laboratory Charges	-	-	2.50	4.95	5.00	5.05	5.10	5.15	5.20	5.26
Patents and Royalties (on Production)	-	-	-	-	-	-	-	-	-	-
Fixed Charges	-	-	109.89	193.04	171.59	150.14	128.70	107.25	85.80	64.35
Depreciation	-	-	109.89	193.04	171.59	150.14	128.70	107.25	85.80	64.35
Property Tax	-	-	-	-	-	-	-	-	-	-
Rent	-	-	-	-	-	-	-	-	-	-
Insurance	-	-	-	-	-	-	-	-	-	-
Plant Overhead	-	-	9.43	18.69	18.88	19.07	19.26	19.45	19.65	19.84
General and Administrative	-	-	12.57	25.36	23.74	22.12	20.51	18.89	17.28	15.67
EBIT (Earning before Interest, Taxes)	-	-	(169.67)	10.37	157.51	184.10	210.73	237.39	264.09	290.82
Taxes	-	-	-	4.15	63.00	73.64	84.29	94.96	105.64	116.33
Net Income	-	-	(169.67)	6.22	94.51	110.46	126.44	142.44	158.45	174.49

Figure 5.5(a). Pro forma income statements, direct CBTL model plant, first 10 years.

Date of First Day in Period	1-Jan-25	1-Jan-26	1-Jan-27	1-Jan-28	1-Jan-29	1-Jan-30	1-Jan-31	1-Jan-32	1-Jan-33	1-Jan-34
Year	2025	2026	2027	2028	2029	2030	2031	2032	2033	2034
Calendar Period	11	12	13	14	15	16	17	18	19	20
Year, from Start of EPC	11	12	13	14	15	16	17	18	19	20
Period of Operation	9	10	11	12	13	14	15	16	17	18
	Period Values					Millions of USD				
Production of DIESEL, Millions of LB per Year	751.6	751.6	751.6	751.6	751.6	751.6	751.6	751.6	751.6	751.6
Domestic	751.6	751.6	751.6	751.6	751.6	751.6	751.6	751.6	751.6	751.6
Export	-	-	-	-	-	-	-	-	-	-
Production, as a % of Design Capacity	100.0%	100.0%	100.0%	100.0%	100.0%	100.0%	100.0%	100.0%	100.0%	100.0%
Product Revenue	507.38	512.46	517.58	522.76	527.99	533.27	538.60	543.98	549.42	554.92
Product DIESEL	363.92	367.56	371.23	374.95	378.70	382.48	386.31	390.17	394.07	398.01
Domestic	363.92	367.56	371.23	374.95	378.70	382.48	386.31	390.17	394.07	398.01
Export	-	-	-	-	-	-	-	-	-	-
By-Product Credit	143.47	144.90	146.35	147.81	149.29	150.78	152.29	153.81	155.35	156.91
Manufacturing Costs	189.79	168.06	146.35	147.81	149.29	150.78	152.29	153.81	155.35	156.90
Operating Costs	112.79	113.92	115.06	116.21	117.37	118.55	119.73	120.93	122.14	123.36
Annual Expenses	-	-	-	-	-	-	-	-	-	-
Raw Material	66.30	66.96	67.63	68.31	68.99	69.68	70.38	71.08	71.79	72.51
Utilities	-	-	-	-	-	-	-	-	-	-
Operating Labor and Supervision	32.67	32.99	33.32	33.66	33.99	34.33	34.68	35.02	35.37	35.73
Maintenance	7.42	7.49	7.57	7.64	7.72	7.80	7.88	7.95	8.03	8.11
Operating Supplies	1.10	1.11	1.12	1.13	1.15	1.16	1.17	1.18	1.19	1.20
Laboratory Charges	5.31	5.36	5.42	5.47	5.52	5.58	5.63	5.69	5.75	5.81
Patents and Royalties (on Production)	-	-	-	-	-	-	-	-	-	-
Fixed Charges	42.90	21.45	-	-	-	-	-	-	-	-
Depreciation	42.90	21.45	-	-	-	-	-	-	-	-
Property Tax	-	-	-	-	-	-	-	-	-	-
Rent	-	-	-	-	-	-	-	-	-	-
Insurance	-	-	-	-	-	-	-	-	-	-
Plant Overhead	20.04	20.24	20.45	20.65	20.86	21.07	21.28	21.49	21.70	21.92
General and Administrative	14.06	12.45	10.84	10.95	11.06	11.17	11.28	11.39	11.51	11.62
EBIT (Earning before Interest, Taxes)	317.59	344.39	371.24	374.95	378.70	382.48	386.31	390.17	394.07	398.01
Taxes	127.04	137.76	148.49	149.98	151.48	152.99	154.52	156.07	157.63	159.21
Net Income	190.55	206.64	222.74	224.97	227.22	229.49	231.79	234.10	236.44	238.81

Figure 5.5(b). Pro forma income statements, direct CBTL model plant, years 11 through 20.

Date of First Day in Period	1-Jan-35	1-Jan-36	1-Jan-37	1-Jan-38	1-Jan-39	1-Jan-40	1-Jan-41	1-Jan-42	1-Jan-43	1-Jan-44
Year	2035	2036	2037	2038	2039	2040	2041	2042	2043	2044
Calendar Period	21	22	23	24	25	26	27	28	29	30
Year, from Start of EPC	21	22	23	24	25	26	27	28	29	30
Period of Operation	19	20	21	22	23	24	25	26	27	28
	Period Values					Millions of USD				
Production of DIESEL, Millions of LB per Year	751.6	751.6	751.6	751.6	751.6	751.6	751.6	751.6	751.6	747.5
Domestic	751.6	751.6	751.6	751.6	751.6	751.6	751.6	751.6	751.6	747.5
Export	-	-	-	-	-	-	-	-	-	-
Production, as a % of Design Capacity	100.0%	100.0%	100.0%	100.0%	100.0%	100.0%	100.0%	100.0%	100.0%	99.5%
Product Revenue	560.47	566.07	571.73	577.45	583.22	589.06	594.95	600.90	606.91	609.63
Product DIESEL	401.99	406.01	410.07	414.17	418.31	422.50	426.72	430.99	435.30	437.25
Domestic	401.99	406.01	410.07	414.17	418.31	422.50	426.72	430.99	435.30	437.25
Export	-	-	-	-	-	-	-	-	-	-
By-Product Credit	158.47	160.06	161.66	163.28	164.91	166.56	168.22	169.91	171.61	172.37
Manufacturing Costs	158.47	160.06	161.66	163.27	164.91	166.56	168.22	169.90	171.60	171.90
Operating Costs	124.59	125.84	127.10	128.37	129.65	130.95	132.26	133.58	134.92	135.09
Annual Expenses	-	-	-	-	-	-	-	-	-	-
Raw Material	73.23	73.97	74.71	75.45	76.21	76.97	77.74	78.52	79.30	79.22
Utilities	-	-	-	-	-	-	-	-	-	-
Operating Labor and Supervision	36.08	36.45	36.81	37.18	37.55	37.93	38.30	38.69	39.07	39.25
Maintenance	8.20	8.28	8.36	8.44	8.53	8.61	8.70	8.79	8.87	8.91
Operating Supplies	1.22	1.23	1.24	1.25	1.27	1.28	1.29	1.30	1.32	1.32
Laboratory Charges	5.86	5.92	5.98	6.04	6.10	6.16	6.22	6.29	6.35	6.38
Patents and Royalties (on Production)	-	-	-	-	-	-	-	-	-	-
Fixed Charges	-	-	-	-	-	-	-	-	-	-
Depreciation	-	-	-	-	-	-	-	-	-	-
Property Tax	-	-	-	-	-	-	-	-	-	-
Rent	-	-	-	-	-	-	-	-	-	-
Insurance	-	-	-	-	-	-	-	-	-	-
Plant Overhead	22.14	22.36	22.58	22.81	23.04	23.27	23.50	23.74	23.97	24.08
General and Administrative	11.74	11.86	11.97	12.09	12.22	12.34	12.46	12.59	12.71	12.73
EBIT (Earning before Interest, Taxes)	402.00	406.02	410.08	414.18	418.32	422.50	426.73	430.99	435.30	437.72
Taxes	160.80	162.41	164.03	165.67	167.33	169.00	170.69	172.40	174.12	175.09
Net Income	241.20	243.61	246.05	248.51	250.99	253.50	256.04	258.60	261.18	262.63

Figure 5.5(c). Pro forma income statements, direct CBTL model plant, years 21 through 30.

Pro forma cash flow projections were also prepared. Figure 5.6 shows the net present value of cash flow over the first twenty-five (25) years, showing a break even by year 20, based on the assumptions of the model as specified in the section regarding Task 3.

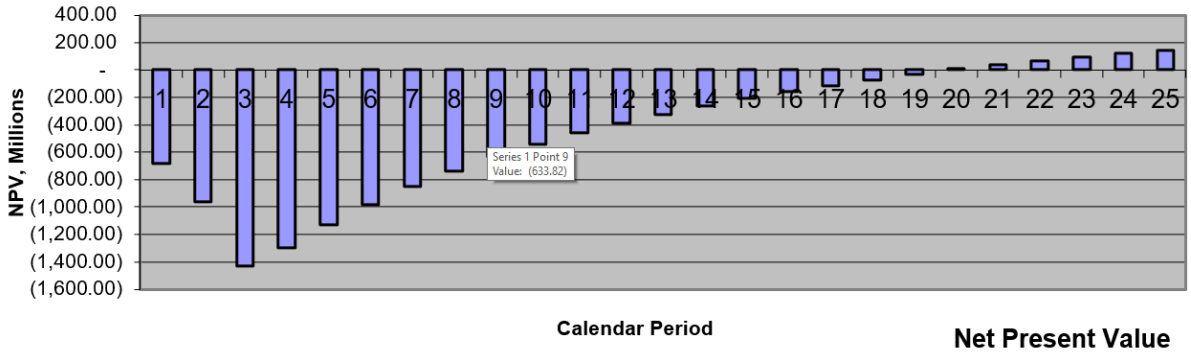

Figure 5.6. Cash flow summary over initial 25 years, indirect CBTL model plant.

Hybrid CBTL (direct CBTL with shale gas) pro forma financial models

Capital expenditures for the hybrid CBTL model plant were estimated at approximately $1.3 billion as illustrated in Figure 5.7.

Capital Expenditures

Summary for Project

Phase	Weeks	Periods
EPC	119.86	2.30
Construction Delay	0.00	0.00
Start-up	40.00	0.77
Production	1413	27.07

	Cashflows in Millions of USD		
	PV of Escalated Total	Escalated Total	Base, Brought to Start of Calendar
Capital Expenditure	1,113.01	1,311.64	1,301.04
Decision Engineering Studies	-	-	-
Owner's Engineering	-	-	-
Fixed Capital Investment	1,005.11	1,168.02	1,161.64
Engineering, Procurement	31.17	34.77	34.03
Materials	647.63	722.36	726.61
Equipment	395.00	434.50	430.19
Bulk Materials	252.64	287.86	296.41
Construction	326.31	410.90	401.00
Working Capital	107.90	143.62	139.40
Start-Up Costs	-	-	-
Catalyst and Chemicals: Initial Charge	-	-	-
Royalties, Initial Fee	-	-	-
Demolition E&C	-	-	-
Land	-	-	-
Return of Working Capital and Salvage Value	28.71	501.03	371.73
Working Capital	10.77	187.89	139.40
Salvage Value: FCI	17.95	313.14	232.33
Salvage Value: Catalyst	-	-	-
Salvage Value: Land	-	-	-

Figure 5-7. Summary of pro forma capital expenditures, hybrid CBTL model plant.

Pro forma income statements were prepared assuming a plant life of thirty (30) years as shown in Figure 5-8(a) through Figure 5.8(c):

Date of First Day in Period	1-Jan-15	1-Jan-16	1-Jan-17	1-Jan-18	1-Jan-19	1-Jan-20	1-Jan-21	1-Jan-22	1-Jan-23	1-Jan-24
Year	2015	2016	2017	2018	2019	2020	2021	2022	2023	2024
Calendar Period	1	2	3	4	5	6	7	8	9	10
Year, from Start of EPC	1	2	3	4	5	6	7	8	9	10
Period of Operation			1	2	3	4	5	6	7	8
	Period Values					Millions of USD				
Production of DIESEL, Millions of LB per Year	-	-	-	704.2	751.6	751.6	751.6	751.6	751.6	751.6
Domestic	-	-	-	704.2	751.6	751.6	751.6	751.6	751.6	751.6
Export	-	-	-	-	-	-	-	-	-	-
Production, as a % of Design Capacity	-	-	-	93.7%	100.0%	100.0%	100.0%	100.0%	100.0%	100.0%
Product Revenue	-	-	-	257.10	277.13	279.90	282.70	285.53	288.38	291.27
Product DIESEL	-	-	-	183.94	198.27	200.25	202.26	204.28	206.32	208.39
Domestic	-	-	-	183.94	198.27	200.25	202.26	204.28	206.32	208.39
Export	-	-	-	-	-	-	-	-	-	-
By-Product Credit	-	-	-	73.16	78.86	79.65	80.44	81.25	82.06	82.88
Manufacturing Costs	-	-	203.92	292.25	275.17	258.11	241.06	224.02	206.99	189.98
Operating Costs	-	-	62.61	108.22	109.30	110.39	111.50	112.61	113.74	114.88
Annual Expenses	-	-	-	-	-	-	-	-	-	-
Raw Material	-	-	29.45	60.46	61.06	61.68	62.29	62.92	63.54	64.18
Utilities	-	-	17.82	25.66	25.91	26.17	26.43	26.70	26.96	27.23
Operating Labor and Supervision	-	-	8.73	12.57	12.70	12.82	12.95	13.08	13.21	13.34
Maintenance	-	-	4.44	6.39	6.45	6.52	6.58	6.65	6.72	6.78
Operating Supplies	-	-	0.76	1.10	1.11	1.12	1.13	1.14	1.16	1.17
Laboratory Charges	-	-	1.42	2.04	2.06	2.08	2.10	2.13	2.15	2.17
Patents and Royalties (on Production)	-	-	-	-	-	-	-	-	-	-
Fixed Charges	-	-	119.62	152.90	135.92	118.93	101.94	84.95	67.96	50.97
Depreciation	-	-	119.62	152.90	135.92	118.93	101.94	84.95	67.96	50.97
Property Tax	-	-	-	-	-	-	-	-	-	-
Rent	-	-	-	-	-	-	-	-	-	-
Insurance	-	-	-	-	-	-	-	-	-	-
Plant Overhead	-	-	6.58	9.48	9.57	9.67	9.77	9.86	9.96	10.06
General and Administrative	-	-	15.11	21.65	20.38	19.12	17.86	16.59	15.33	14.07
EBIT (Earning before Interest, Taxes)	-	-	(203.92)	(35.16)	1.96	21.79	41.64	61.51	81.39	101.29
Taxes	-	-	-	-	0.78	8.72	16.66	24.60	32.56	40.51
Net Income	-	-	(203.92)	(35.16)	1.17	13.08	24.99	36.91	48.83	60.77

Figure 5.8(a). Pro forma income statements, hybrid CBTL model plant, first 10 years.

Date of First Day in Period	1-Jan-25	1-Jan-26	1-Jan-27	1-Jan-28	1-Jan-29	1-Jan-30	1-Jan-31	1-Jan-32	1-Jan-33	1-Jan-34
Year	2025	2026	2027	2028	2029	2030	2031	2032	2033	2034
Calendar Period	11	12	13	14	15	16	17	18	19	20
Year, from Start of EPC	11	12	13	14	15	16	17	18	19	20
Period of Operation	9	10	11	12	13	14	15	16	17	18
	Period Values					Millions of USD				
Production of DIESEL, Millions of LB per Year	751.6	751.6	751.6	751.6	751.6	751.6	751.6	751.6	751.6	751.6
Domestic	751.6	751.6	751.6	751.6	751.6	751.6	751.6	751.6	751.6	751.6
Export	-	-	-	-	-	-	-	-	-	-
Production, as a % of Design Capacity	100.0%	100.0%	100.0%	100.0%	100.0%	100.0%	100.0%	100.0%	100.0%	100.0%
Product Revenue	294.18	297.12	300.09	303.09	306.12	309.18	312.28	315.40	318.55	321.74
Product DIESEL	210.47	212.57	214.70	216.85	219.01	221.21	223.42	225.65	227.91	230.19
Domestic	210.47	212.57	214.70	216.85	219.01	221.21	223.42	225.65	227.91	230.19
Export	-	-	-	-	-	-	-	-	-	-
By-Product Credit	83.71	84.55	85.39	86.25	87.11	87.98	88.86	89.75	90.65	91.55
Manufacturing Costs	172.98	155.99	139.02	140.41	141.82	143.24	144.67	146.11	147.58	149.05
Operating Costs	116.02	117.18	118.36	119.54	120.74	121.94	123.16	124.39	125.64	126.89
Annual Expenses	-	-	-	-	-	-	-	-	-	-
Raw Material	64.82	65.47	66.12	66.79	67.45	68.13	68.81	69.50	70.19	70.89
Utilities	27.51	27.78	28.06	28.34	28.62	28.91	29.20	29.49	29.79	30.08
Operating Labor and Supervision	13.48	13.61	13.75	13.89	14.02	14.16	14.31	14.45	14.59	14.74
Maintenance	6.85	6.92	6.99	7.06	7.13	7.20	7.27	7.34	7.42	7.49
Operating Supplies	1.18	1.19	1.20	1.21	1.23	1.24	1.25	1.26	1.28	1.29
Laboratory Charges	2.19	2.21	2.23	2.26	2.28	2.30	2.32	2.35	2.37	2.40
Patents and Royalties (on Production)	-	-	-	-	-	-	-	-	-	-
Fixed Charges	33.98	16.99	-	-	-	-	-	-	-	-
Depreciation	33.98	16.99	-	-	-	-	-	-	-	-
Property Tax	-	-	-	-	-	-	-	-	-	-
Rent	-	-	-	-	-	-	-	-	-	-
Insurance	-	-	-	-	-	-	-	-	-	-
Plant Overhead	10.16	10.27	10.37	10.47	10.58	10.68	10.79	10.90	11.01	11.12
General and Administrative	12.81	11.56	10.30	10.40	10.50	10.61	10.72	10.82	10.93	11.04
EBIT (Earning before Interest, Taxes)	121.20	141.13	161.07	162.68	164.31	165.95	167.61	169.28	170.98	172.69
Taxes	48.48	56.45	64.43	65.07	65.72	66.38	67.04	67.71	68.39	69.07
Net Income	72.72	84.68	96.64	97.61	98.58	99.57	100.57	101.57	102.59	103.61

Figure 5.8(b). Pro forma income statements, hybrid CBTL model plant, years 11 through 20.

Date of First Day in Period	1-Jan-35	1-Jan-36	1-Jan-37	1-Jan-38	1-Jan-39	1-Jan-40	1-Jan-41	1-Jan-42	1-Jan-43	1-Jan-44
Year	2035	2036	2037	2038	2039	2040	2041	2042	2043	2044
Calendar Period	21	22	23	24	25	26	27	28	29	30
Year, from Start of EPC	21	22	23	24	25	26	27	28	29	30
Period of Operation	19	20	21	22	23	24	25	26	27	28
	Period Values					Millions of USD				
Production of DIESEL, Millions of LB per Year	751.6	751.6	751.6	751.6	751.6	751.6	751.6	751.6	751.6	747.5
Domestic	751.6	751.6	751.6	751.6	751.6	751.6	751.6	751.6	751.6	747.5
Export	-	-	-	-	-	-	-	-	-	-
Production, as a % of Design Capacity	100.0%	100.0%	100.0%	100.0%	100.0%	100.0%	100.0%	100.0%	100.0%	99.5%
Product Revenue	324.96	328.21	331.49	334.80	338.15	341.53	344.95	348.40	351.88	353.46
Product DIESEL	232.49	234.81	237.16	239.53	241.93	244.35	246.79	249.26	251.75	252.88
Domestic	232.49	234.81	237.16	239.53	241.93	244.35	246.79	249.26	251.75	252.88
Export	-	-	-	-	-	-	-	-	-	-
By-Product Credit	92.47	93.39	94.33	95.27	96.22	97.18	98.16	99.14	100.13	100.58
Manufacturing Costs	150.54	152.05	153.57	155.10	156.65	158.22	159.80	161.40	163.01	163.29
Operating Costs	128.16	129.44	130.74	132.05	133.37	134.70	136.05	137.41	138.78	138.98
Annual Expenses	-	-	-	-	-	-	-	-	-	-
Raw Material	71.60	72.32	73.04	73.77	74.51	75.26	76.01	76.77	77.54	77.46
Utilities	30.38	30.69	30.99	31.30	31.62	31.93	32.25	32.58	32.90	33.05
Operating Labor and Supervision	14.89	15.04	15.19	15.34	15.49	15.65	15.80	15.96	16.12	16.19
Maintenance	7.57	7.64	7.72	7.80	7.87	7.95	8.03	8.11	8.19	8.23
Operating Supplies	1.30	1.32	1.33	1.34	1.36	1.37	1.38	1.40	1.41	1.42
Laboratory Charges	2.42	2.44	2.47	2.49	2.52	2.54	2.57	2.59	2.62	2.63
Patents and Royalties (on Production)	-	-	-	-	-	-	-	-	-	-
Fixed Charges	-	-	-	-	-	-	-	-	-	-
Depreciation	-	-	-	-	-	-	-	-	-	-
Property Tax	-	-	-	-	-	-	-	-	-	-
Rent	-	-	-	-	-	-	-	-	-	-
Insurance	-	-	-	-	-	-	-	-	-	-
Plant Overhead	11.23	11.34	11.45	11.57	11.68	11.80	11.92	12.04	12.16	12.21
General and Administrative	11.15	11.26	11.38	11.49	11.60	11.72	11.84	11.96	12.08	12.10
EBIT (Earning before Interest, Taxes)	174.41	176.16	177.92	179.70	181.50	183.31	185.14	187.00	188.87	190.17
Taxes	69.77	70.46	71.17	71.88	72.60	73.32	74.06	74.80	75.55	76.07
Net Income	104.65	105.70	106.75	107.82	108.90	109.99	111.09	112.20	113.32	114.10

Figure 5.8(c). Pro forma income statements, hybrid CBTL model plant, years 21 through 30.

Pro forma cash flow projections were also prepared. Figure 5.9 shows the net present value of cash flow over the first twenty-five (25) years, during which the facility is not projected to have reached break even.

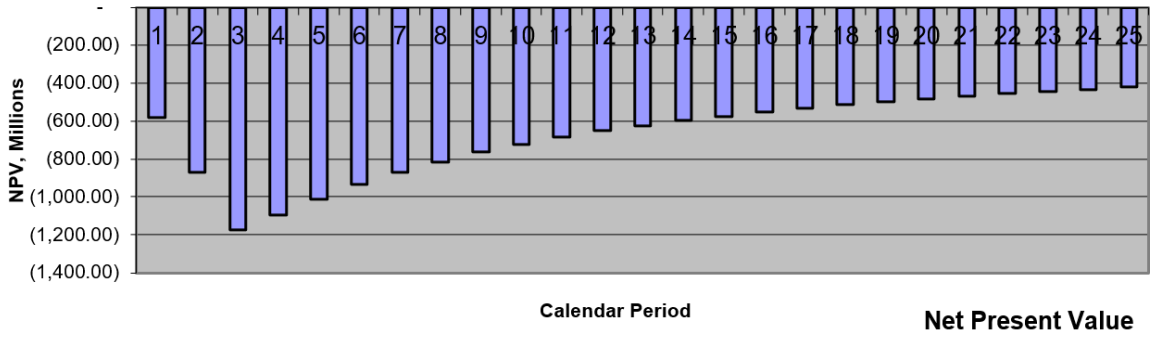

Figure 5.9. Cash flow summary over initial 25 years, hybrid CBTL model plant.

Accomplishments:

- ✓ The project team has evaluated the key variables driving the sensitivity of the direct, indirect, and hybrid CBTL financial models.

Please see the section regarding Task 3.4 for a detailed summary of the sensitivity analyses that were conducted with respect to the CBTL plant models.

Task 5.3 Investor Interest and Financing Analysis

Accomplishments

- ✓ We have prepared an investor prospectus that not only summarizes the pro forma financial projections for the indirect, direct, and hybrid CBTL models, but also provides a framework for discussing certain financial subsidies and incentives, including subsidizing the capital expenditures of the project (for instance, via grants or investment tax incentives) as well as mechanisms to increase revenue on a per-unit basis (for instance, via a per-gallon tax reduction or credit).

- ✓ Various factors were considered, including:
  - Investment conditions
  - Commodity pricing environment
  - Regulatory framework (existing and potential)
  - Project development models and financing options